Developing New Molecular Tools for Biosynthetic Gene Cluster Capture, and Discovery of Novel Antibiotics

Felaine Anne Sumang

Thesis submitted for the degree of Doctor of Philosophy

Newcastle University Biosciences Institute, Faculty of Medical Sciences, Newcastle University

April 2025

Abstract

Actinomycetes are renowned for their ability to produce a wide array of natural products (NPs), with a broad range of applications. NPs are typically encoded by biosynthetic gene clusters (BGCs). Bioinformatic analysis of sequenced Actinomycetes genomes have shown that they possess many BGCs whose potential products are not detected under standard laboratory culture conditions. Advances in genome mining and molecular biology have led to the development of diverse strategies to activate these "cryptic" BGCs, but further improvements in these methods are warranted.

This thesis explores multiple approaches for discovering novel bioactive compounds from Actinomycetes and investigating their BGCs. Chapters 3 and 4 focus on the development of a new bacterial artificial chromosome (BAC) vector, designated pJE2, and optimization of a protocol for genomic library construction enabling the isolation of large BGCs. This approach was applied to *Actinomadura madurae* T576, a producer of unusual sulphated metabolites, resulting in a BAC library from which a clone harbouring the complete 80 kbp BGC responsible for these metabolites was identified. Heterologous expression of this clone in *Streptomyces albus* successfully led to production of the sulphated metabolites. Screening of additional clones also revealed the successful capture of several previously uncharacterized BGCs.

Chapter 5 focuses on a chemical elicitation method, using plant extracts to stimulate NP production in soil-derived Actinomycetes. Notably, hibiscus flower extract induced the production of the antibiotic thiolutin by *Streptomyces* strain MBN 2-2. Further analysis identified hibiscus acid and hydroxycitric acid as the elicitor compounds.

The final chapter centres on associating putative BGCs with the synthesis of three novel antibiotics demurilactone A, persiathiacin, and quinovosamycin. In all three cases, insertional mutagenesis led to the abolition of antibiotic synthesis, thereby validating assignment of the BGCs to their respective antibiotics.

Acknowledgements

I sincerely thank my brilliant supervisors, Prof. Jeff Errington and Dr. Yousef Dashti. Jeff, thank you for the opportunity to be part of your group. It has been a privilege to work alongside you and to learn from your expertise in genetics. I am especially grateful for your patience and guidance in editing my thesis. Yousef, thank you for encouraging me to pursue higher studies and for generously sharing your knowledge in natural products. The projects you entrusted to me became invaluable opportunities to learn and grow in this field. My time working with you has truly been fruitful.

I am grateful to the DOST-SEI for the financial support through the Foreign Graduate Scholarship program. I also extend my thanks to Dr. Emmanuele Severi for providing the Lucigen BAC vector, Prof. Andriy Luzhetskyy for the *Streptomyces* expression strains, Dr. Samiuela Lee and Dr. Biswaranjan Mohanty for LC-MS and NMR support.

To the entire Errington group, both at CBCB, UK and C81 USyd, Australia, thank you for providing such a warm and supportive working environment. Special appreciation to Fatemeh and Sammy whom I've had the pleasure of exchanging insights on natural products. Thanks also to the lab managers and support staff who made life in the lab so much easier.

On a personal note, I want to thank my family, especially my mom, dad, and sisters, for their unwavering support, even from afar. I am also grateful for my old friends from Berea and the new friends I have made along the way. Thank you for being a breather in the middle of busy days. A special mention to Mary, who shared the same UK to Australia journey with me and has become one of my closest friends. Special thanks too to Dashti family, who adopts me every holiday and have become a family away from home.

I could never have completed this PhD without the support of my loving husband, Jovan. Thank you for helping me with my diagrams and for patiently listening, sometimes forcefully but lovingly, to my presentations, random science thoughts, frustrations and lab stories. Your willingness to share in both my burdens and my joys has meant everything to me.

Above all, I give my deepest thanks to God, who is always the First and the Last in every chapter of my life, including this one. Sa Iyo lahat ng papuri!

Table of Contents

Table of Tables

Table of Figures

Abbreviations

% - percent

[M+H]+ - molecular ion plus proton

µg - microgram

µl - microliter

µm - micrometer

µM - micromolar

^{13}C NMR - carbon-13 NMR

^{1}H NMR - proton NMR

A domain- adenylation domain

ACP domain - acyl carrier protein domain

Act - actinorhodin

ACTIMOT- advanced Cas9-mediated in vivo mobilization and multiplication of BGCs

AGE - agarose gel electrophoresis

AGRF - Australian Genome Research Facility

apr - apramycin

ARCs - antibiotic-remodelling compounds

AT - acyl transferase domain

ATP - adenosine triphosphate

BAC - bacterial artificial chromosome

BGC - biosynthetic gene cluster

C domain - condensation domain

CaCl2.2H2O - calcium chloride dihydrate

$CaCO_3$ - calcium carbonate

CAPTURE- Cas12a-assisted precise targeted cloning using in vivo cre-lox recombination

CAS - Chrome Azurol S

cat- chloramphenicol

CATCH- Cas9-assisted targeting of chromosomes segments

CAT-Fishing- CRISPR/Cas12a- and agarose plug-based system for fast biosynthetic gene cluster cloning

CCR regulation - carbon catabolite repression regulation

CDA - calcium-dependent antibiotic

CHEF - clamped homogeneous electric fields

CRISPR - clustered regularly interspaced short palindromic repeats

CYP - cytochrome P450

DAP - diaminopimelic acid

DH domain - dehydratase domain

DI water - deionized water

DiPAC - direct pathways cloning

DMAPP - dimethylallyl diphosphate

DMSO - dimethyl sulfoxide

DMSO-d_6 - deuterated DMSO

DNA - deoxyribonucleic acid

DTT - Dithiothreitol

EDTA - Ethylenediaminetetraacetic acid

ER domain - enoyl reductase domain

ermEp - ermE promoter

EtOAc - ethyl acetate

ExoCET- exonulcease combined with RecET combination

$FeCl_3 \cdot 6H_2O$ - iron(III) chloride hexahydrate

FPP- farnesyl diphosphate

GBLs - gamma-butyrolactones

gDNA - genomic DNA

gen - gentamycin

GGPP- geranylgeranyl diphosphate

GPP - geranyl diphosphate

GYM media - glucose yeast malt extract media

h – hour\s

HCL - hydrochloric acid

HDTMA - hexadecyltrimethylammonium bromide

HiFi- high fidelity

HMW - high molecular weight

HPLC - hi-performance liquid chromatography

HR region - homologous recombination region

iChip - isolation chip

IPP - isopentenyl diphosphate

IPTG - isopropyl β-D-thiogalactopyranoside

ISR - integrase-mediated site-specific recombination

K_2SO_4 - potassium sulfate

kan - kanamycin

kasOp - kasO promoter

kbp - kilobase pairs

kDa - kilodalton

KH_2PO_4 - monobasic potassium phosphate

KOH - potassium hydroxide

KR domain - ketoreductase domain

KS domain - ketosynthase domain

L - liter

LB medium - Luria Bertani medium

LC-HR-MS - liquid chromatography-high resolution mass spectrometry

LC-MS - liquid chromatography-mass spectrometry

LCN - lipid characteristics of Nocardia

LLHR - linear-linear homologous recombination

LMP agarose - low melting point agarose

M - molar

m/z - mass-to-charge ratio

MALDI-TOF-MS - matrix-assisted laser desorption ionization time-of-flight mass spectrometry

Mbp - megabase pairs

MeOH - methanol

mg - milligram

$MgCl_2$ - magnesium chloride

$MgCL_2.6H_2O$ - magnesium chloride hexahydrate

MIC - minimum inhibitory concentration

min - minute

ml- milliliter

mM - millimolar

Mn2+- manganese ion with a +2 charge

MRSA - methicillin-resistant *Staphylococcus aureus*

MS medium - mannitol soy flour medium

MW markers - molecular weight markers

NA - nutrient agar

Na_2HPO_4 - disodium phosphate

NaCl - sodium chloride

nal - nalidixic acid

NEB - New England Biolabs

ng - nanogram

NGS - next-generation sequencing

NMR - nuclear magnetic resonance

NP - natural products

NRPS - non-ribosomal peptide synthetases

NRPs - non-ribosomal peptides

OD - optical density

oriT - origin of transfer

P buffer - protoplast buffer

PAC - P1-derived artificial chromosome

PCP domain - peptidyl carrier protein domain

PCR- polymerase chain reaction

pDNA - plasmid DNA

PEG - polyethylene glycol

PFGE - pulsed field gel electrophoresis

pH - potential of hydrogen

PKS - polyketide synthases

Pol II - RNA polymerase II

psBAC - plasmid Streptomyces bacterial artificial chromosome

PSRs - pathway-specific regulators

PTMs - post-translational modifications

qPCR - quantitative polymerase chain reaction

QVMs - quinovosamycins

RC method - rehydration and centrifugation method

rDNA - ribosomal DNA

Red- undecylprodigiosin

REE - rare earth elements

rif - rifampicin

RiPPs - ribosomally synthesized and post-translationally modified peptides

RNA - ribonucleic acid

rpoβ - RNA polymerase β

rpsL - ribosomal protein S12

rRNA- ribosomal RNA

s - second

SARP - *Streptomyces* activator regulatory proteins

str - streptomycin

TAR - transformation-associated recombination

TBE buffer - Tris-borate EDTA buffer

TE buffer - Tris-EDTA buffer

TE domain - thioesterase domain

TES - [tris(hydroxymethyl)methylamino]-ethanesulfonic acid)

TetR - tetracycline repressor

TFRs - transcriptional regulators

TFs - transcription factors

TFTRs - TetR family transcriptional repressors

TIR - translation initiation region

TSs - terpene synthases

Tun- tunicamycin

U - units

UHPLC-HRMS - ultra-high-performance liquid chromatography-high resolution mass spectrometry

V - volts

VBs - virginiae butanolides

WGS - whole genome sequencing

X-gal- 5-bromo-4-chloro-3-indolyl-β-D-galactopyranoside

YAC - yeast artificial chromosome

YEME medium - yeast extract malt extract

YPD medium - yeast peptone dextrose medium

Zn^{2+}- a zinc ion with a +2 charge

Chapter 1: Chemistry and Biology of Actinomycetes

1.1 Overview of natural product discovery from Actinomycetes

Actinomycetes are a group of high G+C (55-75% guanine and cytosine) Gram-positive bacteria within the Phylum Actinomycetota. These microorganisms are often terrestrial and aquatic by nature. Actinomycetes are renowned for their ability to produce bioactive natural products (NPs), sometimes called secondary or specialized metabolites, including many antibiotics. The first antibiotic from this group, streptomycin, was isolated from *Streptomyces griseus* and successfully used to treat tuberculosis (Schatz, Bugle and Waksman, 1944). This discovery paved the way for other clinically significant antibiotics, including chloramphenicol (1947) (Rebstock, 1949), tetracycline (1948) (Duggar, 1948), erythromycin (1952) (Haight, 1952), and kanamycin A (1957) (Umezawa, 1957), all identified using the "Waksman platform", a bioactivity-guided approach that employs disc diffusion assays to screen crude microbial extracts for antimicrobial activity (Schatz, Bugle and Waksman, 1944) (Figure 1.1 shows a modernised version of the platform).

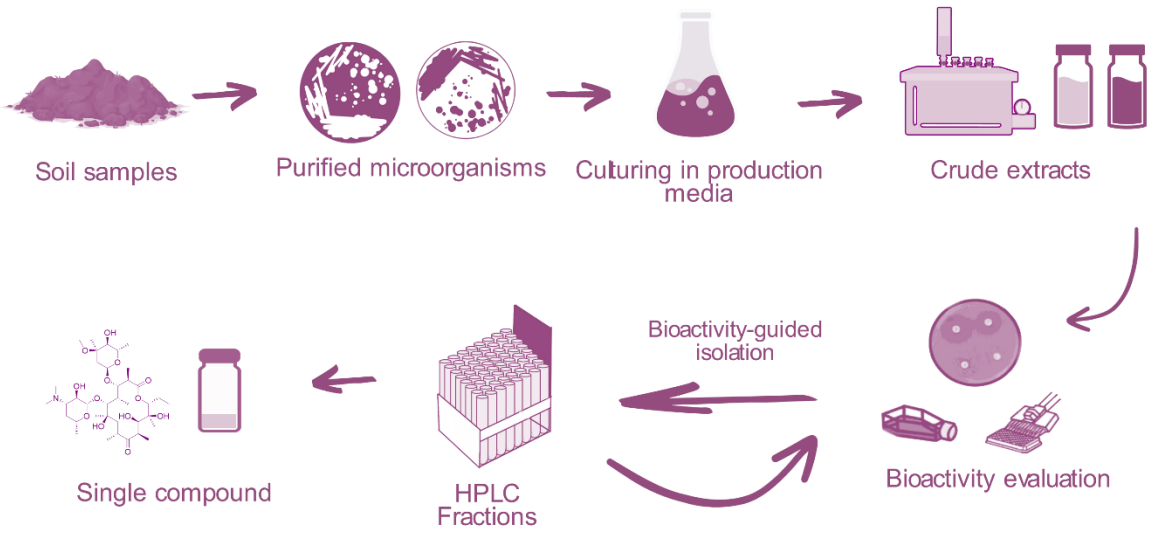

Figure 1.1 Schematic overview of bioassay guided isolation of bioactive NPs produced by microorganisms.

Today, Actinomycetes account for many important classes of antibiotic including aminoglycosides, tetracyclines, amphenicols, macrolides, and glycopeptides (Hutchings, Truman and Wilkinson, 2019; Nair and Abraham, 2020). Some of the early discovered antibiotics remain clinically relevant, as they continue to be used in treating diseases (Farzam K, 2023) and are still being explored for potential applications in other medical conditions (Sime, 2025) despite the emergence of resistant pathogens (Jama-Kmiecik, 2025). Beyond antibiotics, Actinomycetes also produce clinically significant compounds such as: the antifungals amphotericin B and rapamycin (sirolimus); anticancer agents, like anthracyclines,

bleomycin, mitomycin C, dactinomycin (actinomycin D) and doxorubicin; the immunosuppressant cyclosporin; and the metal chelator deferoxamine, which is used to treat iron overdose in patients with anaemia or thalassemia, as well as aluminium toxicity in individuals undergoing dialysis (Nair and Abraham, 2020). Additionally, Actinobacteria play a crucial role in agriculture, contributing to biopesticides such as MYCOSTOP (Finland), which contains dried *Streptomyces griseoviridis* spores and mycelium to control *Fusarium*-induced root, stem, and seed rot, and Actino-Iron (Texas), a biofungicide derived from *Streptomyces lydicus* (Patil *et al.*, 2011). Examples of the diversity of chemical structures for NP molecules made by Actinomycetes are shown in Figure 1.2.

After the 1980s, the discovery of novel compounds from Actinomycetes significantly declined (Van Middlesworth and Cannell, 1998). This led many pharmaceutical companies to abandon NPs as a source of drug discovery. However, since then, advances in genome sequencing, molecular cloning, and bioinformatics have transformed the field of NP discovery. Whole genome sequencing of Actinomycetes revealed that the biosynthetic genes responsible for NP production tended to be clustered into functionally related groups called biosynthetic gene clusters (BGCs). Most of the newly discovered BGCs appeared to remain cryptic or silent under standard culture conditions, so the genome sequencing revealed that organisms tend to have far more potential coding capacity for NPs than is evident from biochemical characterization (Undabarrena *et al.*, 2021; Bentley *et al.*, 2002).

Actinomycetes are thought to produce NPs largely to survive in competitive environments, often as defence mechanisms. However, in standard laboratory culture conditions, where nutrients are abundant and interactions with other organisms are usually absent, many biosynthetic pathways remain inactive, probably due to lack of triggering factors (Atanasov *et al.*, 2021; Hutchings, Truman and Wilkinson, 2019). This has led to the development of a range of new approaches, such as co-culturing, chemical elicitation and molecular genetic manipulation, to stimulate NP production (Rutledge and Challis, 2015).

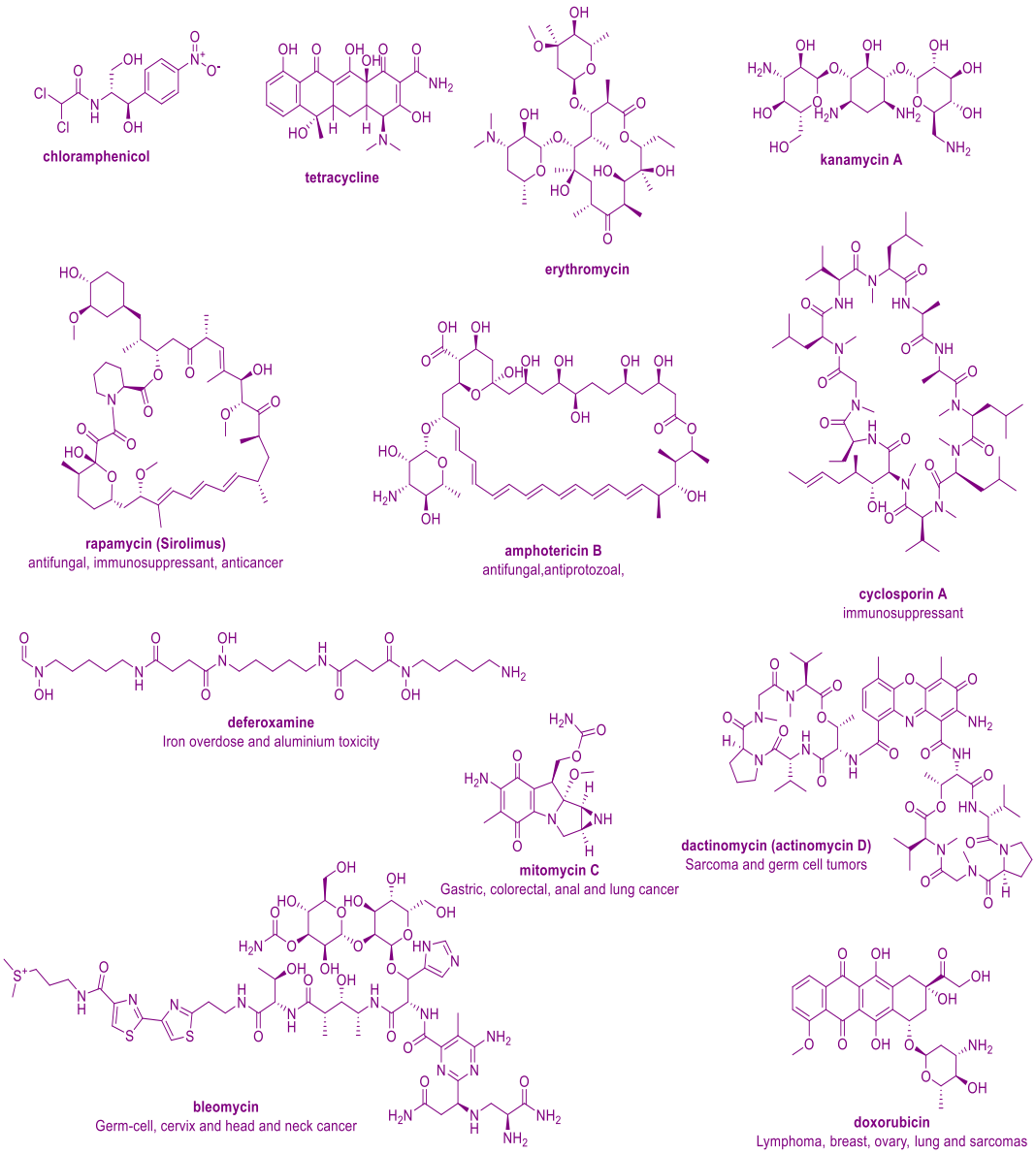

Figure 1.2 Structure of some clinically relevant NPs made by Actinomycetes.

1.2 Classes of natural products based on their biosynthesis

NPs are typically classified according to the biosynthetic pathways through which they are produced. These biosynthetic routes involve precursor molecules and enzymatic machinery that determine the structural diversity of the resulting compounds. Biosynthetic pathways of the major classes of microbial NPs, including polyketides, nonribosomal peptides, ribosomally synthesized and posttranslationally modified peptides, and terpenoids, are discussed below. In

addition to these four, Actinomycetes produce various other types of metabolites generally classified as miscellaneous.

1.2.1 Polyketides

Polyketides are biosynthesized by polyketide synthases (PKS) enzyme systems, which construct complex carbon frameworks from malonyl-CoA and methylmalonyl-CoA. The biosynthetic process involves enzyme complexes organized either modularly or iteratively, depending on the PKS type (Staunton and Weissman, 2001; Shen, 2003). In Type I PKSs, biosynthesis is carried out by large, multifunctional enzymes composed of sequential modules, each responsible for one round of chain elongation. Within each module, domains with specific catalytic functions operate in a coordinated fashion. These domains include acyl transferase (AT), which selects the starting unit and loads it onto the acyl carrier protein (ACP), which delivers it to the ketosynthase (KS) domain. The AT domain of the next module loads the extender unit (typically malonyl-CoA), which is condensed with the growing chain by the KS domain, resulting in elongation of the carbon chain. Additional tailoring domains, such as ketoreductase (KR), dehydratase (DH), and enoyl reductase (ER), sequentially modify the intermediate. Upon completion, the thioesterase (TE) domain cleaves and releases the final polyketide product (Staunton and Weissman, 2001).

In contrast, Type II PKSs consist of discrete, iteratively acting enzymes that repeatedly use a single set of domains to assemble polycyclic polyketides. These systems resemble fatty acid synthases in their repetitive use of catalytic domains but produce structurally distinct scaffolds. Type III PKSs, also known as chalcone-synthase-like PKSs, differ fundamentally from Types I and II. These are homodimeric enzymes that catalyse iterative condensations directly on acyl-CoA substrates, without the involvement of an ACP. As a result, Type III PKSs typically produce smaller polyketides that are mono- or bicyclic in structure (Shen, 2003). Figure 1.3 presents a schematic overview of the structural and mechanistic differences between the PKS types.

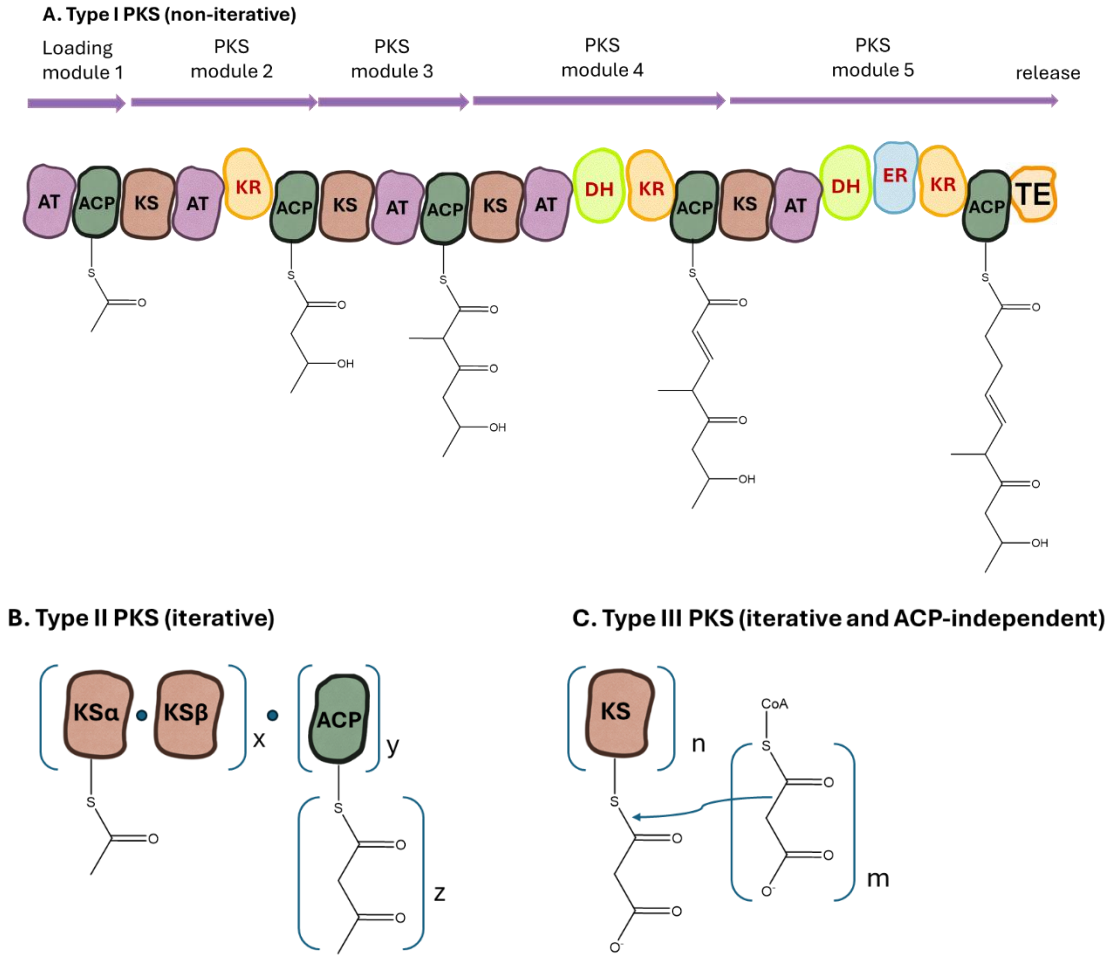

Figure 1.3 Schematic representation of the assembly line machinery of A.) Type I, B.) Type II and C.) Type III PKSs, adopted from (Shen, 2003). AT- acyl transferase; ACP- acyl carrier protein; KS- ketosynthase; KR- ketoreductase; DH- dehydratase; ER- enoyl reductase: TE- thioesterase.

1.2.2 Non-ribosomal peptides

Non-ribosomal peptides (NRPs) are synthesized independently of ribosomes by non-ribosomal peptide synthetases (NRPSs), large multi-enzyme complexes that operate in a modular fashion analogous to PKSs. NRPSs assemble peptide chains from both proteinogenic and non-proteinogenic amino acids. Each module is responsible for the selection and incorporation of a specific amino acid, mediated by a series of conserved domains (Marahiel, 2016; Winn *et al.*, 2016). The adenylation (A) domain activates the amino acid using adenosine triphosphate (ATP); the condensation (C) domain catalyses peptide bond formation; and the peptidyl carrier protein (PCP) domain tethers the growing peptide chain. Figure 1.4 shows a simple diagram of the NRPS assembly line machinery highlighting the role of the three domains. Additional tailoring domains introduce modifications such as oxidation, epimerization, and reduction, leading to structural diversity. Similar to PKSs, NRPSs typically contain a thioesterase (TE)

domain at the end of the assembly line that catalyses product release (Marahiel, 2016; Winn *et al.*, 2016). Hybrid PKS-NRPS systems are also common in Actinobacteria, contributing to a broad range of structurally diverse secondary metabolites. These hybrids result from the integration of PKS and NRPS modules within a single biosynthetic assembly line, or through the sequential action of iterative PKS modules followed by NRPS modules, leading to the formation of polyketide-peptide hybrid structure (Fisch, 2013).

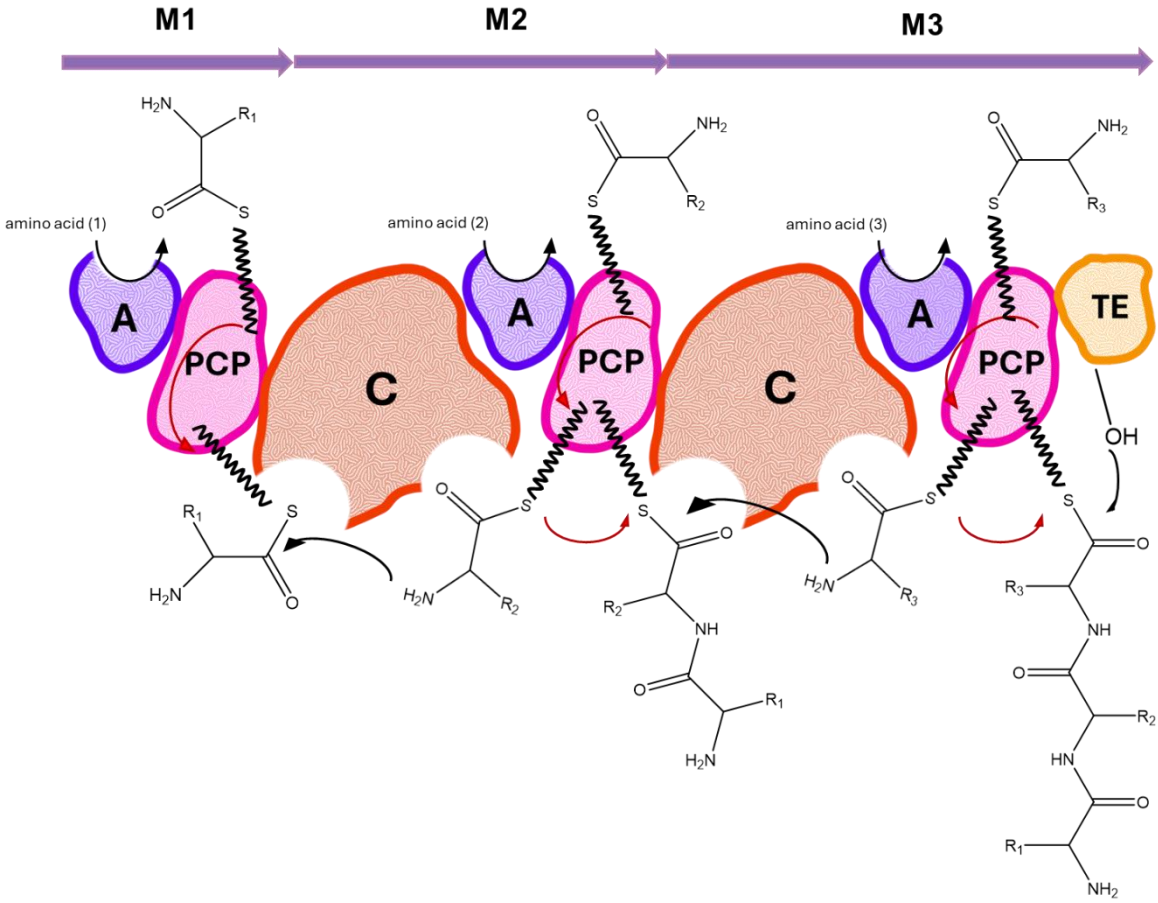

Figure 1.4 Simplified schematic of NRPS assembly line machinery, adapted from (Winn *et al.*, 2016). A- adenylation domain; PCP- peptidyl carrier protein; C- condensation domain.

1.2.3 Ribosomally synthesized and post-translationally modified peptides

Ribosomally synthesized and post-translationally modified peptides (RiPPs) represent a structurally diverse class of natural products that are initially translated by ribosomes as precursor peptides. Typically ranging from 20 to 110 amino acid residues, and then enzymatically modified through post-translational modifications (PTMs) (Arnison *et al.*, 2013). These precursor peptides usually consist of an N-terminal "leader peptide" and a "core peptide," although in some cases, a "follower peptide" is located at the C-terminus (Arnison *et al.*, 2013). Figure 1.5 shows a simplified illustration of RiPP biosynthesis, which involves a leader peptide

that functions as an allosteric regulator, facilitating the proper conformation and activity of the biosynthetic enzymes, while the PTMs are predominantly applied to the core peptide (Yang and Van Der Donk, 2013). PTMs enhance the structural and functional diversity of RiPPs and include processes such as methylation, oxidation, reduction, dehydration, macrocyclization, and the formation of cross-links between amino acid residues (Rubin and Ding, 2020). The modified core peptide remains biologically inactive until proteolytic cleavage removes the leader sequence, typically after completion of all necessary modifications (Arnison *et al.*, 2013; Yang and Van Der Donk, 2013). PTMs are crucial for enhancing the stability, membrane permeability, and bioactivity of RiPPs (Müller, 2018).

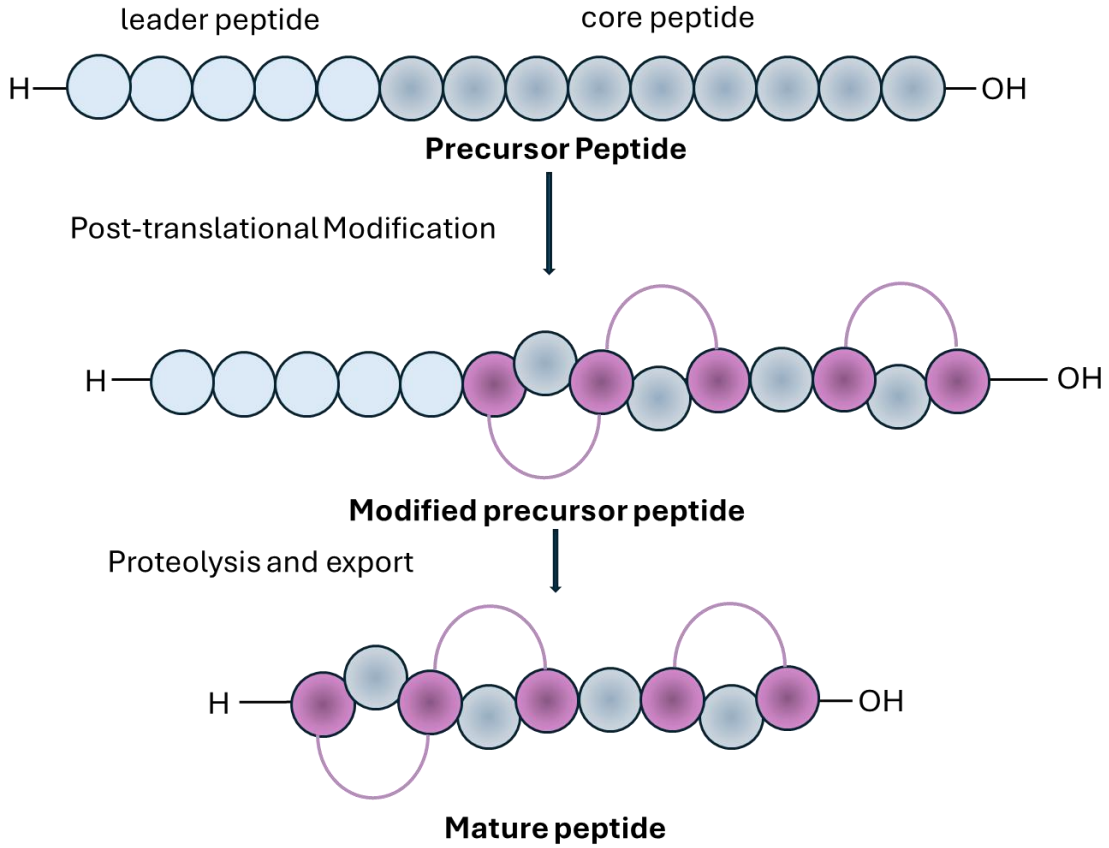

Figure 1.5 Simplified schematic of RiPP biosynthesis, adopted from (Dang and Süssmuth, 2017).

1.2.4 Terpenoids

Terpenoids, also known as isoprenoids, are the largest and most diverse class of natural products, with widespread applications in industries such as food, cosmetics, and fragrance (Silvestre and Gandini, 2008). Beyond their industrial uses, they exhibit a broad spectrum of biological activities, including antimicrobial properties (Cox-Georgian *et al.*, 2019; Silvestre

and Gandini, 2008). Terpenoids are synthesized from five-carbon isoprene units, namely isopentenyl diphosphate (IPP) and dimethylallyl diphosphate (DMAPP). These precursors are converted into various isoprenyl diphosphates of different chain lengths by isoprenyl transferases, producing compounds such as geranyl (GPP), farnesyl (FPP), and geranylgeranyl (GGPP) diphosphates. Terpene synthases (TSs) then catalyse the cyclization of these intermediates to generate a variety of terpenes, including monoterpenes (C10), sesquiterpenes(C15), diterpenes (C20), sesterterpenes (C25), triterpenes (C30), sesquarterpenes (C35), and tetraterpenes (C40) (Figure 1.6) (Tarasova *et al.*, 2023).

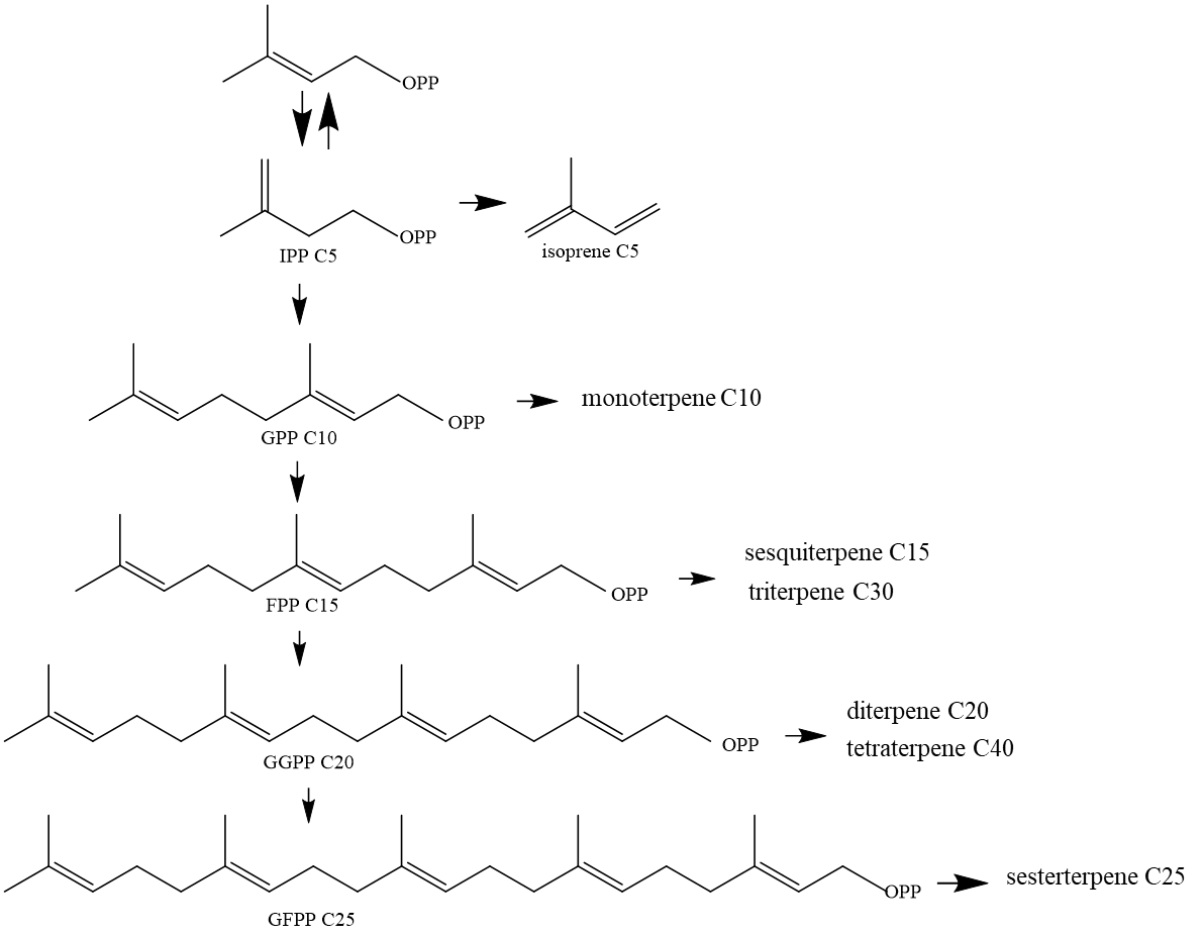

Figure 1.6 Structure of isoprenyl diphosphate units used by terpene synthase in terpenoids biosynthesis, adapted from (Tarasova *et al.*, 2023).

1.3 Biology of Actinomycetes

1.3.1 Taxonomy and classification

The nomenclature associated with traditional "Actinomycetes" has changed numerous times in recent years. Presently, actinomycetes are classified as belonging to the Order Actinomycetales, Class Actinomycetia and Phylum Actinomycetota (Oren and Garrity, 2021). Hereafter, I shall refer to them as Actinomycetes. Most actinomycetes exhibit a filamentous growth pattern,

which initially caused microbiologists to misidentify them as fungi (Williams and Wellington, 1982). They form hyphae partitioned by septa (Klieneberger-Nobel, 1947) and are predominantly aerobic and spore-forming (Waksman and Henrici, 1943). The largest and most extensively studied genus in this order is *Streptomyces*, comprising approximately 700 species (Komaki, 2023).

Before the rise of molecular tools, Actinomycetes were classified using traditional methods based on observable traits. These included the colour of aerial mycelia (e.g., white, grey, red, blue, or violet), the production of melanoid pigments, the presence of reverse-side pigmentation, and the secretion of distinctive soluble pigments. Spore chain morphology including rectiflexibiles, rectinaculiaperti, spirales, or combinations of these, as well as spore surface characteristics, such as smooth, spiny, warty, or hairy textures, were also considered for the classification of Actinomycetes (Sharma, Dangi and Choudhary, 2014).

Beyond morphological differences, Actinomycetes exhibit significant chemotaxonomic diversity, particularly in cell wall composition. A key criterion for differentiation is the presence of diaminopimelic acid (DAP), classifying cell walls into four types (I-IV). Type I contains L-DAP and glycine, Type II includes meso-DAP and glycine, Type III has meso-DAP alone, and Type IV features meso-DAP along with galactose (Goodfellow, 1989). For instance, *Streptomyces* species typically possess Type I cell walls, while *Actinoplanes* exhibit Type II (Lechevalier and Lechevalier, 1970). *Actinomadura* species are associated with Type III, whereas *Nocardia* species have Type IV (Becker, Lechevalier and Lechevalier, 1965; Lechevalier and Lechevalier, 1970).

In addition to cell wall analysis, other chemotaxonomic approaches such as fatty acid profiling, whole-cell composition studies, phage typing, and protein profiling were historically used in genus differentiation (Anderson and Wellington, 2001). For example, *Nocardia* and *Actinomadura* were initially classified as a single genus until lipid analysis identified a lipid characteristics of *Nocardia* (LCN)-A, present only in *Nocardia* species and absent in *Actinomadura*, which led to their reclassification as distinct genera (Mordarska, Mordarski and Goodfellow, 1972). Modern molecular approaches have provided more systematic and robust tools for microbial classification. Prior to the widespread adoption of molecular methods such as 16S ribosomal RNA (rRNA) sequencing, DNA-DNA hybridization was a standard technique used since the 1960s for bacterial taxonomy (Goris *et al.*, 2007). This approach involved comparing the entire genomes of two organisms by assessing the association between their denatured, single-stranded DNA (deoxyribonucleic acid) (Rosselló-Móra, Urdiain and López-López, 2011). However, DNA-DNA hybridization had several limitations such as being time

consuming, labour intensive due to the large amounts of high-quality DNA required (Goris *et al.*, 2007), and was prone to high experimental error and lack of the ability to produce cumulative databases for broader comparisons (Rosselló-Móra, Urdiain and López-López, 2011). As a result, it was gradually replaced by PCR-based techniques like 16S rDNA sequencing, which offered higher efficiency and resolution, enabling the classification of bacteria down to the species and even strain level (Anderson and Wellington, 2001). This method relies on the conserved nature of 16S rRNA genes, which contain both highly conserved and variable regions, allowing for precise phylogenetic comparisons (Woese *et al.*, 1975). With the decreasing cost of sequencing, whole genome sequencing (WGS) is gradually replacing 16S rDNA sequencing. Unlike 16S rRNA, which is primarily used for organism identification, WGS provides the ultimate analysis while also revealing potential BGCs in the genome. These molecular techniques significantly enhance the accuracy and speed of microbial identification, complementing traditional classification methods.

Another approach in bacterial identification is Matrix-Assisted Laser Desorption Ionization Time-Of-Flight Mass Spectrometry (MALDI-TOF-MS), which offers advantages over 16S rRNA sequencing in terms of speed and cost-effectiveness (Seng *et al.*, 2010; Cayrou, Raoult and Drancourt, 2010). Due to these benefits, MALDI-TOF-MS has become the preferred method for identifying bacterial species present in clinical samples (Seng *et al.*, 2010). This technique works by comparing the protein profiles of bacterial isolates against a reference database using the Bruker's MALDI-Biotyper® System (Cayrou, Raoult and Drancourt, 2010). While its efficiency is comparable to 16S rRNA sequencing, some studies indicate that discrepancies encountered with this approach are still resolved using 16S rRNA analysis (Chudzik *et al.*, 2024; Fong *et al.*, 2018). The accuracy of identifying Actinomycetes with this system could be further improved by expanding the Bruker database to include a broader range of Actinomycetes species (Chudzik *et al.*, 2024).

1.3.2 Morphology and life cycle

Actinomycetes have a range of distinct growth habits and cell morphologies, including classical rods and cocci. However, the majority of these organisms, and in general the best NP producers, have a mycelial habit, forming a branching network of hyphae that extend both above the surface of agar plates (aerial hyphae) and within the medium (substrate hyphae) (Sharma, Dangi and Choudhary, 2014). Their morphology varies significantly between genera. *Streptomyces* species, for example, produce stable, powdery aerial mycelium with spore chains. In contrast, *Micromonospora* and *Actinoplanes* lack aerial mycelium entirely, forming only non-fragmenting substrate mycelium. *Actinomadura* and *Thermomonospora* both develop powdery

aerial mycelium but differ in spore structures. *Actinomadura* form short, curly spore chains, while *Thermomonospora* produces branched or clustered single spores (Wellington and Toth, 1994).

Despite their diversity, mycelial Actinomycetes share a common growth pattern and a well-defined life cycle. This cycle has been best studied in the model organism, *Streptomyces coelicolor*, and consists of spore germination, vegetative growth, aerial mycelium formation, and spore development (Figure 1.7) (Chater, Merrick and Parish, 1979). Spore germination is followed by the emergence of hyphal tubes that develop into young mycelial. As the substrate mycelium expands, it gives rise to aerial mycelium. The aerial hyphae then undergo coiling and septum formation (Hopwood, 1988). This leads to the compartmentalization of individual spore cells and is followed by cell wall thickening. In the final stage, the spores mature, round off, and are eventually released, completing the life cycle (Chater, Merrick and Parish, 1979). Sporulation enables Actinomycetes to survive in harsh environments as their spores are highly resistant to desiccation and can be easily dispersed (Hopwood, 1988).

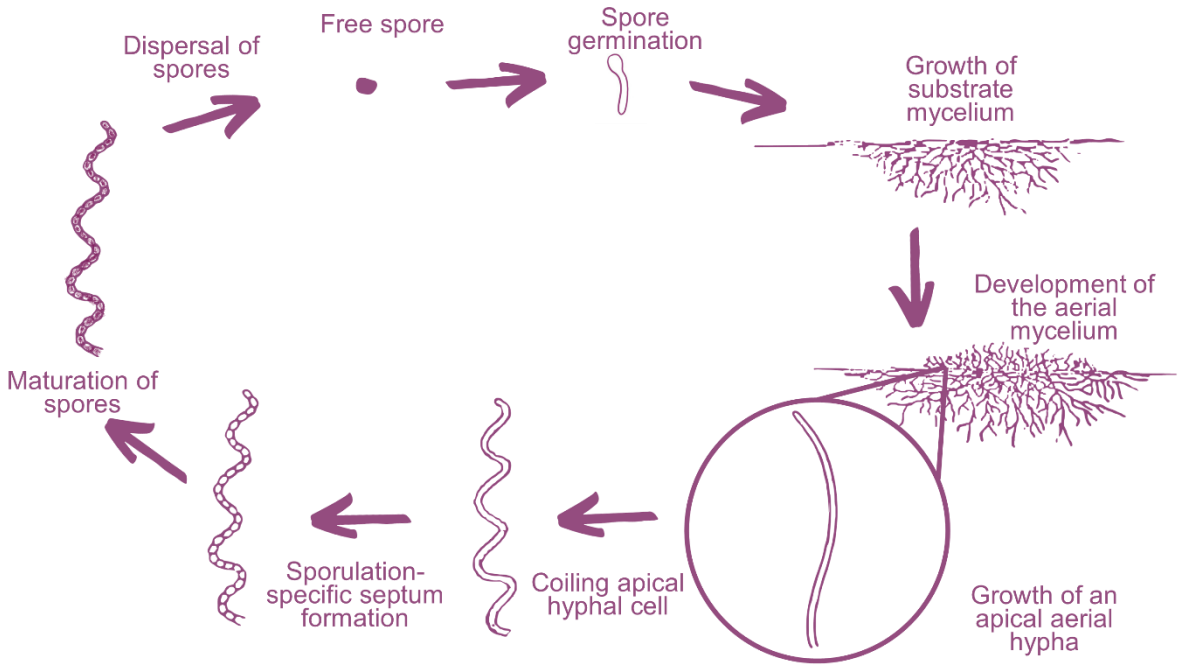

Figure 1.7 Life cycle of *Streptomcyces*. Diagram adopted from (Bunet, 2006).

The physiological and morphological changes in Actinomycetes are closely linked to NP synthesis. Nutrient limitation during stationary phase leads to the lysis of substrate mycelium, releasing nutrients that facilitate aerial mycelium formation (Chater, 1984). Simultaneously, at

the physiological level, NP production is favoured as primary metabolism declines, utilizing stored energy, lipids, proteins, and nucleic acids as building blocks. This process is tightly regulated by specialized genetic pathways dedicated to secondary metabolism (Malik, 1980; Martin and Demain, 1980).

1.3.3 Habitats and ecological roles

Actinomycetes are widely distributed in various habitats, including terrestrial environments, deep sea and mangrove sediments, and as symbionts of plants and animals. They have also been isolated from extreme environments, such as alkaline and volcanic soils, as well as high temperature regions (Bhatti, Haq and Bhat, 2017). Most Actinomycetes are mesophilic, thriving at temperatures between 25-30 °C (Goodfellow and Williams, 1983). They are predominantly found in the surface layers of soil, with their abundance decreasing with depth (Bhatti, Haq and Bhat, 2017). They are responsible for the earthy smell of soil through production of a volatile compound named geosmin (Gerber and Lechevalier, 1965). It is estimated the population of Actinomycetes in soil frequently exceeds 10^6 per gram of soil (Goodfellow and Williams, 1983).

In their natural habitat, Actinomycetes engage in complex interactions with neighbouring or host organisms, including bacteria, plants, and insects. The interactions of Actinomycetes with other microbes can vary widely depending on external factors, such as nutrient availability (Yan *et al.*, 2021; Zeph and Casida Jr, 1986). For instance, studies have reported that predatory behaviour between Gram-positive and Gram-negative bacteria tends to decline in nutrient-rich soils, indicating that such predation is likely non-obligate in nature (Zeph and Casida Jr, 1986). Likewise, research has shown that Actinomycetes may exhibit neutral interactions with neighbouring microbial communities under both nutrient-poor (oligotrophic) and nutrient-rich (eutrophic) conditions (Yan *et al.*, 2021).

Actinomycetes form a symbiotic relationship with plants, especially in the rhizosphere, where they are considered plant-growth-promoting rhizobacteria (PGPR). (Bhatti, Haq and Bhat, 2017; Prashar, Kapoor and Sachdeva, 2014). Plants provide carbon sources like sugars, (Van Der Heijden, Bardgett and Van Straalen, 2008) while the actinomycetes act as decomposers, recycling nutrients by breaking down plant residues using enzymes such as cellulases and ligninases (McCarthy, 1987).

In addition to their roles in nutrient cycling, actinomycetes release various metabolites that influence plant growth and the surrounding microbial community. Some of these metabolites directly inhibit plant pathogens, such as *Fusarium oxysporum* and *Rhizoctonia solani*.

Furthermore, certain actinomycetes, such as the *Streptomyces* strain AgN23, produce galbonolides that supress both plant and fungal enzyme activity. This unique interaction prompts the plant to produce a defence compound called camalexin, which benefits the *Streptomyces* strain by suppressing competing fungi and bacteria, thereby promoting its own colonization (Nicolle *et al.*, 2024).

Actinomycetes function as biostimulants that promote plant growth by producing phytohormones including auxins and cytokinins. (Prashar, Kapoor and Sachdeva, 2014). For instance, a *Streptomyces* strain called *S. nobilis* WA-3, isolated from wheat, was found to produce indole acetic acid (IAA), which significantly increased the shoot length of wheat plants (Anwar, Ali and Sajid, 2016). Similarly, an endophytic *Streptomyces* strain from tomato, *Streptomyces sp.* DBT204, produced the phytohormones IAA and kinetin, improving the growth of both chili and tomato seedlings (Passari et al., 2016).

Actinomycetes also form beneficial relationships with certain insects. For example, Actinomycetes residing on the antennae of leaf cutter ants produce antimicrobial metabolites that selectively inhibit fungal pathogens, while preserving their fungal symbionts (Behie *et al.*, 2017). It was also found that spruce beetles use symbiotic bacteria to protect their galleries from harmful fungi. For example, spruce beetles excrete oral secretions containing bacteria to inhibit the growth of antagonistic fungal species. The strongest antifungal activity was attributed to the isolated non-*Streptomyces* actinomycete, *Micrococcus luteus,* revealing a symbiotic relationship that aids beetle colonization of their host trees (Cardoza, Klepzig and Raffa, 2006).

1.4 Isolation and growth of Actinomycetes

Many methods have been developed for selectively isolating and purifying Actinomycetes. Pre-treatment of samples, e.g. heat treatment, before plating has been effective in eliminating fast-growing Gram-negative bacteria, thereby enhancing the recovery of rare Actinomycete genera such as *Spirilliplanes*, *Actinomadura*, and *Microbispora* (Hayakawa *et al.*, 1991; Tamura, Hayakawa and Hatano, 1997).

Selective isolation media have been devised to specifically promote the growth of Actinomycetes, such as chitin medium, starch-casein medium, and humic acid-vitamin medium (El-Nakeeb and Lechevalier, 1963; Hayakawa and Nonomura, 1989; Williams and Wellington, 1982). Use of antifungal agents, such as cycloheximide and nystatin, enhances isolation efficiency by preventing the overgrowth of fast-growing fungi (Williams and Wellington, 1982). Additionally, a range of antibiotics have been successfully used to isolate specific groups of Actinomycetes, it seems, because organisms producing the antibiotic always carry cognate

resistance genes (Athalye, Lacey and Goodfellow, 1981; Thaker, Waglechner and Wright, 2014).

Beyond selective media, alternative strategies have been employed to isolate rare Actinomycetes. One such method involves plating on top of cellulose ester membrane filters (0.2 and 0.45 μm), through which Actinobacteria mycelia can penetrate, while restricting unwanted bacterial growth (Hirsch and Christensen, 1983). Another widely used technique is the rehydration and centrifugation (RC) method, which has been effective in isolating rare *Streptomyces* and non-*Streptomyces* strains, including *Micromonosporaceae* species (Hayakawa *et al.*, 2000). A sucrose-gradient centrifugation method has been employed specifically for isolating *Nocardia* species (Yamamura, Hayakawa and Iimura, 2003), while calcium carbonate supplementation, combined with the RC method, has been useful in recovering *Actinokineospora* strains (Otoguro *et al.*, 2001).

To address the challenge of isolating "unculturable" bacteria, the isolation chip (iChip) was developed to simulate natural environments. This device includes an agar membrane that traps bacterial cells from an environmental sample. The iChip is designed for return to the original soil environment, allowing bacterial growth to be supported by natural growth factors while preventing contamination, through its semipermeable barrier. The iChip trap version, which uses a 0.2 μm membrane, has further improved the isolation of novel Actinomycete species. (Nichols *et al.*, 2010; Lewis *et al.*, 2010). Additionally, a modified iChip method utilizing a Multiscreen® 96-well plate has been successfully employed to isolate Actinomycetes from beach sediment samples, demonstrating the potential of innovative techniques in microbial discovery (Dos Santos *et al.*, 2022).

1.5 Strategies for in situ activation of cryptic BGCs for discovery NPs

As mentioned earlier, under standard laboratory conditions, most Actinomycetes produce only a limited fraction of their potential NPs, suggesting that many biosynthetic pathways remain silent or weakly expressed. A wide range of methods have been employed in attempts to induce Actinomycetes and other organisms to express a wider range of NP's. Rutledge and Challis (2015) reviewed the field and defined two distinct types of method called pleiotropic and pathway-specific methods. Pleiotropic methods exert a global effect on cells, likely involving impacts on multiple regulatory networks, leading to the activation of more than one BGC. In

contrast, pathway-specific methods target single, identified BGC's (Rutledge and Challis, 2015). Some of these methods are discussed below.

Pleiotropic approaches

1.5.1 Media screening

A simple approach to access the products of cryptic BGCs is to vary the composition of the culture medium. Actinomycetes produce different metabolites depending on the growth medium. Carbon, nitrogen, and phosphorus sources significantly influence the production of NPs. A key regulatory mechanism in bacteria is carbon catabolite repression (CCR) regulation, where in the presence of multiple carbon sources, they preferentially consume one, often glucose, before switching to secondary sources once it is depleted. (Demain, 2020). Adjusting the concentration and timing of glucose supplementation has been shown to impact NP production. For example, natamycin production in *Streptomyces natalensis* was optimized through glucose feeding experiments (Elsayed, Farid and El-Enshasy, 2019). Similarly, nitrogen and phosphorus levels affect NP expression (Shapiro, 2020; Martín, 2004). High nitrogen concentrations often repress production, though some strains preferentially utilize amino acids or nitrate over ammonium salts (Shapiro, 2020). Also, phosphate depletion stimulates NP production although impairing the growth of Actinomycetes (Martín, 2004).

1.5.2 Co-culturing

Co-culturing is the process of growing two or more microbial populations together in the same culture medium. This approach mimics natural environments in which microbes coexist, communicate, and compete for limited resources (Li *et al.*, 2023; Goers, Freemont and Polizzi, 2014). Co-cultures provide a valuable platform for studying microbial interactions and ecological dynamics using model systems (Jessup *et al.*, 2004). Co-culturing has gained prominence in natural product discovery, primarily due to the hypothesis that microbes produce NPs in response to environmental interactions. Furthermore, this approach has the advantage that it does not require extensive genetic manipulation or prior whole-genome sequencing knowledge (Bertrand *et al.*, 2014; Moody, 2014).

Designing an effective co-culture experiment requires consideration of both biotic and abiotic factors. Biotic factors include strain selection, inoculum size, and culture age, all of which can influence the outcome (Selegato and Castro-Gamboa, 2023). For example, co-culturing two marine Actinomycetes, *Saccharomonospora* sp. UR22 and *Dietzia* sp. UR66, isolated from the same Red Sea sponge (*Callyspongia siphonella*), induced the production of two new compounds, saccharomonosporine and convolutamydine F (El-Hawary *et al.*, 2018). Similarly,

NP production in *Streptomyces noursei* was enhanced when co-cultured with *Penicillium rubens*, but only with a 48-hour (h) inoculation delay (Boruta, Ścigaczewska and Bizukojć, 2023).

Abiotic factors such as media composition, incubation duration, and temperature also play a crucial role in co-culture experiments (Selegato and Castro-Gamboa, 2023). For instance, the co-culture of marine a *Streptomyces* and *Bacillus mycoides* led to the production of algicidal compounds tryptamine and bacillamides. This study demonstrated that altering environmental and nutritional conditions, including medium composition, culture method, and pH, significantly influenced tryptamine production (Yu, Hu and Ma, 2015).

The effectiveness of co-culture experiments often depends on the level of microbial interaction (Selegato and Castro-Gamboa, 2023). The most common approach involves direct cell-to-cell contact, as seen in co-culture of *Actinokineospora* sp. EG49 and *Nocardiopsis* sp. RV163, which resulted in the production of three acetamide compounds (Dashti *et al.*, 2014). In another example, co-culturing of *S. coelicolor* and *Aspergillus niger* led to the discovery of two novel compounds (Wu *et al.*, 2015). Alternative methods involve using cell-free supernatants or autoclaved cultures of one the strains instead of live cells. A notable case is the discovery of hydrazine-containing specialized metabolites from *Streptomyces* RKBH-B178 when cultured in the presence of an autoclaved culture of *Mycobacterium smegmatis* (Liang *et al.*, 2019).

1.5.3 Use of chemical elicitors

Chemical elicitation involves the use of small molecules to stimulate NP synthesis. Numerous studies have demonstrated the effectiveness of various chemical elicitors in activating BGCs or enhancing the production of NPs.

Rare earth elements (REEs), such as lanthanum and scandium, have been shown to enhance NP synthesis. As an example, upon supplementation with low concentrations of scandium, 2-25 fold increases in the production of actinorhodin, actinomycin and streptomycin were observed in *S. coelicolor* A3(2), *S. antibioticus* and *S. griseus*, respectively (Kawai *et al.*, 2007). Similarly, it was shown that addition of lanthanum and scandium both enhanced actinorhodin production in *S. coelicolor* A3(2). Transcription analysis with quantitative polymerase chain reaction (qPCR) revealed the activation of 17 additional BGCs in response to scandium treatment (Tanaka, Hosaka and Ochi, 2010).

Common laboratory solvents such as dimethyl sulfoxide (DMSO) and ethanol have also been shown to induce production of NPs. Low concentrations (3%) of DMSO increased the production yields of chloramphenicol, tetracenomycin, and thiostrepton by 2-3 fold in *S.*

venezuelae ATCC1071, *S. glaucescens* and *S. azureus* ATCC14921, respectively (Chen, 2000). Likewise, addition of 6% ethanol at 6 and 13 h post-inoculation of *S. venezuelae* ISP5230 in a galactose-isoleucine-containing medium, led to the production of jadomycin B, a benzoxazolophenanthridine antibiotic (Doull, 1994).

Small molecules that inhibit fatty acid synthesis have also been shown to trigger NP synthesis. Supplementation of a class of fatty acid inhibitors called antibiotic-remodelling compounds (ARCs) in the growth media increased the production of desferrioxamine B and E by *S. pristinaespiralis* ATCC 25486, doxorubicin, baumycin, and three unknown molecules by *S. peucetius* 27952, and an unknown metabolite by *Kutzneria sp.* 744 (Craney, 2012). Further studies on ARCs revealed that they likely activate the regulatory proteins AfsS and AfsR in response to chemical stress, leading to enhanced NP production (Calvelo, 2021).

Other well studied chemical elicitors are gamma-butyrolactones (GBLs). GBLs act as bioregulators or signalling molecules in Actinomycetes, playing a crucial role in activating NP biosynthesis. Early examples included A-factor from *S. griseus* (Khokhlov, 1973) and virginiae butanolides A-C (VBs) which regulate virginiamycin (staphylomycin) production in *S. virginiae* (Yamada, 1987). The mechanism by which GBLs induce the production of NPs involves binding to TetR family transcriptional repressors (TFTRs) leading to conformational changes that release the repressor from DNA, thereby allowing transcription (Zhou, 2021).

Pathway-specific approaches

1.5.4 Promoter engineering

Inducing or enhancing the production of microbial NPs can also be achieved by incorporating strong and efficient promoters to drive gene expression. A prominent example is the *ermE* promoter (*ermEp*), derived from *Saccharopolyspora erythraea,* which drives expression of an erythromycin resistance gene (Bibb, Janssen and Ward, 1985). There are two separate promoters in *ermE* gene, *ermEp*1 and *ermEp*2. An enhanced variant, *ermEp**, was developed by introducing a trinucleotide deletion in *ermEp*1, resulting in increased promoter activity (Bibb *et al.*, 1994). Another widely used promoter is *tipA*, which originates from *S. lividans*. This promoter is inducible in the presence of the antibiotic thiostrepton. However, studies have revealed that the *tipA* gene is not universally present across all *Streptomyces* species (Takano *et al.*, 1995). In 1997, a new promoter, *SF14p*, was characterized from phage 119 of *S. ghanaensis*. *SF14p* consists of two individual phage promoters, 14-Ip and 14-IIp, with the latter exhibiting stronger activity. Remarkably, *SF14p* demonstrates activity comparable to that of *ermEp* (Labes, Bibb and Wohlleben, 1997). Then, in 2005, the *kasO* promoter (*kasOp*) was

isolated from *S. coelicolor*. This promoter is associated with the production of coelimycin and is regulated by two key transcription factors, ScbR and ScbR2 (Takano *et al.*, 2005). To improve its functionality, the *kasOp* was engineered to remove the binding sites for these regulators, resulting in *kasOp**, a variant found to be stronger than both *ermEp** and *SF14p* (Wang *et al.*, 2013). Building on this advancement, *kasOp** was further optimized by creating two libraries of synthetic *kasOp**-based promoters. This involved introducing random mutations in the regions downstream of the -10 sequence and between the -10 and -35 regions. From the 180 synthetic promoters generated, six displayed higher activities than *kasOp**, with SP43 and SP44 emerging as particularly effective variants (Bai *et al.*, 2015). These findings underscore the potential of engineering promoters to achieve enhanced expression of NP biosynthetic genes, paving the way for greater efficiency in NP discovery. These promoters, along with the recently discovered constitutive and synthetic promoters, can be incorporated into the genome of the *Streptomyces* host by homologous recombination or site-specific integration to promote overexpression of the product of interest (Wilkinson *et al.*, 2002).

1.5.5 Transcription factors regulation

Transcription factors (TFs) play a crucial role in regulating NP biosynthesis, often acting as pathway-specific regulators (PSRs) within BGCs. These TFs can function as either activators or repressors, controlling NP production through positive or negative regulation (Martín and Liras, 2010; Xia *et al.*, 2020). Modulating these TFs, either by overexpressing activators or inactivating repressors, has been a key strategy in optimizing NP yields (Martín and Liras, 2010). Most of these activators belong to the family of *Streptomyces* Activator Regulatory Proteins (SARPs). One example is the CcaR protein, which regulates cephamycin and clavulanic acid biosynthesis in *S. clavuligerus* by binding to its own promoter as well as to the bidirectional promoter region, *cefD-cmcI* (Santamarta *et al.*, 2002). Another common group of activators includes Large ATP-binding regulators of the LuxR (LAL) family, such as AveR, which controls avermectin biosynthesis in *S. avermitilis*. Deletion of *aveR* results in a loss of avermectin production, whereas its overexpression significantly increases yields (Guo *et al.*, 2010). Conversely, many negative regulators belong to the TetR (tetracycline repressor) family of transcriptional regulators (TFRs). For example, deletion of *papR3*, a repressor in *S. pristinaespiralis*, results in a 1.4-fold increase in pristamycin production (Meng *et al.*, 2017). Additionally, *wblA* genes, which encode WhiB-like transcription factors, have been widely reported to suppress NP biosynthesis in *Streptomyces*. In *S. venezuelae*, disruption of the *wblA*

gene leads to a 3.5-fold increase in pikromycin production, while its overexpression results in a 2.5-fold decrease (Woo *et al.*, 2014).

1.5.6 Ribosome and RNA polymerase engineering

Another strategy to enhance NP biosynthesis involves introducing antibiotic resistance mutations that affect transcription or protein synthesis and, in turn, for reasons that are not understood, pleiotropically affect secondary metabolism. Antibiotics that have been used for this purpose include gentamicin, streptomycin, thiostrepton, kanamycin, chloramphenicol, and lincomycin, which affect protein synthesis, and rifampicin, which acts on RNA polymerase (Ochi, 2007). For instance, gentamicin-, rifampicin-, and streptomycin-resistant mutants of *S. mauvecolor* have been shown to produce a novel compound, piperidamycin. These mutants had mutations in the *rpoB* or *rpsL* genes, leading to the upregulation of genes involved in piperidamycin biosynthesis (Hosaka *et al.*, 2009). Similarly, site directed mutagenesis generating specific missense mutations in *rpoB* and *rpsL* in *S. chattanoogensis* led to the production of a novel angucycline antibiotic, anthrachamycin (Li *et al.*, 2019b).

1.6 Strategies for cloning and heterologous expression of cryptic BGCs for discovery of NPs

Many of the pathway-specific methods discussed are limited to genetically tractable strains, leaving a significant portion of *Actinomycetes* unexplored. However, advances in genome sequencing and a deeper understanding of the biosynthetic machinery involved in microbial NP production have enabled the development of genomics-driven and pathway-targeted approaches for discovering novel NPs (Rutledge and Challis, 2015). The following strategies focus on isolating BGCs and expressing them heterologously in genetically amenable hosts, allowing for further optimization of expression levels, as well as functional dissection of the genes and associated proteins.

1.6.1 BGC cloning via genomic libraries

Genomic libraries consist of collections of cloned chromosomal DNA fragments. Their construction involves isolating and fragmenting genomic DNA, inserting the fragments into a vector, transferring into a suitable microbial host and recovering large numbers of independent recombinant clones (Figure 1.8). Dut to the large size of some BGCs (e.g. >100 kbp), the process first requires the isolation of intact high molecular weight (HMW) DNA. Problems of DNA fragmentation during extraction and handling, have largely been solved by recent advances in HMW DNA isolation methods such as embedding cells in low melting point agarose to avoid shearing of the DNA (Osoegawa *et al.*, 1998), PEG-mediated and freeze-

thawing strategy (Bey *et al.*, 2010) and the nuclei method, a method used to isolate DNA from eukaryotic nuclei (Zhang *et al.*, 2012). Preparation of the DNA fragments for cloning can be done in various ways, including complete or partial digestion with restriction endonucleases (Duke, Chervenak and Cohen, 1983) or physical methods, such as sonication (Deininger, 1983). DNA fragment ends can be processed to facilitate ligation with the vector. Then, the DNA can be size fractionated to the preferred size, which eliminates the smaller DNA fragments that would otherwise be preferentially cloned.

Library construction varies considerably in terms of the cloning vector, host strain and DNA manipulation methods. Some of the vectors used for microbial NP discovery are briefly discussed below.

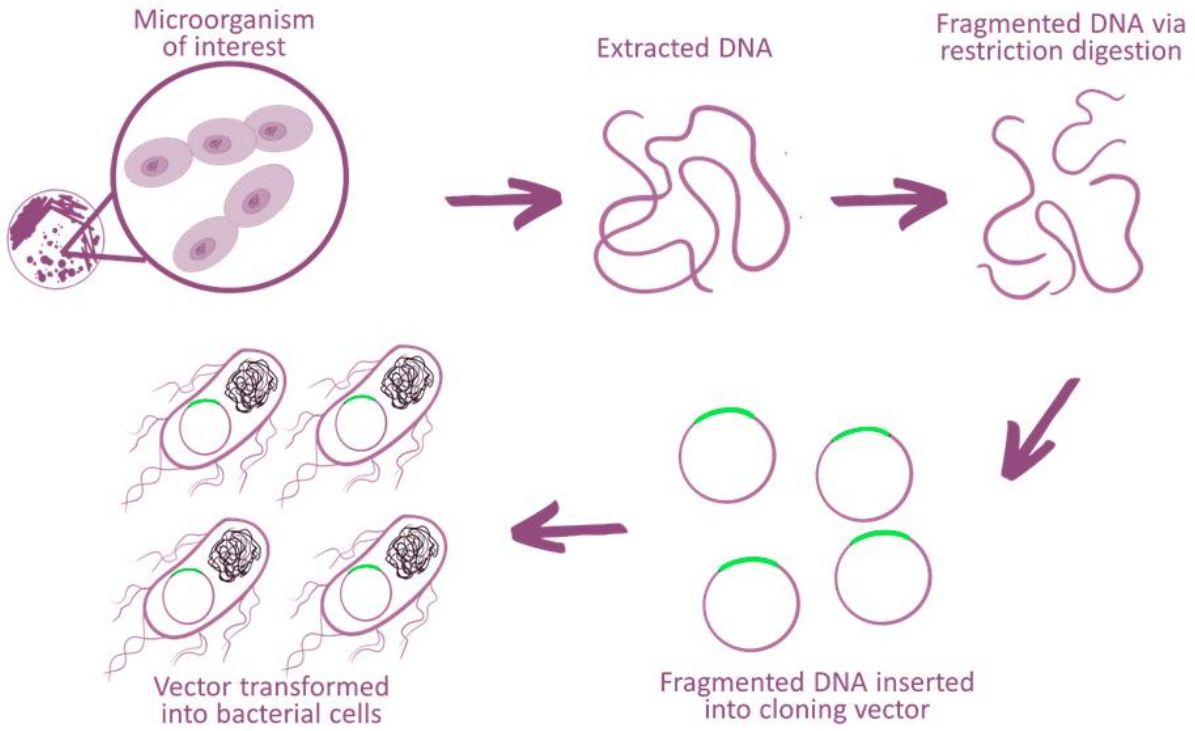

Figure 1.8 General overview of the gDNA library generation process.

Cosmids

Cosmid vectors contain a lambda *cos* DNA sequence enabling it to be packaged *in vitro* into bacteriophage lambda capsids, which can then infect *E. coli* cells with very high efficiency. Some cosmid vectors, however, have a high copy number, which can make the resulting plasmids unstable. In addition, this type of vector can only accommodate insert sizes of 50 kbp or less (Brenner and Miller, 2014), whereas BGCs from Actinomycetes are often >50 kbp and can extend to >100 kbp (Gomez-Escribano and Bibb, 2012). Examples of cosmid vectors

available are Supercos1 (Agilent), which was utilized for constructing a genomic DNA library for whole-genome sequencing of *S. coelicolor* (Gust *et al.*, 2003), pFD666, which was employed to clone a chitosanase-encoding gene from *Kitasatosporia* N174 (Denis and Brzezinski, 1992) and pTOYAMAcos, which is an integrative cosmid vector that was used to clone rebeccamycin from *Lechevalieria aerocolonigen*es (Onaka *et al.*, 2003).

Fosmids

Fosmid cloning vectors, such as pFOS1 (Kim *et al.*, 1992), are similar to cosmid vectors with regards to insert size but are derived from the *E. coli* F plasmid, which has a low copy number. Given that function, fosmids are more stable than cosmid vectors, which made them more efficient vectors for making DNA libraries from organisms with complex genomes such as Actinomycetes (Saraswathy and Ramalingam, 2011). The downside of such vectors is that the low copy number makes the derivative plasmids difficult to purify and characterise. Unfortunately, many BGCs encoding interesting NPs are too large to be cloned by lambda packaging. This problem was overcome when various vectors capable of accommodating much larger fragments of DNA were developed.

Bacterial artificial chromosome (BAC)

The first BAC vector, pBAC108L (Shizuya *et al.*, 1992), based on the F factor replication origin, was shown to accommodate inserts of up to 300 kbp. One example of using this approach to capture BGCs in Actinomycetes is the cloning of a 128 kbp segment of DNA from *S. roseosporus* NRRL11379 (Miao *et al.*, 2005). Genomic libraries of both genetically tractable and intractable strains can be made with BAC vectors.

P1-derived artificial chromosome (PACs)

PAC vectors have an origin of replication from *E. coli* phage P1, which replicates as a stable circular plasmid in lysogenised cells. Similar to the BAC vectors, PACs can accept large insert sizes with high level of structural and segregational stability due to its low copy number maintenance (Gomez-Escribano and Bibb, 2012). In recent years, probably the most common and effective Actinomycete library cloning has been done by the Canadian company BioS&T, using pESAC (*E. coli-Streptomyces* artificial chromosome) vectors first developed by Sosio et

al. (2000). These vectors have the advantage that they can also be conjugated into *Streptomyces* host strains and stably integrated into the host chromosome.

Yeast artificial chromosome (YACs)

YAC vectors are based on replication functions from budding yeast and can accommodate much larger inserts (up to 3000 kbp) in the host yeast cells; however, they are poor in terms of structural and segregational stability (Saraswathy and Ramalingam, 2011). YAC DNAs are frequently rearranged, or some portions are deleted. In addition, as for the low copy number bacterial vectors, it is difficult to obtain workable amounts of DNA from YACs (Brenner and Miller, 2014). Therefore, YAC vectors are probably the least preferred choice in cloning BGCs from Actinomycetes.

1.6.2 Direct BGC cloning methods

There are several established methods for the direct cloning and expression of BGCs, and while they vary in specific strategies, they generally follow a similar three-step workflow: (1) isolation of the target BGC, (2) capture of the BGC of interest, and (3) transfer into a heterologous host for expression (Figure 1.9). This section will focus on the first two steps. The final step, the BGC transfer to heterologous host, is commonly achieved through transformation or conjugation and is largely dependent on the chosen heterologous host, which will be discussed in the next section. Table 1.1 below summarizes commonly used direct capture methods for cloning BGCs from Actinomycetes, including their strategies for BGC isolation and capture, along with their respective advantages and disadvantages.

BGC isolation can be achieved either *in vivo* or *in vitro*. *In vivo* approaches such as psBAC and ISR involve the integration of genetic elements flanking the target BGC, facilitating homologous recombination to excise and capture the cluster within the host cell (Du *et al.*, 2015; Liu *et al.*, 2009). A more recent method, ACTIMOT, utilizes CRISPR technology to introduce targeted DNA breaks, enabling the release of the BGC *in vivo* (Xie *et al.*, 2024). *In vitro* methods, such as TAR cloning, CAPTURE, and CAT-FISHING, typically rely on either restriction enzyme digestion or CRISPR-Cas systems to process HMW gDNA for BGC isolation (Yamanaka *et al.*, 2014; Enghiad *et al.*, 2021; Liang *et al.*, 2022).

Similarly, BGC capture can also occur either *in vivo* or *in vitro*. Methods like TAR and CAT-FISHING employ homologous recombination in yeast or *E. coli*, enabling circularization of the capture vector with the target BGC within the cell (Yamanaka *et al.*, 2014; Liang *et al.*, 2022). In contrast, techniques such as DiPaC and ExoCET use high-fidelity (HiFi) DNA assembly or

T4 ligase, respectively, to circularize the BGC *in vitro* before transformation into *E. coli* (Greunke *et al.*, 2018; Yuan *et al.*, 2023).

Each of these approaches presents distinct advantages and limitations. For instance, methods like TAR, CATCH, CAT-FISHING, and ACTIMOT require highly specialized cloning vectors with flanking homology arms (Yamanaka *et al.*, 2014; Liang *et al.*, 2022; Xie *et al.*, 2024; Jiang *et al.*, 2015). PCR-dependent strategies such as DiPaC can be particularly challenging when working with Actinomycetes, due to their high GC content, which increases the risk of mutation or instability during amplification (Greunke *et al.*, 2018). Meanwhile, *in vivo* recombination methods like psBAC and ISR are limited to strains that are genetically tractable (Du *et al.*, 2015; Liu *et al.*, 2009).

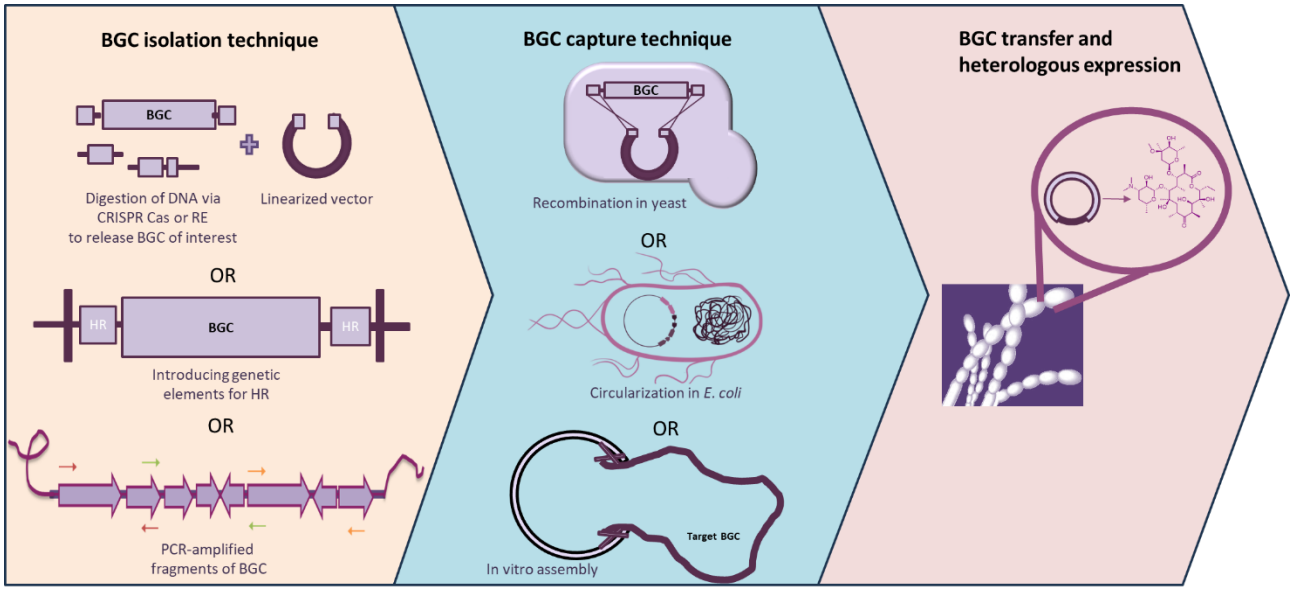

Figure 1.9 General workflow for direct BGC cloning approaches.

Table 1.1 Summary of direct BGC cloning methods and their associated advantages and disadvantages.

Method	BGC isolation technique	BGC capturing technique	Advantage	Disadvantage	BGC cloned/ Reference
psBAC- plasmid *Streptomyces* bacterial artificial chromosome	Unique restriction site and psBAC backbone are introduced on each end of BGC of interest	*In vivo*. Two consecutive homologous recombination events in the chromosome	Allows control over the length of the captured BGC without requiring prior DNA isolation	Only feasible with genetically tractable organisms; laborious	90 kbp meridamycin (Liu *et al.*, 2009)
ISR-integrase-mediated site-specific recombination	$attB_6$ and $attP_6$ sites are incorporated at each end of the target BGC	*In vivo*, introduction of an $int_{\phi BTI}$-bearing plasmid pIJ10500 for site-specific recombination between $attB_6$ and $attP_6$	Permits targeted capture of BGCs of defined lengths without DNA isolation	Only feasible with genetically tractable organisms; laborious	Actinorhodin, napsamycin and daptomycin (Du *et al.*, 2015)
DiPAC- Direct Pathways Cloning	BGC fragments are amplified via PCR using HiFi Taq Polymerase	*In vitro*, assembly of BGC fragments and capture vector is done via HiFi assembly technology and transform ligation product to *E. coli* host	Technically easier and rapid; allows refactoring of BGC	Prone to mutations and not applicable to large BGCs	Phenazine BGC and erythromycin (Greunke *et al.*, 2018)
TAR/TAR-CRISPR-Transformation-Associated Recombination	Homologous arm "hooks" on each end of the linearized TAR vector are used to capture the BGC from digested gDNA	*In vivo*, homologous recombination in yeast to circularize the capture plasmid and BGC of interest	Can be used to clone larger BGCs with high efficiency	Laborious process and needs yeast spheroplast transformation	Taromycin A (Yamanaka *et al.*, 2014); oxomilbemycins BGC (Li *et al.*, 2019a)
LLHR- RecET-linear-linear homologous recombination based approach	Linear capture vector with two homologous arms is used to capture BGC from digested gDNA	*In vivo*, homologous recombination in *E. coli* strain GB05-dir which carries an integrated RecET-Redγ system	Utilizes *E. coli* as cloning host	Recircularization of the empty vector results in empty clones	luminmycin A and luminmide A and B (Fu *et al.*, 2012)

ExoCET- Exonuclease combined with RecET combination	Linear capture vector with two homologous arms is used to capture BGC from digested gDNA	*In vitro,* annealing the linear capture vector and target BGC is achieved using T4 polymerase then transformed into an *E. coli* host	Utilizes *E. coli* as cloning host	Requires highly specialized vectors	142 kbp BGC from virus genome (Yuan *et al.*, 2023)
CAPTURE- Cas12a-assisted precise targeted cloning using *in vivo* Cre-*lox* recombination	Cas12a is used to introduce staggered cuts into gDNA to release the BGC, which is then assembled with PCR-amplified DNA receivers via a T4 DNA polymerase exo+ fill-in assembly strategy	*In vivo*, circularization is done via Cre-*lox* recombination with the aid of the helper plasmid pBE14 in *E. coli*	High cloning efficiency and can be applied to clone large BGCs	Involves several steps including purification of Cas12a and *in vitro* assembly of BGC and curing of the helper plasmid	Cloned 43 uncharacterized BGCs (Enghiad *et al.*, 2021)
ACTIMOT- Advanced Cas9-mediaTed *In vivo* MObilization and mulTiplication of BGCs	Directly nick and capturing the target BGC within the cell by employing the release plasmid (pRel) which includes a codon-optimized Cas9 gene, and a single-guide RNA (sgRNA) cassette	*In vivo*, capture plasmid, pCap, is introduced into the Actinomycete, to facilitate BGC relocation	Does not require genomic DNA isolation; can be used to relocate and amplify BGCs within the cell; can be used for BGC activation	Only applicable to genetically tractable Actinomycetes	Actimotins (Xie *et al.*, 2024)
CATCH- Cas9-assisted targeting of chromosomes segments	Cas9 protein is used to cut the HMW gDNA in a in an agarose plug	*In vitro*, target DNA fragment is ligated to a PCR-amplified vector via Gibson assembly then transformed into an *E.coli* host	Employs Cas9-mediated precise cleavage to isolate the BGC	Exhibits low efficiency in cloning fragments bigger than 100 kbp; does require purification of Cas9 protein and requires purification of HMW gDNA in an agarose plug	Jadomycin (Jiang *et al.*, 2015)

In vitro λ packaging mediated cloning	Cas9 protein is used to digest HMW gDNA	*In vitro*, digested gDNA is ligated to *Eco*RV-linearized pJTU2554. Ligation product was then in vitro packaged into phage particles to transfect *E. coli*	Takes advantage of Cas9-mediated precise cleavage to isolate the BGC	*In vitro* λ packaging system is limited to 50 kbp BGCs which is below the size of many BGCs from Actinomycetes	Tü3010 and sisomicin (Tao *et al.*, 2019)
CAT-Fishing-CRISPR/Cas12a-and Agarose plug-based sysTem for Fast bIoSyntHetIc geNe cluster cloninG	Cas12a is used to digest the HMW gDNA to generate sticky ends	*In vitro*, Cas12-digested gDNA is ligated into a Cas12-digested capture vector using a ligase enzyme, followed by transformation into *E. coli*.	Cost-effective and employs Cas12-mediated precise cleavage to isolate the BGC	Low efficiency that can be improved if HMW gDNA is isolated in agarose plugs. Requires purification of Cas12 protein	110 kbp gene for a cryptic polyketide (Liang *et al.*, 2022)

1.6.3 Gene transfer from E. coli to Streptomyces

Transformation

Transformation refers to the direct uptake of DNA from the surrounding environment (Bibb, Ward and Hopwood, 1978). In *Streptomyces*, two commonly employed transformation methods are polyethylene glycol (PEG)-mediated protoplast transformation and electroporation. Protoplast transformation involves enzymatically removing the cell wall, typically with lysozyme, followed by the introduction of DNA in the presence of PEG. The resulting transformants are plated on regeneration medium, and antibiotic selection is applied by overlaying with the appropriate antibiotic (Bibb, Ward and Hopwood, 1978). Electroporation, by contrast, involves exposing a mixture of cells and DNA to a short, high-voltage electrical pulse, which creates temporary pores in the cell membrane through which DNA can enter (Pigac and Schrempf, 1995). This method can be applied to both protoplasts (Pigac and Schrempf, 1995) and intact cells (Mazy-Servais, Baczkowski and Dusart, 1997).

Conjugation

Bacterial conjugation is the process of transferring genes between donor and recipient organisms, involving direct cell-cell contact. Donor cells, in most cases have a conjugative plasmid, which encodes all of the proteins needed for interactions with a recipient cell, often involving synthesis of a pilus, and factors needed for gene transfer (Curtiss III, 1969; Grohmann, Muth and Espinosa, 2003). Another key element is the *oriT* (origin of transfer) sequence, which is the target for initiation of the DNA transfer process. The *E. coli-Streptomyces* shuttle vectors often utilise the conjugation system from plasmid RP4, or the closely related plasmid RK2, that can be either transferable or non-transferable (depending on the presence/ absence of *oriT*), and the *tra* genes which are responsible for gene transfer (Simon, Priefer and Pühler, 1983). Shuttle plasmids with an *oriT* sequence can be "mobilised" by the conjugative plasmid and thereby transferred into the *Streptomyces* host. Within *Streptomyces*, the shuttle plasmids are maintained either by self-replication, or by integration into the host chromosome. The site-specific integration system of *Streptomyces* phage ϕC31 has been used extensively (Kuhstoss and Rao, 1991; Thorpe, Wilson and Smith, 2000). This process requires the presence of an *attB* site in the *Streptomyces* chromosome and its corresponding *attP* sequence in the vector, as well as the *int* gene, encoding the integrase enzyme. Integration of large BGCs at this site does not seem to have an effect on growth or sporulation of the host strain (Gomez-Escribano and Bibb, 2012).

Some *Streptomyces* hosts, importantly including *S. coelicolor*, have a restriction system against methylated DNA (González-Cerón, Miranda-Olivares and Servín-González, 2009). This is

problematic for conjugation of genomic libraries since they are usually prepared in DNA-methylating strains like *E. coli* DH10β. To tackle this, a methylation-deficient *E. coli* strain ET12567 was developed for conjugation in *Streptomyces*. *E. coli* ET12567 is not a suitable primary cloning host because of its low transformation efficiency (Gomez-Escribano and Bibb, 2011). To get around this, a tri-parental mating method was developed (Kieser *et al.*, 2000). An efficient *E. coli* host carrying the cloning vector with the target BGC is mixed with *E. coli* ET12567 typically containing the non-transmissible driver plasmid pUZ8002, which carries RK2-derived gene transfer functions (Figure 1.10)

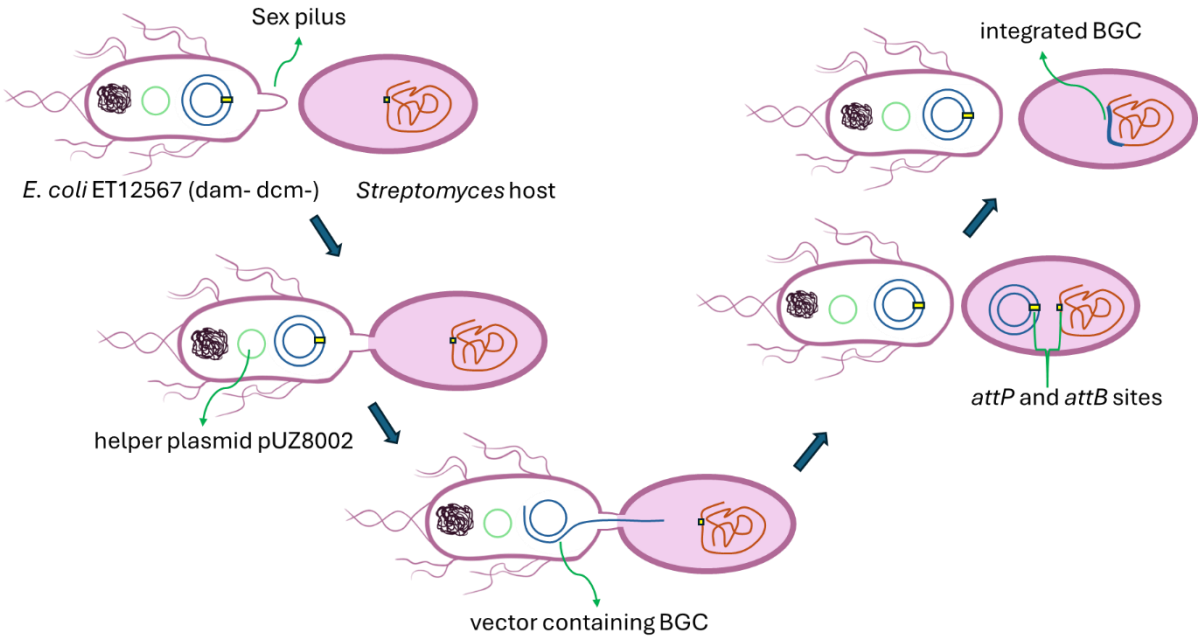

Figure 1.10 Conjugation in *Streptomyces* via dam⁻ and dcm⁻ *E. coli* ET12567 with helper plasmid pUZ8002.

1.6.4 Heterologous expression of BGCs in Streptomyces host strains

Transferring a BGC into a *Streptomyces* host does not necessarily ensure successful production of the corresponding NP. In a review summarizing successful expression of 90 NPs in a heterologous host (Nah *et al.*, 2017), it was reported that 83% of the BGCs had been cloned in an integrative vector by generation of a DNA library. Among the 90 targeted NPs, 60% were efficiently integrated into the host genome, while 37% remained self-replicative. Most BGCs were introduced into well-studied *Streptomyces* strains such as *S. coelicolor*, *S. lividans*, and *S. albus* with the latter used in approximately 12% of the cases. However, the expression levels of these compounds varied significantly. Only 14% of the NPs showed enhanced production in the heterologous host compared to their native strains, while 12% exhibited reduced yields. The

remaining studies did not provide comparative data. These findings underscore that efficient expression remains a major bottleneck in heterologous NP discovery. Several factors can influence this outcome, including the compatibility of the heterologous host, availability of necessary biosynthetic precursors, and the presence of regulatory elements like strong promoters (Bibb, Janssen and Ward, 1985).

Streptomyces *expression host*

One critical factor is the choice of expression host. There are several important considerations in choosing a *Streptomyces* host. First, the strain should be amenable to genetic manipulation and easily manipulated by conjugation or transformation. Second, it should possess regulatory mechanisms that will promote the expression of introduced BGCs. Third, the host should be able to provide sufficient precursors for biosynthesis of the BGC product (Kang and Kim, 2021).

Several *Streptomyces* strains, particularly *S. albus*, *S. coelicolor* and *S. lividans*, have commonly been used as expression hosts for NP synthesis (Myronovskyi and Luzhetskyy, 2019; Baltz, 2010; Kang and Kim, 2021). *S. coelicolor* is an excellent host because of its well characterized genetic system and ability to produce various kinds of NPs (Hopwood, 1967; Gomez-Escribano and Bibb, 2011). *S. lividans* is closely related to *S. coelicolor*, as both strains share a common ancestor, *S. violaceoruber* (Hatano, Tamura and Nishii, 1994; Duangmal, Ward and Goodfellow, 2005). *S. lividans* has an advantage over *S. coelicolor* in its ability to accept methylated DNA (Kieser *et al.*, 1982). Although closely related, these strains can behave differently as expression hosts (Baltz, 2010). For example, novobiocin was expressed both in *S. coelicolor* M152 and *S. lividans* TK24 but the yields were 31 mg/L and less than 1 mg/L respectively (Eustáquio *et al.*, 2005). Meanwhile, *S. lividans* 1326 is the preferred host for synthesis of capreomycin (Felnagle *et al.*, 2007) and viomycin (Barkei *et al.*, 2009). *S. albus* has a smaller genome than the first two hosts and is also a robust expression host. For example, synthesis of iso-migrastatin was found to be highest in *S. albus* J1074 (46 mg/L), followed by *S. lividans* K4-112 (25 mg/L), then *S. coelicolor* M1152 (23 mg/L), and least in *S. avermitilis* SUKA5 (4.2 mg/L) (Feng *et al.*, 2009). Similarly, expression of the fredericamycin BGC yielded almost 132 mg/L in *S. albus* J1074, while no production was detected in *S. lividans* K4-114 (Chen, Wendt-Pienkowski and Shen, 2008).

Selecting an appropriate host for expressing a target BGC often requires a trial-and-error approach, making the possession of a diverse set of potential host strains advantageous. For example, there are claims that NRPS and RiPP BGCs are suitable for expression in *S. lividans*

while PKSs are produced at higher levels in *S. albus* and *S. coelicolor* (Myronovskyi and Luzhetskyy, 2019).

A current strategy in the field involves engineering streamlined, genome-minimized strains or introducing targeted mutations to enhance NP production. Deletion of endogenous BGCs not only reduces background metabolite noise but also minimizes competition for precursors, thus improving detection of the desired products. This has led to the development of engineered strains like *S. lividans* YA10 (Ahmed *et al.*, 2020), K4-114 (Ziermann and Betlach, 1999) and *S. albus* Del1-14 (Myronovskyi *et al.*, 2018). As described above, mutations in the *rpoB* and *rpsL* genes (Ochi and Hosaka, 2013) lead to enhanced NP production and have been incorporated into *S. coelicolor* expression strains M1152 and M1154 (Gomez-Escribano and Bibb, 2011). In general, the deletions and mutations introduced into expression strains do not seem to have affected growth or sporulation, which supports both long term strain preservation and efficient genetic manipulation (Gomez-Escribano and Bibb, 2011). Table 1.2 outlines commonly used *Streptomyces* expression hosts and summarizes their genetic modifications aimed at improving NP biosynthesis.

Table 1.2 Summary of commonly used *Streptomyces* expression hosts.

Expression host	Parent strain	Genetic manipulation	Remarks	BGC cloned/ Reference
S. coelicolor				
S. coelicolor M1146 (Gomez-Escribano and Bibb, 2011)	*S. coelicolor* M145	Deletion of 4 BGCs: actinorhodin, prodiginines, calcium-dependent antibiotic (CDA) and CPK	Deletion of the 4 clusters eliminated competition for precursors. Deletions also simplified the chromatography, enhancing the detection of weakly produced metabolites. *S. coelicolor* can have issues accepting methylated DNA.	streptophenazines (Bauman *et al.*, 2019)
S. coelicolor M1152 (Gomez-Escribano and Bibb, 2011)	*S. coelicolor* M1146	point mutations in the RNA polymerase *β* (*rpoB)*	Generally, enhance the production of NPs	indolocarbazole (ICZ) from *S. sanyensis* (Li *et al.*, 2013); Thiolactomycin (Tang *et al.*, 2015)
S. coelicolor M1154 (Gomez-Escribano and Bibb, 2011)		point mutations in the *rpoB* and *rpsL* (ribosomal protein S12)		hibarimicins (Liu *et al.*, 2024)
S. lividans				
S. lividans 1326	Original strain also known as *S. lividans* 66		Can take methylated DNA Loss of SLP2 and SLP3 has been associated with a reduction in chromosomal recombination.	capreomycin (Felnagle *et al.*, 2007); viomycin (Barkei *et al.*, 2009)
S. lividans TK24 (Kieser *et al.*, 1982)	*S. lividans* 1326	streptomycin-resistant derivative of *S. lividans* 1326, via multiple rounds of protoplasting and		tuberactinomycin and viomycin for biosynthetic studies (Barkei *et al.*, 2009)

		regeneration, resulting in the loss of autonomous plasmids, SLP2 and SLP3		
S. lividans K4-114 and *S. lividans* K4-155 (Ziermann and Betlach, 1999)	*S. lividans* TK24	Removal of the actinorhodin biosynthetic cluster. *S. lividans* K4-114 and K4-155 and genetically identical. Strain K4-155 is a clone obtained using suicide vector.	Enhanced NP production due to elimination of competition for precursor molecules	platencins (Smanski *et al.*, 2012)
S. lividans ΔYA9, ΔYA10 and ΔYA11 (Ahmed *et al.*, 2020)	*S. lividans* TK24	Strain ΔYA9- with 9 deleted clusters and 1 native *attB* site Strain ΔYA10 – 10 deleted clusters and 2 *attB* sites Strain ΔYA11- 11 deleted clusters and 3 *attB* sites	Deletion of 9-11 BGCs gave a cleaner metabolic background, and the additional *attB* sites enable accommodation of extra copies of the BGC, potentially giving a higher NP yield. Strain ΔYA9 has a higher conjugation efficiency than the other two.	curacozole derivatives (Hollands *et al.*, 2024)
S. albus				
S. albus J1074 (Chater and Wilde, 1976)	*S. albus* G	Loss of its *SalI* restriction enzyme system	Facilitating the recovery of recombinant plasmids containing *Sal*I sites	antitumor steffimycin (Gullón *et al.*, 2006); spinosad (Tan *et al.*, 2017)
S. albus Del14 (Myronovskyi *et al.*, 2018).	*S. albus* J1074	15 clusters were removed	Mainly to facilitate heterologous expression by providing a cleaner metabolite background for easy compound detection and higher production yields	fralnimycin (Myronovskyi *et al.*, 2018); nybomycin (Rodríguez Estévez *et al.*, 2018)
S. albus B2P1, B3P1	*S. albus* Del14	strain B2P1- one additional *attB* site	Having extra *attB* sites enables accommodation of extra copies	didesmethylmensacarcin, griseorhodin A,

and B4 (Myronovskyi *et al.*, 2018).		strain B3P1- two additional *attB* sites strain B4- four canonical *attB* sites	of the BGC, potentially giving a higher NP yield	aloesaponarin II, cinnamycin and didemethoxyaranciamycinone (Myronovskyi *et al.*, 2018).

1.7 Project aims

Overall, this study aimed at identifying and characterizing novel bioactive compounds from Actinomycetes, using molecular and chemical approaches, and screening the compounds for antimicrobial activity. Then to investigate their biosynthesis and, for antimicrobial compounds, determine their mode of action.

The first main aim was to develop an efficient cloning strategy for capturing BGCs responsible for producing novel compounds and to enable heterologous expression in a suitable host.

The second main aim was to employ chemical elicitation strategies to induce NP production by activating cryptic biosynthetic pathways.

The final aim was to use molecular genetics to verify the identities of BGCs postulated to be responsible for the production of novel antibiotics, thereby providing insights into the biosynthetic mechanisms underlying natural product synthesis.

Chapter 2: Materials and Methods

2.1 Microbial culture conditions and maintenance

Various culture media were used for NP production by Actinomycetes. Depending on the strain growth and production of the target metabolites, either liquid or solid YEME, ISP2, GYM or R2YE media were used (Table 2.1). Cultures were incubated at 30 °C for 7-10 days depending on the strain's growth phase. Liquid cultures were shaken at 180 rpm.

To prepare gDNA of Actinomycetes, strains were grown in Yeast Extract Malt Extract (YEME) medium for 2-3 days in a shaking incubator at 30 °C. To obtain dispersed cell growth, baffled Erlenmeyer flasks were used, sometimes with addition of 10% (v/v) glycine to the medium.

Actinomycetes were maintained on YEME agar at room temperature for 2-3 weeks. For long-term storage, glycerol stocks were prepared. Typically, strains were grown in Mannitol Soy flour (MS) medium (Table 2.1) for sporulation, and spores were harvested after 3-4 days by adding sterile water and then scraping them with a sterile loop. The spores were collected in a sterile 50 mL centrifuge tube, vortexed, and filtered using a syringe with sterile non-absorbent cotton. The filtered spores were centrifuged and resuspended in 1-2 mL of 25% (v/v) glycerol (depending on the pellet size) in sterile cryotubes, which were stored at -80°C.

Liquid Luria Bertani (LB) medium (Table 2.1) was used for *Escherichia coli*, *Bacillus subtilis*, and *Staphylococcus aureus* cultures incubated at 37 °C. *Cryptococcus neoformans* and *Candida albicans* were cultured in liquid Yeast Peptone Dextrose (YPD) medium (Table 2.1) incubated at 30 °C on a shaking incubator. For solid cultures, *E. coli*, *B. subtilis*, and *S. aureus* were grown on Nutrient agar (NA), and *C. neoformans* and *C. albicans* were grown on YPD agar. The agar plates were incubated overnight at either 37 °C for bacteria or 30 °C for yeasts. For long-term storage, glycerol stocks were prepared by growing the strains overnight in liquid culture, then mixing 750 µL of the culture with an equal volume of 50% (v/v) glycerol in cryotubes. Glycerol stocks were stored at -80°C.

The following antibiotics and supplements were incorporated into either liquid or solid culture media, as applicable (Table 2.2).

Table 2.1 Culture media recipes.

Yeast- extract malt-extract (YEME)	Per L: 3g Yeast extract 3g Malt extract 5g Peptone 10g glucose 20g agar (for solid)

Luria-Bertani (LB)	Per L: 10 g Tryptone 5 g Yeast Extract 10 g NaCl pH 7.0
Nutrient agar (NA)	Per 1 L: 28 g Nutrient Agar
YPD	Per 1 L: 20 g of Peptone 10 g of yeast extract 20 g of Glucose
ISP2	Per 1 L: 4 g Yeast extract 10 g Malt extract 4 g Glucose 20 g Agar
GYM	4 g Glucose 4 g Yeast extract 10 g Malt extract 2 g CaCO3 20 g Agar
Mannitol Soy (MS) agar	Per 400 mL: 8 g Soy Flour 8 g Mannitol 8 g Agar
R2YE	Per L: 103 g sucrose 0.25 g K_2SO_4 10.12 $MgCL_2.6H_2O$ 10 g glucose 0.1 g casaminoacids 5 g yeast extract 3 g proline 3 g $CaCl_2.2H_2O$

Table 2.2. List of antibiotic and media supplements.

Antibiotic/supplement	Stock concentration	Final concentration

Apramycin (Apr)	50 mg/mL	*E. coli* 50 µg/mL Actinomycetes 50 µg/mL For overlaying after conjugation on Actinomycetes 30 µg/mL
Kanamycin (Kan)	20 mg/mL	*E. coli* 20 µg/mL
Chloramphenicol (Cat)	35 mg/mL	*E. coli* 10 µg/mL
Nalidixic acid (Nal)	30 mg/mL	Overlaying 20 µg/mL
X-gal	20 mg/mL	*E. coli* 8 µg/mL
IPTG	1 M	*E. coli* 200 µM
Arabinose	1000 X	BAC replicator cells 1X
Glycine	10 % (v/v)	Actinomycetes 0.5% (v/v)
$MgCl_2$	1 M	100 mM

2.2 Strains, plasmids and primers

Strains, plasmids and primers which were used or generated in this work are shown in Tables 2.3, 2.4 and 2.5.

Table 2.3 Strains used and generated in this study.

Name	Genotype/comment	Reference or commercial source
E. coli DH10β	F– *mcrA* Δ(*mrr-hsdRMS-mcrBC*) φ80*lacZ*ΔM15 Δ*lacX74 recA1 endA1 araD139* Δ (*ara-leu*)7697 *galU galK* λ– *rpsL*(Str^R) *nupG*	(Grant *et al.*, 1990)
E. coli ET12567 [pUZ8002]	F- dam-13::Tn9 dcm-6 hsdM hsdR zjj-202::Tn10 recF143 galK2 galT22 ara-14 lacY1 xyl-5 leuB6 thi-1 tonA31 rpsL136 hisG4 tsx-78 mtl-1 glnV44	(Kieser *et al.*, 2000)
E. coli BAC replicator cells	F - *mcr*A Δ(*mrr-hsd*RMS-*mcr*BC) *end*A1 *rec*A1 Φ80d*lac*ZΔM15 Δ*lac*X74 *ara*D139 Δ(*ara, leu*)7697 *gal*U *gal*K *rps*L *nup*G λ- *ton*A (StrR)	Lucigen
Steptomyces lividans 1326	Wild type (WT)	(Kieser *et al.*, 1982)
Streptomyces coelicolor M1152	With *rpoβ* point mutations	(Gomez-Escribano and Bibb, 2011)
Streptomyces albus J1074	Lack of *Sal*I restriction system	(Chater and Wilde, 1976)
Streptomyces lividans YA10	10 cluster deleted from *S. lividans* TK24	(Ahmed *et al.*, 2020)

Streptomyces albus Del14	14 clusters deleted on *S. albus* J1074	(Myronovskyi *et al.*, 2018)
S. albus J1074 (pJE-2)	*S. albus* J1074 with empty pJE-2	This work
S. albus J1074 (pJE2-4G5)	*S. albus* J1074 with clone pJE2-4G5	This work
S. albus Del14 (pJE-2)	*S. albus* Del14 with empty pJE-2	This work
S. lividans YA10 (pJE-2)	*S. lividans* YA10 with empty pJE-2	This work
S. albus Del14 (pJE2-4G5)	*S. albus* Del14 with clone pJE2-4G5	This work
S. lividans YA10 (pJE2-4G5)	*S. lividans* YA10 with clone pJE2-4G5	This work
S. albus Del14 (pJE2-1D1)	*S. albus* Del14 with clone pJE2-1D1	This work
S. lividans YA10 (pJE2-1D1)	*S. lividans* YA10 with clone pJE2-1D1	This work
S. albus Del14 (pJE2-1G12)	*S. albus* Del14 with clone pJE2-1G12	This work
S. lividans YA10 (pJE2-1G12)	*S. lividans* YA10 with clone pJE2-1G12	This work
S. lividans YA10 (pJE2-1G9)	*S. lividans* YA10 with clone pJE2-1G9	This work
Streptomyces strain DEM21308	Demurilactone producing strain	(Dashti *et al.*, 2022)
Streptomyces strain DEM21308-Ω*dmlE*	*Streptomyces* strain DEM21308 with insertional mutagenesis on *dmlE*	This work
Actinokineospora UTMC 2248	Persiathiacin producing strain	(Dashti *et al.*, 2024)
Actinokineospora UTMC 2248-*perX*	*Actinokineospora* UTMC 2248 with insertional mutagenesis on *perX*	This work
Streptomyces strain PR3G	Quinovosamycin 4 producing strain	(Sumang, Errington and Dashti, 2025)
Streptomyces strain PR3G_*quiQ*	*Streptomyces* strain PR3G with insertional mutagenesis on *quiQ*	This work

Table 2.4 Plasmids used or generated in this study.

Name	Comment	Reference or construction details
pSET152	*aac(3)-IV, intC31, attP, traJ*	(Bierman *et al.*, 1992)
pSMART-BAC	*cmr, sopABC, ori2, oriV*	Lucigen
pJE-1	*aac(3)-I*, sopABC, ori2, oriV, intC31, attP, traJ*, *Xho*I cloning site	This work, Gibson assembly
pJE-2	*aac(3)-IV, sopABC, ori2, oriV, intC31, attP, traJ, Bam*HI cloning site	This work, Gibson assembly
pJE2-4G5	pJE-2 with 120 kbp 4G5 clone with whole region 5 (BGC for sulphated compound)	This work, BAC library
pJE2-4F3	pJE-2 with 100 kbp 4F3 clone with partial region 5 (BGC for sulphated compound)	This work, BAC library
pJE2-1D1	pJE-2 with 124 kbp 1D1 clone with whole region 4	This work, BAC library
pJE2-1G12	pJE-2 with 63 kbp 1G12 clone with whole region 7	This work, BAC library
pJE2-1G9	pJE-2 with 118 kbp 1G9 clone with whole region 27	This work, BAC library

pET28a T7pCONS TIR-1 sfGFP	pET28a with a T7 promoter fixed and a synthetically evolved translation initiation region (TIR)	(Shilling *et al.*, 2020)
pSET-*dmlE*	pSET with *dmlE* fragment used for insertional mutagenesis to disrupt *dml* cluster	This work, Gibson assembly
pSET-*perX*	pSET with *perX* fragment used for insertional mutagenesis to disrupt *per* cluster	This work, Gibson assembly
pSET-*quiQ*	pSET with *quiQ* fragment used for insertional mutagenesis to disrupt *qui* cluster	This work, Gibson assembly

aac(3)-IV, apramycin-resistance gene
intC31, phiC31 integrase gene
attP, phiC31 attachment site
traJ, transfer of genes
cmr, chloramphenicol resistance gene
sopABC, plasmid partitioning genes in F plasmid
ori2, (or *oriS*), single-copy origin of replication
oriV, high-copy origin of replication

Table 2.5 Primers and other synthesized oligonucleotides used in this study.

Primer name	Sequence (5' to 3')	Comment
pSET-152_pJE-F	GCCTTTCGTTTTAGGTTCATGTGCAGCTCCATC	For creating pJE
pSET-152_pJE-R	CAAGTGTGTCGCTCAGGCTTCCCGGGTGTCT	For creating pJE
pSMART-pJE-F	CCGGGAAGCCTGAGCGACACACTTGCATCG	For creating pJE
pSMART-pJE-R	AATCGATGTCGACCACACTGGCTCACCTTCG	For creating pJE
I-SceITer-F	TGAGCCAGTGTGGTCGACATCGATTAGGGATAACA GGGTAATCAAATAAAACGAAAGGCTCAGTCGAAAG ACTGGGCCTTTCGTTTTA	Synthesized terminator and I-*Sce*I site
I-SceITer-R	TGCACATGAACCTAAAACGAAAGGCCCAGTCTTTC GACTGAGCCTTTCGTTTTATTTGATTACCCTGTTATC CCTAATCGATGTCGAC	
pJE-SalI-XhoI-F	GGTACGCGTCGATTATCTTGAGAATGACCACTGCTG TGAGC	Direct site mutagenesis for changing *Sal*I site to *Xho*I in pJE1
pJE-SalI-XhoI-R	GCTCACAGCAGTGGTCATTCTCAAGATAATCGACGC GTACC 5	
pJE-BamHI-F	CGAAGGTGAGCCAGTGTGGGATCCATCGATTAGGG ATAACAGG	Direct site mutagenesis for changing *Xho*I site of pJE-1 to *Bam*HI (pJE-2)
pJE-BamHI-R	CCTGTTATCCCTAATCGATGGATCCCACACTGGCTC ACCTTCG	
Validation clone F	CGTTCTGTCCGTCACTTCC	For structure validation of clones in pJE vector via sequencing
Validation clone R	CGGTGGTGATAAACTTATCATC	

Sulfo-screen-F	GACCGCGTGGACGGAGCCGT	For screening sulfotransferase gene in gDNA library of T576
Sulfo-screen-R	CCGTATCGACCTGGGCTCGT	
Region 2 F	GAGGACATCCATCCGC	For screening region 2 in gDNA library of T576
Region 2R	CTCGTACTCCAGGGC	
Region 4 F	AGGACATCCTCCCGC	For screening region 4 in gDNA library of T576
Region 4 R	GCTCGTGGACACCGT	
Region 7 F	CGCTGCGACGGTCTG	For screening region 7 in gDNA library of T576
Region 7 R	GAGGGCGGTCACGAC	
Region 14 F	GATCAAGGACCTCGCC	For screening region 14 in gDNA library of T576
Region 14 R	GTGTCGGTGGTGTAC	
Region 24 F	GTGGCGATCACCGGG	For screening region 24 in gDNA library of T576
Region 24 R	ACCGGGAGCCGGTAG	
Region 25 F	ATGACGCGCCAGGAG	For screening region 25 in gDNA library of T576
Region 25 R	GCCGAGTTGTGGCCG	
Region 27 F	TCAGGGCTCAGTCCG	For screening region 27 in gDNA library of T576
Region 27 R	GATGAACGTCGCCGC	
Region 28 F	TGCTGGTGACGCTCG	For screening region 28 in gDNA library of T576
Region 28 R	GCCGGTTCGACGCAG	
Region 29 F	CTACTCGCCCCAGCG	For screening region 29 in gDNA library of T576
Region 29 R	GCACGCGGAGCTGGA	
pSET-dmlE-F	CTGGTACCAGAACCTGCGCACGAGACACCCGGGAAGCCTG	For assembly of pSET-*dmlE*
pSET-dmlE-R	AGCGCTTCCCAGGAGATCTCAGCTTGCATGCCTGCAGGTC	
dmlE-pSET-F	GACCTGCAGGCATGCAAGCTGAGATCTCCTGGGAAGCGCT	
dmlE-pSET-R	CAGGCTTCCCGGGTGTCTCGTGCGCAGGTTCTGGTACCAG	
check1-dmlE-F	GACCTGGACGGGCGCTAC	Verify insertion and position of pSET-*dmlE* to *Streptomyces* 21308-dmlE
check1-dmlE-R	CTCTAGAGTCGACCTGCAGC	
check2-dmlE-F	GCCAGGTGCGAATAAGGGAC	
check2-dmlE-R	GCCGTCTCCTCCAGCCAGAA	

UTMC-perX-F	GACCTGCAGGCATGCAAGCTGAGTTCTACCGCGACCCGCA	For assembly of pSET-*perX*
UTMC-perX-R	CAGGCTTCCCGGGTGTCTCGCCGGAAGAACGACCGGAACG	
pSET-perX-F	CGTTCCGGTCGTTCTTCCGGCGAGACACCCGGGAAGCCTG	
pSET-perX-R	TGCGGGTCGCGGTAGAACTCAGCTTGCATGCCTGCAGGTC	
PR3G-quiQ-F	GACCTGCAGGCATGCAAGCTCTGCAGCGTCTCGGCCATGC	For assembly of pSET-*quiQ*
PR3G-quiQ-R	CAGGCTTCCCGGGTGTCTCGCAGGGTGAGGAGGCGTCGCG	
pSET-quiQ-F	CGCGACGCCTCCTCACCCTGCGAGACACCCGGGAAGCCTG	
pSET-quiQ-R	GCATGGCCGAGACGCTGCAGAGCTTGCATGCCTGCAGGTC	

2.3 Molecular biology procedures

2.3.1 Plasmid DNA (pDNA) miniprep

E. coli plasmids were prepared by inoculating a single colony into 10 mL LB supplemented with appropriate antibiotic and grown overnight at 37 °C in a shaking incubator. The cultures were then centrifuged (16 x g for 10 min in an Eppendorf microcentrifuge) and the cell pellet was used for plasmid isolation using a QIAprep Spin Miniprep Kit from Qiagen following the manufacturer's protocol. To obtain more concentrated pDNA for follow up studies, 30 µL of deionized (DI) water (20 µL if the plasmid is a low copy number) was used for the final elution.

2.3.2 Genomic DNA isolation

To prepare gDNA, strains were grown in liquid culture as described in section 2.1. Then, 1 mL of culture was centrifuged to obtain the cell pellet for gDNA isolation using Promega's Wizard® Genomic DNA Purification Kit. The final volume used to resuspend the gDNA was 30-50 µL of the provided rehydration buffer, depending on the pellet size.

2.3.3 DNA quantification

Quantification of pDNA, gDNA or purified PCR products was done using a NanoDrop™ One/OneC Microvolume UV-Vis Spectrophotometer from Thermo Fisher Scientific. 2 µL of the sample was loaded to check the quantity in ng/µL and the A260/280 absorbance ratio was measured to determine DNA purity.

2.3.4 Oligonucleotides

DNA oligonucleotide primers (Table 2.5) for sequencing or PCR amplification were designed with Snapgene (SnapGene | Software for everyday molecular biology) and ordered from

Eurogentec (www.eurogentec.com/life-science.html) or Integrated DNA Technologies (Integrated DNA Technologies | IDT (idtdna.com).

2.3.5 Polymerase chain reaction (PCR)

PrimeSTAR GXL DNA Polymerase (Takara), which is reliable in amplifying from high-GC Actinomycete genomes, was used for PCR reactions. Table 2.6 shows the typical reaction mixture, and the PCR profile is given in Table 2.7. PCR reactions were done on a MiniAmp™ Thermal Cycler from Thermo Fisher Scientific.

Table 2.6 PCR reaction mix.

Component	Amount in 50 µL reaction
5X GXL Buffer	10 µL
dNTPS	4 µL
10 µM forward primer	2 µL
10 µM reverse primer	2 µL
DMSO	2 µL
PrimeSTAR® GXL DNA Polymerase	1 µL
Template DNA	Variable, typically 1 µL
DNAse and RNAse free water	Make to 50 µL

Table 2.7 PCR profile.

Thermocycling step		Temperature	Time
Initial denaturation		98 °C	1 min
PCR cycles	Denaturation	98 °C	10 s
	Annealing	60-65 °C	40 s
	Extension	72 °C	30 s
Final extension		72 °C	7 min
Hold		4 °C	indefinitely

2.3.6 Agarose gel electrophoresis (AGE)

AGE is used to separate DNA fragments based on their size and shape. The marker used was a 1kbp ladder from NEB. Samples were mixed with loading dye (NEB, 6X purple gel loading dye) to a final concentration of 1X before loading to the gel. Agarose gels were prepared to 1 % (w/v) concentration in 0.5X TBE (Table 2.8). SYBR Green (Thermo Fisher) or Nancy-520 (Sigma Aldrich), were added to final concentrations of 400X and 200X, respectively, to visualize DNA bands. Gel imaging was done on a Biorad ChemiDoc™ MP imaging system. For DNA bands needing to be extracted, a blue light illuminator (Thermo fisher) was used.

Table 2.8 TBE buffer solution recipe.

Buffers	
10 X TBE	Per L:

	108 g Tris base 55 g boric acid 7.4 g disodium EDTA dihydrate
0.5X TBE (1:20 dilution from 10X TBE) 1X TBE (1:10 dilution from 10XTBE)	Per L 5.4 g Tris Base 2.75 g boric acid 0.37 g Disodium EDTA dihydrate

2.3.7 PCR products purification and gel extraction

QIAquick PCR Purification Kit (Qiagen) was used for purification of PCR products and restriction digestion reactions, following the manufacturer's protocol. The purified DNA was eluted with nuclease-free water, typically 10-20 µL, depending on the desired final concentration.

For gel extraction, the target band on the agarose gel was cut out and the DNA was purified using a QIAquick Gel Extraction Kit (Qiagen), following the manufacturer's protocol. The final DNA was eluted with nuclease-free water, typically 10-15 µL, depending on the desired final concentration.

2.3.8 Restriction digestion

Restriction enzymes were obtained from NEB and were used following the manufacturer's protocols, using their recommended buffers and concentration of DNA and enzyme. Typically, restriction digests were carried out in a 37 °C incubator for 1 h.

2.3.9 Dephosphorylation reaction

Dephosphorylation was performed to stop the re-ligation of digested plasmids, using 1 µL (20 U/µL) of Alkaline Phosphatase (Calf Intestinal Alkaline Phosphatase; Promega), added to the restriction digestion mixture.

2.3.10 Ligation

T4 DNA ligase (NEB) was used to ligate DNA fragments, following the manufacturer's instructions. Usually, reactions had a total volume of 10 µL, with vector:insert ratio of 1:2. Reaction mixtures were incubated at room temperature overnight.

2.3.11 Gibson assembly

NEBuilder HIFI Master Mix from NEB was used to assemble plasmids by the Gibson method. The primers for amplification were designed to produce 20 bp overlapping. Assembly was

performed following the manufacturer's protocol. Typically, 1:2 vector: insert ratio was used with 50 µg of vector. The assembly mix was incubated at 50 °C for 1 h. Then, 2 µL of the reaction mixture was transformed into electrocompetent cells following the protocol described in section 2.4.2.

2.3.12 DNA sequencing

Plasmids and PCR products were sequenced by Sanger sequencing at the MRC PPU unit at Dundee University (www.dnaseq.co.uk) or the Australian Genome Research Facility (AGRF) (Sanger Sequencing — AGRF).

For whole genome sequencing (WGS), cultures were prepared as outlined in section 2.1. Approximately 30–50 mg of wet cell mass (equivalent to 4×10^9 to 6×10^9 cells) were preserved in an inactivation buffer and submitted to MicrobesNG (Birmingham University, UK) or sequencing using both Nanopore and Illumina platforms.

2.3.13 Partial fill-in method

The Klenow fragment of DNA polymerase (NEB) was used for partial fill-in reactions with digested pDNA or gDNA. The standard partial fill-in reaction mixes used for the digested pJE vector and digested HMW gDNA are shown in Table 2.9. The reaction mixture was incubated at room temperature for 30 mins, then purified using a PCR purification kit (section 2.3.7).

Table 2.9 Partial fill-in reaction mix.

Component	Amount
Digested pDNA/gDNA	3 µg
10x fill-in buffer	5 µL
10 mM dTTP	2 µL
10 mM dCTP	2 µL
5 units (U) /µL klenow fragment	2 µL
Nuclease free water	Up to 25 µL

2.3.14 HMW gDNA isolation in DNA plugs

YEME containing 0.5% (v/v) glycine was used to grow Actinomycete strains for gDNA isolation. The cultures were incubated at 30 °C with continuous shaking for 2 days until a dispersed cell culture was achieved. The cells were then filtered using a 100 µm cell strainer and washed twice with 30% (w/v) sucrose. The washed cells were embedded in 1% (w/v) low

melting point (LMP) using an agar plug moulder. The process of isolating HMW DNA embedded in the agarose plugs, including the lysis and separation of DNA from proteins as well as the buffer recipes, were as described for BAC library construction (Osoegawa *et al.*, 1998). The agarose plugs containing HMW DNA could be stored in TE buffer at 4°C for at least 4 weeks without affecting the DNA quality.

2.3.15 Partial digestion

For partial digestion the HMW DNA fragments isolated from agarose plugs were incubated in 1 mL of 1 mM Tris, 5 mM NaCl, 0.1 mM dithiothreitol (DTT), containing 4 units of *Sau*3AI (NEB) for 4 h. $MgCl_2$ was then added to a final concentration of 10 mM, to initiate digestion, and the plugs were incubated at 37 °C to different time points (0, 2.5, 5, 7.5, 10 and 20 mins). To stop the digestion, plugs were immediately transferred to 50 mM (ethylenediaminetetraacetic acid) EDTA with 1 mg/mL proteinase K and were incubated for 30 mins at 37 °C.

2.3.16 Pulsed field gel electrophoresis (PFGE)

Partially digested HMW DNA samples were separated by PFGE (Schwartz and Cantor, 1984) using a CHEF (clamped homogeneous electric fields) Mapper system from Biorad, CHEF-DR II. The plugs were loaded in 0.75% LMP agarose using NEB Midrange PFGE markers to enable size estimation of the fragments. The plugs were run in 0.5X TBE Buffer with thiourea, with conditions of 0.1-25 s initial and final time, 6 V/cm for 20 h.

2.3.17 Fragment recovery using agarase

Blue light illuminator (Thermo fisher) was used to visualize the gel, and fragments greater than 50 kbp were selected and extracted from LMP agarose using agarase (Thermo fisher) following the manufacturer's protocol. To check the quantity and quality of the fragments for the ligation procedure, the recovered DNA fragments were subjected to AGE using 1% (w/v) agarose (section 2.3.6).

2.3.18 Vector preparation

The cloning vector pJE-2 was digested and dephosphorylated with enzymes *Bam*HI and alkaline phosphatase simultaneously, to linearise the plasmid and prevent the vector from re-ligating. To check the vector preparation, digested and dephosphorylated vector samples were subjected to ligation and transformation into DH10β. Absence of transformants indicated that

the vector was completely digested, and that the phosphorylation was successful. After quantifying the concentration, aliquots of the vector were kept at -20 °C for follow up studies.

2.3.19 Cloning via ligation

HMW DNA fragments from gDNA were obtained by *Sau*3AI digestion and by size fractionation on LMP agarose gel. The recovered HMW DNA fragments were then cloned into the digested and dephosphorylated pJE-2 vector using NEB T4 ligase, with a 10:1 molar ratio of vector:insert. The ligation reaction was left overnight at room temperature.

2.3.20 Drop dialysis method

Drop dialysis was done to the ligation mix to remove the salts that highly affect the electroporation. The ligation mix was drop-dialyzed on Millipore filters (type VS, 0.025 mm) for 2 h against 0.5X TBE buffer at room temperature.

2.4 Transformation

2.4.1 Preparation of electrocompetent cells of E. coli *DH10β and ET12567 [pUZ8002]*

Strains DH10β or ET12567 [pUZ8002] were grown in LB overnight with shaking at 37 °C. In the morning 1 mL of culture was diluted into 100 mL of fresh LB and cultured until an OD_{600nm} of 0.5 was reached. The cells were centrifuged, and the pellet was washed twice with ice cold 10% (v/v) glycerol, then resuspended in 2 mL ice cold 10% (v/v) glycerol. Aliquots of 50 µL per tube were prepared and snap frozen using liquid nitrogen before storing at -80 °C.

2.4.2 E. coli *transformation via electroporation*

Electrocompetent cells were thawed on the ice for about 5-10 mins before addition of 2 µL of plasmid, ligation mix or assembly mix. The mixture was then transferred to a pre-chilled 1 mm cuvette for transformation by a Biorad Gene Pulser Xcell™ electroporator in a pre-set bacterial profile for a 1 mm gap cuvette with 1.8 kV, 25 µF capacitance and 200 Ω resistance. Cells were then transferred to a microcentrifuge tube containing 750 µL LB and incubated at 37 °C with shaking for 1 h. The mixture was then plated on agar plates supplemented with appropriate antibiotics.

2.4.3 Protoplast preparation and transformation

Protoplasts were prepared by growing the strain at 30 °C in YEME for 2 days. To promote a dispersed culture 10% (w/v) sucrose was added to the culture medium. The cells were then passed through a 70 µm nylon cell filter. The filtrate was centrifuged and the cell pellet was washed twice with 0.3 M sucrose. Cells were resuspended in 7 mL protoplast buffer (P buffer,

Table 2.10) with 2 mg/mL lysozyme and subsequently incubated for 15 mins at 30 °C. To check if the protoplast preparation was successful, 5 µL of cells were inspected by microscopy. Protoplasts were then centrifuged for 15 mins at 2000 g, and the pellet resuspended in 1 mL P buffer could be stored at 4 °C for 1-2 weeks without affecting its quality.

For transformation, protoplasts were diluted 1:10 in P buffer and 2-4 µg of pDNA was added to the cells, followed by addition of 200 µL of transformation buffer. The mixture was spread into 2 pre-dried R2YE agar plates which were incubated at 30°C. The following day, one plate from each transformation was overlaid with 1 mL of DI water containing apramycin at a final concentration of 30 µg/mL, while another plate was left without antibiotic to assess the protoplast regeneration efficiency.

Table 2.10 P buffer recipe.

P buffer	Per 50 mL: 40 mL P buffer (Per L: 103 g sucrose,0.25 g K_2SO_4, 10.12 $MgCL_2.6H_2O$) 5 mL $CaCl_2.2H_2O$ 5 mL TES (2-[Tris(hydroxymethyl)methylamino]-ethanesulfonic acid) 500 µL 0.5 % (w/v) of KH_2PO_4

2.5 Conjugation

Plasmids were first transformed into to electrocompetent ET12567 [pUZ8002] cells, using the transformation protocol described in section 2.4.2. The transformation mixture was directly inoculated into LB broth with appropriate antibiotics and grown overnight at 37 °C with shaking. The next morning, 100 µL of the grown culture was refreshed in 10 mL LB broth with antibiotics and grown to an OD_{600nm} 0.5. The culture was centrifuged and washed twice with LB, then resuspended in 100 µL LB. Simultaneously, 25 µL of spores (thawed from -80 °C) were added to 300 µL LB and incubated at 50 °C for 15 mins to trigger germination. The heat shock spores were then mixed with the ET12567 [pUZ8002] cells and plated out in MS medium supplemented with 100 mM $MgCl_2$. The next morning, the plates were overlayed with the

proper antibiotics (Table 2.2) used for selection. Colonies that grew were patched into agar with supplied antibiotics.

2.6 Preparation of crude extracts

2.6.1 Bacterial extract preparation

For characterization of specialized metabolite production, Actinomycetes were cultured using conditions described section 2.1. To prepare crude extracts from solid media, agar was cut into smaller pieces and transferred into vials or a glass container. The agar pieces were then covered with either ethyl acetate (EtOAc) or methanol (MeOH), depending on the solvent best suited for extracting the target compound of interest, and left for at least 3 h before filtering through Whatman no. 1 filter paper, then concentrated using a Büchi rotary evaporator. The concentrated crude extract was then transferred to appropriate glass tubes and dried using a Genevac EZ-2 4.0 centrifugal evaporators. Dried crude extracts were stored at -20 °C.

For crude extracts from isolates grown in liquid culture, samples were centrifuged at 4,200 rpm for 20 mins. The supernatant was then filtered through Whatman no.1 filter paper and passed through a C18 column, followed by flash chromatography clean up, as discussed in section 2.11.1. Cleaned up extract was dried in a Genevac evaporator and stored at -20 °C for further studies.

2.6.2 Plant extract preparation

Hibiscus sp. flowers (Zindee) purchased from a public store were ground using a mortar and pestle. Then, 30 g of the ground plant material was transferred into a glass container to which 200 mL of MeOH was added. The mixture was continuously mixed using a magnetic stirrer for at least 3 h at room temperature. The MeOH extract was then filtered using Whatman no. 1 filter paper and concentrated on a rotary evaporator. The concentrated extract was transferred into pre-weighed glass vials and dried in a Genevac. The weight of the dried *Hibiscus* extract was determined and a stock of 18 mg/mL in DMSO was stored at -20 °C before use.

2.7 Antibacterial activity assays

A disc diffusion assay was used to determine the activity of the crude extracts, HPLC fractions or pure compounds against pathogenic microbes including *Bacillus subtilis*, *Escherichia coli*, *Staphylococcus aureus*, *Cryptococcus neoformans*, and *Candida albicans*. Briefly, an overnight culture of the bacterium or fungus was refreshed by inoculating 50 µl of the grown culture into 5 mL of LB or YPD and cultured at 37 °C or 30 °C to an OD_{600nm} of ~ 0.5. Crude extracts or pure compounds in DMSO were diluted if necessary. 10-20 µl of extracts or compounds were

pipetted onto sterile 6 mm filter discs and dried. Meanwhile, lawn of the bacteria was spread on the agar plates using sterile cotton buds to achieve uniformity. Then, the dried disc containing extract/fraction/compound was placed on the microbial lawn and the plates were incubated at 30 °C or 37 °C overnight. Zones of inhibition were measured the next day.

2.8 Determining minimum inhibitory concentration (MIC) value

Overnight culture of the target pathogen was refreshed in LB or YPD liquid medium and let to grow to OD_{600nm} ~ 0.5 for about 2-3 h. Meanwhile, serial dilutions of pure compound in DMSO were prepared from stock solution. Refreshed cultures were further diluted to final concentrations of 1:10,000 for *B. subtilis S. aureus*, and *E. coli*, or 1:100 for *C. neoformans* and *C. albicans*. Then, 198 µl of the diluted culture was pipetted into sterile 96 well plate using multichannel pipettor. Then 2 µl of the of the serially diluted compound added on each well except for wells for negative control on which 2 µl DMSO added. The plate was then sealed by Breathe-Easy sealing films (ProSicetech) and run overnight on plate reader (Tecan) at either 37 °C or 30 °C with shaking. The absorbance at A_{600nm} were measured every 6 mins. The resulting absorbance data exported to an excel file and growth curve were generated using Prism software (Graphpad).

2.9 Chrome Azurol S (CAS) assay

The CAS solution was prepared following the procedure described in literature (Alexander and Zuberer, 1991). Three different solutions, solutions A, B, C, were prepared according to the recipe given on Table 2.11. Solution B was slowly added to solution A while stirring continuously, followed by the addition of solution C. The mixture was then brought to a final volume of 100 mL with MilliQ water. Just before use, 87.3 mg of sulfosalicylic acid was added to the mixture. Stock solutions of 5 mg/mL for ethylenediaminetetraacetic acid (EDTA), citric acid, hydroxycitric acid, hibiscus acid dimethyl ester, and hydroxycitric acid 1,3-dimethyl ester were prepared in MilliQ water and then diluted with the CAS solution to obtain final concentrations of 25, 20, 15, 10, 5.0, 2.5, 1.0, 0.5, 0.25, 0.1, 0.05, and 0.01 mg/mL in a 100 µL total reaction volume. MilliQ water and EDTA were used as negative and positive controls, respectively.

Table 2.11 CAS assay solutions recipe.

CAS assay solution A	Per 25 mL of milliQ: 21.9 mg of hexadecyltrimethylammonium bromide (HDTMA)
CAS assay solution B	1.5 mL of 1 mM FeCl3·6H2O in 10 mM HCl and mix with 7.5 mL of 2 mM CAS

CAS assay solution C	Per 50 mL of milliQ: 9.76 g of 2-(N-morpholino)ethanesulfonic acid (MES) pH 5.6 using 1 N KOH

2.10 Protein purification and expression

The target gene for protein expression was cloned into an optimized pET28 plasmid, pET28a T7pCONS TIR-2, via Gibson assembly (Addgene Plasmid #154464) (Shilling et al., 2020). The assembled vector was validated through restriction digestion and sequencing before being transformed into *E. coli* BL21. The transformed *E. coli* BL21 cells were cultured overnight at 37 °C, then refreshed in 1L of LB medium until the OD_{600} reached 0.5–0.6. Protein expression was induced by adding 0.5 mM IPTG to the culture, which was then incubated overnight at 15 °C with shaking. Cells were then harvested by centrifugation at 4,000 rpm for 15 mins at 4 °C (Thermo Scientific™ Sorvall™ LYNX 6000). The cell pellet was resuspended in 20 mL of binding buffer (Table 2.12) containing an EDTA-free cOmplete Ultra protease inhibitor tablet (Roche). Cell lysis was performed via sonication, with pulses of 10 s and 10 s off at 20% amplitude for a total of 5 mins. The lysate was centrifuged at 17,000 rpm for 1 h at 4°C, and supernatant filtered through a 0.45 µm syringe filter. The filtered lysate was then subjected to HiTrap Chelating HP column (Cytiva) loaded with Ni^{2+} ions, following the manufacturer's protocol. Elution was performed using a gradient of imidazole concentrations (20 mM, 50 mM, 100 mM, 200 mM, and 500 mM) (Table 2.12). A 10 µL aliquot of each eluted fraction was mixed with 10 µL of NEB blue protein loading dye and incubated at 95 °C for 5 mins. The denatured protein samples were resolved on a pre-cast 8–16% (w/v) MP TGX gel (Bio-Rad Laboratories) using a Bio-Rad Mini-PROTEAN electrophoresis cell at 120 V for 45 mins in 1X Tris-Glycine buffer (Bio-Rad Laboratories). A Broad Range (10–250 kDa) color-coded Prestained Protein Marker (Cell Signaling Technologies) was used to estimate protein sizes. The gel was stained for 1 h using a coomassie brilliant blue R250 staining solution (Table 2.12) and subsequently destained for 1 h using a destaining solution (Table 2.12). For further destaining, the gel was then incubated in distilled water overnight with gentle shaking at room temperature.

Table 2.12 Protein purification solutions recipe.

Binding buffer	0.02 M Na_2HPO_4 0.5 M NaCl

Elution buffer	0.02 M Na_2HPO_4 0.5 M NaCl 20 mM, 50mM, 100mM, 200mM, 500mM imidazole
Staining solution	Per 1L: 1g Coomassie brilliant blue R250 100 mL Acetic acid 500 mL MeOH
Destaining solution	Per 1L: 100 mL Acetic acid 500 mL MeOH

2.11 Purification and fractionation methods

2.11.1 Flash chromatography

Flash chromatography is done either to fractionate or clean-up crude extracts using HyperSep C18 column (Thermo Scientific). The column was prepared by elution of 2 volumes of MeOH followed by 2 volumes of DI water. Then, the filtered liquid extract was pass through the column. For simple clean up of the liquid extract, two volumes of DI water were used before the extract was eluted with two volumes of methanol. For fractionation, different concentrations of MeOH from low to high was used to elute the column until the final elution by two volumes of MeOH which was dried using Genevac.

2.11.2 High performance liquid chromatography (HPLC)

HPLC was used to fractionate crude extracts. The dried extract was dissolved in 1 mL of MeOH, pipetted to a dental cotton, and left to air-dry under a fume hood. The dental cotton containing the extract was placed into a cartridge (10 × 30 mm) and connected to a semi-preparative reverse-phase C18 Betasil column (20 mm × 150 mm or 21.2 mm x 250mm). Preparative HPLC (Agilent 1260 Infinity II) was employed for extract fractionation using the following conditions: an initial phase of 5% (v/v) acetonitrile for 5 mins, followed by a linear gradient from 5% to 95% (v/v) acetonitrile over 55 mins, then held at 100% (v/v) acetonitrile for the final 5 mins, with a flow rate of 9 mL/min or 12 mL/min. Fractions were collected every 30 or 60 s over the 60-min runtime. The collected fractions were directly tested for activity and/or analysed by LC-MS, then were dried on a Genevac and then sent for NMR analysis.

2.12 Structural Analysis

2.12.1 Liquid chromatography mass spectrometry

LC-MS analysis was done to detect the presence of known or unknown compounds on the crude extract or fractions from HPLC. LC-HR-MS analysis was performed on Thermo Vanquish UHPLC connected to a Proshell 120 EC-C18 column (2.1 × 100 mm, 1.9 μm) linked to an Orbitrap IQ-X Tribrid or Exploris 120 mass spectrometer. 50 μL of HPLC fractions were directly transferred to LC-MS vials or 96-well plate for analysis while EtOAc or MeOH extracts of solid cultures or liquid crude extracts were centrifuged twice for 10 mins using maximum rpm prior to LC-MS analysis.

2.12.2 Nuclear magnetic resonance (NMR)

Samples for NMR were resuspended in 170 μL dimethyl sulfoxide-d 6 (Sigma Aldrich or Cambridge Isotope Laboratories) or other deuterated solvents and were transferred to 3 mm NMR tubes (Bruker). NMR spectra were recorded on a Bruker 600 MHz spectrometer equipped with a TCI cryoprobe at 25 °C. The ^{1}H and ^{13}C NMR chemical shifts were referenced to the DMSO-d_6 solvent peaks at δ_H 2.50 and δ_C 39.52 or other deuterated solvent peaks.

Chapter 3: Construction of the pJE Cloning and Expression Vectors, and Construction of Preliminary Genomic Libraries

3.1 Introduction

Genomic libraries are constructed by large scale cloning of random fragments of genomic DNA (gDNA) into a suitable vector, generally a plasmid (Nierman and Feldblyum, 2001). In the area of NP discovery, gDNA library construction is a useful tool for cloning large fragments for expression of cryptic BGCs. One important element in cloning BGCs is the design of the cloning vector. A plasmid cloning vector is an autonomously replicating vehicle designed to enable the isolation and amplification of desired DNA sequences (Snyder, Champness and Champness, 2007). Plasmid vectors are easy to manipulate and purify. They can also function as shuttle vectors, facilitating the transfer of genes between organisms, such as from *E. coli* to *Streptomyces* (Snyder, Champness and Champness, 2007). As a result, cloning vectors have become essential molecular tools in NP discovery, enabling the manipulation, expression, and study of BGCs involved in secondary metabolite production (Atanasov *et al.*, 2021). They help overcome challenges associated with the genetic manipulation of actinomycetes, which are often relatively intractable. The success of BGC cloning vectors depends on certain key features, such as target insert size, copy number, selectable markers, and cloning sites (Preston, 2003). For cloning large DNA fragments, high copy number vectors are generally avoided due to instability. Instead, some low copy number plasmid derivatives, such as the original bacterial artificial chromosome vectors (BACs), can accommodate inserts up to 300 kbp, based on their F factor based replication system (replicon), including the *oriS* and *repE* genes, and partitioning genes (*sopA*, *sopB* and *sopC*) (Shizuya *et al.*, 1992). Most conventional plasmids use antibiotic resistance genes as selectable markers, allowing for the selection of plasmid-containing cells. Apramycin is widely used in *Streptomyces* research because it can be used to select recombinants in both *E. coli* and *Streptomyces* and usually exhibits a low false positive rate (Feng, Kim and Brady, 2010). The cloning site is the region where foreign DNA is inserted, generally comprising one or more unique restriction endonuclease recognition sites. The target DNA fragments can then be prepared with compatible cohesive ends to enable efficient ligation (Preston, 2003).

In this project, we developed novel cloning and expression vectors, pJE-1 and pJE-2, by integrating features from two well-established vectors. pSMART BAC (Lucigen) is derived from F factor-based BAC vector, pBeloBACII (Woo *et al.*, 1994). It is specifically designed for constructing shotgun libraries for whole-genome sequencing, while reducing transcriptional interference from inserted DNA (Godiska *et al.*, 2005). The second component, pSET152, is a widely used shuttle vector that can undertake site-specific integration at the bacteriophage ϕC31 attachment site (*attB* site) (Bierman *et al.*, 1992), which is present in many *Streptomyces*

genomes (Kuhstoss and Rao, 1991). Additionally, pSET152 can be mobilized from *E. coli* to *Streptomyces* via conjugation, facilitated by an origin of transfer (*oriT*) from plasmid RK2 (Mazodier, Petter and Thompson, 1989). The pJE vectors were constructed by combining elements of the two vectors, to enable efficient cloning, integration, and expression of BGCs in *Streptomyces*, thereby enhancing NP discovery.

3.2 Results and discussion

3.2.1 Construction and features of the pJE-1 vector

The pJE-1 vector (Figure 3.1) was assembled from four fragments: two amplified by PCR from Lucigen's pSMART BAC v2 (~ 6kbp), one from pSET152 (~ 4 kbp), and a short synthesized fragment containing *Sal*I and I-*Sce*I restriction sites, along with transcription terminators. Primer sequences and the synthesized fragment details are provided in Table 2.5. Site-directed mutagenesis was used to introduce a unique *Xho*I site for cloning by the partial fill in method because the fragment amplified from pSET152 contains other *Sal*I sites. The gross structure of pJE-1 was confirmed by restriction digestion with *Xcm*I and *Pvu*II, which produced bands of the expected sizes (Figure 3.2). The pJE-1 vector has the following features derived from pSMART BAC and pSET152 as seen in Figure 3.1. The *ori2* replicon maintains a low copy number plasmid characteristic of bacterial F plasmid, enabling stable maintenance of large DNA inserts. However, its copy number can be increased to a medium level via *oriV*, which, in the BAC replicator (Lucigen) host strain, is inducible by expression of the *trfA* gene in the presence of L-arabinose (Wild, Hradecna and Szybalski, 2002). Plasmids can therefore be stably maintained at low copy number and then amplified to facilitate screening or plasmid purification. Additionally, pJE-1 carries the phage ϕC31 integrase gene to facilitate site-specific integration into the chromosomes of many Actinomycetes (Kuhstoss and Rao, 1991). Other key features of pJE-1 include a unique *Xho*I cloning site and an apramycin resistance gene for use as selectable marker in both *E. coli* and *Streptomyces*. Furthermore, terminators flanking the cloning site prevent unwanted transcription from the vector into the insert, reducing the risk of instability and cloning bias.

The effectiveness of the arabinose induction system was confirmed by growing cultures of *E. coli* BAC replicator containing pJE-1 in the presence and absence of arabinose and extracting pDNA. Gel electrophoresis **(**Figure 3.3**)** confirmed that the yield of plasmid was greatly enhanced following growth in the presence of L-arabinose.

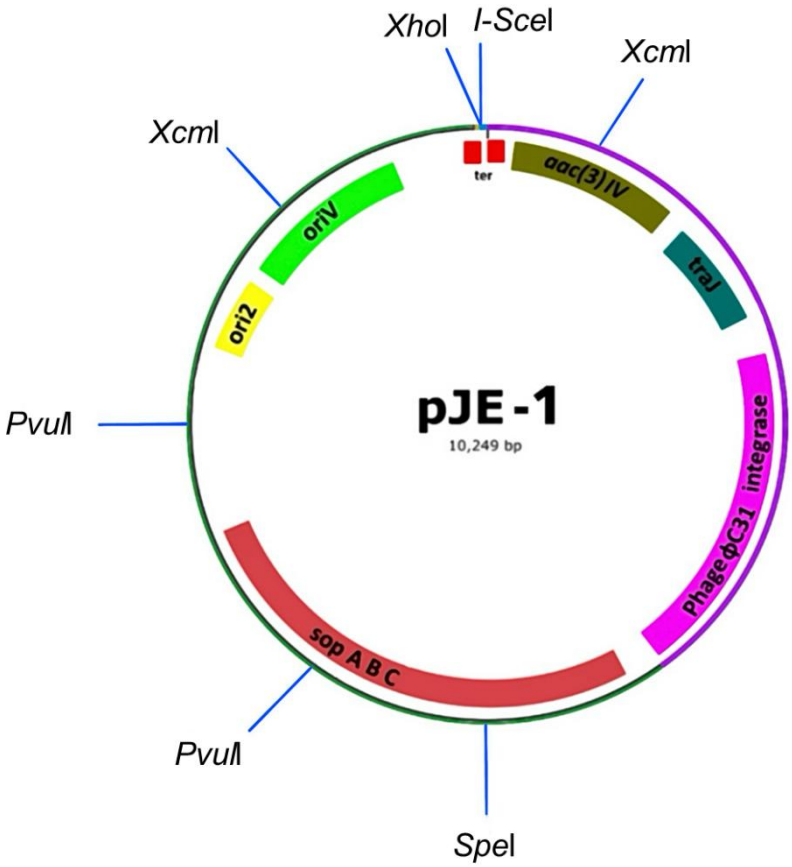

Figure 3.1. Plasmid map of the pJE-1 cloning and expression vector.

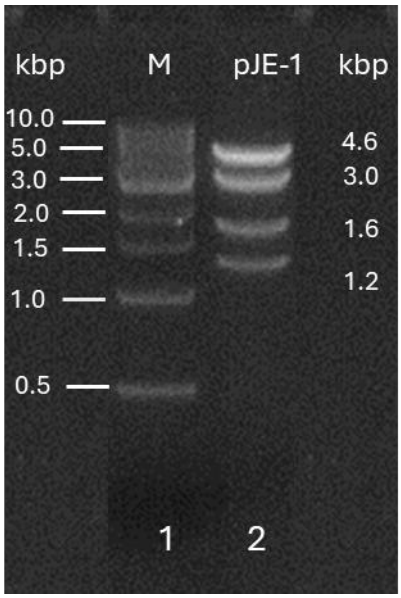

Figure 3.2. AGE photo (1% (w/v) agarose, 0.5X TBE,100 V,1 h) to validate the structure of pJE-1 via restriction digestion. Lane 1, molecular weight (MW) Markers (1kb ladder); lane 2, restriction digest using restriction enzymes *Xcm*I and *Pvu*II (with expected sizes to the right).

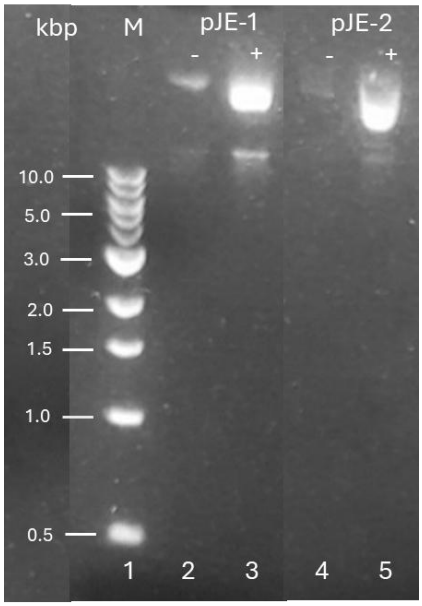

Figure 3.3. AGE photo (1% (w/v) agarose, 0.5X TBE,100 V,1 h) to illustrate copy number amplification of pJE-1 and pJE-2. Lane 1, 1kb marker; lanes 2-3, pJE-1 with (+) and without (-) arabinose; lanes 4-5, pJE-2 with (+) and without (-) arabinose.

3.2.2 Genomic library construction via the partial fill-in method

The partial fill-in method is illustrated in Figure 3.4. Vector and insert are digested with different restriction endonucleases generating 4 bp 5' overhangs. DNA polymerase is then used to fill in two of the four overhanging residues. In both cases, the remaining 2 bp overhangs are no longer capable of base pairing, thus the vector cannot self-ligate, nor can inserts join to each other end-to-end. However, for certain pairs of enzymes, the partially filled in ends become compatible, as for the *Bgl*II and *Xho*I sites shown in the Figure. (Hung and Wensink, 1984). In gDNA library construction, this approach is beneficial for two reasons. First, it prevents vector self-ligation, thereby preventing the recovery of vector molecules with no inserts. Second, it prevents insert-insert connections, thereby generating recombinants exclusively with single insertions (Zabarovsky and Allikmets, 1986). To evaluate the utility of the pJE-1 cloning vector, a pilot genomic library was constructed using this method. To start, high molecular weight (HMW) gDNA was extracted using a phenol-chloroform method and was subsequently digested using *Bgl*II (A^GATCT). This enzyme was chosen because its AT-rich recognition site is expected to produce relatively large fragments from the GC-rich chromosomal DNA. The *Bgl*II-digested fragments were partially filled in with dGTP and dATP. In parallel, the *Xho*I-linearized vector was partially filled-in with dTTP and dCTP, resulting in compatible ends between the vector and insert, as illustrated in Figure 3.4 (Zabarovsky and Allikmets, 1986).

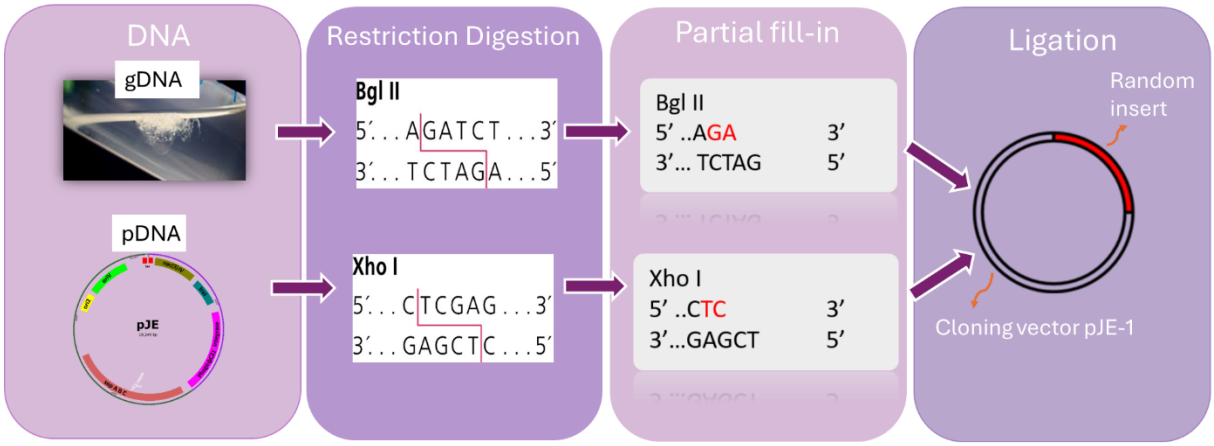

Figure 3.4 Diagram of partial fill-in method employed for cloning gDNA fragments in pJE-1.

To confirm that the partial fill-in strategy was functioning efficiently, electrocompetent DH10β cells were transformed with equimolar amounts of the following DNA preparations: digested pJE-1 (Figure 3.5A), digested and ligated pJE-1 (Figure 3.5B), and ligated pJE-1 after partial fill-in (Figure 3.5C). Apramycin-resistant transformants were only obtained when the vector was cleaved and ligated without partial fill-in, confirming that the vector was fully digested and successfully end-filled, as expected. To assess the vector's ability to incorporate partially end-filled chromosomal DNA, ligation reactions were performed using 35 ng of vector with varying insert concentrations, followed by transformation of DH10β cells. As shown in Table 3.1, transformants were obtained at all insert concentrations, but curiously, with no clear correlation between insert amount and yield of transformants. A total of 374 clones were obtained.

To test for the cloning efficiency and assess the insert size distribution, nine randomly selected clones were analysed. Based on the pJE-1 restriction map (Figure 3.1), digestion with *Spe*I and *Xcm*I was expected to generate three vector derived fragments (1.6, 4.0 and 4.5 kbp), with inserts affecting the size of the 1.6 kbp fragment. As shown in Figure 3.6**,** all plasmids exhibited loss of the small fragment, replaced by one or more larger fragments, indicating a low frequency of vector only clones. However, the insert sizes were generally relatively low, ranging from 300 bp to 10 kbp, as indicated above each lane, and no clones exceeded 20 kbp. This emphasised the need to size fractionate the target DNA before cloning.

To optimize insert size*,* gDNA was extracted from agarose-embedded cells (section 2.3.14) to minimize shearing, followed by partial digestion with *Sau*3AI (section 2.3.15). Complete digestion with *Bgl*II was avoided because it could fragment BGCs into non-functional pieces or generate fragments too large for cloning. Partial digestion with *Sau*3AI was preferred as it has only a four-base recognition sequence, therefore cutting frequently, while generating the

same sticky ends as *Bgl*II. Initially, the same partial fill-in approach was applied to *Sau*3AI-digested fragments cloned into *Xho*I-digested pJE-1. However, despite repeated attempts, library construction was largely unsuccessful, generating no colonies after transformation, perhaps because of the low binding efficiency afforded by 2 bp sticky ends.

Figure 3.5 LB agar plates (with apramycin) after transformation of electrocompetent DH10β with (A) digested pJE-1; (B) digested and ligated pJE-1; (C) ligated pJE-1 after partial fill-in using Klenow polymerase.

Table 3.1. Number of colonies obtained after ligation with varying insert concentrations.

Concentration of insert	No. of colonies
20ng	17
40ng	34
80ng	36
120ng	83
160ng	44
200ng	32
240ng	25
280ng	29
320ng	74
Total	**374 colonies**

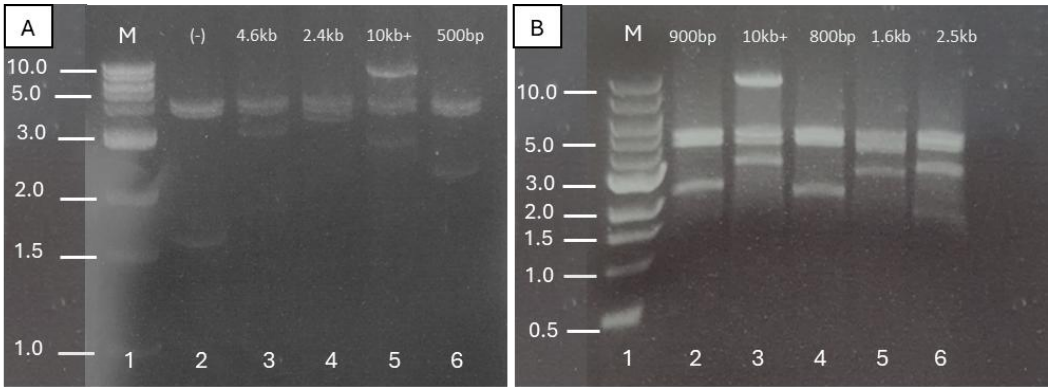

Figure 3.6 Agarose gel electrophoresis image for insert size determination (1% (w/v) agarose, 0.5X TBE,100V,1 h). (A) Lane 1, 1 kb marker; lane 2, digested empty pJE; lanes 3-6, random clones digested with *Xcm*I and *Spe*I. (B) Lane 1, 1 kb marker; lanes 2-6, random clones digested with the same enzymes. The number above each lane indicates the approximate insert size.

3.2.3 Construction of pJE-2

To overcome the limitations of the partial fill-in method, we decided to switch to an alternative cloning strategy using 4 bp overhangs instead of 2, while preventing vector re-ligation using alkaline phosphatase. To implement this strategy, site-directed mutagenesis was used to replace the unique *Xho*I cloning site of pJE-1 with *Bam*HI (primers listed in Table 2.5). The resulting vector, pJE-2 (Figure 3.7), retained all features of pJE-1 except for the new cloning site. The structure was verified by sequencing, and restriction digestion with *Bam*HI and *Hind*III, yielding the expected band sizes of 6.3 kbp, 3 kbp and 1 kbp (Figure 3.8). Additionally, as for

pJE-1, the copy number of pJE-2 was amplified when cultured with L-arabinose, as shown by the increase in pDNA yield (Figure 3.3, lanes 4-5).

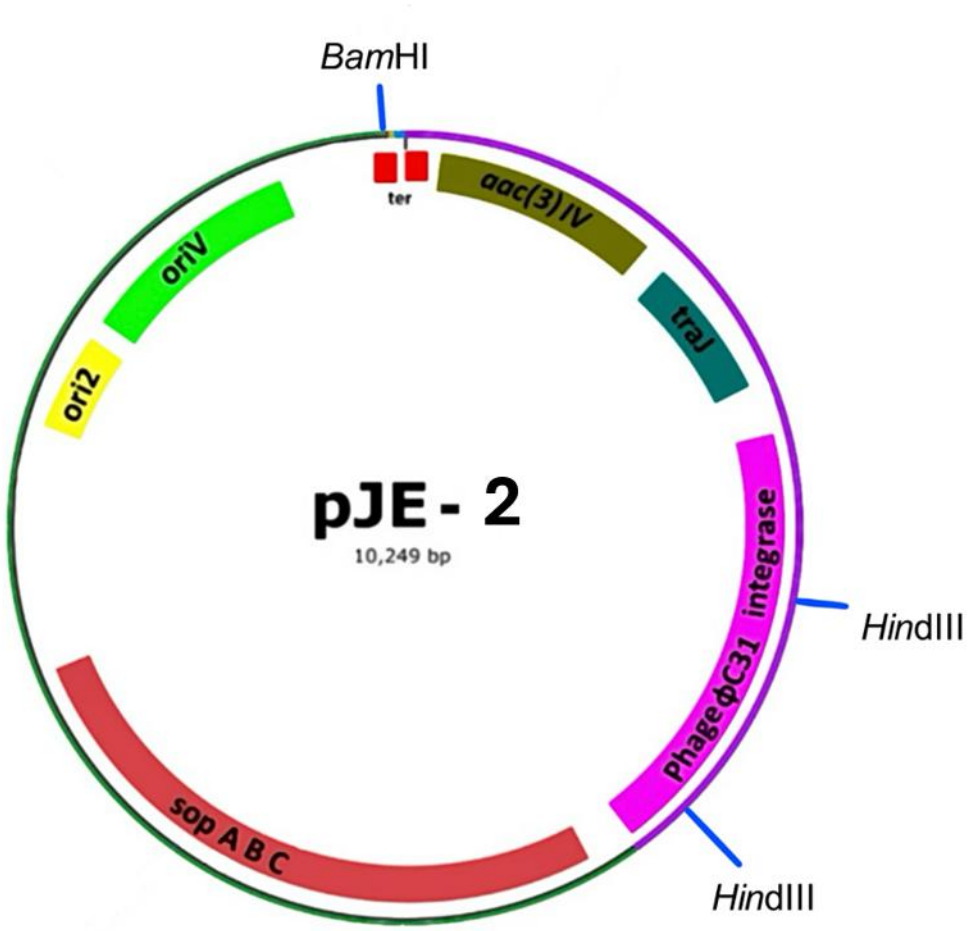

Figure 3.7 Plasmid map of the pJE-2 cloning and expression vector with a unique *Bam*HI cloning site.

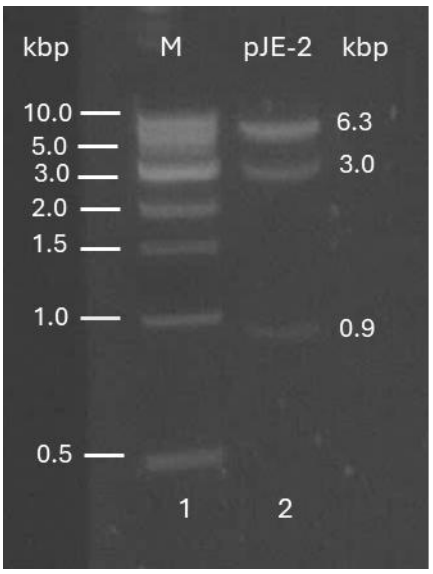

Figure 3.8 AGE photo (1% (w/v) agarose, 0.5X TBE,100 V, 1h) to validate pJE-2 via restriction digestion using restriction enzymes *Bam*HI and *Hin*dIII. Lane 1, 1kb marker; lane 2, pJE-2 (with expected sizes to the right).

3.2.4 Vector phosphatase cloning method

The vector phosphatase cloning method uses alkaline phosphatase treatment to remove the 5'-phosphate from the sticky ends generated by cleavage of the vector at its cloning site. pJE-2 was digested with *Bam*HI and simultaneously dephosphorylated. To test for the efficiency of cleavage and dephosphorylation, electrocompetent *E. coli* DH10β cells were transformed with either (A) digested and dephosphorylated or (B) digested, dephosphorylated, and ligated pJE-2. No transformants were obtained, confirming the effectiveness of vector preparation (data not shown). Successful cloning also depends on high-quality HMW gDNA. *Streptomyces werraensis* "MY12", was selected for a pilot study because it is easy to grow. Growth conditions were optimized in YEME media supplemented with 0.5% (w/v) glycine, which can increase cell wall sensitivity to lysozyme and hence the release of DNA (Zhang *et al.*, 1999). Figure 3.9 shows that DNA isolated from *Streptomyces werraensis* culture grown in YEME-glycine (lanes 2 and 3) formed a single, slow-moving band, indicative of high molecular weight, whereas the DNA from an equivalent culture grown without glycine (lane 4) appeared more degraded.

The HMW gDNA embedded in agarose was subjected to partial digestion with *Sau*3AI at different time points (0, 5, 10, 15, 20 and 30 min). Figure 3.10 shows PFGE results, with size selection carried out on the 10- and 15-min samples (white boxes). The DNA was recovered using agarase treatment and samples run on AGE (Figure 3.11). Both samples formed discrete bands, running well behind the 10 kbp marker, indicating a high MW and minimal shearing.

The estimated concentration of recovered fragments was ~45-50 ng/µL, based on approximate equivalence to the concentration of the lowest band NEB 1 kb marker (42 ng/µL).

The recovered DNA fragments and prepared vector were ligated using T4 ligase, and subjected to drop dialysis, to reduce the salt concentration and prevent arcing during electroporation (Willson and Gough, 1988). The ligation product was transformed into electrocompetent BAC replicator cells and plated in apramycin plates for selection. Eight random clones from each set of libraries were picked for validation of the insert size via restriction digestion. Figure 3.12 presents restriction digestion results with *Xcm*I and *Sna*BI of 8 random clones from the 10 min time point (red box) and 8 from the 15 min time point (yellow box). Lane 2 (digested pJE-2 control) shows three bands corresponding to the empty vector (~5.6 kbp, ~3 kbp, and ~1.6 kbp). The presence of an insert was evident upon replacement of the lowest band in the gel by several other fragments of various sizes and, to a first approximation, the size of the insert should be proportional to the number of additional fragments. Among the random clones, only three empty clones (lanes 11, 12, and 14) were observed in the 15 min sample suggesting a small percentage of clones without inserts, and many clones appeared to have large inserts. To obtain a more accurate estimation of insert size, the ends of the inserts were sequenced using primers (validation clone F and validation clone R; see Table 2.5) reading in from the vector, either side of the *Bam*HI cloning site. The sequences of 9 clones were then mapped onto the *Streptomyces werraensis* genome. Figure 3.13 shows the distribution and estimated sizes of the cloned fragments, which ranged from 31 to 60 kbp and were broadly distributed across the genome.

Figure 3.9 PFGE of HMW gDNA extracted from *Streptomyces werraensis*. Lane 1, midrange PFGE marker; lanes 2-3, gDNA from cells with 0.5% (w/v) glycine (+); lane 4, gDNA from cells grown without glycine (-).

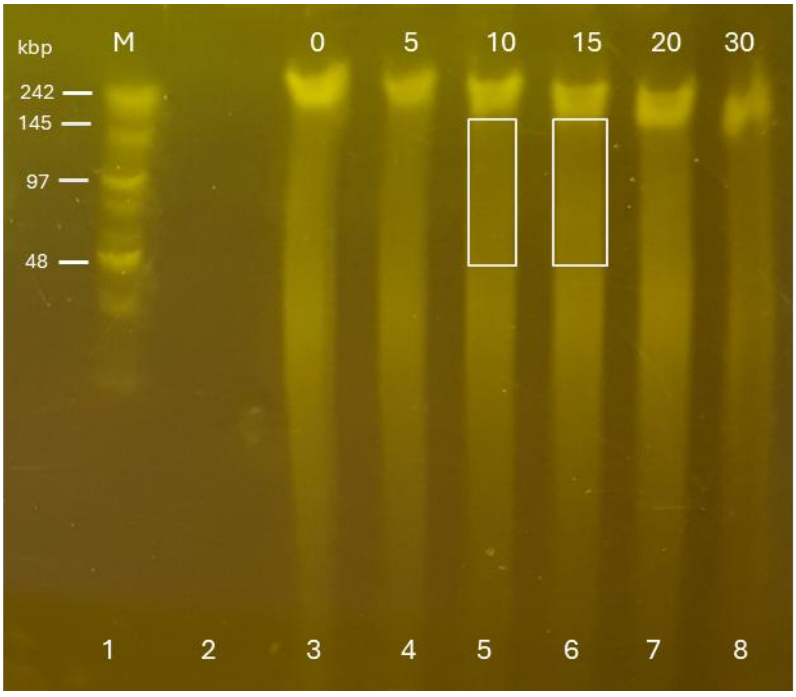

Figure 3.10 PFGE run on the CHEF DR II 200V, with 0.1-25 s switching times, for 20 h in 0.75% (w/v) LMP agarose and 0.5X TBE: lane 1, midrange PFGE marker; lanes 3-8, gDNA of *Streptomyces werraensis* strain partially digested with *Sau*3AI for 0, 5, 10, 15, 20 or 30 min; white boxes, selection range for the 10 and 15-min digested fragments.

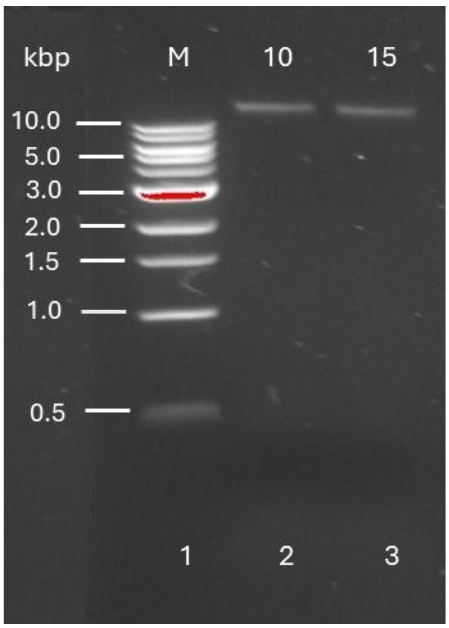

Figure 3.11 AGE image showing the recovery of partially digested *Streptomyces werraensis* gDNA from LMP agar after agarase treatment (1% (w/v) agarose, 0.5X TBE, 100V, 1 h). Lane 1, 1 kbp marker; lanes 2-3, size selected fragments recovered from the 10 and 15 min time points, respectively.

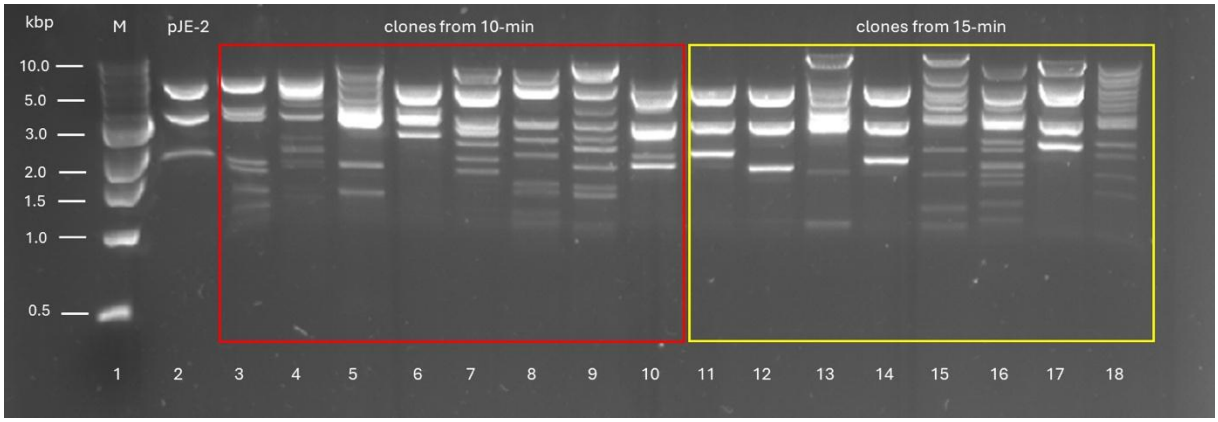

Figure 3.12 AGE image for validation of insert presence and size (1% (w/v) agarose, 0.5X TBE, 100V, 1 h) Lane 1, 1 kb marker; lane 2, digested empty pJE-2; lanes 3-10 (red box), eight random clones from the 10 min time point digested with *Xcm*I and *Sna*BI; lanes 11-18 (yellow box), eight random clones from the 15 min time point digested with *Xcm*I and *Sna*BI. Plasmids were amplified by culture growth in the presence of arabinose.

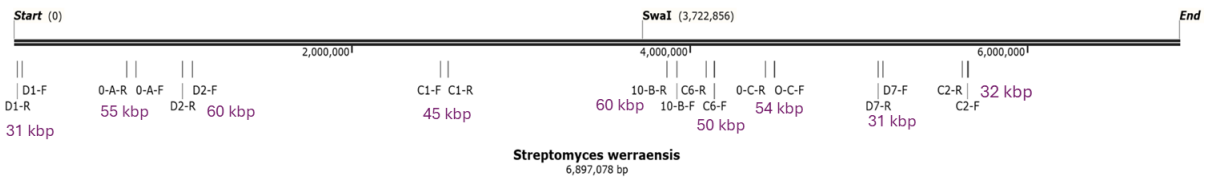

Figure 3.13 Genome map of *Streptomyces werraensis* and distribution of the 9 cloned segments determined by insert-end sequencing.

3.3 Conclusion

In this study two new efficient cloning vectors were assembled and demonstrated to be extremely useful in the construction of random, HMW genomic libraries. The vectors were designed to enable cloning of DNA fragments bearing 5'-TGCA-3' (pJE-1) or 5'-GATC-3' (pJE-2). In the absence of arabinose, the low copy number F-based replication and stability functions enable stable maintenance of clones with large DNA inserts, while addition of arabinose greatly facilitates clone characterization by increasing the copy number.

Library construction was strongly influenced by the methodology used for HMW gDNA isolation and partial digestion. Embedding cells in agarose plugs limits the shearing of the HMW DNA, which is crucial for capturing large BGCs in an intact manner. Additionally, optimizing the partial digestion time points, employing low-melting-point agarose for fragment recovery, and using drop dialysis for buffer exchange, significantly improved insert size and transformation efficiency.

It emerged that the vector-phosphatase approach using the unique *Bam*HI site of pJE-2 provided an efficient method for vector preparation. While partial fill-in prevents vector self-ligation and cloning of tandem target fragments, its efficiency may be limited for large DNA fragments with only 2-base pair overhangs, although this conclusion is based on a small number of experiments. Ultimately, the vector-phosphatase method appears to have efficiently generated a library with large, cloned segments. Use of pJE-2 to generate a highly representative genomic library is described in the next chapter.

Chapter 4: DNA Library Preparation using Vector pJE-2 and Gene Cluster Expression in *Streptomyces* Hosts

4.1 Introduction

A genomic library is a comprehensive collection of clones representing the entire genome of an organism. The construction of a genomic library begins with the isolation of high-quality genomic DNA, followed by fragmentation into smaller pieces, typically using restriction digestion. These DNA fragments are then inserted into a suitable cloning vector and transformed into *E. coli*. As a result, the genomic library contains copies of the organism's complete genetic information (Singh *et al.*, 2021).

Discovery that Actinobacteria possess cryptic biosynthetic gene clusters (BGCs) that are not reflected in their observable metabolic profiles first emerged from sequencing of the *Streptomyces coelicolor* A3(2) genome via cosmid library construction (Bentley *et al.*, 2002). This discovery led scientists to develop methods for accessing these cryptic or "silent" BGCs. One strategy involved constructing genomic libraries to capture and clone the silent BGCs, which could then be expressed in heterologous hosts to uncover novel NPs (Park *et al.*, 2022; Martínez-Burgo *et al.*, 2014). Details of the different types of cloning vectors such as cosmids, BACs, PACs and YACs and their advantages and disadvantages are discussed in section 1.6.1.

Efforts have been made to increase the insert size of the constructed gDNA libraries, since most of the BGCs responsible for the production of antibiotics such as daptomycin, erythromycin, vancomycin are large, often exceeding 50 kbp (Gomez-Escribano and Bibb, 2012; Baltz, 2019) and it is important to be able to study and manipulate entire functional BGCs.

Recent advances in BGC cloning from Actinomycetes both *in vivo* and *in vitro*, have largely centred around targeted cloning strategies, often leveraging CRISPR-Cas9 technology (Wan, Ma and Yuan, 2023), which are described in detail with their respective pros and cons in chapter one (section 1.6.2). While constructing a genomic DNA library can be time-consuming and labour-intensive, compared to targeted cloning strategies, it offers a significant advantage by being applicable to genetically intractable or even potentially, uncultured organisms. This makes genomic library construction a valuable approach for uncovering the biosynthetic potential of rare and less-studied microorganisms.

Here, the pJE-2 vector (as described in the previous chapter) was used to generate a genomic library from an interesting laboratory strain, *Actinomadura madurae* T576 (Figure 4.1a), which makes a series of novel sulphated compounds. The tentative structure of the major compound is shown in Figure 4.1b. A crude extract of *A. madurae* T576 also exhibits bioactivity against *Bacillus subtilis* (unpublished work). This strain has so far been refractory to genetic

manipulation. Construction of a gDNA library would provide an alternative way to access its biosynthetic potential.

Regardless of the cloning method employed, characterization of the products of cloned BGCs requires their expression in a host capable of synthesising the encoded NP molecules. Important attributes of an effective expression host include: genetic tractability, minimal background production of native secondary metabolites, absence of inherent biological activity, rapid growth, and high production yields of heterologously expressed BGCs (Baltz, 2010). Early examples of widely used heterologous hosts include *Streptomyces albus* J1074 (Chater and Wilde, 1976), *Streptomyces lividans* 1326 (Thompson, Ward and Hopwood, 1982), and *Streptomyces coelicolor* strains M1146, M1152, and M1154 (Gomez-Escribano and Bibb, 2011), which were discussed in section 1.6.4.

Recent advancements in this area have focused on the development of "cluster-free" *Streptomyces* hosts. These engineered strains lack endogenous BGCs, thereby significantly reducing background metabolite production and enhancing the detection of heterologously expressed products. Some strains have also been modified to enable extra copies of the cloned BGC to be inserted, to increase synthesis of the target compound. Notable examples include *S. albus* Del14 (Myronovskyi *et al.*, 2018) and *S. lividans* YA10 (Ahmed *et al.*, 2020), which were both genome minimized version of *S. albus* J1074 and *S. lividans* TK24 respectively.

In this study, both *S. albus* Del14 and *S. lividans* YA10 were utilized as expression hosts for BGCs derived from *A. madurae* T576. The primary objective was to clone the BGC responsible for producing the novel sulphated metabolites and then successfully express it in one of these improved hosts.

4.2 Results and Discussion

4.2.1 Genomic Library Preparation from A. madurae T576

HMW gDNA from *A. madurae* T576 was extracted using the method described in chapter 3. The cells of this strain, even when grown on YEME supplemented with 0.5% (w/v) glycine, tend to clump together. To address this, a 100 µm nylon cell strainer (Falcon) was used to separate the cells prior to washing and embedding in agarose plugs. Genomic DNA was partially digested with *Sau*3AI for different time periods (0, 2.5, 5, 7.5, 10 and 15 mins), and ligated to the *Bam*HI-digested pJE-2 vector. Figure 4.2 shows the results of separating the digested DNA samples using an optimized CHEF-DR II protocol. DNA fragments from the 2.5- and 5-minute digests (highlighted in white boxes) were selected for size >50 kbp, and recovered from the gel segment using the agarase method (chapter 2.3.17). Samples of the recovered

fragments were subjected to AGE (Figure 4.3). The presence of intact bands above the 10 kb marker (from the 1 kb NEB ladder) indicated that the recovered fragments were large and mainly free from degradation. These fragments were ligated to the pJE-2 vector and transformed into BAC replicator cells, with selection for apramycin. 8 clones were picked from each transformation and grown in the presence of arabinose. Amplified plasmids were isolated and digested with *SnaB*I and *Xcm*I to estimate their insert sizes (Figure 4.4). Clones from the 5-minute digest (red box) generally contained larger inserts with fewer empty vectors, for reasons that are not clear. In total, 576 clones were preserved in 96 well plates.

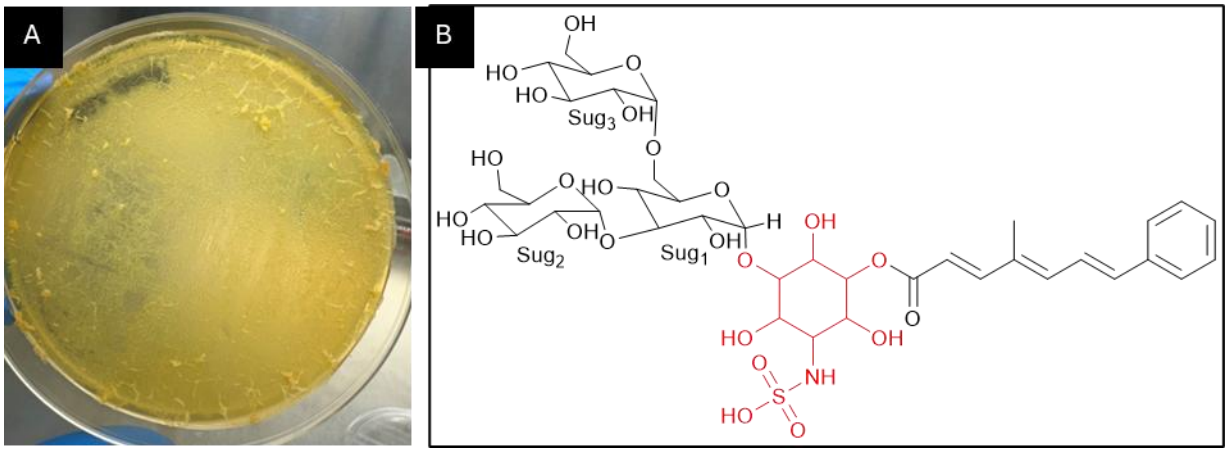

Figure 4.1 A, *A. madurae* T576 grown on YEME agar. B, tentative chemical structure of novel sulphated compounds from *A. madurae* T576.

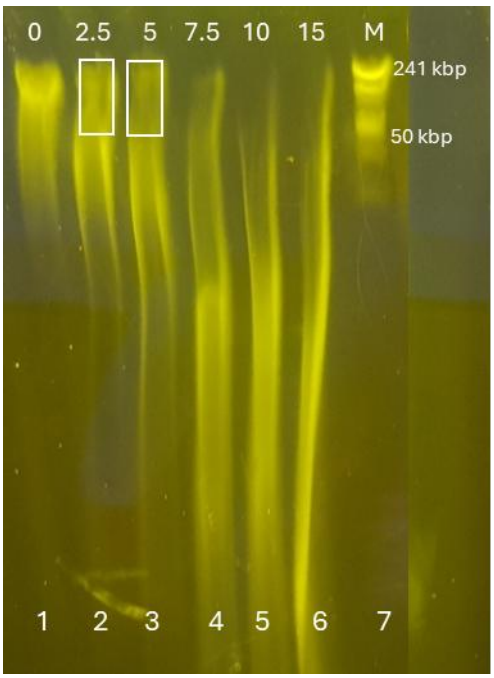

Figure 4.2 PFGE run on CHEF DR II (200V, 0.1-25 s switch time, 20 h) using 0.75% (w/v) LMP agarose in 0.5X TBE. Lanes 1-6: HMW *A. madurae* T576 DNA partially digested with *Sau*3AI for 0, 2.5, 5, 7.5, 10 and 15 mins, respectively; lanes 7: MidRange PFGE marker (NEB); white boxes highlight the regions used for size selection**.**

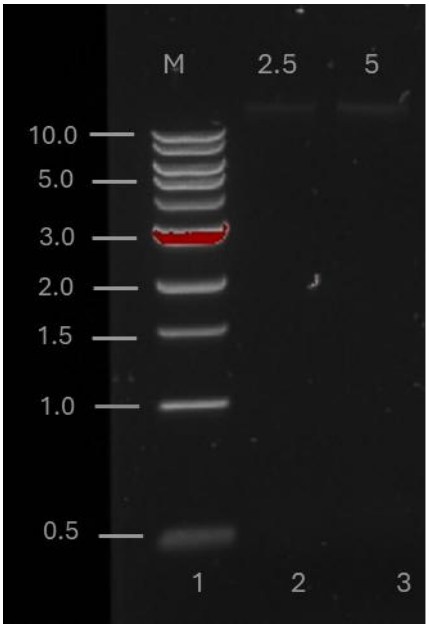

Figure 4.3 AGE of size selected DNA fragments recovered from the gel shown in Figure 4.2 (100V, 1h, 1% (w/v) agarose, 1X TBE). Lane 1, 1-kbp DNA marker; lanes 2-3, recovered fragments from the 2.5- and 5-min timepoints, respectively.

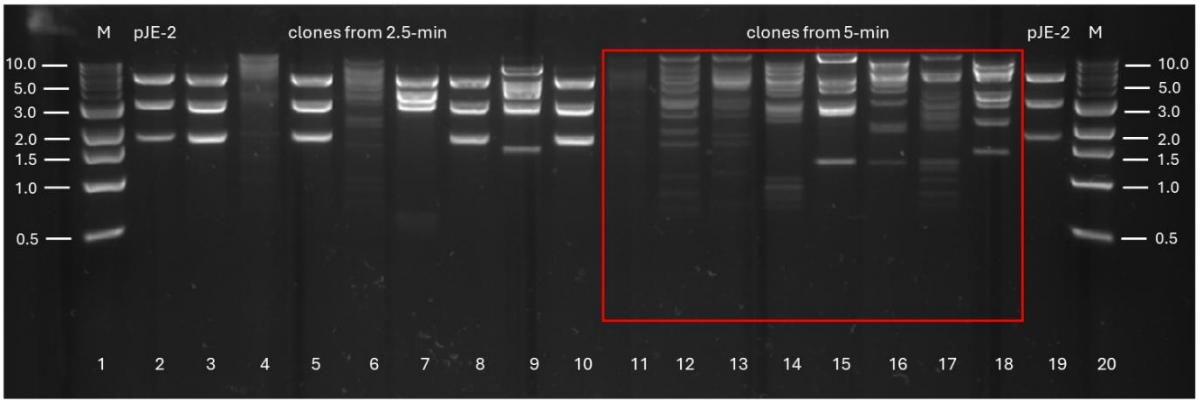

Figure 4.4 AGE for characterization of inserts in the *A. madurae* T576 genomic library (100V, 1 h, 1% (w/v) agarose, 1X TBE). Lane 1, 1-kbp DNA marker; lanes 2 and 19, pJE-2 vector digested with *SnaB*I and *Xcm*I; lanes 3-18, eight random clones from the partially digested fragments of the 2.5-min (3-10) or 5-min (11-18) BAC libraries; lane 20, 1 kb DNA marker.

4.2.2 Cloning of the potential BGC linked to the novel sulphated compounds

The genome of *A. madurae* T576 is 9.4 Mbp in size and was sequenced using a combination of Nanopore and Illumina technologies, performed by MicrobesNG (Birmingham University, UK). Analysis of the genomic sequence using antiSMASH 7.0 (Blin et al., 2021) identified a total of 29 BGCs (Table 4.1). Among these, region 5, which was predicted to be an ~80 kbp hybrid BGC combining features of both Types I and III polyketide synthase (PKS) systems, was of particular interest. Table 4.2 summarizes the genes with their predicted functions in the potential BGC for the sulphated compounds. The cluster includes several genes predicted to be associated with inositol biosynthesis (highlighted in blue) and sulfotransferase genes (highlighted in green), consistent with their potential role in biosynthesis of the sulphated metabolites

Table 4.1 Summary of all regions of *A. madurae* T576 based on antiSMASH results.

Region	Type	From	To	Most similar known cluster		similarity
Region 1	Betalactone	508,405	538,270			
Region 2	NRPS	690,974	763,600	crochelin A	NRP + Polyketide	12%
Region 3	Redox-co factor	889,330	911,509	sch-47554/Sch-47555	Polyketide	3%
Region 4	NRPS-like	1,399,737	1,462,386	coprisamide C/ coprisamide D	NRP	21%
Region 5	T1PKS, T3PKS	1,526,244	1,605,633	5-dimethylallylindole-3-acetonitrile	Other	55%
Region 6	terpene, lanthipeptide-class-iv	1,786,998	1,826,182	hopene	Terpene	38%
Region 7	PKS-like	2,882,636	2,923,673	vazabitide A	NRP	15%
Region 8	Terpene	2,999,847	3,022,123	pyrroloformamide A/ pyrroloformamide B/ pyrroloformamide D/ pyrroloformamide C	NRP + Other	12%
Region 9	Terpene	3,273,280	3,299,312	hopene	Terpene	46%
Region 10	Terpene	3,955,294	3,976,214	frankiamicin	Polyketide	14%
Region 11	Terpene	4,136,545	4,157,648			
Region 12	lanthipeptide-class-ii	4,214,163	4,236,604	cinnamycin B	RiPP	26%
Region 13	Terpene	4,288,152	4,309,056	isorenieratene	Terpene	18%
Region 14	T1PKS	4,430,990	4,476,602	maklamicin	Polyketide	4%
Region 15	phosphonate	5,429,216	5,440,082			
Region 16	lanthipeptide-class-iv	5,614,509	5,637,466			
Region 17	T3PKS	5,679,807	5,720,451	lagunapyrone A/ lagunapyrone B/ lagunapyrone C	Polyketide	22%
Region 18	Terpene	6,675,568	6,696,761	2-methylisoborneol	Terpene	50%
Region 19	NI-siderophore	6,774,740	6,806,530	peucechelin	NRP	15%

Region 20	Terpene	7,623,221	7,644,240	chlortetracycline	Polyketide	8%
Region 21	RiPP-like	7,720,936	7,731,745			
Region 22	Ectoine	8,003,646	8,014,041	ectoine	Other	75%
Region 23	Betalactone	8,126,777	8,157,301	fengycin	NRP	20%
Region 24	T2PKS	8,265,541	8,338,140	WS 79089B/ benaphthamycin/ WS 79089D/ WS 79089A/WS 79089C	Polyketide	10%
Region 25	T2PKS, PKS-like	8,341,629	8,414,065	sch-47554/Sch-47555	Polyketide	9%
Region 26	thiopedptide	8,458,472	8,489,364	GE2270A	RiPP: thiopeptide	22%
Region 27	lanthipeptide-class-i	8,520,429	8,546,078	SF2487	Polyketide	8%
Region 28	NRP-metallophore,NRPS	8,933,137	9,005,805	madurastatin D1/D2/C1	NRP	37%
Region 29	T1PKS, oligosaccharide	9,087,549	9,157,195	calicheamicin	Polyketide	50%

Blue – regions screened in the generated *A. madurae* T576 BAC library

Table 4.2 Gene names in the potential sulphated compounds BGC and their predicted function.

Locus_Tag	Predicted / known protein function
T576_01470	Baeyer-Villiger monooxygenase
T576_01471	hypothetical protein
T576_01472	Serine 3-dehydrogenase
T576_01473	Trypsin
T576_01474	10 kDa chaperonin 1
T576_01475	putative glycosyltransferase
T576_01476	Arylsulfotransferase
T576_01477	6-deoxyerythronolide-B synthase EryA2
T576_01478	Narbonolide/10-deoxymethynolide synthase PikA1
T576_01479	Linear gramicidin synthase subunit D
T576_01480	alpha/beta hydrolase
T576_01481	glycosyltransferase
T576_01482	Arylsulfotransferase
T576_01483	MATE family efflux transporter
T576_01484	Beta-glucosidase BoGH3B
T576_01485	Thioesterase PikA5
T576_01486	Sulfotransferase family protein
T576_01487	Alpha-pyrone synthesis polyketide synthase-like Pks11
T576_01488	condensation domain-containing protein
T576_01489	hypothetical protein
T576_01490	hypothetical protein
T576_01491	hypothetical protein
T576_01492	Arylsulfotransferase
T576_01493	hypothetical protein
T576_01494	Transcriptional regulatory protein DegU
T576_01495	Inositol-1-monophosphatase
T576_01496	Polyketide synthase PksL
T576_01497	UDP-4-amino-4-deoxy-L-arabinose--oxoglutarate aminotransferase
T576_01498	Inositol-3-phosphate synthase
T576_01499	Mycocerosic acid synthase-like polyketide synthase
T576_01500	MIO-dependent tyrosine 2,3-aminomutase
T576_01501	Long-chain-fatty-acid--CoA ligase
T576_01502	3-oxoacyl-[acyl-carrier-protein] synthase 2

T576_01503	3-oxoacyl-[acyl-carrier-protein] synthase 2
T576_01504	Mycocerosic acid synthase
T576_01505	3-oxoacyl-[acyl-carrier-protein] reductase FabG1
T576_01506	hypothetical protein
T576_01507	MFS transporter
T576_01508	MFS transporter
T576_01509	hypothetical protein
T576_01510	Regulatory protein AfsR
T576_01511	helix-turn-helix transcriptional regulator
T576_01512	Nucleoid-associated protein Lsr2
T576_01513	Mitomycin radical oxidase
T576_01514	HTH-type transcriptional regulatory protein GabR
T576_01515	MFS transporter small subunit
T576_01516	Oxalate:formate antiporter
T576_01517	MFS transporter
T576_01518	HTH-type transcriptional repressor KstR2

Green- sulfotransferase genes
Blue- genes involve in inositol biosynthesis

To investigate the involvement of this BGC in the biosynthesis of the target compounds, the constructed gDNA library was screened using primers specific to the sulfotransferase gene (Sulfo-screen-F and Sulfo-screen-R; sequences provided in Table 2.5**)**. Clones were induced with arabinose to increase the yield of plasmid DNA for screening. Then, the plasmid DNAs from each row of colonies in the 96-well plates were pooled and subjected to PCR amplification. Figure 4.5 shows the screening results for plates I and II. The positive controls (lanes 2 and 19), derived by using gDNA from *A. madurae* T576, consistently yielded a 1.25 kb amplicon, corresponding to the expected product size. In contrast, PCR amplification of pooled pDNA from rows F and G of plate I produced distinct bands of different sizes, which did not match the positive control, indicating possible non-specific amplification. Screening of plates III and IV, as shown in Figure 4.6, revealed positive signals in lanes 16–18 (highlighted with a red box), corresponding to pooled pDNA from rows F, G, and H of plate IV. These bands matched the size of the positive control amplicon (lane 19), suggesting the presence of the target gene. To identify the individual positive clones, pDNA from each well in the corresponding rows was further screened. (Hereafter, clones are given designations corresponding to the plate number, row and then well number.) Gel analysis (Figure 4.7) identified four clones 4F3, 4G5, 4H6, and 4H9 as positive by PCR. These candidates were further validated by insert-end sequencing to confirm their integrity and assess whether they contained the complete BGC. Sequencing

results showed that clones 4H6 and 4H9 were false positives. Clone 4F3 (yellow in Figure 4.8), while approximately 100 kbp in size, did not contain the full BGC (black in Figure 4.8). In contrast, clone 4G5 (pink in Figure 4.8) was identified as a ~120 kbp construct containing the complete BGC of interest. These results identified clone 4G5 as the lead candidate for further investigation into the biosynthesis of the novel sulphated compounds.

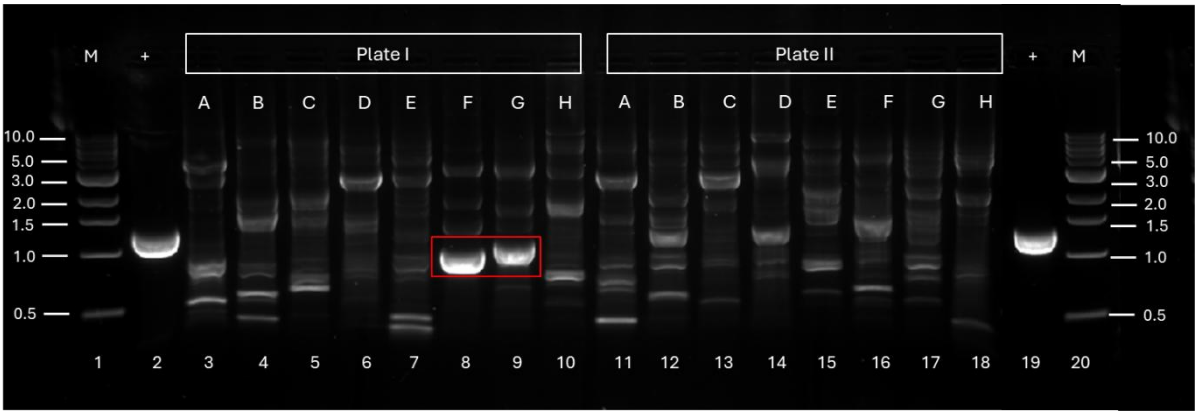

Figure 4.5 AGE image of library screening for the sulfotransferase gene (100V, 1h, 1% (w/v) agarose, 1X TBE). Lanes 1 and 20, 1-kbp marker; lanes 2 and 19, positive controls (gDNA template); lanes 3-10, pooled pDNA from plate I rows A-H; lanes 11-18, pooled pDNA from plate II rows A-H; red box, bands possibly matching the positive controls.

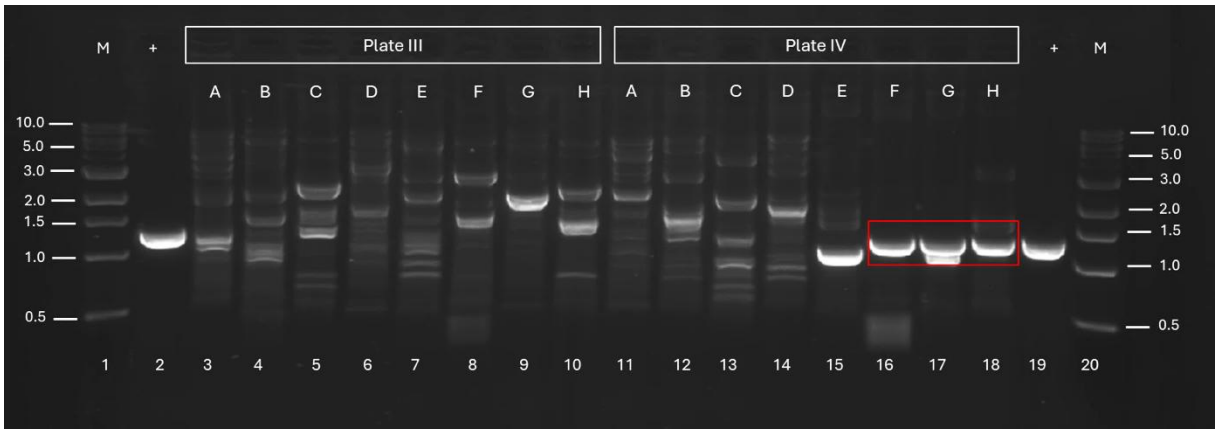

Figure 4.6 AGE image of library screening for the sulfotransferase gene (100V, 1 h, 1% (w/v) agarose, 1X TBE). Lanes 1 and 20, 1-kb marker; lanes 2 and 19, positive controls (gDNA template); lanes 3-10, pooled pDNA from plate III rows A-H; lanes 11-18, pooled pDNA from plate IV rows A-H; red box, bands possibly matching the positive controls.

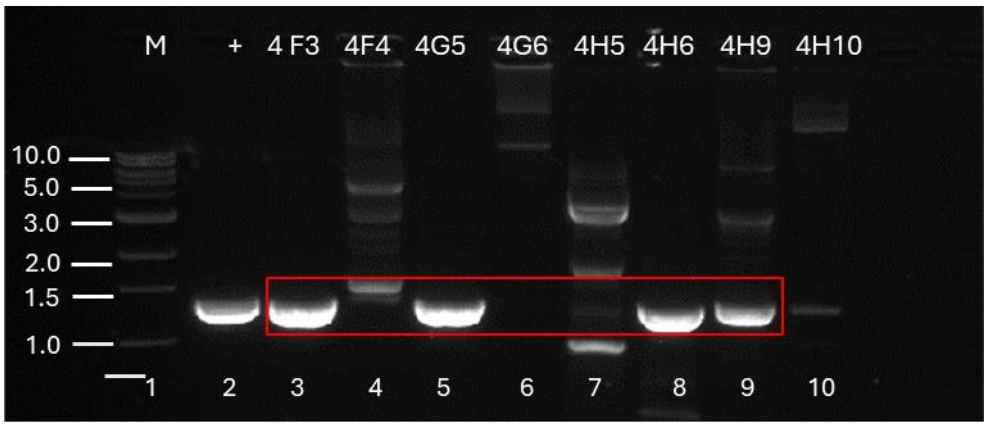

Figure 4.7 AGE image of library screening for the sulfotransferase gene (100V, 1 h, 1% (w/v) agarose, 1X TBE). Lane 1, 1-kbp marker; lane 2, positive control (gDNA template); lanes 3-4, pDNA from 4F3 and 4F4; lanes 5-6, pDNA from 4G5 and 4G6; lanes 7-8, pDNA from 4H5 and 4H6; lanes 9-10, pDNA from 4H9 and 4H10; red box, bands possibly matching the positive controls.

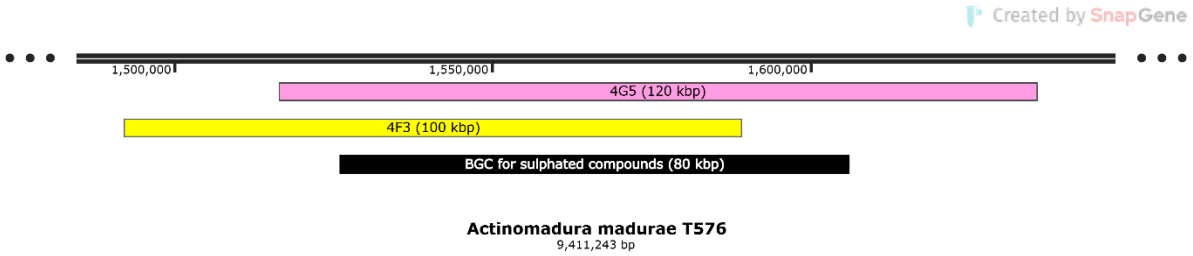

Figure 4.8 Graphical presentation of the coverage of clone 4G5 (120 kbp, pink) and clone 4F3 (100 kbp, yellow) vs potential BGC for the sulphated compounds (80 kbp, black) after insert-end sequencing.

4.2.3 Screening the A. madurae *T576 gDNA Library for other BGCs*

The antiSMASH analysis of *A. madurae* T576 (Table 4.1) revealed additional regions that appear potentially cryptic or uncharacterized due to their low percentage similarity to entries in the antiSMASH database and other databases like MIBiG (Blin *et al.*, 2023). Among these, nine regions—2, 4, 7, 14, 24, 25, 27, 28 and 29 (highlighted in blue in Table 4.1)—were selected for targeted screening. To facilitate this, specific primer pairs were designed for each region, with their sequences listed in Table 2.5.

The genomic library of *A. madurae* T576 was screened using the same pooled pDNA approach as employed above. Each plate was further grouped by pooling rows A and B, C and D, E and F, and G and H, resulting in a total of four pooled pDNA samples per plate. When a positive signal was detected, the process was refined by screening individual rows within the pooled sample and subsequently narrowing it down to individual clones. This stepwise approach allowed for the identification of specific clones harbouring the BGCs of interest.

Region 2 BGC

Region 2 is a 72.6 kbp predicted NRPS cluster that exhibits low (12%) similarity to siderophore crochelin A (Baars *et al.*, 2018), suggesting the potential for a novel metabolite. The screening results for region 2 (Figure 4.9) indicated positive signals in rows C and D of plate IV matching the mobility of the positive control (lane 19). Further screening identified clone 4C11 as a candidate with a positive signal for region 2 (Figure 4.10). To test this, the clone was subjected to insert-end sequencing. However, the results suggested that clone 4C11 was a false positive, indicating the amplicon did not originate from the desired region, or possibly that the clone contained more than one insert. Interestingly, in Figure 4.10, the amplicon from clone 4C11 appeared slightly larger than the positive control. This size discrepancy raised the possibility that the primers annealed to off-target sites in the template pDNA.

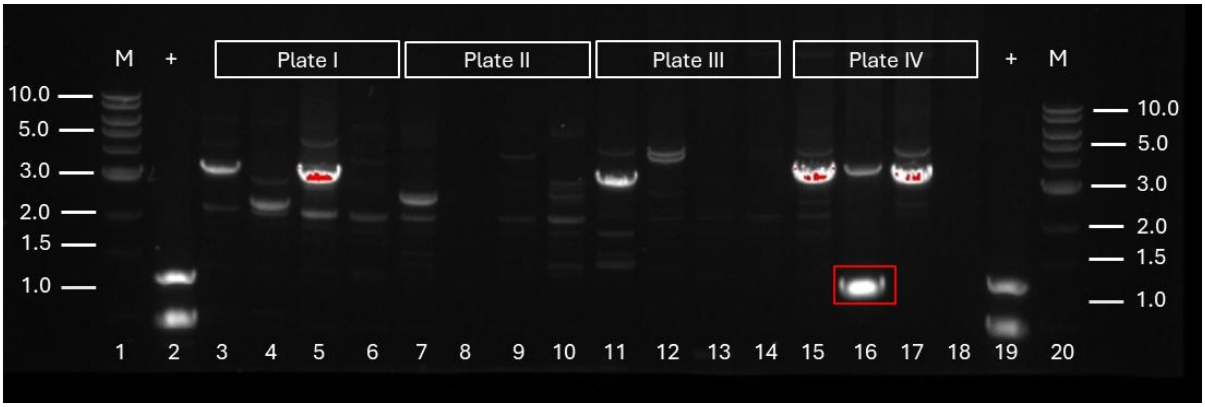

Figure 4.9 AGE image of library screening for the region 2 (100V, 1 h, 1% (w/v) agarose, 1X TBE). Lanes 1 and 20, 1-kbp marker; lanes 2 and 19 positive controls (gDNA template); lanes 3-6, pooled pDNA from plate I rows A-H; lanes 7-10, pooled pDNA from plate II rows A-H; lanes 11-14, pooled pDNA from plate III rows A-H; lanes 15-18, pooled pDNA from plate IV rows A-H; red box, band possibly matching the positive controls.

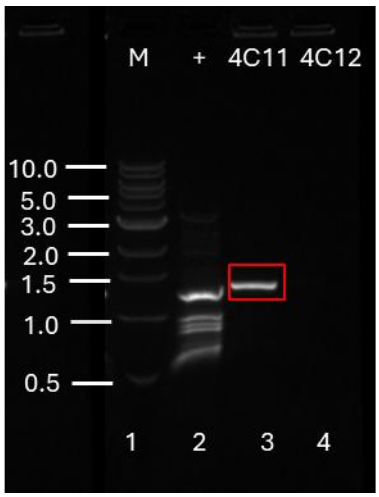

Figure 4.10 AGE image of library screening for region 2 (100V, 1 h, 1% (w/v) agarose, 1X TBE). Lane 1, 1-kbp marker; lanes 2 positive control (gDNA template); lanes 3-4, pDNA from 4C11 and 4C12; red box, bands possibly matching the positive controls.

Region 4 BGC

Region 4 was identified as an NRPS-like BGC with an estimated size of approximately 62.6 kbp. The antiSMASH analysis revealed that it shares 21% similarity to the antibiotic coprisamide C/D (Shin *et al.*, 2021). Screening the 4 plates gave a positive PCR signal with the pooled samples from rows C and D of plate I (Figure 4.11). Further analysis narrowed the positive signal to an individual clone, designated as 1D1 (Figure 4.12). End-sequencing of clone 1D1 revealed that this clone is approximately 124 kbp in length and successfully harbours the entirety of the 62.6 kbp region 4 (Figure 4.13). This result establishes 1D1 as a key clone for further investigating the biosynthesis of compounds associated with region 4, potentially unlocking insights into the production of coprisamide-like molecules.

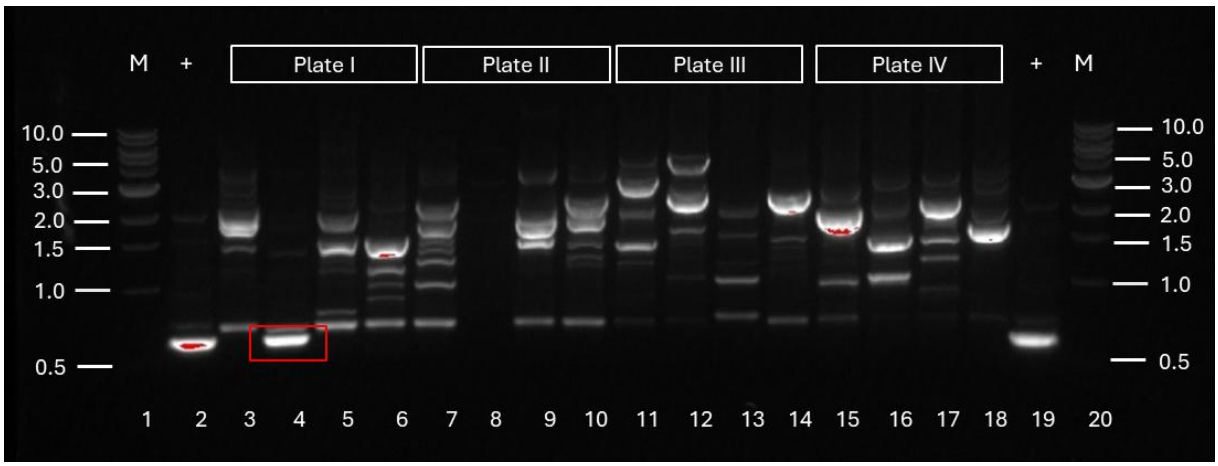

Figure 4.11 AGE image of library screening for the region 4 (100V, 1 h, 1% (w/v) agarose, 1X TBE). Lanes 1 and 20, 1-kbp marker; lanes 2 and 19, positive controls (gDNA template); lanes 3-6, pooled pDNA from plate I rows A-H; lanes 7-10, pooled pDNA from plate II rows A-H; lanes 11-14, pooled pDNA from plate III rows A-H; lanes 15-1,8 pooled pDNA from plate IV rows A-H; red box, band possibly matching the positive controls.

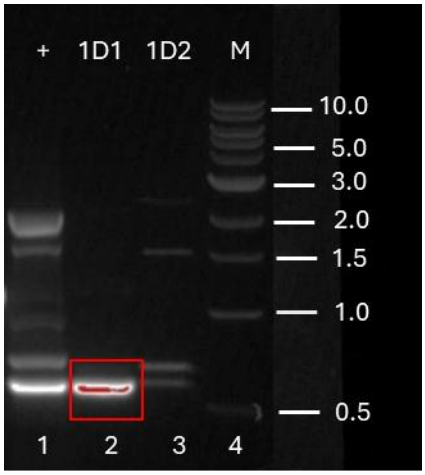

Figure 4.12 AGE image of library screening for region 4 (100V, 1 h, 1% (w/v) agarose, 1X TBE). Lane 4, 1-kbp marker; lanes 1 positive control (gDNA template); lanes 2-3, pDNA from 1D1 and 1D2; red box, band possibly matching the positive controls.

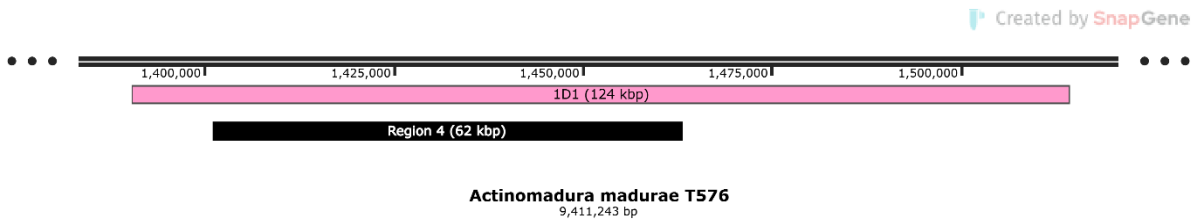

Figure 4.13 Graphical presentation of the coverage of clone 1D1 (124 kbp, pink) vs region 4 (62 kbp, black) after insert-end sequencing.

Region 7 BGC

Region 7 contains a PKS-like BGC with an estimated size of 41 kbp and a 15% similarity to vazabitide A (Hasebe *et al.*, 2016). PCR screening (Figure 4.14), revealed positive signals in

lanes 6 and 7, corresponding to pooled samples from plate I rows G and H and plate II rows A and B. To pinpoint the source of these signals, the pooled samples were further analysed at the row level, confirming positive results from plate I row G and plate II row B. Single-clone screening subsequently identified clones 1G12 and 2B9 as the sources of the positive signals, as depicted in Figure 4.15. Insert-end sequencing of these clones was performed to determine their genomic composition (Figure 4.16), revealing that clone 1G12 (pink) has a 63.6 kbp insert, while that of clone 2B9 (yellow) measures 48.7 kbp. While clone 2B9 does not span the entirety of the 41 kbp region 7, the larger 2G12 clone is sufficient to cover the complete cluster.

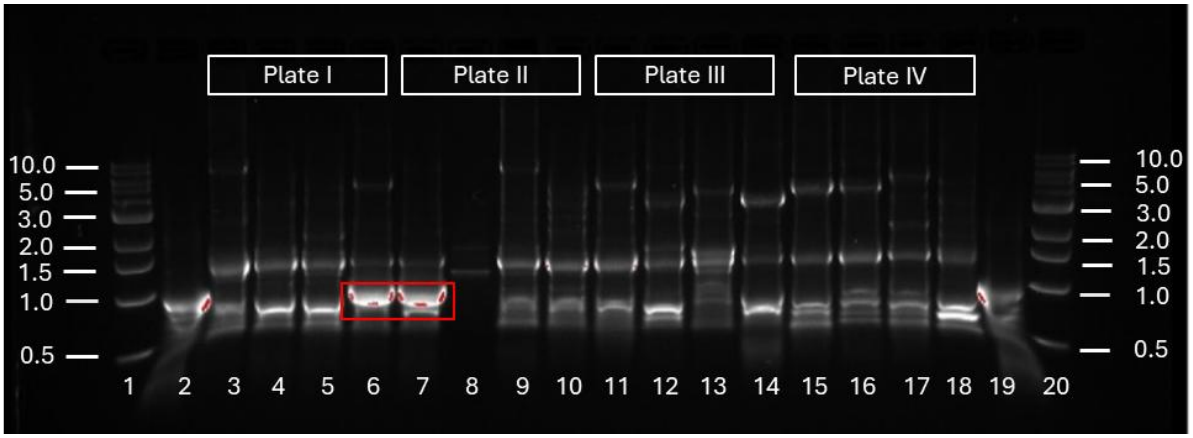

Figure 4.14 AGE image of library screening for the region 7 (100V, 1 h, 1% (w/v) agarose, 1X TBE). Lanes 1 and 20, 1-kbp marker; lanes 2 and 19 positive controls (gDNA template); lanes 3-6, pooled pDNA from plate I rows A-H; lanes 7-10, pooled pDNA from plate II rows A-H; lanes 11-14, pooled pDNA from plate III rows A-H; lanes 15-18, pooled pDNA from plate IV rows A-H; red box, bands possibly matching the positive controls.

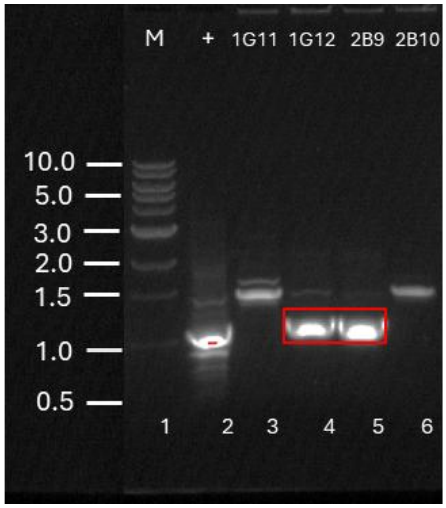

Figure 4.15 AGE image of library screening for region 7 (100V, 1 h, 1% (w/v) agarose, 1X TBE). Lane 1, 1-kbp marker; lane 2, positive control (gDNA template); lanes 3-4, pDNA from 1G11 and 1G12; lanes 5-6, pDNA from 2B9 and 2B10; red box, bands possibly matching the positive controls.

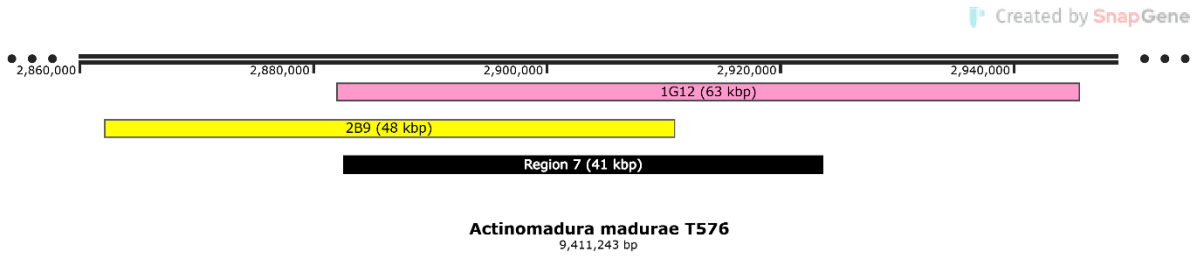

Figure 4.16 Graphical presentation of the coverage of clone 1G12 (63 kbp, pink) and clone 2B9 (48 kbp, yellow) vs region 7 (41 kbp, black) after insert-end sequencing.

Region 14 BGC

Region 14 is a 45.6 kbp T1 PKS BGC with low (4%) similarity to the antibiotic maklamicin (Igarashi *et al.*, 2011), as determined by ClusterBlast. Screening results revealed two pooled pDNA samples that produced positive signals, specifically from plate II rows G and H, and plate III rows C and D (Figure 4.17). Individual row analysis revealed positive signals from plate II rows G and H, but no signal was detected in plate III rows C and D (data not shown). Subsequent PCR screening of clones from rows G and H on plate II showed five positive signals in lanes 6, 8, 9, 13, and 14 (Figure 4.18). However, the bands corresponding to these positive clones were slightly greater in size than expected from the positive control. These discrepancies in the fragment sizes suggested non-specific binding of the designed primers. One of the identified clones, 2G8, was sent for end sequencing, which confirmed it to be a false positive, consistent with the observed size mismatch with the positive control.

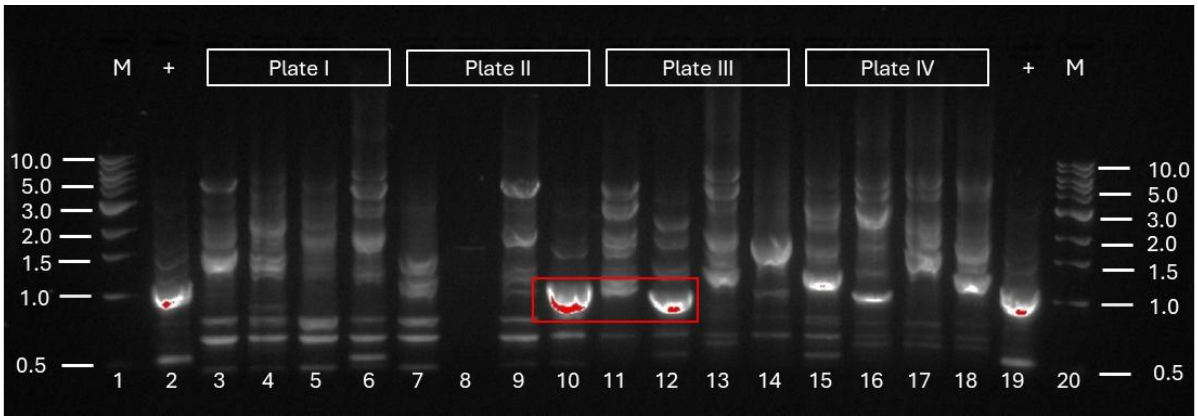

Figure 4.17 AGE image of library screening for the region 14 (100V, 1 h, 1% (w/v) agarose, 1X TBE). Lanes 1 and 20, 1 kbp marker; lanes 2 and 19, positive controls (gDNA template); lanes 3-6, pooled pDNA from plate I rows A-H; lanes 7-10, pooled pDNA from plate II rows A-H; lanes 11-14, pooled pDNA from plate III rows A-H; lanes 15-18, pooled pDNA from plate IV rows A-H; red box, bands possibly matching the positive controls.

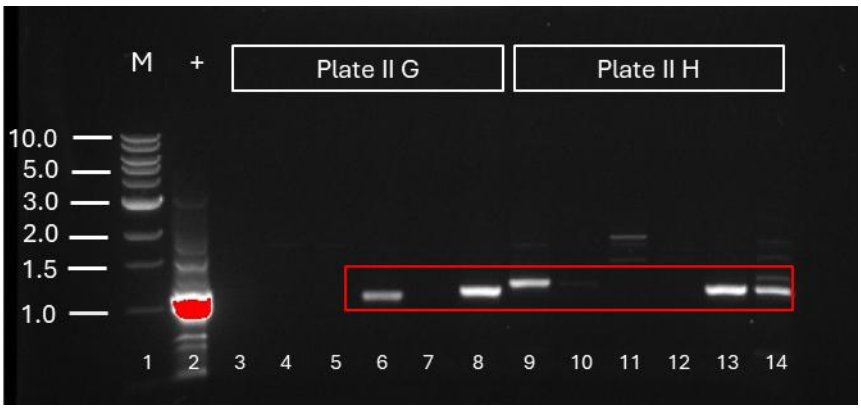

Figure 4.18 AGE image of library screening for region 14 (100V, 1 h, 1% (w/v) agarose, 1X TBE). Lane 1, 1-kb marker; lanes 2, positive control (gDNA template); lanes 3-8, pooled pDNA from plate II row G; lanes 9-14, pooled pDNA from plate II row H; red box, bands possibly matching the positive controls.

Region 24 BGC

Region 24 is a 72.5 kbp BGC, identified as a Type II PKS cluster with a 10% similarity to the antibiotic benaphthamycin (Ritzau *et al.*, 1997). Screening results for region 24 showed two pooled pDNA samples exhibiting signals matching the positive control (Figure 4.19). These positive signals were found in pooled pDNA from plate II rows E and F, as well as plate III rows A and B. Further analysis revealed that clones 2E12 and 3B8 exhibited band sizes similar to those of the positive control (Figure 4.20). However, insert-end sequencing revealed that 2E12 (pink) and 3B8 (yellow) had inserts of 60.6 kbp and 40 kbp, respectively, smaller than the target region (Figure 4.21), indicating that these clones only partially overlapped the target region.

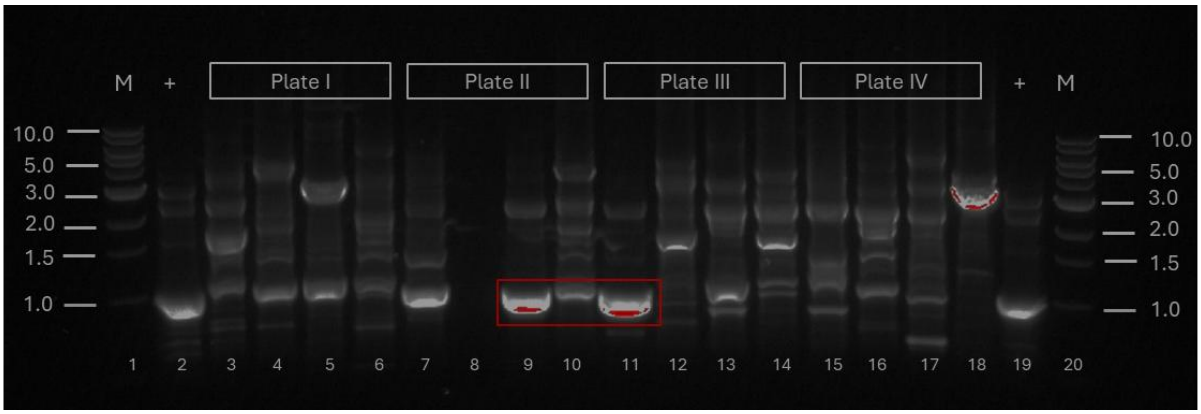

Figure 4.19 AGE image of library screening for the region 24 (100V, 1 h, 1% (w/v) agarose, 1X TBE). Lanes 1 and 20, 1-kbp marker; lanes 2 and 19, positive controls (gDNA template); lanes 3-6, pooled pDNA from plate I rows A-H; lanes 7-10, pooled pDNA from plate II, rows A-H; lanes 11-14, pooled pDNA from plate III rows A-H; lanes 15-18, pooled pDNA from plate IV rows A-H; red box, bands possibly matching the positive controls.

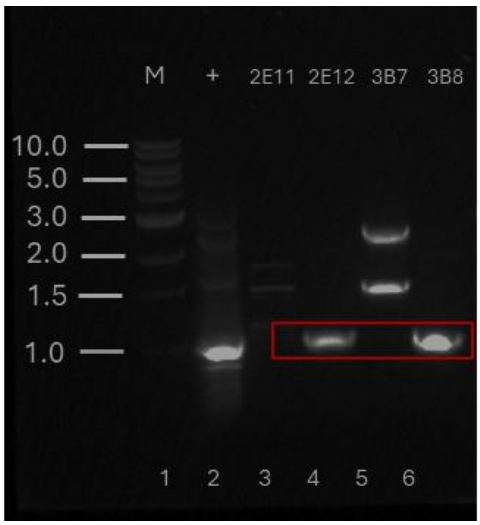

Figure 4.20 AGE image of library screening for region 24 (100V, 1 h, 1% (w/v) agarose, 1X TBE). Lane 1, 1-kbp marker; lane 2, positive control (gDNA template); lanes 3-4, pDNA from 2E11 and 2E12; lanes 5-6, pDNA from 3B7 and 3B8; red box, bands possibly matching the positive controls.

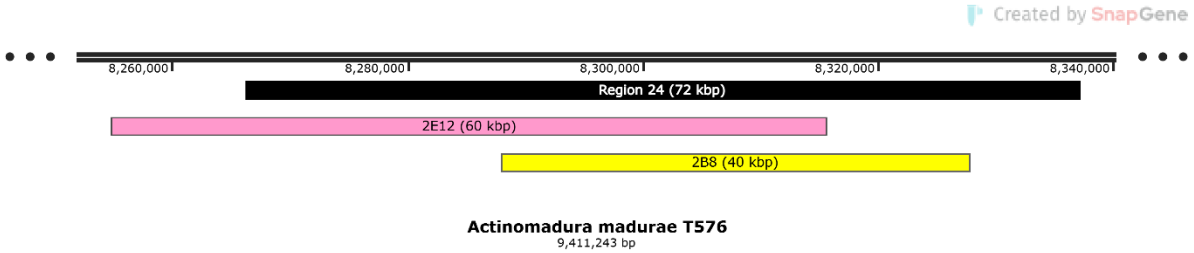

Figure 4.21 Graphical presentation of the coverage of clone 2E12 (60 kbp, pink) and clone 3B8 (40 kbp, yellow) vs region 24 (72 kbp, black) after insert-end sequencing.

Region 25 BGC

Region 25 is predicted to be a type II PKS-like cluster spanning 62.4 kbp, which shares 9% similarity with an unidentified cluster. During the screening of region 25, a positive signal was detected from a pooled pDNA sample derived from plate IV rows G and H (Figure 4.22). Further analysis identified clone 4H12 as the source of the positive signal (Figure 4.23). This clone was subsequently subjected to insert-end sequencing, revealing an insert of 47.5 kbp (pink in Figure 4.24), which falls short of the required 62.4 kbp to fully encompass region 25.

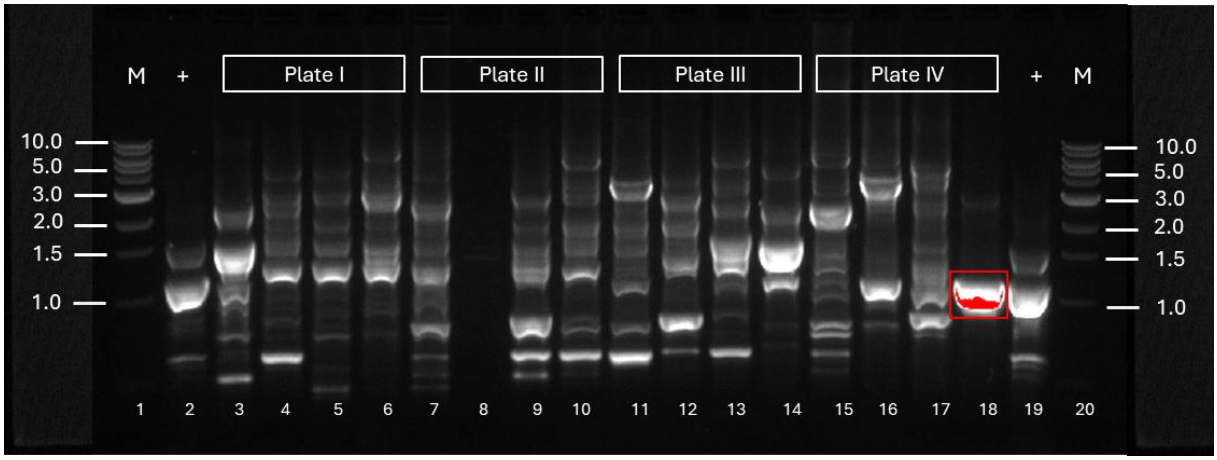

Figure 4.22 AGE image of library screening for the region 25 (100V, 1 h, 1% (w/v) agarose, 1X TBE). Lanes 1 and 20, 1-kbp marker; lanes 2 and 19, positive controls (gDNA template); lanes 3-6, pooled pDNA from plate I rows A-H; lanes 7-10, pooled pDNA from plate II rows A-H; lanes 11-14, pooled pDNA from plate III rows A-H; lanes 15-18 pooled pDNA from plate IV rows A-H; red box, band possibly matching the positive controls.

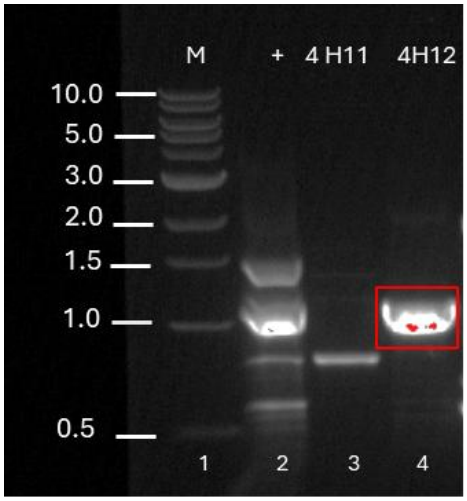

Figure 4.23 AGE image of library screening for region 25 (100V, 1 h, 1% (w/v) agarose, 1X TBE). Lane 1, 1-kbp marker; lane 2 positive control (gDNA template); lanes 3-4, pDNA from 4H11 and 4H12; red box, band possibly matching the positive controls.

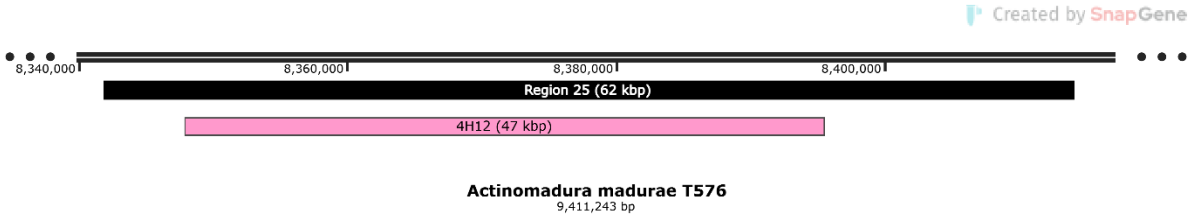

Figure 4.24 Graphical presentation of the coverage of clone 4H12 (47 kbp, pink) vs region 25 (62 kbp, black) after insert-end sequencing.

Region 27 BGC

Region 27, identified as encoding a small lanthipeptide, spans 25.6 kbp and shares 8% similarity with an unknown lanthipeptide. Figure 4.25 presents the screening results for region 27 in which a positive signal was observed in lanes 6 and 16, corresponding to rows G and H of plate I and rows C and D of plate IV. Further screening led to the identification of clone 1G9 as the positive hit, as shown in Figure 4.26. Insert-end sequencing revealed insert of 118 kbp that includes the entire 25.6 kbp region (Figure 4.27).

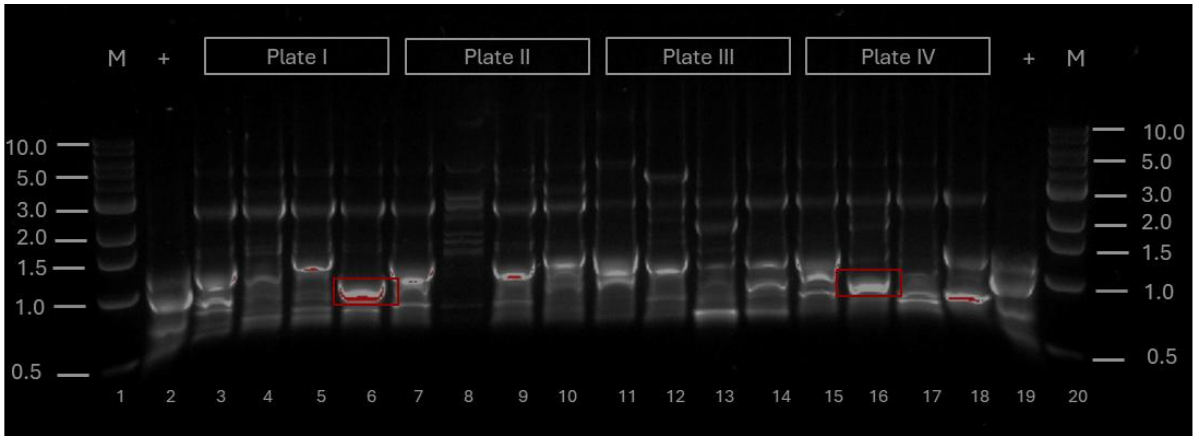

Figure 4.25 AGE image of library screening for the region 27 (100V, 1 h, 1% (w/v) agarose, 1X TBE). Lanes 1 and 20, 1-kbp marker; lanes 2 and 19, positive controls (gDNA template); lanes 3-6, pooled pDNA from plate I rows A-H; lanes 7-10, pooled pDNA from plate II, rows A-H; lanes 11-14, pooled pDNA from plate III rows A-H; lanes 15-18 pooled pDNA from plate IV, rows A-H; red boxes, bands possibly matching the positive controls.

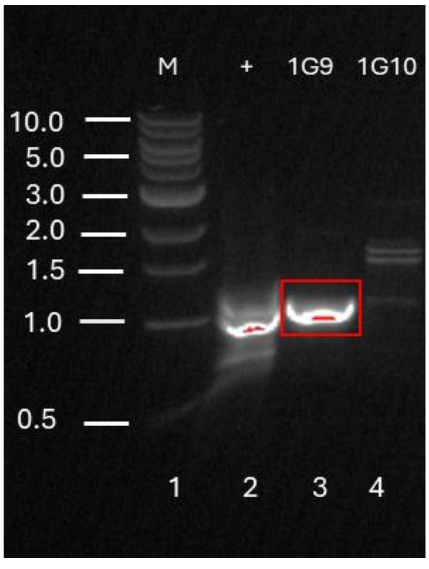

Figure 4.26 AGE image of library screening for region 27 (100V, 1 h, 1% (w/v) agarose, 1X TBE). Lane 1, 1-kbp marker; lane 2, positive control (gDNA template); lanes 3-4, pDNA from 1G9 and 1G10; red box, bands possibly matching the positive controls.

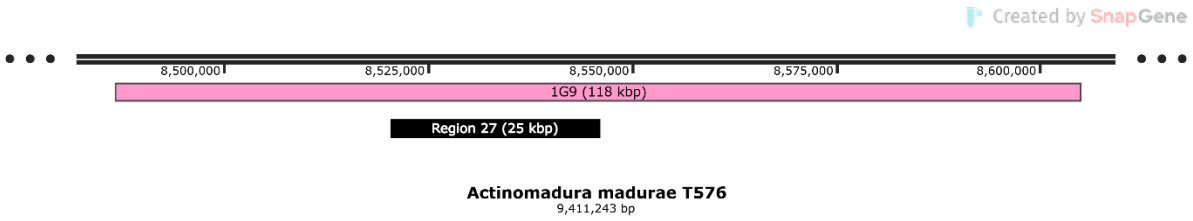

Figure 4.27 Graphical presentation of the coverage of clone 1G9 (118 kbp, pink) vs region 27 (25 kbp, black) after insert-end sequencing.

Region 28 BGC

Region 28 is an NRPS-like cluster, with an estimated size of 72.6 kbp that exhibits 37% similarity to the known siderophore madurastatin (Harada *et al.*, 2004). Screening results showed two pooled pDNA samples which yielded positive signals from plate IV rows E and F, and plate IV rows G and H (Figure 4.28). Further analysis led to the identification of two positive clones, 4E2 and 4G9 as seen in Figure 4.29. Unfortunately, insert-end sequencing revealed that although clone 4G9 (pink in Figure 4.30), at 93.5 kbp, was big enough to cover the 72.6 kbp cluster, it was missing the first 12 kbp of the cluster. Clone 4E2 (yellow in Figure 4.30) was 60 kbp, and therefore too small to encompass region 28.

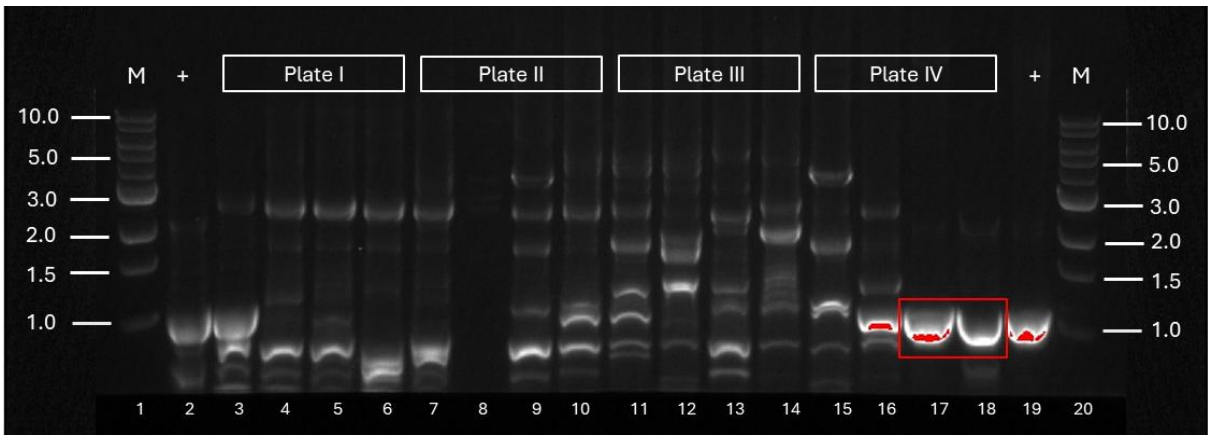

Figure 4.28 AGE image of library screening for the region 28 (100V, 1 h, 1% (w/v) agarose, 1X TBE). Lanes 1 and 20, 1-kbp marker; lanes 2 and 19, positive controls (gDNA template); lanes 3-6, pooled pDNA from plate I rows A-H; lanes 7-10 pooled pDNA from plate II rows A-H; lanes 11-14, pooled pDNA from plate III rows A-H; lanes 15-18, pooled pDNA from plate IV rows A-H; red box, bands possibly matching the positive controls.

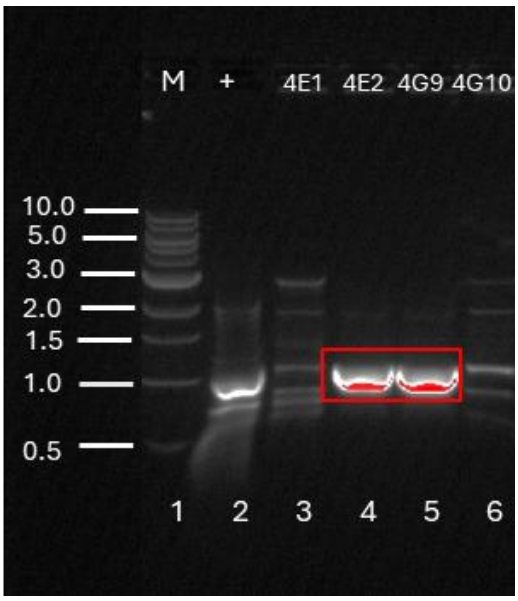

Figure 4.29 AGE image of library screening for region 28 (100V, 1 h, 1% (w/v) agarose, 1X TBE). Lane 1, 1-kbp marker; lane 2, positive control (gDNA template); lanes 3-4, pDNA from 4E1 and 4E2; lanes 5-6, pDNA from 4G9 and 4G10; red box, bands possibly matching the positive controls.

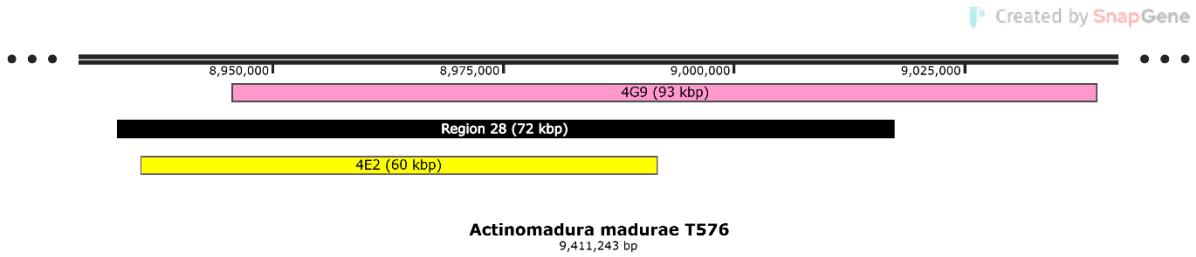

Figure 4.30 Graphical presentation of the coverage of clone 4G9 (93 kbp, pink) and clone 4E2 (60 kbp, yellow) vs region 29 (72 kbp, black) after insert-end sequencing.

Region 29 BGC

Lastly, region 29 is a predicted TypeI-PKS cluster of approximately 69.6 kbp, with 50% similarity to the antitumor NP, calicheamicin (Zein *et al.*, 1988). Initial screening revealed a positive signal corresponding to plate I rows A and B (lane 3 in Figure 4.31). Further analysis led to the identification of positive clone 1B6. However, as seen in Figure 4.32, although clone 1B6 produced a distinct band, the size was slightly larger than the positive control. Insert-end sequencing identified a 70 kbp insert, which did contain the desired PCR target, but did not encompass the full 69.6 kbp of region 29 (Figure 4.33).

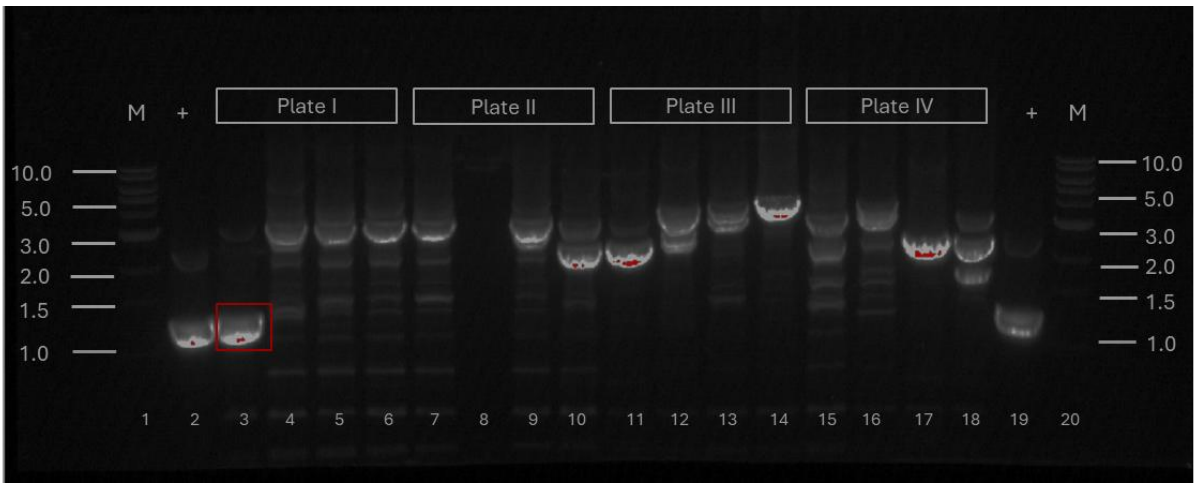

Figure 4.31 AGE image of library screening for the region 29 (100V, 1 h, 1% (w/v) agarose, 1X TBE). Lanes 1 and 20, 1-kbp marker; lanes 2 and 19, positive controls (gDNA template); lanes 3-6, pooled pDNA from plate I rows A-H; lanes 7-10, pooled pDNA from plate II rows A-H; lanes 11-14, pooled pDNA from plate III rows A-H; lanes 15-18, pooled pDNA from plate IV rows A-H; red box, bands possibly matching the positive controls.

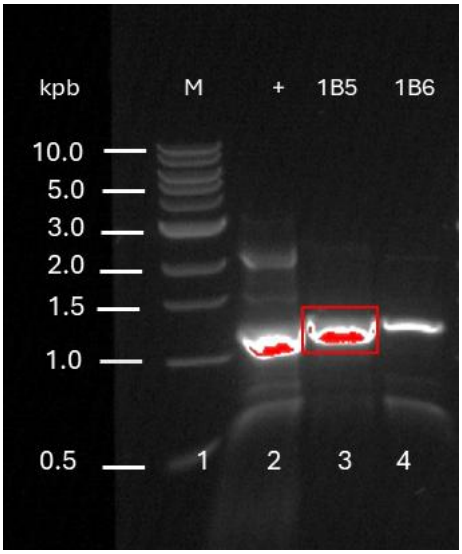

Figure 4.32 AGE image of library screening for region 29 (100V, 1 h, 1% (w/v) agarose, 1X TBE). Lane 1, 1-kb marker; lane 2, positive control (gDNA template); lanes 3-4, pDNA from 1B5 and 1B6; red box, band possibly matching the positive controls.

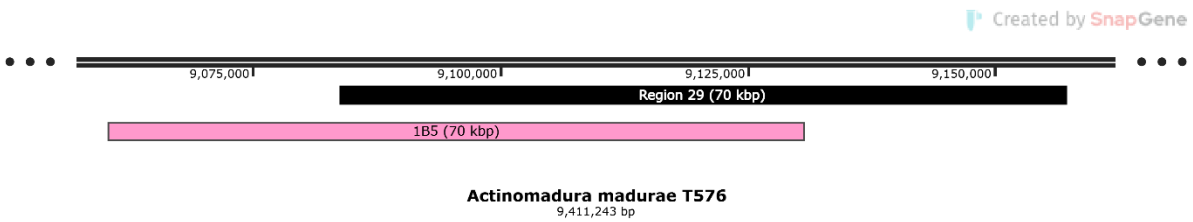

Figure 4.33 Graphical presentation of the coverage of clone 1B5 (70 kbp, pink) vs region 29 (70 kbp, black) after insert-end sequencing.

In summary, this section focused on the screening of the *A. madurae* T576 gDNA library, with 10 regions selected for detailed analysis from the 29 BGCs identified in the *A. madurae* T576 genome. Table 4.3 shows a summary of the regions screened with their respective size and clone. Of these, 4 regions (highlighted in blue) were successfully cloned, including the potential cluster thought to be involved in the biosynthesis of a novel sulphated compound series. Table 4.3 also shows the number of *Sau*3AI sites for each region. While there is a possibility that more *Sau*3AI sites might correlate with unsuccessful cloning, as seen with regions 24, 25, and 29, this pattern is inconsistent with regions 2 and 28 in comparison to region 5. Moreover, since the T576 gDNA library was originally screened for region 5, it is possible that other regions were overlooked. Therefore, a definitive conclusion could not be made about the correlation between the number of *Sau*3AI sites and the successful capture BGCs. Nonetheless, the successfully cloned regions provide a useful starting point from which to study the genetic potential of strain *A. madurae* T576.

Table 4.3 Summary of 10 regions screened from *A. madurae* T576 library with their respective sizes, number of *Sau*3AI sites and clone size.

Region	Size (kbp)	Number of *Sau*3AI sites	Clone (size kbp)
Region 2	72.6	497	-
Region 4	62.6	346	1D1 (124)
Region 5	80	507	4G5 (120)
Region 7	41	262	1G12 (63)
Region 14	45.6	287	-
Region 24	72.5	540	2E12 (60)
Region 25	62.4	532	4H12 (47)
Region 27	25.6	193	1G9 (118)
Region 28	72.6	486	4G9 (93)
Region 29	69.6	528	1B5 (70)

4.3 Conjugation and expression of cloned BGCs in *Streptomyces* hosts

4.3.1 Conjugation and expression of clone 4G5 bearing the BGC for sulphated compounds

The 120 kbp clone 4G5, which contains an 80 kbp BGC potentially involved in the production of novel sulphated compounds, was successfully conjugated into three different laboratory expression hosts: *Streptomyces albus* J1074, *Streptomyces coelicolor* M1152, and *Streptomyces lividans*. The conjugation results varied qualitatively among the hosts, with more colonies observed for *S. lividans*, followed by *S. coelicolor* M1152, and least for *S. albus* J1074, after selection with apramycin (Figure 4.34). Whole genome sequencing confirmed that the entire BGC was successfully cloned, and no mutations were observed within the cluster from clone 4G5 in the BAC replicator strain and from one successful conjugant from each of the *S. albus* J1074, *S. lividans*, and *S. coelicolor* M1152 hosts.

Purified conjugants of each strain were cultured in liquid YEME medium at 30°C for 5 days to assess the production of the sulphated compounds. The conditions used were as previously optimized for the production of the sulphated compounds by *A. madurae* T576 (work of Fatemeh Mazraatitajabadi). Notably, the *S. albus* J1074 (pJE2-4G5) conjugant exhibited a more pronounced yellow tint compared to the parent strain, *S. albus* J1074, as shown in Figure 4.35. This distinct coloration is a characteristic of the sulphated compounds originally isolated from *A. madurae* T576 (Dashti, personal communication), suggesting that the conjugant might be making the sulphated compounds. However, initial experiments failed to detect compounds with the expected mass.

To increase the chances of detecting the target sulphated compounds, I carried out experiments with the parent *Actinomadura* strain to further optimise production and detection of the sulphated compounds. A range of growth conditions and extraction methods were tested in order to detect synthesis of the sulphated compounds. This included culturing in both solid and liquid media of YEME, GYM, R2YE, and ISP4. For extraction, ethyl acetate and methanol were used for solid cultures, while C18 column flash chromatography was applied to liquid cultures. The optimised conditions to detect the sulphated compounds involved culturing in R2YE (both liquid and solid) and extracting with C18 HyperSep columns for liquid cultures and methanol for solid cultures.

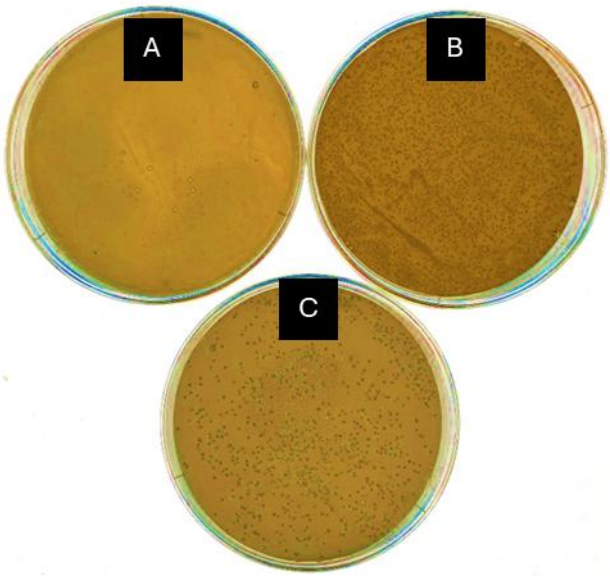

F**igure 4.34** Apramycin-resistant colonies obtained after conjugating the clone 4G5 clone into: A, *S. albus* J1704; B, *S. lividans* 1326; C, *S. coelicolor* M1152.

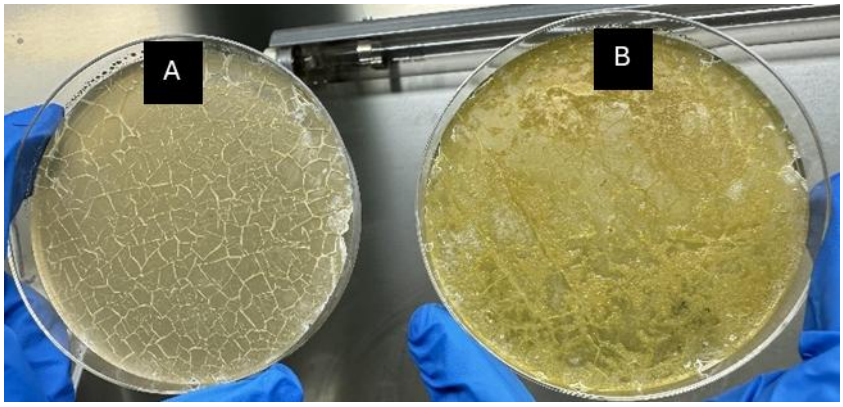

Figure 4.35 Comparison of A, *S. albus* J1074 and B, *S. albus* J1074 (pjE2-4G5) after growth on YEME agar for 5 days.

To facilitate the expression of the target BGC, improved host strains were acquired from Luzhetskyy's laboratory (Myronovskyi *et al.*, 2018) (see section 1.6.4). The 4G5 clone was subsequently conjugated with the engineered strains, *S. albus* Del14 and S. *lividans* YA10, again selecting for apramycin resistance. Successful conjugants from *S. albus* Del14 and S. *lividans* YA10 were subjected to the optimised condition, as described above, to detect the sulphated compounds. Conjugants of *S. albus* Del14 and S. *lividans* YA10 with empty pJE-2 vector were used as negative controls. Figure 4.36 shows a comparative analysis of the two expression hosts, including controls. After 5–7 days of incubation on R2YE medium at 30°C. *S. albus* Del14 (pJE2-4G5) exhibited a prominent yellow coloration, consistent with earlier observations from the *S. albus* J1074 (pJE2-4G5) strain. In contrast, *S. lividans* YA10 (pJE2-4G5) showed no significant pigment changes upon receiving the plasmid.

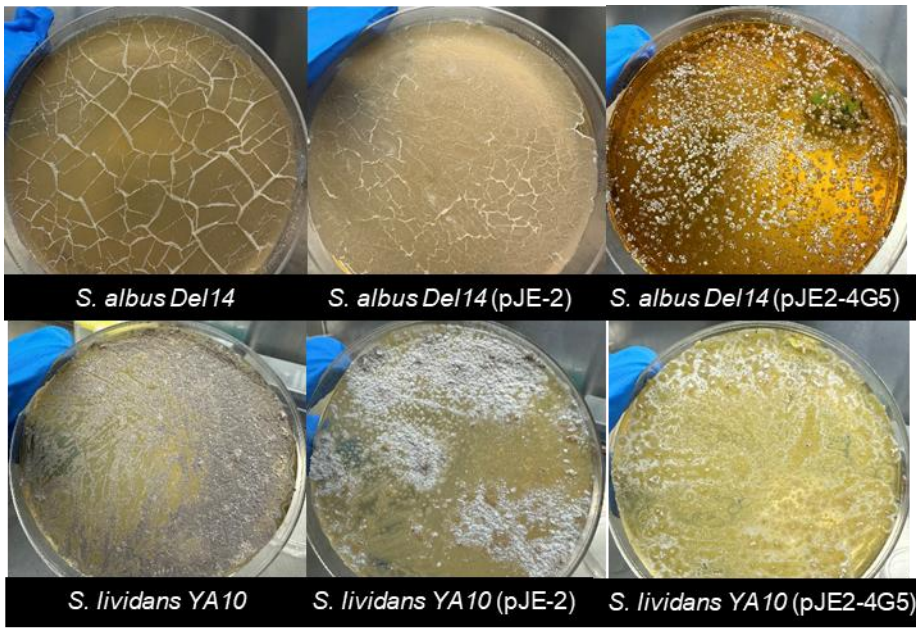

Figure 4.36 *S. albus* Del14, *S. albus* Del14 (pJE-2), *S. albus* Del14 (pJE2-4G5), *S. lividans* YA10, *S. lividans* YA10 (pJE-2) and *S. lividans* YA10 (pJE2-4G5) grown on R2YE agar for 5-7 days.

LC-MS analysis of liquid cultures, examining both supernatants and cell extracts, confirmed the synthesis of the sulphated compounds by *S. albus* Del14 (pJE2-4G5) but not by *S. lividans* YA10 (pJE2-4G5). Figure 4.37 shows the detection of compounds in the supernatant of the liquid cultures. The detected sulphated compounds have $[M+H]^+$ of 942.28, matching the expected mass of the target molecule. Interestingly, the same mass consistently appeared at four different retention times, but this was also the same for the parent strain. The expression of the target compound was similarly detected in solid cultures of *S. albus* Del14 (pJE2-4G5) grown on R2YE and YEME media, with methanol used as the extraction solvent (Figures 4.38 and 4.40). Conversely, the use of ethyl acetate as the extraction solvent failed to reveal the compound (Figures 4.39 and 4.41).

Further optimization led to the use of methanol as extraction method for cells grown in liquid R2YE. Using these conditions, comparison of *A. madurae* T576 and *S. albus* Del14 (pJE2-4G5) did not just detect the target sulphated compounds (Figure 4.42) but revealed an additional peak with a retention time of 4.05 min and an $[M+H]^+$ of 1008.33 (Figure 4.43). Notably, this additional mass was absent in the *S. albus* Del14 strain carrying the empty pJE2 vector. This observation suggests the possible expression of a compound related to the target sulphated metabolites, potentially pointing to previously uncharacterized compounds derived from the same biosynthetic pathway.

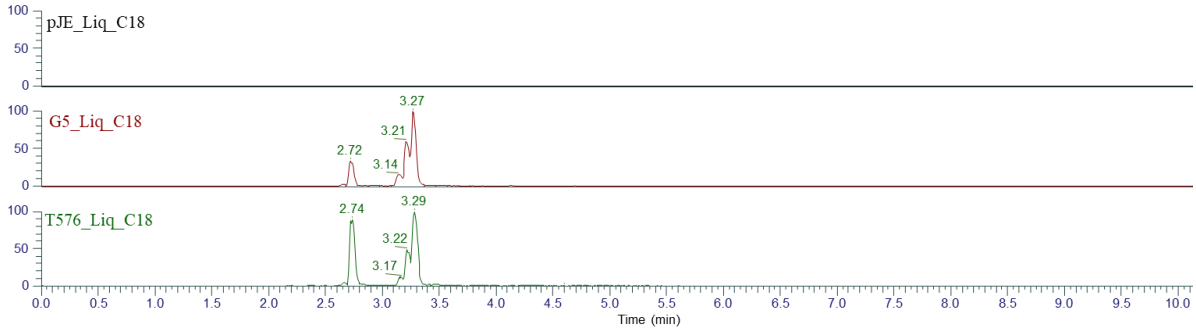

Figure 4.37 Comparison of the extracted ion chromatograms for *m/z* 942.28 from UHPLC-HRMS analyses of culture extracts of *S. albus* Del14 (pJE-2), *S. albus* Del14 (pJE2-4G5) and *A. madurae* T576 cells (top to bottom) grown in R2YE liquid media extracted using C18 flash chromatography.

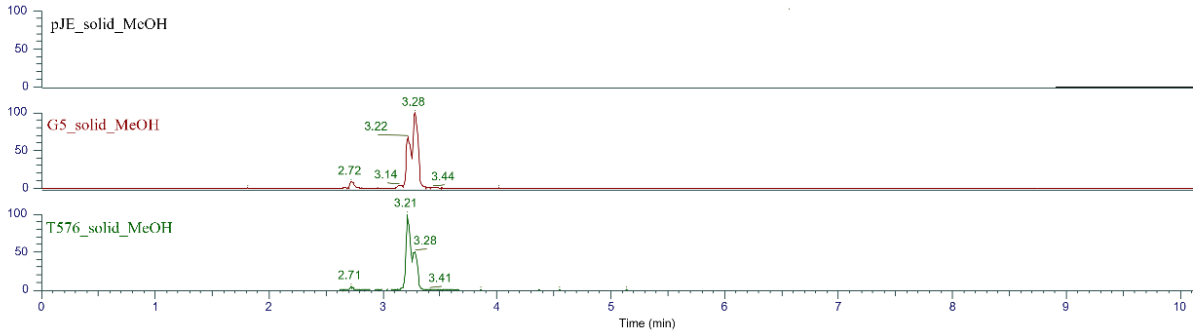

Figure 4.38 Comparison of the extracted ion chromatograms for *m/z* 942.28 from UHPLC-HRMS analyses of culture extracts of *S. albus* Del14 (pJE-2), *S. albus* Del14 (pJE2-4G5) and *A. madurae* T576 cells (top to bottom) grown in R2YE solid media extracted with methanol.

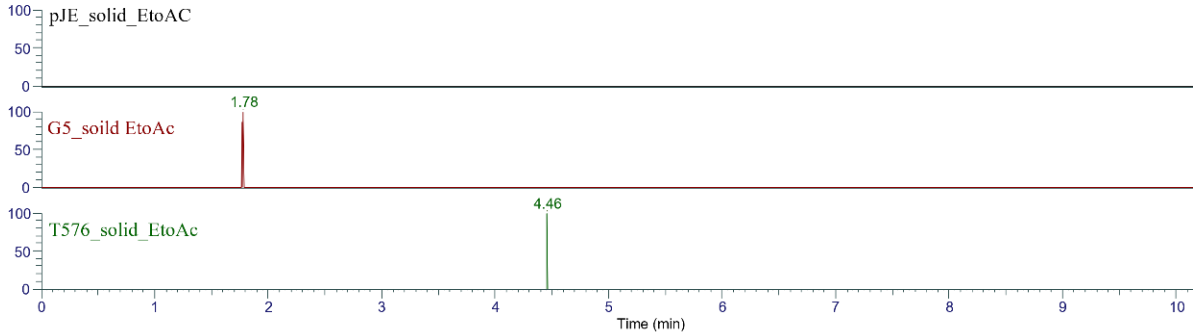

Figure 4.39 Comparison of the extracted ion chromatograms for *m/z* 942.28 from UHPLC-HRMS analyses of culture extracts of *S. albus* Del14 (pJE-2), *S. albus* Del14 (pJE2-4G5) and *A. madurae* T576 cells (top to bottom) grown in R2YE solid media extracted with ethyl acetate.

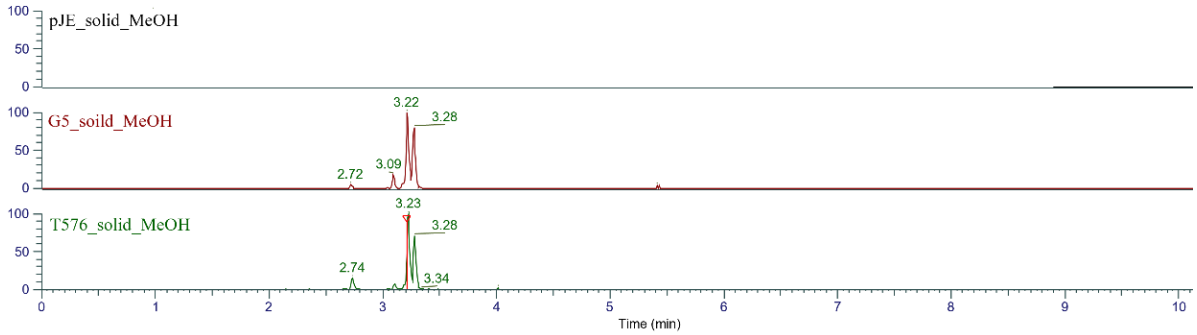

Figure 4.40 Comparison of the extracted ion chromatograms for *m*/*z* 942.28 from UHPLC-HRMS analyses of culture extracts of *S. albus* Del14 (pJE-2), *S. albus* Del14 (pJE2-4G5) and *A. madurae* T576 cells (top to bottom) grown in YEME solid media extracted with methanol.

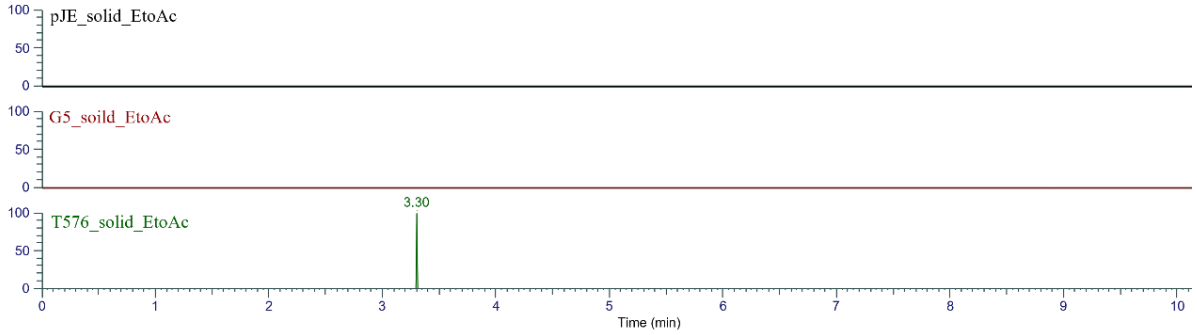

Figure 4.41 Comparison of the extracted ion chromatograms for *m*/*z* 942.28 from UHPLC-HRMS analyses of culture extracts of *S. albus* Del14 (pJE-2), *S. albus* Del14 (pJE2-4G5) and *A. madurae* T576 cells (top to bottom) grown in YEME solid media extracted with ethyl acetate.

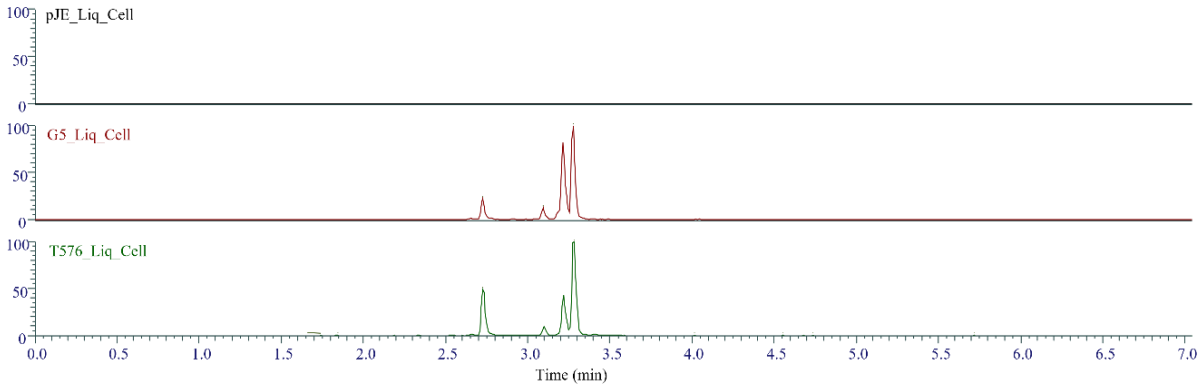

Figure 4.42 Comparison of the extracted ion chromatograms for *m*/*z* 942.28 from UHPLC-HRMS analyses of culture extracts of *S. albus* Del14 (pJE-2), *S. albus* Del14 (pJE2-4G5) and *A. madurae* T576 cells (top to bottom) grown in R2YE liquid media extracted with methanol.

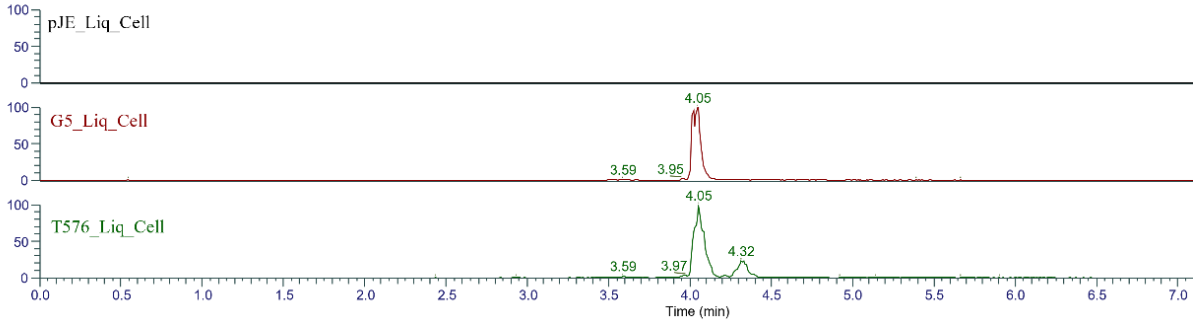

Figure 4.43 Comparison of the extracted ion chromatograms for *m/z* 1008.33 from UHPLC-HRMS analyses of culture extracts of *S. albus* Del14 (pJE-2), *S. albus* Del14 (pJE2-4G5) and *A. madurae* T576 cells (top to bottom) grown in R2YE liquid media extracted using methanol from cells.

4.3.2 Conjugation and expression of other cloned BGC

Clones harbouring the other biosynthetic regions isolated as above were also introduced into *S. albus* Del14 and *S. lividans* YA10 for heterologous expression. Clones 1D1 and 1G12, containing the entireties of region 4 and 7, respectively, were successfully conjugated into both expression hosts. However, clone 1G9, a 118 kbp fragment harbouring region 27, could only be successfully conjugated into *S. lividans* YA10, likely due to its larger size or some other incompatibility with the host system. Another possible explanation for the failed conjugal transfer of clone 1G9 to *S. albus* Del14 is its possible toxicity in the *Streptomyces* host.

Following successful conjugation, the engineered strains were cultivated on both solid and liquid R2YE and YEME media to evaluate the synthesis of secondary metabolites. Extracts from these cultures were analysed using LC-MS to detect any production of compounds associated with the cloned BGCs. Unlike the noticeable changes observed in *S. albus* (pJE2-4G5), Figure 4.44 shows no visible changes occurred in *S. albus* Del14 or *S. lividans* YA10 harbouring clones 1D1 and 1G12 compared with their counterparts carrying the empty vector pJE-2. A similar observation was made for *S. lividans* YA10 (pJE2-1G12), with the exception that its growth was noticeably slower than the other conjugants possibly, due to its large insert size.

Following analysis of the LC-MS extracts from both liquid and solid cultures grown in YEME and R2YE media, using the same extraction procedure previously described, no additional peaks were detected for the conjugants of *S. albus* Del14 (pJE2-1G9) or *S. lividans* YA10 (pJE2-1G9). Similarly, no unique peaks were observed in *S. lividans* YA10 (pJE2-1G12) (data not shown).

Initially, a distinct peak with an $[M+H]^+$ of 569.31 was detected in *S. albus* Del14 (pJE2-1D1) (data not shown). The peak was consistently observed in extracts from cells grown in both liquid

and solid YEME media, with methanol used as the extraction solvent. However, after repeating the same conditions, LC-MS data showed that the peak was present both in extracts of *S. albus* Del14 and *S. albus* Del14 (pJE-2) which means it is from the medium or produced by the host strain (data not shown).

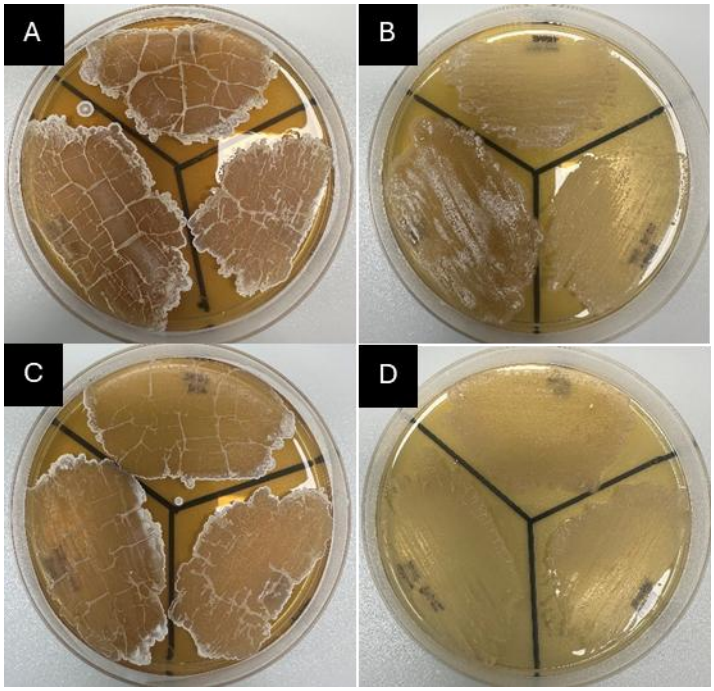

Figure 4.44 From top to clockwise. All grown for 7 days in YEME
A) *S. albus* Del14; *S. albus* Del14 (pJE-2); *S. albus* Del14 (pJE2-1D1).
B) *S. lividans* YA10; *S. lividans* YA10 (pJE-2); *S. lividans* YA10 (pJE2-1D1).
C) *S. albus* Del14; *S. albus* Del14 (pJE-2); *S. albus* (pJE2-1G12).
D) *S. lividans* YA10; *S. lividans* YA10 (pJE-2); *S. lividans* YA10 (pJE2-1G12).

4.4 Discussion

This study resulted in the successful cloning and preliminary characterization of multiple BGCs from the genome of *A. madurae* T576. Among the successfully cloned regions, an 80 kbp BGC encoding novel sulphated compounds was efficiently conjugated and expressed in a heterologous *Streptomyces* host, validating the assignment of the BGC and its functional activity. This finding suggests that the established protocol of gDNA library construction using the cloning vector pJE-2 can be used to clone and express large BGCs of Actinomycetes for NP discovery.

Throughout this process, several factors affecting both the cloning and expression of target compounds were identified. In the cloning phase, factors such as the quality of HMW gDNA and the optimization of partial digestion time points were found to significantly impact the size and integrity of the cloned fragments (Osoegawa *et al.*, 1998). For compound expression, the

choice of heterologous host (Myronovskyi and Luzhetskyy, 2019; Kang and Kim, 2021; Baltz, 2010), the composition of the growth medium (Bode *et al.*, 2002), and the method of metabolite extraction (Pinu, Villas-Boas and Aggio, 2017) were all pivotal in detecting the target compound. These factors highlight the interconnection of the different experimental stages, from identifying BGCs to characterizing the resulting metabolites.

However, this strategy comes with notable limitations. The preparation of high-molecular-weight genomic DNA and the subsequent PCR-based screening are both labour-intensive and time-consuming. Moreover, there is no assurance of capturing an intact BGC, as demonstrated by the incomplete recovery of regions 24 and 28. This is likely attributed to the use of the frequent-cutting restriction enzyme *Sau*3AI, which indiscriminately cleaves the DNA, making it difficult to avoid breaks within the cluster. To overcome this, several strategies can be implemented. One potential solution is refining the methodology for gDNA library preparation, particularly focusing on size selection and optimizing partial digestion time points to enable the cloning of larger fragments, potentially up to and beyond 200 kbp. Alternatively, as detailed in section 1.6.3, various direct cloning techniques such as TAR cloning, CAPTURE, and CATCH which offer efficient, time-saving alternatives for capturing entire BGCs.

Expression of the sulphated compounds were found to be more efficient using *S. albus* Del14 as expression host and R2YE as culture medium, coupled with methanol as extraction solvent. This underscores the critical role of selecting an effective extraction method for accurately identifying and quantifying target compounds from biological samples. Methanol is a polar extraction solvent that can be used to extract intracellular metabolites since it can disrupt the cell wall (Pinu, Villas-Boas and Aggio, 2017). This can possibly explain the detection of compounds from cells both from liquid and solid cultures when methanol was used as extraction solvent. However, sulphated compounds were also detectable at low concentration from liquid culture after passing it through C18 column, potentially because it can also be secreted into the culture medium or released by cell lysis. On the other hand, the additional mass, of [M+H]+ 1008.33, which is possibly related to the sulphated compounds, was only detected with cells from liquid culture using methanol as solvent, which might support the hypothesis that the compound is intracellular.

Although regions 4, 7, and 27 were successfully cloned and conjugated, novel metabolites were not detected under the conditions used for the sulphated compound. This suggests that further optimization, such as modifying the growth media, refining the extraction protocol, or employing alternative expression hosts may be necessary to detect the expression of the corresponding compounds

Chapter 5: Hibiscus Acid and Hydroxycitric Acid Dimethyl Esters from Hibiscus Flowers Induce Production of Dithiolopyrrolone Antibiotics by *Streptomyces* strain MBN2-2

Published in:

***Natural Products and Bioprospecting* 2024, 14.1:40**

5.1 Introduction

Plant-microbe interactions in the rhizosphere has been a focal point of many ecological studies (Jacoby *et al.*, 2017). These interactions can be mutually beneficial or potentially harmful. In the realm of resource exchange, plants contribute significantly by supplying microbes with essential components such as carbon in form of sugar (Van Der Heijden, Bardgett and Van Straalen, 2008). In return, microbes play a crucial role in converting organically-bound nitrogen, phosphorus, and sulphur in the soil into bioavailable forms, facilitating optimal nutrient absorption by plants through mineralization (Van Der Heijden, Bardgett and Van Straalen, 2008). Other examples include heterotrophic bacteria that have the ability to convert atmospheric nitrogen into ammonia through enzymatic processes catalysed by nitrogenase (Franche, Lindström and Elmerich, 2009); bacteria that produce hydrolytic enzymes crucial for breaking down insoluble organic polymers into simpler forms; and siderophore producing microbes that aid in scavenging iron and other essential minerals. Ultimately, these nutrients become available for plants to utilize (Vurukonda, Giovanardi and Stefani, 2018; Bhatti, Haq and Bhat, 2017). To make the most of this relationship, plants have developed strategies such as releasing molecules like flavonoids to attract beneficial microbes, while concurrently deterring phytopathogens, thus shaping their root microbiome (Sasse, Martinoia and Northen, 2018).

Organisms from the Phylum Actinomycetota are common inhabitants of the soil and rhizosphere, and frequently can synthesise a wide range of specialised metabolites that are thought to be involved in adapting the organisms to their highly competitive environment, including symbiotic interactions with plants in the rhizosphere (Bhatti, Haq and Bhat, 2017; Takeuchi *et al.*, 1996; De Simeis and Serra, 2021; Van der Meij *et al.*, 2017). For example, a specific category of bacteria known as plant growth-promoting rhizobacteria exhibits the capability to synthesize compounds like indole-3-acetic acid and gibberellic acid, which play pivotal roles in enhancing plant growth (Strzelczyk and Pokojska-Burdziej, 1984).

It is now well established that the genomes of the majority of Actinomycetes harbor numerous biosynthetic gene clusters (BGCs) that are either not expressed or expressed poorly under conventional laboratory culture conditions (Nett, Ikeda and Moore, 2009; Dashti *et al.*, 2017). One approach used to induce the production of compounds encoded by these cryptic BGCs is to mimic natural environments by co-cultivating two different Actinomycete strains or an Actinomycete strain with a fungal counterpart. This method has successfully led to the production of compounds that are not generated in independent cultures (Dashti *et al.*, 2014). Taking inspiration from the interactions between plants and microbes, we aimed to mimic this

phenomenon and investigate plant extracts as elicitors to induce the production of specialized metabolites from Actinomycetota strains isolated from plant rhizospheres. Here, we present our findings that hibiscus acid dimethyl ester (**3**) and hydroxycitric acid 1,3-dimethyl ester (**4**) from hibiscus induce production of the broad-spectrum antibiotics thiolutin (**1**) and aureothricin (**2**).

5.2 Results and Discussion

5.2.1 Induction of thiolutin and aureothricin from strain MBN 2-2 using hibiscus extract

For this induction study, 24 actinobacteria isolated from plant rhizosphere environments were selected. Plant extracts such as hibiscus flowers, sage leaves, cinnamon, coriander seeds, turmeric, and musk root were used as elicitors. These extracts were prepared using the method outlined in section 2.6.2. The extracts were tested at two final concentrations of 4.5 and 18 mg/mL, by adding them to overnight cultures of actinobacteria in YEME liquid medium. After seven days of incubation, 1 mL of the cultures was centrifuged, and the supernatants were subjected to analysis by LC-MS. Concurrently, their antimicrobial activity against various microorganisms including *Escherichia coli*, *Bacillus subtilis*, *Staphylococcus aureus*, *Cryptococcus neoformans*, and *Saccharomyces cerevisiae* were assessed by following the disc diffusion assay method described in section 2.7. The culture supernatant of one *Streptomyces* isolate, designated as MBN2-2, exhibited significant antimicrobial activity against all tested microorganisms when cultivated in the presence of hibiscus extract (Figures 5.1 and 5.2). This antimicrobial activity was absent when the strain was cultured without hibiscus extract. Comparison of the LC-HR-MS chemical profiles of these two cultures revealed two distinctive peaks in the profile of MBN2-2 cultured with hibiscus extract, which were absent in the non-treated culture (Figure 5.3). These peaks corresponded to $[M+H]^+$ masses at *m/z* 229.0100 and 243.0257 (Figure 5.4), indicating molecular formulae of $C_8H_8N_2O_2S_2$ and $C_9H_{10}N_2O_2S_2$, respectively. Database searches identified thiolutin and aureothricin, respectively, as likely candidates for the active molecules (Figure 5.5).

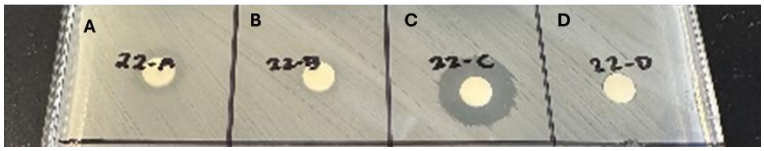

Figure 5.1. Disc diffusion assay of culture supernatant of *Streptomyces* strain MBN2-2 against a lawn of *B. subtilis*. Paper discs were treated with culture supernatant of *Streptomyces* strain MBN2-2, supplemented as follows: A) nothing added; B) DMSO; C-D) hibiscus extract at a final concentration of (C) 4.5 mg/mL or (D) 18 mg/mL. Image from (Sumang *et al.*, 2024).

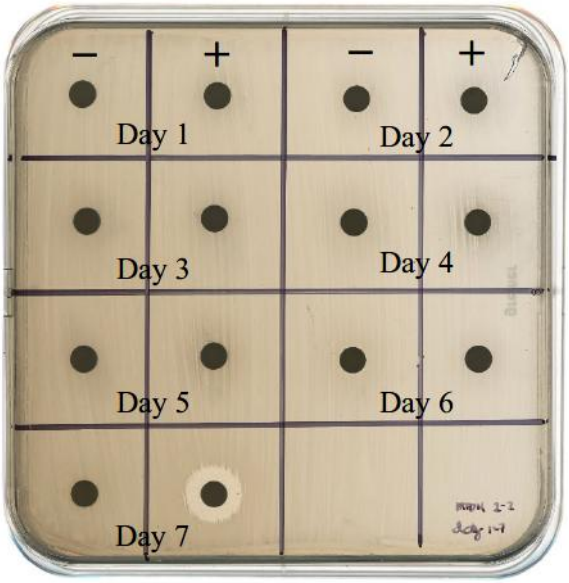

Figure 5.2. Effect of time of culture incubation and presence of hibiscus extract in the culture medium on production of antibiotic activity against *B. subtilis*. *Streptomyces* strain MBN2-2 was cultured in YEME with (+) and without (-) added 4.5 mg/mL of hibiscus extract for 7 days. Image from (Sumang *et al.*, 2024).

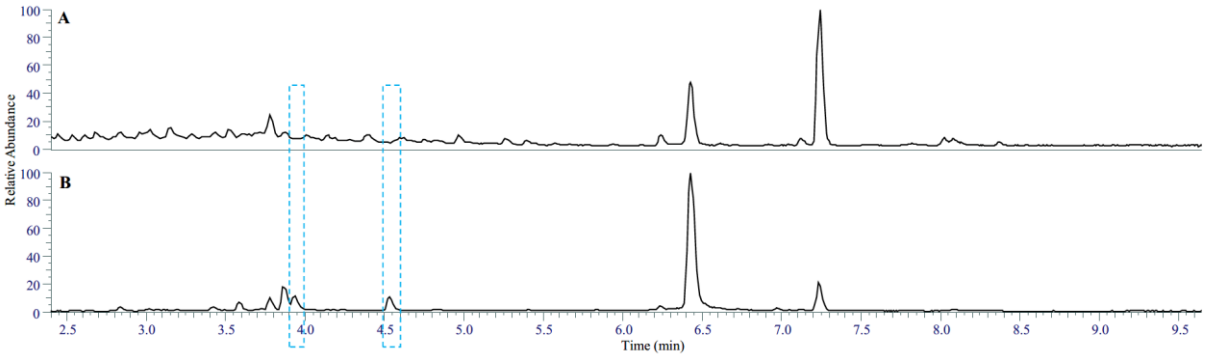

Figure 5.3. Total ion chromatogram from LC-HR-MS analyses of culture supernatant of *Streptomyces* strain MBN2-2 grown **A)** without and **B)** with extract of hibiscus flower added to the culture media. Image from (Sumang *et al.*, 2024).

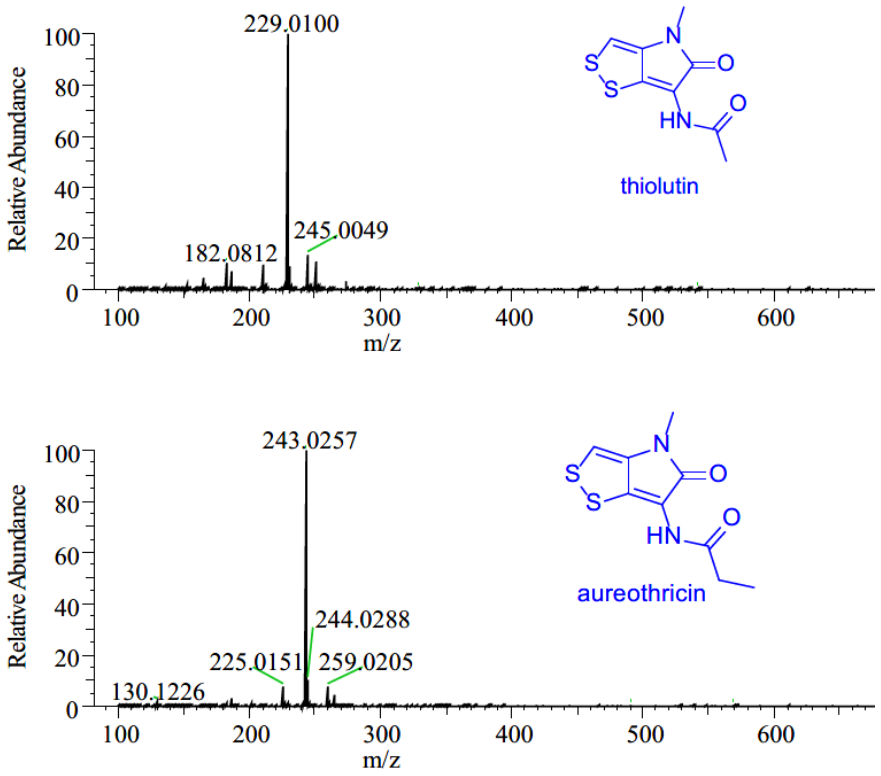

Figure 5.4. High resolution mass spectrometry of induced metabolites thiolutin and aureothricin. Image from (Sumang *et al.*, 2024).

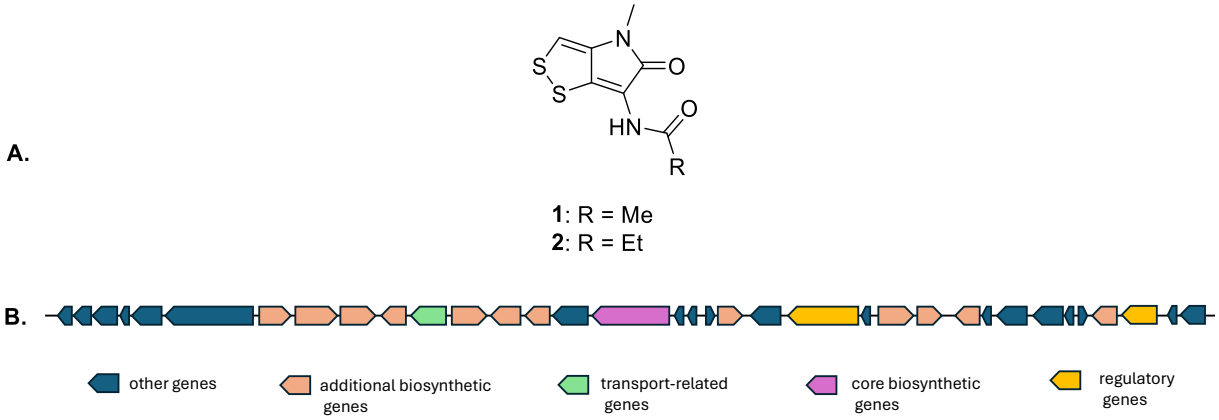

Figure 5.5. A.) Structure of thiolutin (**1**) and aureothricin (**2**) produced by *Streptomyces* strain MBN2-2 in presence of the extract of hibiscus flower in culture media. B.) Thiolutin BGC from *Streptomyces* MBN 2-2. Coloured blocks indicate annotated gene functions. Image from (Sumang *et al.*, 2024).

To substantiate the above observations the *Streptomyces* strain MBN2-2 was cultured at large scale (250 mL in YEME medium) with and without hibiscus extract. After seven days of incubation, ethyl acetate extracts were prepared from the cultures and subjected to semipreparative HPLC fractionation. A bioassay-guided approach was employed to identify the active fractions. Upon pairwise comparison of the HPLC fractions derived from the cultures

with and without hibiscus extract, it was found that fractions 23 and 26 from the extract obtained in the presence of hibiscus exhibited an induced antimicrobial activity. LC-HR-MS analysis confirmed that these fractions contained compounds with masses corresponding to thiolutin and aureothricin, respectively. Subsequent verification of their structures was achieved through NMR spectroscopy (Figures 5.7-5.9) and the NMR data is shown in Table 5.1

Both thiolutin and aureothricin belong to a class of natural products distinguished by a unique bicyclic structure containing a dithiolopyrrolone ring system consists of a five-membered pyrrolone ring fused with a five-membered ring containing two sulfur atoms (Celmer and Solomons, 1955). Dithiolopyrrolones (DTPs) have been isolated from various bacteria, including *Streptomyces albus* (Celmer *et al.*, 1952), *Saccharothrix algeriensis* (Merrouche *et al.*, 2020), *Xenorhabdus bovienii* (McInerney *et al.*, 1991), and *Alteromonas rava* (Shiozawa *et al.*, 1993). This class of compounds are known for their wide range of activities against several pathogenic microbes, including *S. aureus*, *E. coli*, *Klebsiella pneumoniae*, *Listeria monocytogenes*, *Candida albicans*, *Aspergillus carbonarius*, and *Fusarium culmorum* (Celmer and Solomons, 1955; Oliva *et al.*, 2001; Merrouche *et al.*, 2020). Interestingly, in addition to their broad-spectrum activity against different phytopathogenic bacteria and fungi, compounds **1** and **2** have shown strong activity against *Erwinia amylovora*, a bacterium that is responsible for apple fire blight (Nguyen *et al.*, 2024). Furthermore, in *in vivo* experiments they have been effective in suppressing tomato bacterial wilt and apple fire blight (Nguyen *et al.*, 2024). The antibiotic mode of action of thiolutin is attributed to interruption of diverse cellular pathways (Li *et al.*, 2014). It is suggested that the disulfide bond of the thiolutin is reduced in the cell and subsequently chelates Zn^{2+}, leading to inhibition of multiple metalloproteins. The reduced form also interacts with Mn^{2+} to inhibit the RNA polymerase II (Pol II) transcription initiation (Qiu *et al.*, 2024).

We then sequenced the genome of MBN2-2 (section 2.3.12), and bioinformatics analysis revealed the presence of a gene cluster capable of supporting the biosynthesis of thiolutin and aureothricin (GenBank number: PP747228). Figure 5.5 B shows the antiSMASH 8.0.2 prediction of the 48 kbp thiolutin BGC and its annotated genes. The BGC of thiolutin contains the same core biosynthetic genes as that of other structurally closely related DTPs such as holomycin (Li *et al.*, 2014). Its main NRPS genes encode the typical domain triad, cyclization (Cy), adenylation (A), and thiolation (T), that incorporates L-cysteine as the building block (Li *et al.*, 2014; Pansomsuay *et al.*, 2025). The cluster also includes oxidoreductase genes, one of which is responsible for disulfide bond formation, and an *N*-acetyltransferase that catalyses acetyl group transfer from acetyl-CoA to generate an acetylated intermediate (Li *et al.*, 2014;

Pansomsuay *et al.*, 2025). The key structural difference between holomycin and thiolutin is the *N*-methyl group at the endocyclic amide of thiolutin, introduced by an *N*-methyltransferase (Chen, Johnson and Li, 2023). Although an *N*-methyltransferase gene is present within the thiolutin BGC, in vitro studies showed it is not involved in thiolutin biosynthesis (Chen, Johnson and Li, 2023; Huang *et al.*, 2015). Instead, an *N*-methyltransferase located outside the thiolutin BGC was identified to catalyse *N*-methylation in DTPs (Chen, Johnson and Li, 2023).hap

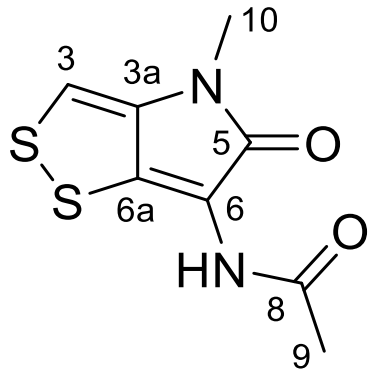

Figure 5.6. Structure of thiolutin with numbering used in NMR table.

Table 5.1 ^{1}H and ^{13}C NMR data of thiolutin (DMSO-d_6).

Position	δ_C	δ_H
3	110.9	7.33, s
3a	136.0	
5	166.2	
6	114.8	
6a	132.4	
8	168.9	
9	22.4	2.02, s
10	27.5	3.25, s
NH		9.98, s

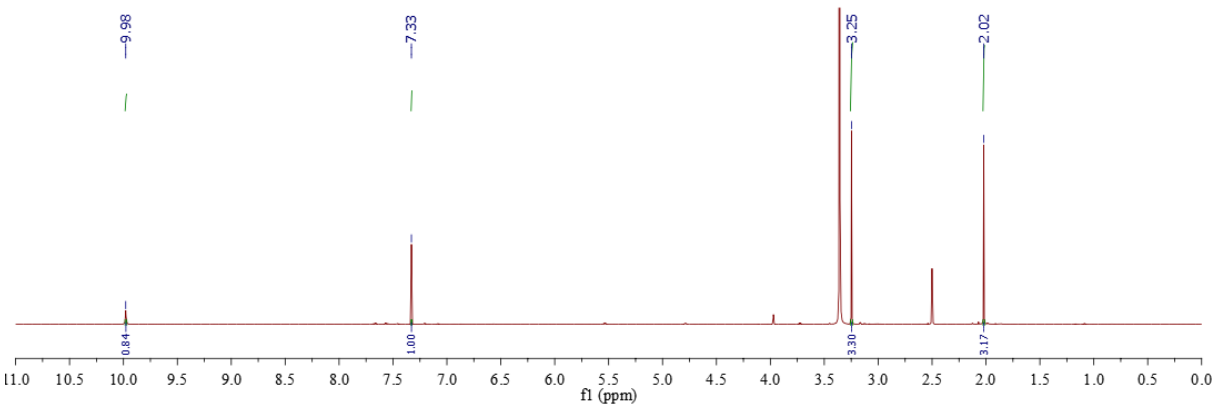

Figure 5.7. ^{1}H NMR spectrum of thiolutin in DMSO-d_6. Image from (Sumang *et al.*, 2024).

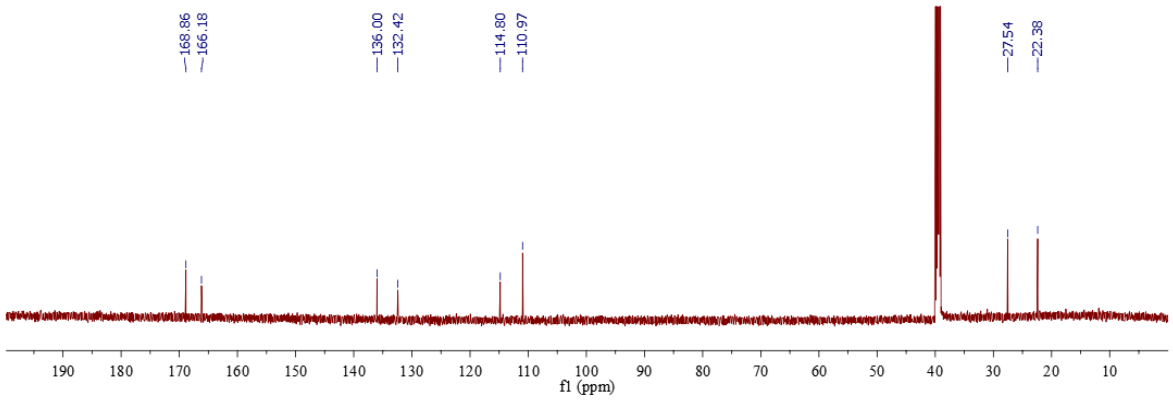

Figure 5.8. ^{13}C NMR spectrum of thiolutin in DMSO-d_6. Image from (Sumang *et al.*, 2024).

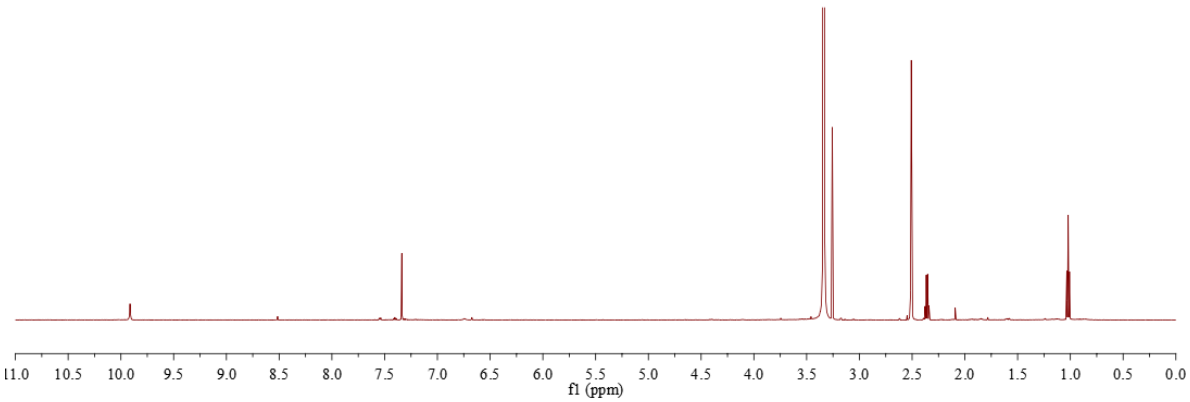

Figure 5.9. ^{1}H NMR spectrum of aureothricin in DMSO-d_6. Image from (Sumang *et al.*, 2024).

5.2.2 Hibiscus acid and hydroxycitric acid triggers production of thiolutin and aureothricin from strain MBN 2-2

Our next objective was to identify the compound/s from the hibiscus extract that were responsible for triggering thiolutin and aureothricin production. A methanolic extract of hibiscus flower was fractionated via semipreparative HPLC. The dried fractions were then resuspended in DMSO and added to overnight cultures of MBN2-2. Analysis of the cultures

after seven days revealed that fractions 8 and 11 induced thiolutin and aureothricin production. LC-HR-MS analysis of these fractions revealed $[M+H]^+$ peaks at *m/z* 219.0499 ($C_8H_{11}O_7$) and 237.0604 ($C_8H_{13}O_8$), potentially corresponding to hibiscus acid dimethyl ester (**3**) and hydroxycitric acid 1,3-dimethyl ester (**4**), respectively (Figure 5.10). The identities of these compounds were confirmed by ^{1}H NMR spectroscopy (Figures 5.11 and 5.12). While it has been reported that plant exudates can contain citric acid and that this can enhance the colonization of beneficial microbes in the rhizosphere (Jiao *et al.*, 2022), we are not aware of reports that citric acid or related compounds such as hydroxycitric acid or its methyl esters, can induce the production of specialized metabolites in actinobacteria. To explore this possibility, a similar induction study was conducted using citric acid and hydroxycitric acid. LC-HR-MS profiling and antibacterial activity assays indeed confirmed the production of thiolutin and aureothricin induced by both compounds.

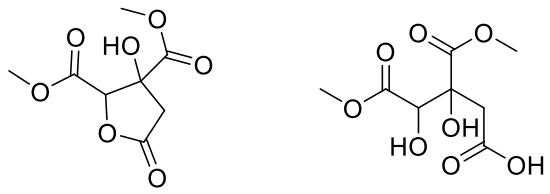

3 **4**

Figure 5.10. Structure of elicitors hibiscus acid dimethyl ester (**3**) and hydroxycitric acid 1,3- dimethyl ester (**4**) identified in the extract of hibiscus flower. Image from (Sumang *et al.*, 2024).

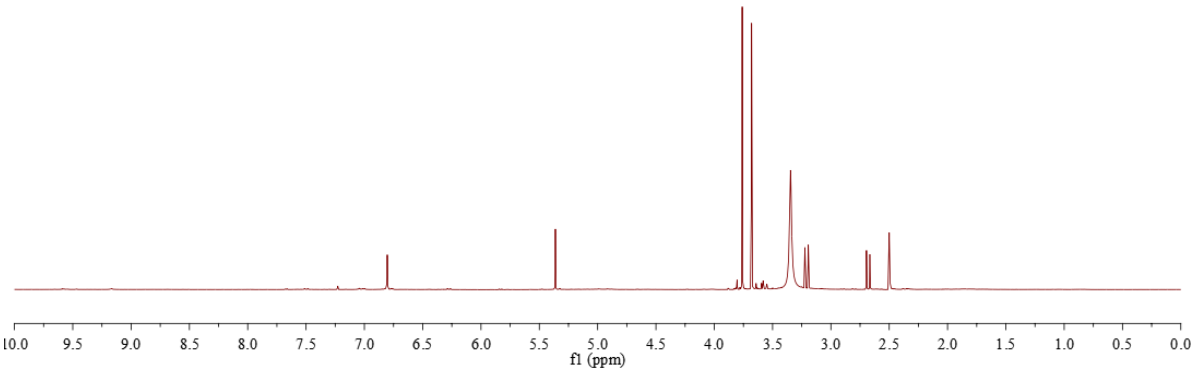

Figure 5.11. ^{1}H NMR spectrum of hibiscus acid dimethyl ester in DMSO-d_6. Image from (Sumang *et al.*, 2024).

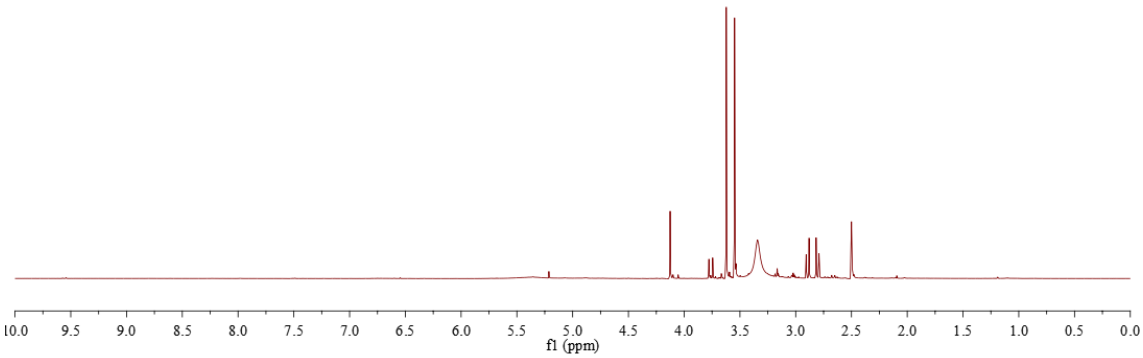

Figure 5.12. ^{1}H NMR spectrum of hydroxycitric acid 1,3-dimethyl ester in DMSO-d_6. Image from (Sumang *et al.*, 2024)

5.2.3 Role of iron in production of thiolutin and aureothricin from strain MBN 2-2

How thiolutin and aureothricin are induced by the addition of hibiscus acid dimethyl ester, hydroxycitric acid dimethyl ester, citric acid, and hydroxycitric acid remains unclear. Citric acid is recognized as an iron chelator, and various citrate-containing metabolites, such as staphyloferrin B, achromobactin, and vibrioferrin, have been recognised as siderophores produced by bacteria for iron acquisition (Ribeiro, Sousa and Simões, 2022; Cheung, Murphy and Heinrichs, 2012). Hence, we speculated that iron availability might have a role in triggering the production of thiolutin and aureothricin. Previous studies have demonstrated that iron starvation can activate certain BGCs (Traxler *et al.*, 2013; Küberl *et al.*, 2020; Vior *et al.*, 2014b). Additionally, a single biosynthetic pathway that can produce bagremycins under iron depletion conditions, also produces ferroverdins when iron is abundant (Martinet *et al.*, 2019). Here, it seemed possible that citrate, hydroxycitrate, and related analogues might chelate free iron ions present in the medium, leading to iron starvation and consequent induction of thiolutin and aureothricin production. Alternatively, the complexes formed by these compounds with iron could be taken up by bacterial transporter systems supporting the activity of enzymes requiring iron for their function.

A Chrome Azurol S (CAS) assay (section 2.9) was used to test whether hibiscus acid dimethyl ester, hydroxycitric acid 1,3-dimethyl ester, and hydroxycitric acid can chelate iron. As shown in Figure 5.13, all compounds tested can chelate iron, albeit less avidly than citric acid. We then tested whether iron alone could induce thiolutin and aureothricin production. Compounds **1** and **2** were both made when either Fe^{2+} (iron (II) sulphate), or Fe^{3+} (iron (III) chloride) were added to a culture of *Streptomyces* strain MBN2-2, at a concentration of 0.75 mg/mL (Figure 5.14), confirming the direct involvement of iron in triggering their biosynthesis.

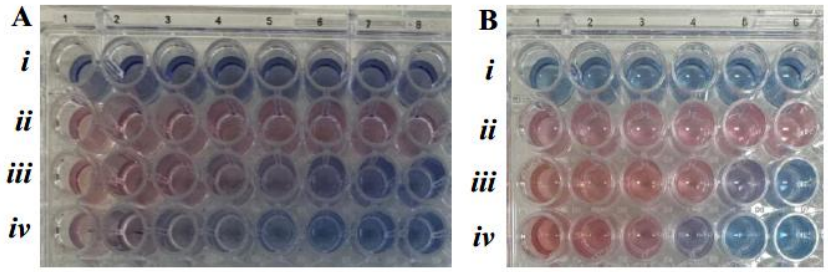

Figure 5.13 A) CAS assay results of ***i*:** milliQ water (negative control), ***ii*:** EDTA (positive control), ***iii*:** citric acid and ***iv*:** hydroxycitric acid, in concentrations 5.0, 2.5, 1.0, 0.5, 0.25, 0.1, 0.05 and 0.01 mg/mL (left to right). **B**) CAS assay results of ***i*:** milliQ water (negative control), ***ii*:** EDTA (positive control), ***iii*:** fraction 8 (dimethyl hibiscus acid), and ***iv*:** fraction 11 (dimethyl hydroxycitric acid), in concentrations 25.0, 20, 15, 10, 5.0, 2.5 mg/mL (left to right).

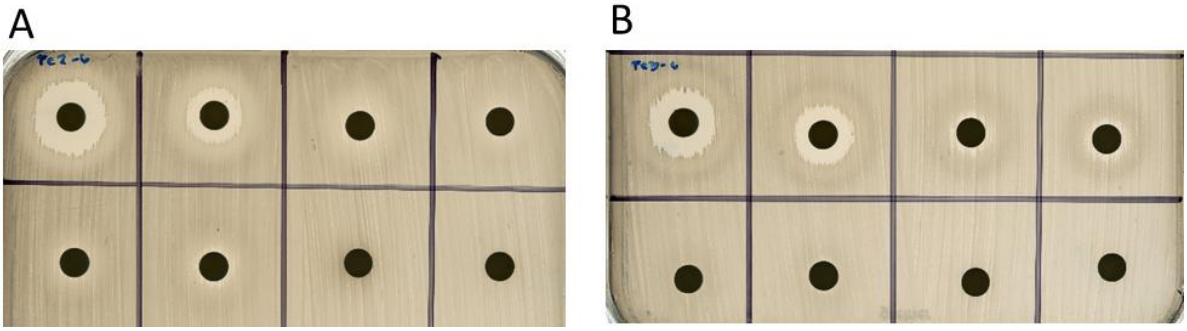

Figure 5.14. Effect of iron concentration on antibiotic production by *Streptomyces* strain MBN2-2. Disc diffusion assay on a lawn of *B. subtilis*. Discs were impregnated with 10 µL of supernatant from a 7 day old culture of *Streptomyces* strain MBN2-2 supplemented with A) Fe^{2+}, B) Fe^{3+}, at concentrations of 1, 0.75, 0.5, 0.25, 0.1, 0.05, 0.025 mg/mL (top left to bottom right), with the last a blank control.

5.3 Conclusions

Understanding the interactions between microbes and plants at the molecular level is of great importance. Several microbial specialized metabolites have been identified to be beneficial for plants through their insecticide (e.g. spinosad and abamectin) and fungicide activity (e.g. Burkholdines) (Dayan, Cantrell and Duke, 2009; Lin *et al.*, 2012), or by promoting plant growth (e.g. indole-3-acetic acid and gibberellic acid) (Strzelczyk and Pokojska-Burdziej, 1984). Considering that these interactions should be reciprocal, we tried to assess the effects of plant extracts on the production of specialized metabolites by Actinomycetes strains isolated from the plant rhizosphere. This led to identification of hibiscus acid dimethyl ester and hydroxycitric acid 1,3-dimethyl ester from hibiscus flowers as elicitors that induce production of the broad-spectrum antibiotics thiolutin and aureothricin by *Streptomyces* strain MBN2-2.

Chapter 6: Linking Biosynthetic Gene Clusters to the Production of Novel Specialized Metabolites and Exploring their Bioactivity and Mechanism of Action

Published in:

***ACS Infectious Diseases* 2022, 8, 2253-2258**

***ACS Infectious Diseases* 2024, 11, 155-163**

***Bioorganic Chemistry* 2025, 160, 108431**

6.1 Introduction

Genes responsible for the biosynthesis of NPs in Actinomycetes are organized into BGCs. One critical step in understanding NP biosynthesis involves linking the specific BGC that encodes enzymes responsible for the biosynthesis of a given compound. This requires understanding of the biosynthetic pathways associated with various NP classes, including their precursor molecules and the enzymes involved in each step which is further discussed in section 1.2. Identifying these genes responsible for these enzymatic reactions opens new avenues for advanced applications such as biosynthetic pathway engineering, mutasynthesis, and combinatorial biosynthesis, aimed at enhancing NP discovery and production (Pham *et al.*, 2019). The major focus of this chapter is on validating the identities of the BGCs involved in production of demurilactone A, persiathiacin A, and quinovosamycins, via insertional mutagenesis. Additionally, mechanism of resistance to persiathiacin and biological activity of quinovosamycin Q4 were investigated.

6.2. Linking *dml* biosynthetic gene cluster to demurilactone A production in *Streptomyces* DEM 21308

6.2.1 Background

Demurilactone A is a novel polyene macrolide (Figure 6.1), produced by *Streptomyces* strainDEM21308 (Dashti *et al.*, 2022). Although the compound showed no activity against various tested bacteria and fungi, it effectively inhibited the growth of non-walled, Gram-positive *Bacillus subtilis* (referred to as “L-forms”) at a minimum inhibitory concentration (MIC) of 16 µg/mL. L-forms are cell wall-deficient bacteria, first observed following accidental isolation of a wall-less *Streptobacillus moniliformis* (Klieneberger, 1935). Research on L-forms, particularly regarding their role as pathogens, has garnered significant interest. Studies have shown that L-forms can be isolated from infected human and animal samples using osmoprotective media and have the ability to revert to a walled form, suggesting their potential involvement in recurrent infections (Errington *et al.*, 2016). Therefore, identifying compounds

that inhibit the growth of L-forms could provide valuable therapeutic strategies for combating persistent infections.

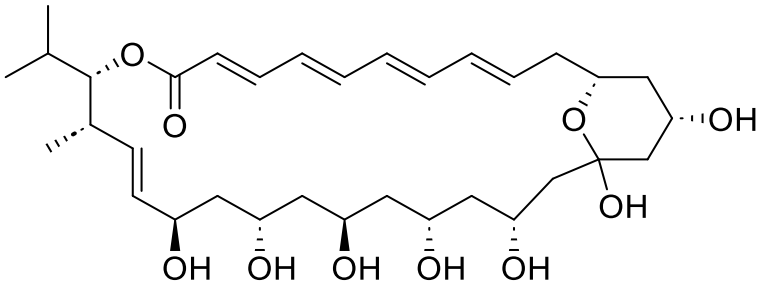

Figure 6.1 Structure of demurilactone A. Figure from (Dashti *et al.*, 2022).

Bioinformatic analysis of the genome sequence of *Streptomyces* DEM21308 using antiSMASH 7.0 revealed several polyketide synthase (PKS) gene clusters. Among them, only one cluster contained the 15 modules required to assemble the demurilactone backbone. This cluster, designated *dml*, comprises five PKS genes: *dmlE*, *dmlF*, *dmlG*, *dmlH*, and *dmlI*). Figure 6.2 illustrates the proposed assembly line machinery for demurilactone A biosynthesis (work of Dr. Yousef Dashti).

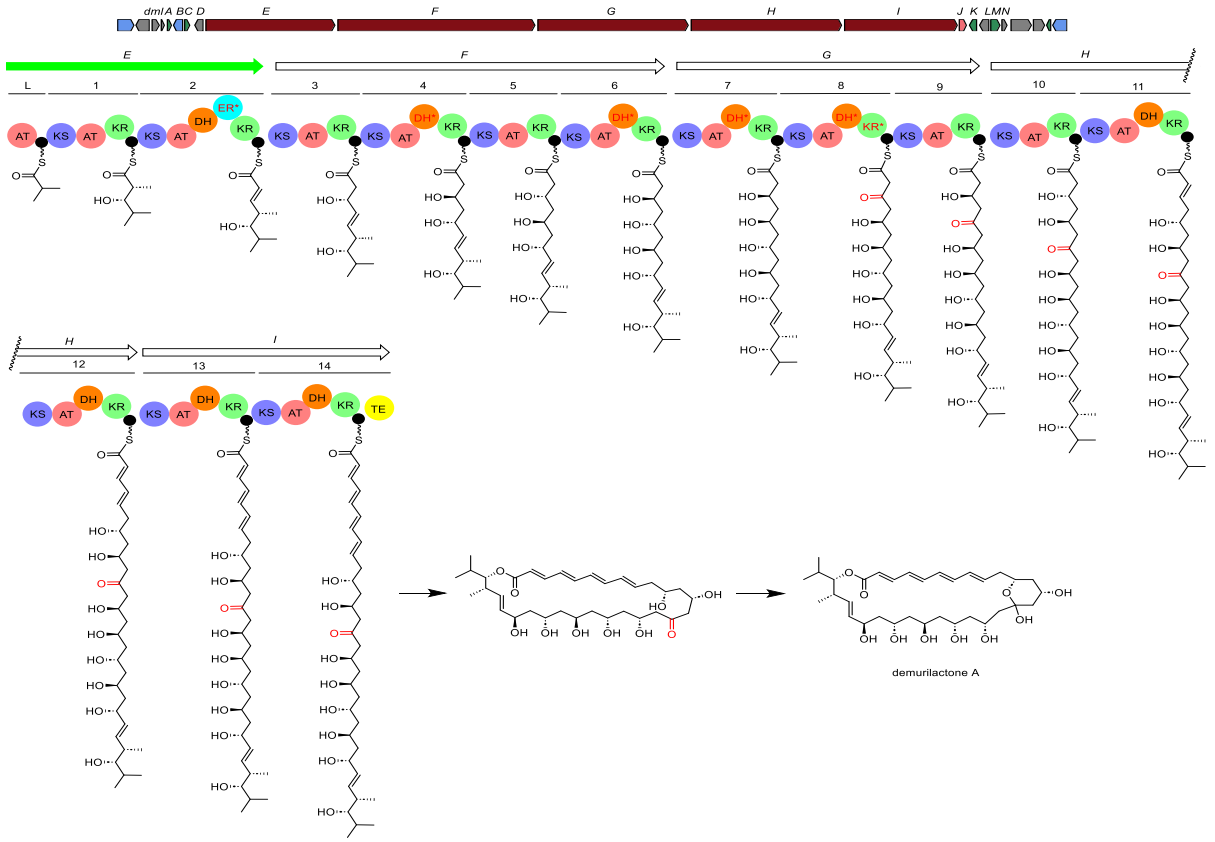

Figure 6.2 The *dml* gene cluster and proposed biosynthetic pathway of demurilactone A. Abbreviations: AT- acyltransferase; KS- ketosynthase; KR- ketoreductase; DH- dehydratase; ER- enoyl reductase; TE- thioesterase. Acyl carrier proteins are shown in black circles. Inactive domains are shown with asterisk in red colour. *dmlE* highlighted in green. Figure from (Dashti *et al.*, 2022).

6.2.2 Gene disruption of the proposed dml *cluster*

If the cluster described above was genuinely responsible for synthesis of demurilactone, disruption of one or more of the key genes in the cluster should abolish production of the compound. Initially, several plasmids developed for gene deletion in *Streptomyces,* including pCRISPomyces2, pCRISPR-cas9, and PYH7 were used in attempts to generate a markerless deletion of *dmlE* (highlighted in green in Figure 6.2). However, attempts to obtain the required mutant by conjugation of the constructed vectors into the *Streptomyces* strain were unsuccessful. We then turned to an insertional mutagenesis approach to inactivate the *dml* gene cluster using a pSET-based vector, as illustrated in Figure 6.3.

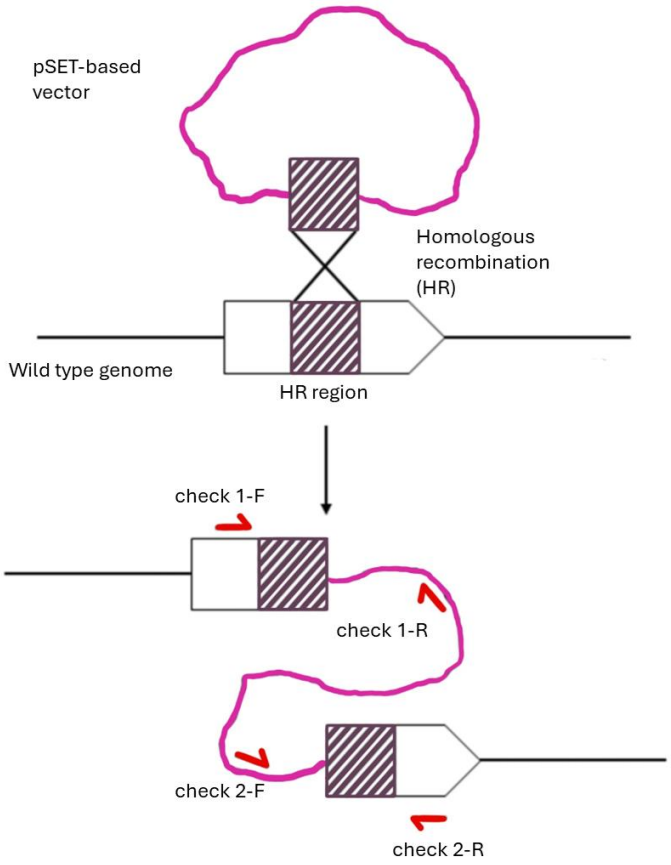

Figure 6.3 Schematic representation of the single crossover insertion of the pSET-*dmlE* vector into the genome of *Streptomyces* DEM21308. Red arrows show the locations of primers designed to validate the insertion event.

To construct a suitable vector, a 3.5 kbp fragment from pSET152 containing the origin of replication, the apramycin resistance gene, and the *traJ* gene, was PCR-amplified and ligated to a PCR-amplified 2 kbp internal fragment of the *dmlE* gene. The map of resulting 5.5 kbp construct, designated pSET-*dmlE*, is shown in Figure 6.4. The integrity of pSET-*dmlE* was confirmed by restriction digestion and sequencing. Because the inserted DNA segment is internal to the *dmlE* gene, integration by a single crossover event (Figure 6.3) results in a partial duplication of the target gene. Crucially, both of the gene copies are truncated and therefore likely to be non-functional. The vector was transformed into *E. coli* ET12567 [pUZ8002] and then mixed with *Streptomyces* DEM21308 to enable conjugative transfer of the pSET derivative. Conjugants were selected for resistance to apramycin. Because pSET-*dmlE* cannot replicate autonomously in *Streptomyces* and lacks the phiC31 integrase, conjugants were

expected to arise by homologous recombination, involving the internal portion of the *dmlE* gene.

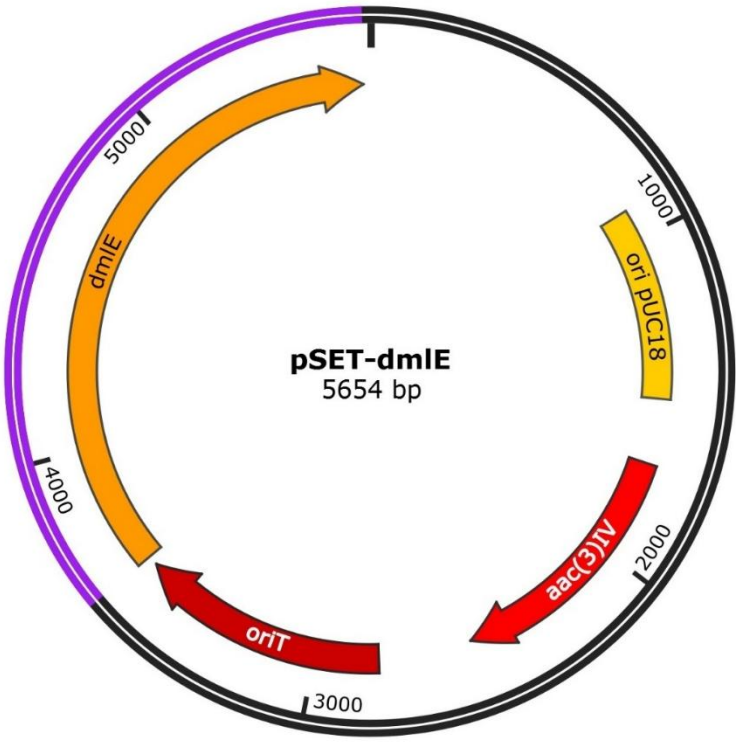

Figure 6.4 Plasmid map of pSET-*dmlE* vector used for *dmlE* inactivation in *Streptomyces* DEM21308. Note that the *dmlE* sequence indicated is an internal segment of the gene lacking both N- and C-terminal coding regions.

To verify the chromosomal insertion site of the vector, PCR amplification was performed using primer pairs targeting the regions indicated by the red arrows in Figure 6.3, using gDNA extracted from a presumptive conjugant. As shown in Figure 6.5, PCR yielded ~2kbp bands flanking each side of the inserted fragment, confirming the successful single-crossover insertion of the pSET-*dmlE* vector. To determine whether insertional mutagenesis affected the production of demurilactone A, both the mutant and wild type strains were grown on solid GYM media. After 7 days, agar plates were extracted with methanol and analysed by UHPLC-HR-MS. Comparative metabolic profiling (Figure 6.6) revealed that demurilactone A was produced only by the wild type strain. This provides direct evidence that the *dmlE* gene, at least, and presumably the whole *dml* BGC, is required for demurilactone A biosynthesis.

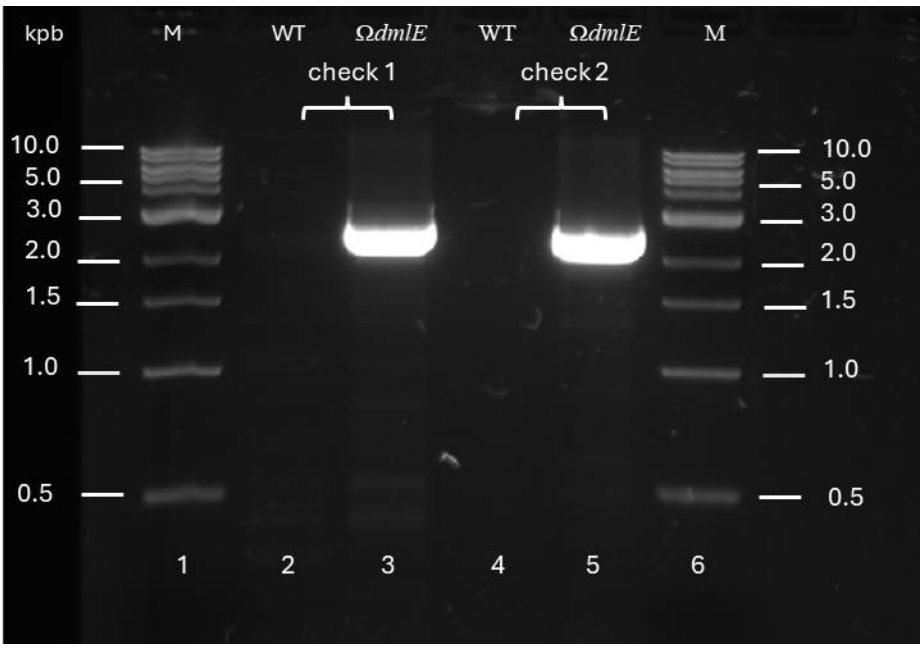

Figure 6.5. AGE image showing PCR verification of vector insertion in *Streptomyces* strain 21308-Ω*dmlE* (100 V, 1 hr, 1% (w/v) agarose, 1X TBE). Lanes 1 and 6: 1kb DNA marker; lanes 2-3: wild type and mutant gDNA with primer pair check1; lanes 4-5: wild type and mutant gDNA with primer pair check2. Image adapted from (Dashti *et al.*, 2022).

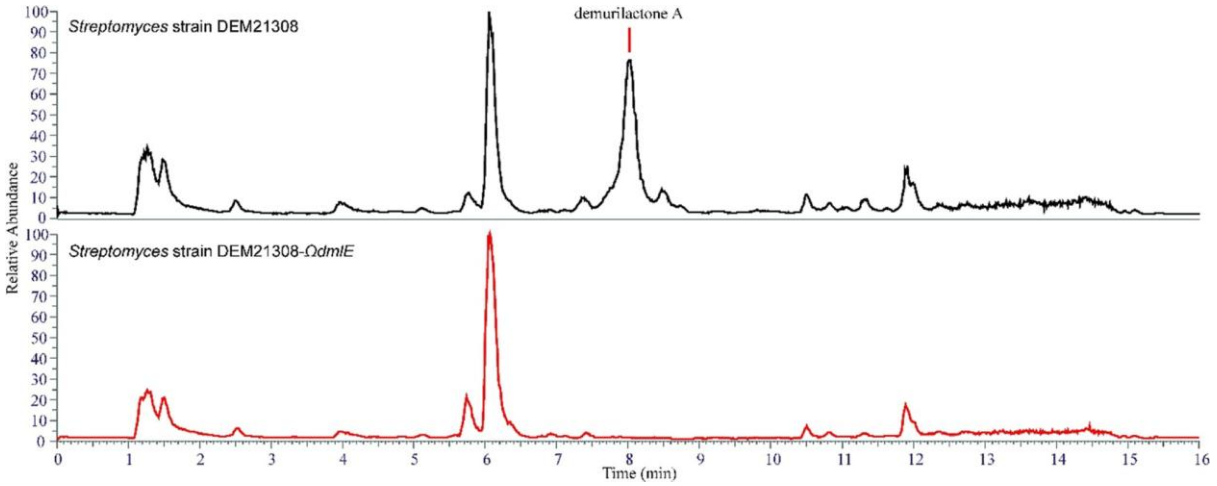

Figure 6.6. Comparison of LC–MS profiles of culture extracts from *Streptomyces* strain DEM21308 and *Streptomyces* strain DEM21308-Ω*dmlE*. Figure adapted from (Dashti *et al.*, 2022).

6.3 Linking the *per* gene cluster to persiathiacin production and mechanism of action of persiathiacin

6.3.1 Background

Thiopeptides, also known as thiazolyl peptides, are highly modified macrocyclic peptides that belong to the RiPPs family of natural products (Bagley *et al.*, 2005). A key structural feature of thiopeptides is the presence of a six-membered nitrogen-containing ring (Just-Baringo, Albericio and Álvarez, 2014), which forms the basis for their classification into different series

(series a to e) (Vinogradov and Suga, 2020). Thiopeptides are also categorized based on macrocycle size, with studies suggesting a correlation between macrocycle size and biological activity (Vinogradov and Suga, 2020).

Persiathiacins are newly identified polyglycosylated thiopeptide antibiotics produced by *Actinokineospora* UTMC 2248 (Dashti *et al.*, 2024). These 26-membered thiopeptides belong to series e, along with nocathiacin, nosiheptide, and philipimycin (Dashti *et al.*, 2024). The major compound, persiathiacin A, exhibits potent antibacterial activity against methicillin-resistant *Staphylococcus aureus* (MRSA) and multidrug-resistant *Mycobacterium tuberculosis* (Dashti *et al.*, 2024).

In the study focused on the discovery and biosynthesis of persiathiacins (Dashti *et al.*, 2024), a gene cluster containing 33 genes (designated *per*) was proposed to be involved in the persiathiacin production. Bioinformatics analysis of the *per* BGC revealed a high percentage of similarity with the gene clusters of closely related thiopeptides nosiheptide (*nos*) and nocathiacin (*noc*). The persiathiacin biosynthesis pathway includes 6 cytochrome P450 (CYP) enzymes (*perB, perC, perT, perU, perV* and *perX*), five of which show significant similarity to CYP in the *noc* BGC. The only CYP-encoding gene absent from the *noc* BGC was *perX*, which is hypothesized to catalyse the hydroxylation of the central thiazole ring, forming the attachment site for the three sugars, as shown in Figure 6.7 (hydroxyl attached by PerX shown in red). Overproduction and purification of PerX, followed by *in vitro* enzyme assays with nosiheptide, resulted in the expected hydroxylated products, although the yield was insufficient for full structural characterization. Similarly, overexpression of *perX* in the nosiheptide producing strain did not produce the desired yield despite detection of hydroxylated nosiheptide by HPLC-HR-MS. In this study, I attempted to use insertional mutagenesis of *Actinokineospora* UTMC 2248, via protoplast formation, to validate the role of the *perX*. I also investigated the mechanism of resistance to persiathiacin.

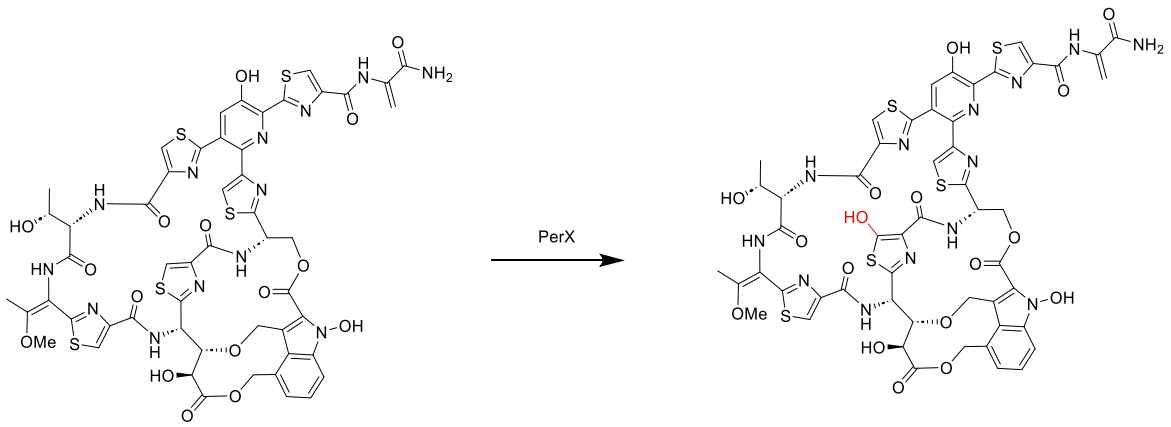

Figure 6.7 Chemical structure of core persiathiacin highlighting the hydroxylation of the thiazole ring to form attachment for the trisaccharide which is hypothesized to be catalysed by PerX.

6.3.1 Insertional mutagenesis of perX *using protoplast formation*

A similar approach to that described in the previous section was employed to inactivate *perX* in *Actinokineospora* UTMC 2248. A pSET-based vector was constructed by replacing the integrase gene of pSET152 with a 2 kb internal fragment of the *perX* gene, as illustrated in Figure 6.3. A map of the assembled vector, named pSET-*perX*, is shown in Figure 6.8, and the primer sequences used for amplification are listed in Table 2.5. Again, because the inserted fragment was internal to the *perX* gene, it would generate a gene disruption upon single-crossover integration into the UTMC 2248 genome. Despite multiple attempts, no genuine conjugants were obtained following conjugation of pSET-*perX* into *Actinokineospora* UTMC 2248 using *E. coli* ET12567 [pUZ8002]. This is likely due to the strain's inability to sporulate on solid media; spores are the preferred starting material for preparation of the well dispersed cultures needed for efficient conjugation (Mazodier, Petter and Thompson, 1989). Moreover, when grown in liquid culture, the cells tend to aggregate, further reducing conjugation efficiency.

Protoplast transformation was then employed as an alternative strategy with which to introduce pSET-*perX* into *Actinokineospora* UTMC 2248. The protoplast formation protocol (section 2.4.3), was adapted from MacNeil and Klapko (MacNeil and Klapko, 1987). Figure 6.9 shows *Actinokineospora* UTMC 2248 cells before (A) and after (B) treatment with protoplast buffer containing lysozyme. Microscopic images were captured under 100x oil-immersion objective. The spherical morphology of the cells in Figure 6.9B, in contrast to the branched mycelia in Figure 6.9A, indicates successful removal of the cell wall.

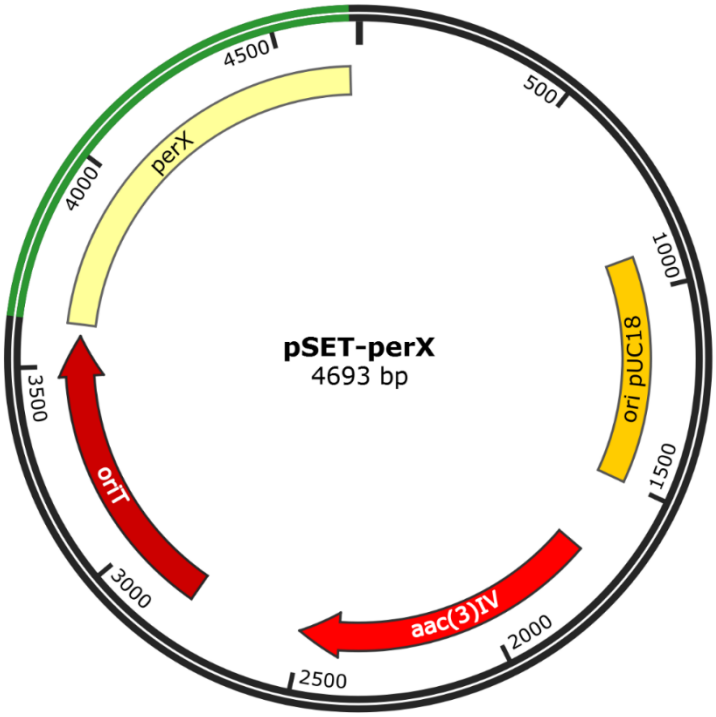

Figure 6.8 Plasmid map of pSET-*perX* used for inactivation of *perX* gene in *Actinokineospora* UTMC 2248.

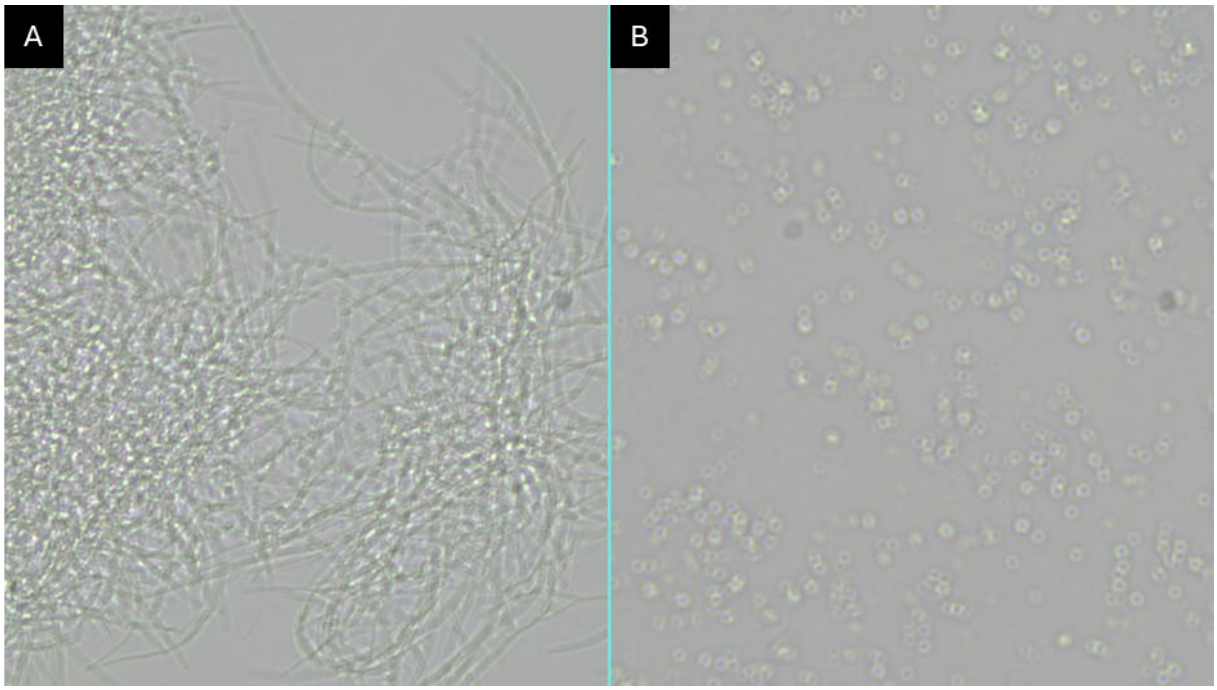

Figure 6.9 *Actinokineospora* UTMC 2248 before (A) and after (B) treatment with protoplast buffer containing lysozyme for 30 min. Images taken under 100x oil immersion objective.

The resulting protoplasts were subjected to PEG-mediated transformation using 2 µg of pSET-*perX* plasmid DNA and subsequently plated onto pre-dried R2YE medium. After overnight incubation at 30 °C, an apramycin overlay was applied for the selection of transformants, and the plates were returned to 30 °C to allow protoplast regeneration. Colonies began appearing

between 4 to 10 days post-selection. One apramycin-resistant colony, designated UTMC-*perX* was selected for metabolic production. Figure 6.10 shows a comparison of the metabolic profiles of the wild type and mutant strains. A distinct mass shift corresponding to loss of the trisaccharide moiety was observed, consistent with expectation for the loss of *perX* function. These results demonstrate that direct insertional mutagenesis via protoplast transformation is a viable strategy for future functional studies of genes involved in persiathiacin biosynthesis.

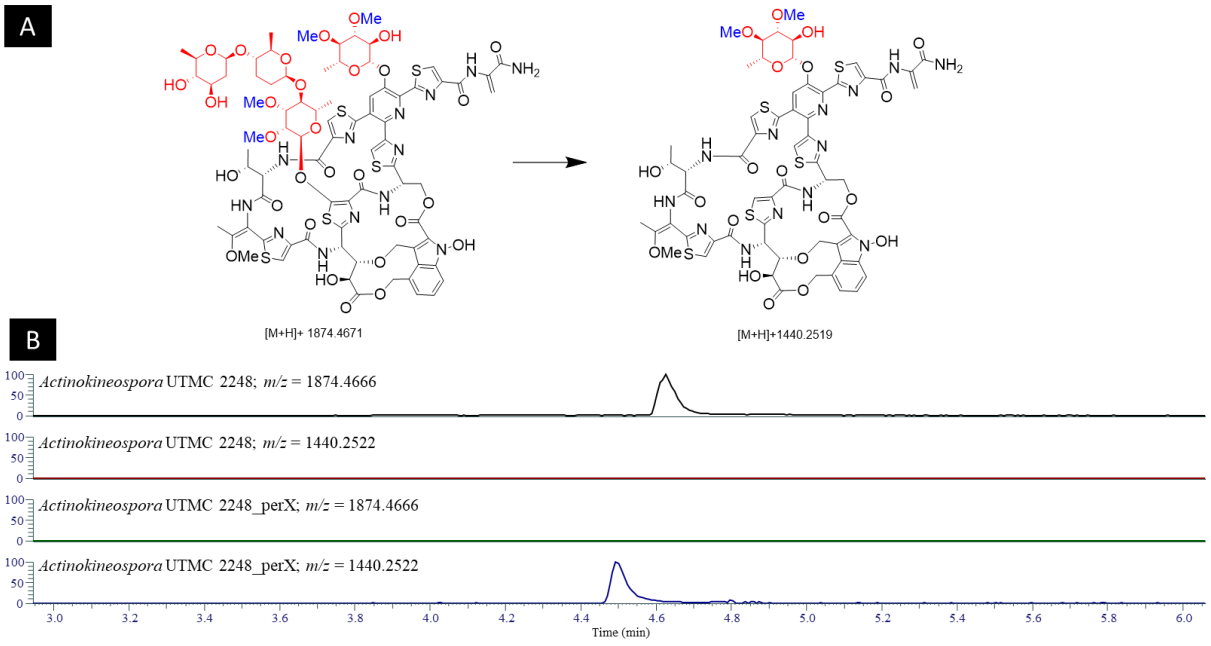

Figure 6.10 A) Left- chemical structure of persiathiacin highlighting the sugar moieties; $[M+H]^+$ 1874.46. Right- chemical structure of persiathiacin after removal of trisaccharide attached to central thiazole ring; $[M+H]^+$1844.25. B) Extracted ion chromatograms at *m/z* 1874.4666 (black) and 1440.2522 (red) from UHPLC-HR-MS analyses of culture extracts from *Actinokineospora* UTMC 2248 in comparison with extracted ion chromatograms at *m/z* 1874.4666 (green) and 1440.2522 (blue) in *Actinokineospora* UTMC 2248_perX.

6.3.2. Mechanism of resistance to persiathiacin

In vitro biochemical assays demonstrated that persiathiacin inhibits protein translation at both the initiation and elongation phases (Woodgate *et al.*, 2024). To further investigate the mechanisms of resistance, persiathiacin-resistant *Bacillus subtilis* 168CA mutants were generated by culturing *B. subtilis* on plates containing varying concentrations of persiathiacin (10–30 µg/mL). Whole genome sequencing analysis of the resulting mutants revealed various mutations in the *rplK* gene, which encodes ribosomal protein L11. Most mutations involved

deletions at Proline 22, a known binding site for the thiopeptides thiostrepton and nosiheptide (Woodgate *et al.*, 2024; Wimberly *et al.*, 1999; Harms *et al.*, 2008).

A similar mutation pattern was observed in *S. aureus* persiathiacin-resistant mutants.

Figure 6.11 shows an alignment of the *rplK* gene amplified and sequenced from wild type *S. aureus* with six mutant sequences. Table 6.1 presents the genotypic variations and their corresponding mutations detected in the six resistant strains. Mutants Sa-1 and Sa-2 (purple, Figure 6.11) harboured single base pair deletions at positions 169 and 340, respectively, resulting in premature stop codons (UAA). Mutants Sa-3 and Sa-4 (blue, Figure 6.11) carried a single base pair deletion of A at position 19, leading to a frameshift. Mutants Sa-5 and Sa-6 (yellow, Figure 6.11) both exhibited 57 bp deletions from position 87 to 143. The identical mutations observed in Sa-3/Sa-4 and Sa-5/Sa-6 suggest that they may be clonal descendents rather than independent mutants. Since only the *rplK* region was sequenced in a limited number of *S. aureus* mutants, additional resistance mechanisms to persiathiacin A, beyond L11 mutations, cannot be excluded.

Collectively, these findings indicate that mutations in *rplK* are a key driver of persiathiacin resistance. Further growth analysis comparing one of the *B. subtilis* 168CA persiathiacin resistant mutants (designated *mutD*) and wild-type *B. subtilis* 168CA revealed impaired growth in the mutant strain, both in presence and absence of persiathiacin, resembling the phenotype of an *rplK* knockout strain (*B. subtilis* 168CA Δ*rplK*) (Figure 6.12).

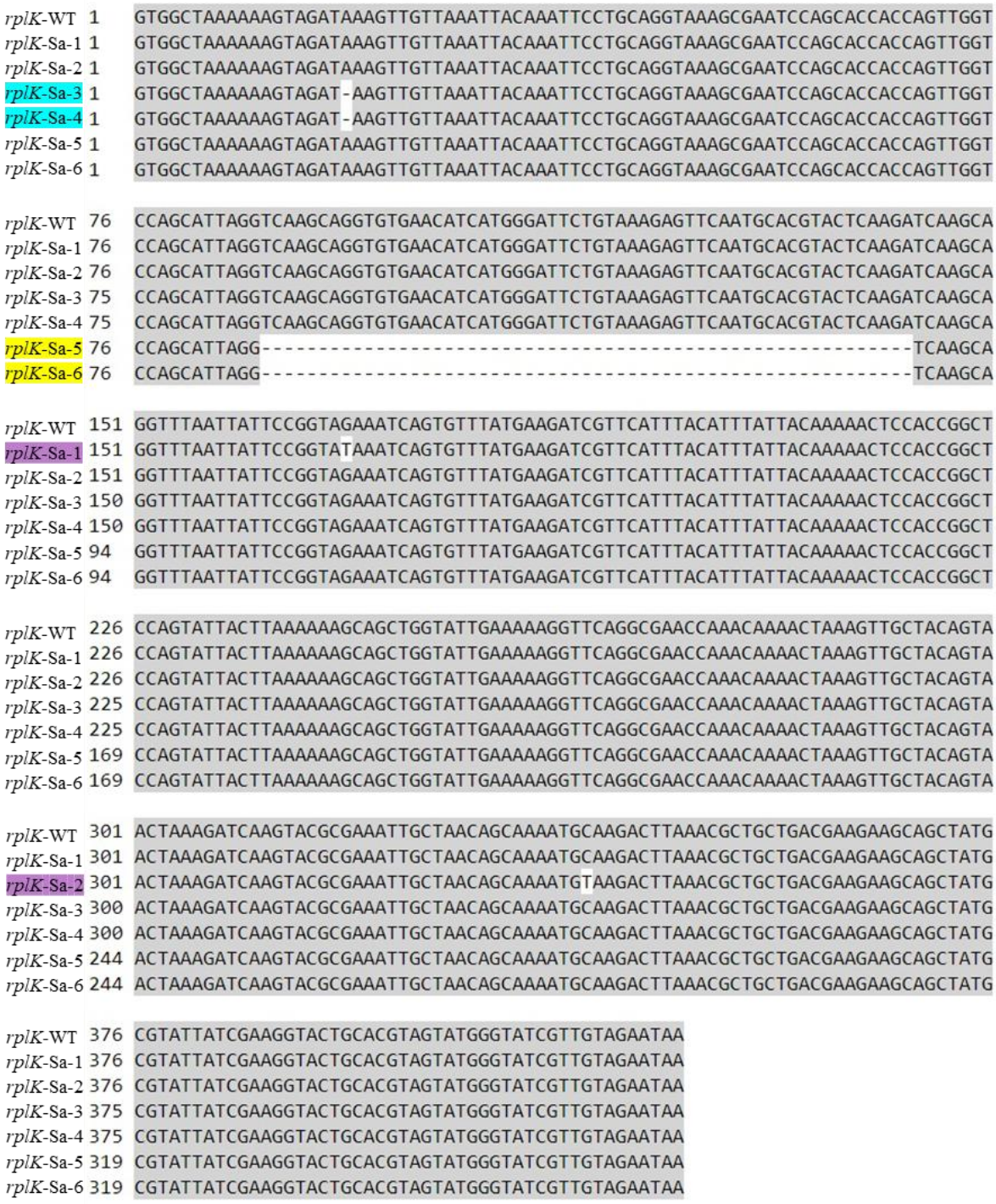

Figure 6.11 Multiple sequence alignment of *rplK* from *S. aureus* (*rplK*-WT) and persiathiacin A resistant *S. aureus* isolates (*rplK* Sa1-6). Image adapted from (Woodgate *et al.*, 2024).

Table 6.1 Table of the persiathiacin-resistant *S. aureus* mutants and their genotype changes.

Mutant	Genotype changes	Genetic mutation
rplK-Sa-1	Substitution at position 169	Stop codon
rplK-Sa-2	Substitution at position 340	Stop codon
rplK-Sa-3	1 bp deletion at position 19	Frameshift mutation
rplK-Sa-4	1 bp deletion at position 19	Frameshift mutation

rplK-Sa-5	57 bp deletion at positions 87 to 143	Deletion mutation
rplK-Sa-6	57 bp deletion at positions 87 to 143	Deletion mutation

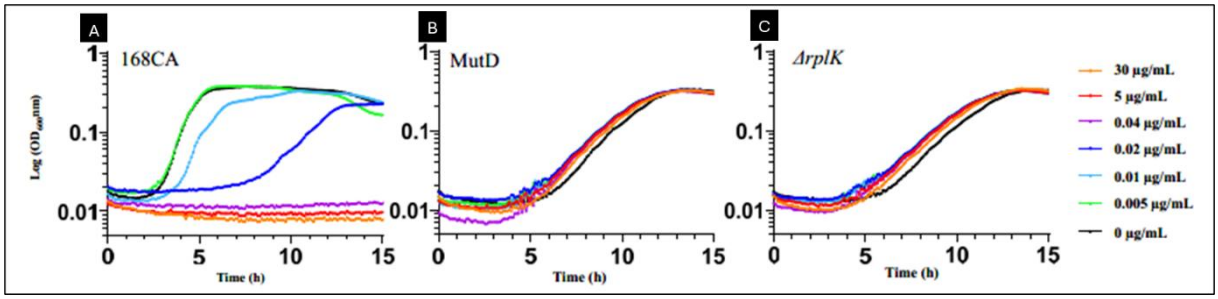

Figure 6.12 Comparative growth curve of: A) *B. subtilis;* B) *mutD*; C) *ΔrplK* grown in LB medium with varying concentrations of persiathiacin, as indicated. Image adapted from (Woodgate *et al.*, 2024).

6.4 Biosynthesis and biological activity of quinovosamycins

6.4.1 Background

Nucleoside antibiotics are a class of NPs derived from nucleosides and nucleotides. They exhibit a broad range of biological activities, including antibacterial, antifungal, antitumor, antiviral, herbicidal, and insecticidal effects. This wide spectrum of activity arises from their ability to interfere with key biosynthetic processes such as nucleic acid, protein, and glycoprotein synthesis; all pathways in which nucleosides and nucleotides play essential roles (Isono, 1988). Notably, their mode of action is closely tied to their chemical structure. For instance, nucleoside analogues primarily inhibit nucleic acid synthesis, while acylated or glycosylated nucleosides tend to disrupt protein and glycan biosynthesis (Isono, 1988).

Quinovosamycins (QVMs) are nucleoside antibiotics originally isolated from *Streptomyces niger*. Structurally, they are closely related to tunicamycin, with the only difference being that the *N*-acetylglucosamine residue in tunicamycin (Tun) is replaced by *N*-acetylquinovosamine in QVMs (Figure 6.13A) (Price *et al.*, 2016). To date, three analogues (Q1–Q3) have been identified, distinguished by variations in the fatty acid chain attached to the tunicamine core (Figure 6.13B) (Price *et al.*, 2016). Our paper (Sumang, Errington and Dashti, 2025) reports the discovery of a new QVM analogue, Q4, and proposes a different biosynthetic pathway deviating from that previously suggested for QVM biosynthesis (Price *et al.*, 2016). Additionally, the antimicrobial activity of Q4, including MIC values was evaluated.

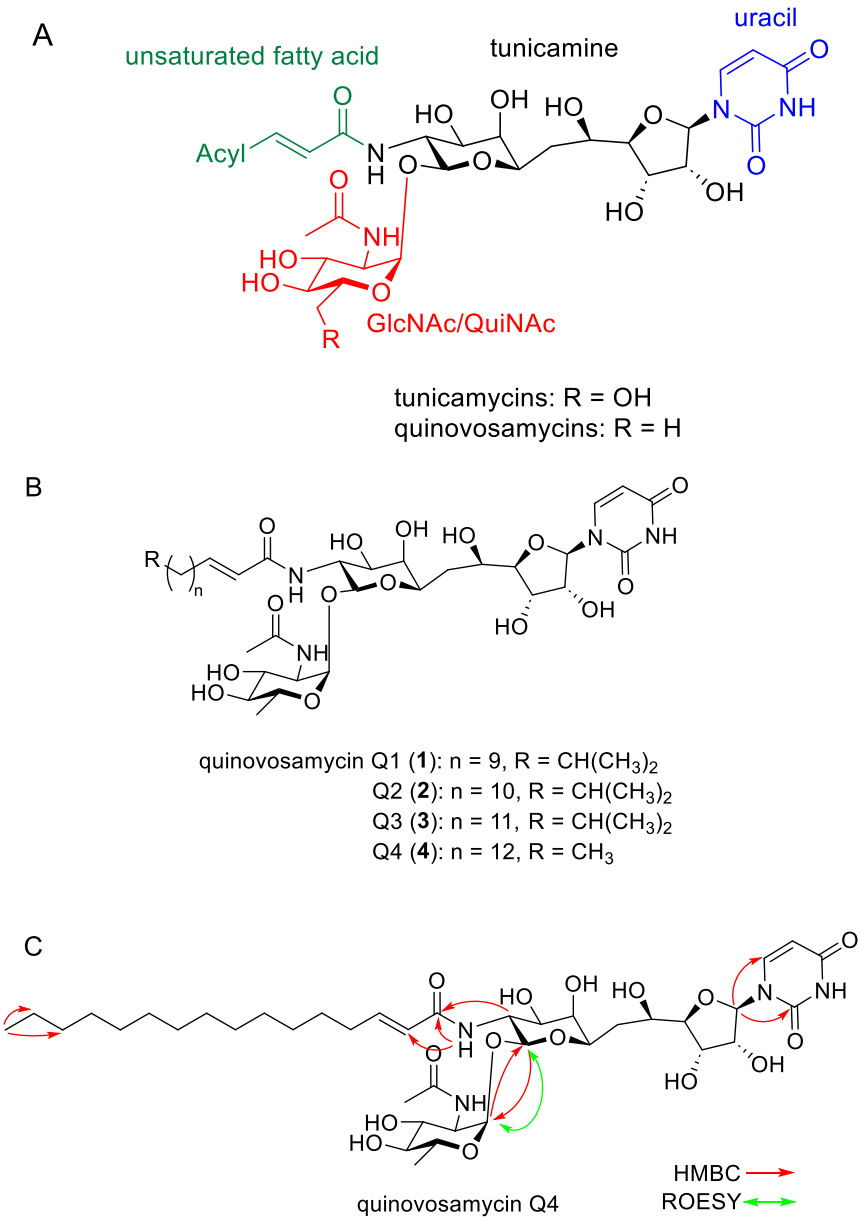

Figure 6.13 (A) Chemical structure of quinovosamycins and tunicamycins. (B)Structure of QVM analogues (Q1-Q4). (C)Structure of Q4 with key HMBC and ROESY correlations. Figure adapted from (Sumang, Errington and Dashti, 2025)

6.4.2 Purification and structure elucidation of Q4

The novel quinovosamycin analogue, Q4, was purified from *Streptomyces* strain PR3G, a strain isolated from rhizosphere. This strain was selected from an Actinobacterial extract library after its crude extract demonstrated strong antimicrobial activity against *Cryptococcus neoformans*, *Candida albicans*, and *Bacillus subtilis*. For large-scale production, *Streptomyces* strain PR3G was cultivated on 1L YEME agar plates for seven days, followed by methanol extraction of the cells. Bioactivity-guided fractionation was performed using preparative HPLC, and the structure of the active compounds were elucidated by NMR and mass spectrometry. Two of the

bioactive fractions were found to share the same molecular formula, $C_{39}H_{64}N_4O_{15}$. One was confirmed as Q2 based on NMR analysis, which features a branched fatty acid tail (Price *et al.*, 2016), while the other contained a straight-chain fatty acid tail, identifying it as the novel analogue, Q4 (Figure 6.13C) (work of Dr, Yousef Dashti). A detailed discussion of the structural elucidation based on 1D and 2D NMR experiments, is provided in our published study (Sumang, Errington and Dashti, 2025). The key difference between Q2 and Q4 is the presence of a triplet methyl group with characteristic chemical shift, which is indicative of a straight fatty acid chain, found exclusively in the fatty acid moiety of Q4.

6.4.3 Biosynthesis of Q4

To investigate the biosynthesis of QVMs, *Streptomyces* strain PR3G was sequenced using both Nanopore and Illumina technologies, and the genome was subsequently assembled. Bioinformatics analysis of the assembled genome revealed a biosynthetic gene cluster (GenBank accession number PQ628243) containing genes highly homologous to *tunA-tunN*, which are involved in tunicamycin biosynthesis (Figure 6.14A). Previous studies have postulated that the *tun* BGC may also be responsible for QVM biosynthesis (Price *et al.*, 2016). It was hypothesized that a putative reductase could directly reduce UDP-GlcNAc-5,6-ene (**5**) to UDP-D-QuiNAc (**11**), serving as a precursor for QVMs (Figure 6.14B). Additionally, *tunD* was proposed to have relaxed substrate specificity, allowing it to glycosylate intermediate **9** with either UDP-GlcNAc or UDP-D-QuiNAc, leading to the formation of tunicamycin and quinovosamycins, respectively (Price *et al.*, 2016).

Upstream of *tunA-tunN* in the *Streptomyces* strain PR3G genome, we identified several gene (designated *quiO-quiS*) predicted to encode enzymes involved in sugar modification and attachment (Figure 6.14B). QuiS is a putative thymidylyltransferase, likely responsible for activating GlcNAc-1-phosphate, a precursor for both UDP-Glc-5,6-ene (**6**) and UDP-D-QuiNAc (**11**). QuiR, predicted to be an NAD-dependent epimerase/dehydratase, likely functions as a 4,6-dehydratase generating UDP-4-keto-6-deoxy-α-D-GlcNAc (**10**), while QuiP, a putative FAD-dependent oxidoreductase, is proposed to reduce intermediate **10** to UDP-D-QuiNAc (**11**). Finally, the glycosyltransferase QuiQ could catalyse the attachment of UDP-D-QuiNAc (**11**) to intermediate **9**, forming **12** during quinovosamycin biosynthesis.

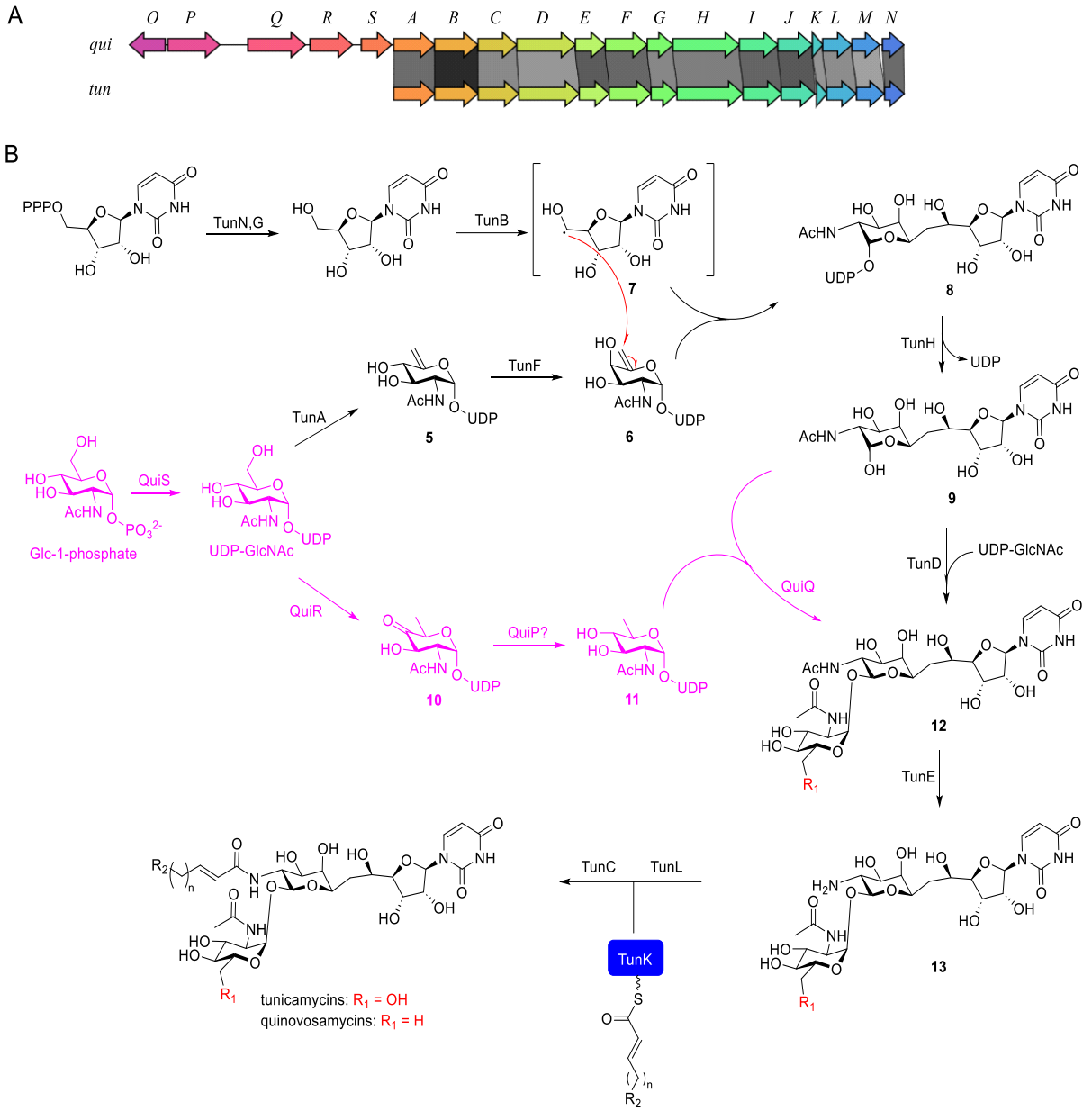

Figure 6.14 A) Organization of the *qui* and *tun* biosynthetic gene clusters. B) Proposed biosynthesis of quinovosamycins and tunicamycins (proposed function of new enzymes are shown in purple). Image adapted from (Sumang, Errington and Dashti, 2025).

6.4.4 Insertional mutagenesis of the quiQ *gene*

To experimentally verify the role of these newly identified genes in QVM biosynthesis, insertional mutagenesis was performed on *quiQ*, one of the predicted essential genes, using a pSET-derived vector, again containing an internal segment of the gene. The 4.8 kbp construct (Figure 6.15) was introduced into *Streptomyces* PR3G by conjugation, and successful transconjugants were grown in YEME medium. After five days of growth, cells were extracted with methanol and analysed by UHPLC-HR-MS for metabolic profiling (Figure 6.16). The absence of QVM analogues in the mutant strain confirmed the essential role of the *quiQ* gene in QVM biosynthesis.

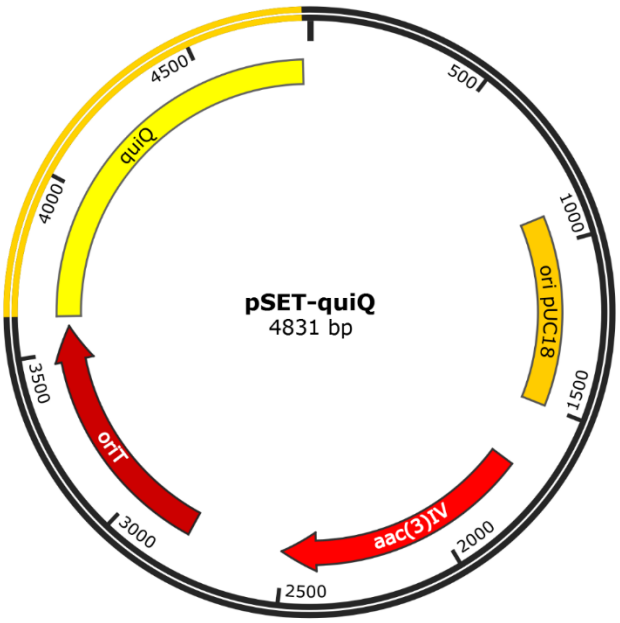

Figure 6.15 Plasmid map of pSET-*quiQ* used for insertional mutagenesis and inactivation of *quiQ* on *Streptomyces* strain PR3G.

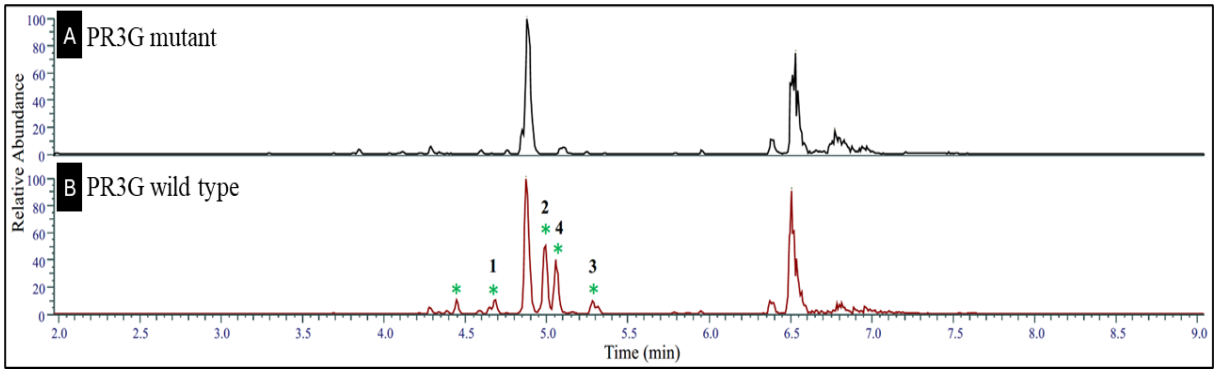

Figure 6.16 Total ion chromatogram from UHPLC-HR-MS analyses of **A)** mutant strain with insertional mutagenesis in *quiQ* and **B)** wild type *Streptomyces* strain PR3G. Peaks corresponding to quinovosamycins (Q1-Q4) are annotated with green stars, whose structures were confirmed by NMR. Image adapted from (Sumang, Errington and Dashti, 2025).

To evaluate whether the newly identified analogue, Q4, retained the antimicrobial activity characteristic of other quinovosamycin and tunicamycin derivatives, it was tested against *C. neoformans* H99, *C. albicans*, and *B. subtilis*. As shown in Figure 6.17, Q4 exhibited MIC values of 0.03 µg/mL, 0.5 µg/mL, and 0.125 µg/mL against *C. neoformans*, *C. albicans*, and *B. subtilis*, respectively, demonstrating its potent and broad spectrum antimicrobial activity.

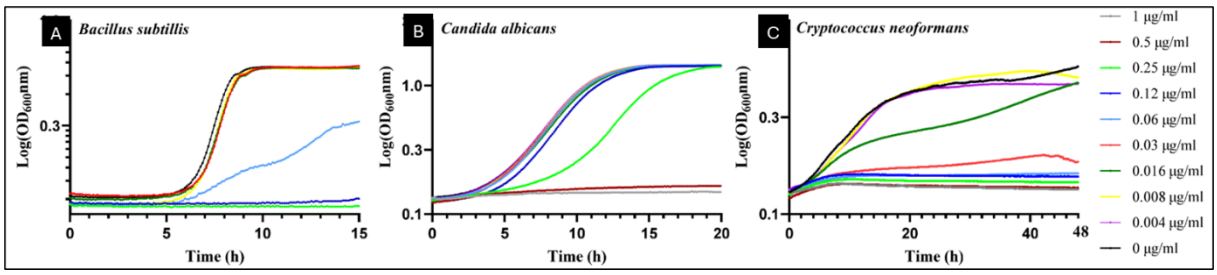

Figure 6.17 Growth curve of A) *B. subtilis*; B) *C. albicans* and C) *C. neoformans* H99 grown with various concentrations of Q4 grown in 30 °C with shaking, and OD600 measurements were made at 6 min intervals. Image adapted from (Sumang, Errington and Dashti, 2025).

Chapter 7: Summary, Impact, and Future Directions

7.1 Overview

This thesis focuses on the discovery and characterization of NPs from Actinomycetes and is organized into three main parts. The first part presents a molecular approach for capturing BGCs and heterologously expressing them in a *Streptomyces* host. The second part explores the use of plant extracts as chemical elicitors to stimulate NP production in Actinomycetes. The final part integrates linking BGCs to the production of novel antibiotics, investigating their biosynthetic pathways, and examining mechanisms of resistance. This chapter provides a summary of the key findings from each study, highlights their significance to the scientific community, and outlines potential future research directions.

7.2 A new method for capturing large BGCs based on the pJE vectors

The ability to capture and heterelogously express intact BGCs is an important method that helps drive NP discovery forward, especially via the expression of cryptic BGCs from genetically intractable strains (Nah *et al.*, 2017; Park *et al.*, 2022). One important factor in BGC capture is the cloning vector. Chapter 3 focuses on the construction of two new vectors, pJE-1 and pJE-2, which were shown to be effective for constructing gDNA libraries with very large inserts. The F-based replication system of the pJE vectors ensured stable maintenance of large DNA inserts, while the inducible copy-number control facilitated clone characterization. Optimized methodologies such as the use of agarose plugs, partial digestion, recovery of digested fragments from agarose, and drop dialysis significantly improved DNA integrity, insert size, and transformation efficiency. The vector-phosphatase method using the *Bam*HI site of pJE-2 efficiently produced a representative library with large cloned fragments, as compared to the partial- fill in strategy using pJE-1. Chapter 4 describes the use of pJE-2 and the optimized protocol described in chapter 3 in making a representative gDNA library from the *Actinomadura madurae* T576 strain that produces novel sulphated compounds. Multiple BGCs from *A. madurae* T576 were successfully cloned, including an ~80 kbp BGC encoding the sulphated compounds. This BGC was functionally validated through heterologous expression in *S. albus* Del14, leading to the production of the expected compounds. Compound detection was strongly influenced by host strain, culture medium, and extraction method. Methanol extraction was found to be more effective, suggesting that the compounds are largely intracellular but can also be secreted in low amounts. Despite these successes, challenges remain, including the labour-intensive preparation of high-quality genomic DNA, the risk of BGC fragmentation by frequent-cutting enzymes such as *Sau*3AI, and the absence of detectable metabolites from some successfully cloned and conjugated regions. Nevertheless, this work

demonstrates a validated workflow from BGC capture to compound expression for NP discovery in Actinomycetes.

Although most of the recently developed biosynthetic gene cluster (BGC) capturing techniques emphasize direct capture using CRISPR Cas9 technology (Xu and Wright, 2019; Wan, Ma and Yuan, 2023), constructing gDNA libraries using the pJE vector still remains highly advantageous. This approach allows for the simultaneous capture of multiple BGCs in a single gDNA library and is particularly useful for genetically intractable and slow growing strains. Moreover, the design of pJE can be further optimized and serves as a progenitor for future cloning vector development. A key advantage of the pJE vector is its switchable copy number, from low to medium copy, mediated by the presence of *oriS* and *oriV*. In addition, pJE can integrate into common *Streptomyces* hosts through the phiC31 integration system. Among the widely used cloning vectors capable of accommodating large DNA inserts is pESAC13 derived from the vectors described by Sosio et al. (Sosio, Bossi and Donadio, 2001). This vector can conjugate into *Streptomyces* but is commercially owned by Bio S&T (Banque pESAC13, sur Bio S&T). Another BAC-based vector, pStreptoBAC V, can only be maintained at low copy number and does not possess the phiC31 system, so it requires protoplast transformation for transfer to a heterologous host. This vector was used to clone and subsequently express in *S. lividans* TK64 the daptomycin BGC (Miao *et al.*, 2005). Similarly, the pHL921/931 vectors are low copy but incorporate the phiC31 systeem, and they have been successfully used to clone and express streptothricin and borrelidin BGCs from *Streptomyces rochei* (Xu et al., 2016). While low copy number vectors provide stable maintenance of large DNA inserts, they have the disadvantage of yielding low DNA recovery for downstream analysis. The incorporation of the phiC31 system, however, offers a strong advantage by enabling conjugation across different *Streptomyces* hosts. The pMBD vector series further expands available options by providing a combination of low and high copy vectors, all of which utilize phiC31 integration system (Martinez *et al.*, 2004). By contrast, the pJW series also employ *oriV* to switch between low and high copy numbers but lack phiC31, and they are mostly applied in plant systems (Wild, Hradecna and Szybalski, 2002). Taken together, these features highlight the distinct advantages of the pJE vector, making it an efficient tool for cloning large DNA inserts and advancing NP discovery in Actinomycetes.

Future directions should focus on strategies that enable cloning of larger DNA inserts, which are often critical for capturing complete BGCs. This may include optimizing partial restriction digestion methods and refining methods for recovering intact HMW DNA fragments. Since screening of the resulting clones can be time-consuming and labor-intensive, incorporating

PCR-based fingerprinting with universal primers for NRPSs and PKSs would be highly beneficial (Ayuso-Sacido and Genilloud, 2005). This approach would provide an overview of the genetic content of each clone. For the expression of sulfated compounds, the introduction of stronger promoters such as SP44 (Bai *et al.*, 2015), *kasO*p* (Wang *et al.*, 2013), and P_{30S} (Huang *et al.*, 2025) could significantly improve yields of the target metabolites. In contrast, regions 4, 7, and 27, although successfully cloned, failed to show expression under the same conditions applied for expression of sulphated compounds, indicating the need for alternative strategies. These include use of different heterologous hosts, such as *Streptomyces venezuelae* (Jung et al., 2006) or *Streptomyces avermitilis* SUKA17 (Komatsu *et al.*, 2013), and optimizing culture conditions by testing a variety of growth media to facilitate compound production (Bode *et al.*, 2002). Alternatively, the lack of expression may indicate the presence of transcriptional regulators that keep these clusters silent. To overcome this, one approach is to overexpress potential activators such as LAL family proteins (Laureti *et al.*, 2011), while another is to delete repressors such as TetR-like regulators within the cloned BGCs (Alberti *et al.*, 2019), thereby unlocking silent pathways and promoting compound expression.

7.3 Use of plant extracts to induce NP production in Actinomycetes

Chapter 5 explored how phytochemicals can act as elicitors to activate silent BGCs in Actinomycetes. The main strategy used for this study was to incorporate different plant extracts to Actinomycetes isolated from rhizhosphere. One of the strains, *Streptomyces* MBN2-2, when grown with hibiscus extract, produced two compounds not detected in cultures without the extract, thiolutin and aureothricin, both classified as broad-spectrum DTP antibiotics. Streptomyces strain MBN2-2,—thiolutin and aureothricin, both recognized as broad-spectrum DTP antibiotics. LC-HR-MS confirmed their presence through distinct peaks corresponding to the known masses of these antibiotics, and their structures were validated through NMR spectroscopy. Further analysis of the hibiscus extract revealed two active compounds, hibiscus acid dimethyl ester and hydroxycitric acid 1,3-dimethyl ester, which were identified as the inducers of DTP production. Given the structure of the compounds and their ability to chelate iron, the role of iron in regulating DTP biosynthesis was investigated. Supplementing the culture medium directly with iron ions (Fe^{2+} or Fe^{3+}) also induced the production of thiolutin and aureothricin, suggesting a link with iron availability. Thus, the proposed mechanism is that these phytochemicals alter iron availability in the culture media, triggering the activation of DTP antibiotics in *Streptomyces* MBN2-2.

This work demonstrates how plant-microbe interactions can be intentionally replicated under laboratory set-up to stimulate NP production in *Actinomycetes*. The study specifically demonstrates that iron chelation by small organic molecules functions as a biochemical signal that activates distinct antibiotic pathways, providing key insights for the development of molecules designed to serve as elicitors of antibiotic production. Future directions for this study include providing a clear mechanism by which iron availability influences the induction of DTPs. This could involve examining iron regulatory proteins (Cheng *et al.*, 2018), siderophore systems (Barona-Gomez *et al.*, 2006), and transcription factors that connect iron sensing to gene cluster activation (Vior *et al.*, 2014a). Expanding the screening to additional plant extracts or a broader range of *Actinomycetes* strains may also reveal new elicitors and lead to the discovery of novel antibiotics. Another valuable line of research is exploring the ecological role of these compounds in the rhizosphere (Stringlis *et al.*, 2018), particularly whether hibiscus plants produce them to shape microbial communities (Nicolle *et al.*, 2024) or suppress pathogenic organisms (Viaene *et al.*, 2016).

7.4 Linking BGCs to novel antibiotics

Chapter 6 emphasizes the link between the predicted BGCs and the production of novel antibiotics, namely demurilactone A, persiathiacins, and quinovosamycin 4. Demurilactone A, a polyene macrolide synthesized by *Streptomyces* DEM21308, was shown to inhibit the growth of L-form *B. subtilis* with a minimum inhibitory concentration (MIC) of 16 µg/mL (Dashti *et al.*, 2022) highlighting its potential as a therapeutic agent for persistent infections (Errington *et al.*, 2016). Persiathiacins are polyglycosylated thiopeptide antibiotics produced by *Actinokineospora* UTMC 2248, which share structural similarity to nocathiacin, nosiheptide, and philipimycin (Dashti *et al.*, 2024). Persiathiacin A exhibits strong antibacterial activity against MRSA and multidrug-resistant *M. tuberculosis* (Dashti *et al.*, 2024). Quinovosamycins, on the other hand, are nucleoside antibiotics that are structurally related to tunicamycins. Quinovosamycin 4, a newly discovered analogue isolated from *Streptomyces* PR3G, differs from previously reported analogues by having a straight-chain fatty acid tail. This compound exhibited potent activity against *C. neoformans*, *C. albicans*, and *B. subtilis* with MIC values of 0.03 µg/mL, 0.5 µg/mL, and 0.125 µg/mL, respectively (Sumang, Errington and Dashti, 2025). Meanwhile, additional research on quinovosamycin biosynthesis explored the function of upstream genes present in the *qui* BGC but absent from the *tun* BGC. Specifically, QuiS, QuiR, and QuiP are suggested to act sequentially in the activation and modification of sugar precursors, ultimately leading to the formation of UDP-D-QuiNAc during the biosynthetic

pathway. Subsequently, the glycosyltransferase QuiQ is predicted to catalyze the attachment of UDP-D-QuiNAc to generate quinovosamycin (Sumang, Errington and Dashti, 2025).

In all cases, gene inactivation was achieved through direct insertional mutagenesis, using a pSET-based vector introduced into the respective producing strains either by conjugation or protoplast transformation. Integration of the pSET-based vector resulted in a single cross-over event that disrupted essential genes within the BGCs. The complete loss of antibiotic production in the resulting transformants provided clear evidence for the involvement of these BGCs in the biosynthesis of the respective antibiotics. Linking a BGC to production of a specific antibiotic is the first step in undertanding the biosynthesis of the compound. This knowledge enables the engineering of biosynthetic pathways to increase yield, create improved analogues, or produce the compound in alternative hosts (Pham et al., 2019). As an example, current research is directed toward improving the solubility of persiathiacin by employing a gene inactivation strategy, as highlighted in this study.

Further studies were also conducted on the mechanism of resistance to persiathiacin A. These investigations revealed that persiathiacin-resistant mutants of *B. subtilis* and *S. aureus* acquired mutations in the *rplK* gene, which encodes the L11 ribosomal protein that acts as the binding site for thiopeptides (Woodgate *et al.*, 2024). Alongside the discovery of new antibiotics, it is crucial to investigate the molecular mechanisms underlying antibiotic resistance. Understanding these mechanisms enables the development of strategies to prevent or overcome resistance, thereby enhancing the effectiveness and longevity of both existing and new antibiotics (Lin *et al.*, 2015). This knowledge can also guide the design of new drugs that avoid or counteract resistance (Blair *et al.*, 2015).

References

Ahmed, Y., Rebets, Y., Estévez, M. R., Zapp, J., Myronovskyi, M. and Luzhetskyy, A. (2020) 'Engineering of Streptomyces lividans for heterologous expression of secondary metabolite gene clusters', *Microbial cell factories,* 19, pp. 1-16.

Alberti, F., Leng, D. J., Wilkening, I., Song, L., Tosin, M. and Corre, C. (2019) 'Triggering the expression of a silent gene cluster from genetically intractable bacteria results in scleric acid discovery', *Chemical science,* 10(2), pp. 453-463.

Alexander, D. and Zuberer, D. (1991) 'Use of chrome azurol S reagents to evaluate siderophore production by rhizosphere bacteria', *Biology and Fertility of soils,* 12, pp. 39-45.

Anderson, A. S. and Wellington, E. (2001) 'The taxonomy of Streptomyces and related genera', *International journal of systematic and evolutionary microbiology,* 51(3), pp. 797-814.

Anwar, S., Ali, B. and Sajid, I. (2016) 'Screening of rhizospheric actinomycetes for various in-vitro and in-vivo plant growth promoting (PGP) traits and for agroactive compounds', *Frontiers in microbiology,* 7, pp. 1334.

Arnison, P. G., Bibb, M. J., Bierbaum, G., Bowers, A. A., Bugni, T. S., Bulaj, G., Camarero, J. A., Campopiano, D. J., Challis, G. L. and Clardy, J. (2013) 'Ribosomally synthesized and post-translationally modified peptide natural products: overview and recommendations for a universal nomenclature', *Natural product reports,* 30(1), pp. 108-160.

Atanasov, A. G., Zotchev, S. B., Dirsch, V. M. and Supuran, C. T. (2021) 'Natural products in drug discovery: advances and opportunities', *Nature reviews Drug discovery,* 20(3), pp. 200-216.

Athalye, M., Lacey, J. and Goodfellow, M. (1981) 'Selective isolation and enumeration of actinomycetes using rifampicin', *Journal of Applied Microbiology,* 51(2), pp. 289-297.

Ayuso-Sacido, A. and Genilloud, O. (2005) 'New PCR primers for the screening of NRPS and PKS-I systems in actinomycetes: detection and distribution of these biosynthetic gene sequences in major taxonomic groups', *Microbial ecology,* 49(1), pp. 10-24.

Baars, O., Zhang, X., Gibson, M. I., Stone, A. T., Morel, F. M. and Seyedsayamdost, M. R. (2018) 'Crochelins: siderophores with an unprecedented iron-chelating moiety from the nitrogen-fixing bacterium Azotobacter chroococcum', *Angewandte Chemie,* 130(2), pp. 545-550.

Bagley, M. C., Dale, J. W., Merritt, E. A. and Xiong, X. (2005) 'Thiopeptide antibiotics', *Chemical reviews,* 105(2), pp. 685-714.

Bai, C., Zhang, Y., Zhao, X., Hu, Y., Xiang, S., Miao, J., Lou, C. and Zhang, L. (2015) 'Exploiting a precise design of universal synthetic modular regulatory elements to unlock the microbial natural products in Streptomyces', *Proceedings of the National Academy of Sciences,* 112(39), pp. 12181-12186.

Baltz, R. H. (2010) 'Streptomyces and Saccharopolyspora hosts for heterologous expression of secondary metabolite gene clusters', *Journal of Industrial Microbiology and Biotechnology,* 37(8), pp. 759-772.

Baltz, R. H. (2019) 'Natural product drug discovery in the genomic era: realities, conjectures, misconceptions, and opportunities', *Journal of Industrial Microbiology and Biotechnology,* 46(3-4), pp. 281-299.

Barkei, J. J., Kevany, B. M., Felnagle, E. A. and Thomas, M. G. (2009) 'Investigations into viomycin biosynthesis by using heterologous production in Streptomyces lividans', *Chembiochem,* 10(2), pp. 366-376.

Barona-Gomez, F., Lautru, S., Francou, F.-X., Leblond, P., Pernodet, J.-L. and Challis, G. L. (2006) 'Multiple biosynthetic and uptake systems mediate siderophore-dependent iron acquisition in Streptomyces coelicolor A3 (2) and Streptomyces ambofaciens ATCC 23877', *Microbiology,* 152(11), pp. 3355-3366.

Bauman, K. D., Li, J., Murata, K., Mantovani, S. M., Dahesh, S., Nizet, V., Luhavaya, H. and Moore, B. S. (2019) 'Refactoring the cryptic streptophenazine biosynthetic gene cluster unites phenazine, polyketide, and nonribosomal peptide biochemistry', *Cell chemical biology,* 26(5), pp. 724-736. e7.

Becker, B., Lechevalier, M. and Lechevalier, H. (1965) 'Chemical composition of cell-wall preparations from strains of various form-genera of aerobic actinomycetes', *Applied Microbiology,* 13(2), pp. 236-243.

Behie, S. W., Bonet, B., Zacharia, V. M., McClung, D. J. and Traxler, M. F. (2017) 'Molecules to ecosystems: Actinomycete natural products in situ', *Frontiers in microbiology,* 7, pp. 2149.

Bentley, S. D., Chater, K. F., Cerdeño-Tárraga, A.-M., Challis, G. L., Thomson, N., James, K. D., Harris, D. E., Quail, M. A., Kieser, H. and Harper, D. (2002) 'Complete genome sequence of the model actinomycete Streptomyces coelicolor A3 (2)', *nature,* 417(6885), pp. 141-147.

Bertrand, S., Bohni, N., Schnee, S., Schumpp, O., Gindro, K. and Wolfender, J.-L. (2014) 'Metabolite induction via microorganism co-culture: a potential way to enhance chemical diversity for drug discovery', *Biotechnology advances,* 32(6), pp. 1180-1204.

Bey, B. S., Fichot, E. B., Dayama, G., Decho, A. W. and Norman, R. S. (2010) 'Extraction of high molecular weight DNA from microbial mats', *Biotechniques,* 49(3), pp. 631-640.
Bhatti, A. A., Haq, S. and Bhat, R. A. (2017) 'Actinomycetes benefaction role in soil and plant health', *Microbial pathogenesis,* 111, pp. 458-467.

Bibb, M. J., Janssen, G. R. and Ward, J. M. (1985) 'Cloning and analysis of the promoter region of the erythromycin resistance gene (ermE) of Streptomyces erythraeus', *Gene,* 38(1-3), pp. 215-226.

Bibb, M. J., Ward, J. M. and Hopwood, D. A. (1978) 'Transformation of plasmid DNA into Streptomyces at high frequency', *Nature,* 274(5669), pp. 398-400.

Bibb, M. J., White, J., Ward, J. M. and Janssen, G. R. (1994) 'The mRNA for the 23S rRNA methylase encoded by the ermE gene of Saccharopolyspora erythraea is translated in the absence of a conventional ribosome-binding site', *Molecular microbiology,* 14(3), pp. 533-545.

Bierman, M., Logan, R., O'brien, K., Seno, E., Rao, R. N. and Schoner, B. (1992) 'Plasmid cloning vectors for the conjugal transfer of DNA from Escherichia coli to Streptomyces spp', *Gene,* 116(1), pp. 43-49.

Blair, J. M., Webber, M. A., Baylay, A. J., Ogbolu, D. O. and Piddock, L. J. (2015) 'Molecular mechanisms of antibiotic resistance', *Nature reviews microbiology,* 13(1), pp. 42-51.

Blin, K., Shaw, S., Augustijn, H. E., Reitz, Z. L., Biermann, F., Alanjary, M., Fetter, A., Terlouw, B. R., Metcalf, W. W. and Helfrich, E. J. (2023) 'antiSMASH 7.0: new and improved predictions for detection, regulation, chemical structures and visualisation', *Nucleic acids research,* 51(W1), pp. W46-W50.

Bode, H. B., Bethe, B., Höfs, R. and Zeeck, A. (2002) 'Big effects from small changes: possible ways to explore nature's chemical diversity', *ChemBioChem,* 3(7), pp. 619-627.

Boruta, T., Ścigaczewska, A. and Bizukojć, M. (2023) 'Investigating the Stirred Tank Bioreactor Co-Cultures of the Secondary Metabolite Producers Streptomyces noursei and Penicillium rubens', *Biomolecules,* 13(12), pp. 1748.

Brenner, S. and Miller, J. H. (2014) *Brenner's encyclopedia of genetics.* Elsevier Science.
Bunet, R. (2006) *Investigation of the Regulatory Mechanism of ScbA and ScbR, Two Genes Involved in the Synthesis and Sensing of [gamma]-butyrolactones & Identification of Iron Transport Genes in Streptomyces Coelicolor A3 (2).* Eberhard-Karls-Universität zu Tübingen.

Calvelo, V. Y., Crisante, D., Elliot, M., & Nodwell, J. R (2021) 'The ARC2 response in Streptomcyes coelicolor requires the global regulatory genes afsR and afsS.', *Microbiology,* 167(5), pp. 001047.

Cardoza, Y. J., Klepzig, K. D. and Raffa, K. F. (2006) 'Bacteria in oral secretions of an endophytic insect inhibit antagonistic fungi', *Ecological Entomology,* 31(6), pp. 636-645.

Cayrou, C., Raoult, D. and Drancourt, M. (2010) 'Matrix-assisted laser desorption/ionization time-of-flight mass spectrometry for the identification of environmental organisms: the Planctomycetes paradigm', *Environmental Microbiology Reports,* 2(6), pp. 752-760.

Celmer, W. D. and Solomons, I. (1955) 'The structures of thiolutin and aureothricin, antibiotics containing a unique pyrrolinonodithiole nucleus', *Journal of the American Chemical Society,* 77(10), pp. 2861-2865.

Celmer, W. D., Tanner Jr, F. W., Harfenist, M., Lees, T. and Solomons, I. (1952) 'Characterization of the antibiotic thiolutin and its relationship with aureothricin', *Journal of the American Chemical Society,* 74(24), pp. 6304-6305.

Chater, K., Merrick, M. and Parish, J. (1979) 'Developmental biology of prokaryotes', *ed. P. Jh. Blackwell Publishing, Oxford, United Kingdom*, pp. 93-114.

Chater, K. F. (1984) 'Morphological and physiological differentiation in Streptomyces', *Microbial development*, pp. 89-116.

Chater, K. F. and Wilde, L. (1976) 'Restriction of a bacteriophage of Streptomyces albus G involving endonuclease SalI', *Journal of bacteriology,* 128(2), pp. 644-650.

Chen, G., LI, X., Waters, B., & Davies, J. (2000) 'Enhanced production of microbial metabolites in the presence of dimethyl sulfoxide', *The Journal of antibiotics,* 53(10), pp. 1145-1153.

Chen, X., Johnson, R. M. and Li, B. (2023) 'A permissive amide N-methyltransferase for dithiolopyrrolones', *ACS catalysis,* 13(3), pp. 1899-1905.

Chen, Y., Wendt-Pienkowski, E. and Shen, B. (2008) 'Identification and utility of FdmR1 as a Streptomyces antibiotic regulatory protein activator for fredericamycin production in Streptomyces griseus ATCC 49344 and heterologous hosts', *Journal of bacteriology,* 190(16), pp. 5587-5596.

Cheng, Y., Yang, R., Lyu, M., Wang, S., Liu, X., Wen, Y., Song, Y., Li, J. and Chen, Z. (2018) 'IdeR, a DtxR family iron response regulator, controls iron homeostasis, morphological differentiation, secondary metabolism, and the oxidative stress response in Streptomyces avermitilis', *Applied and Environmental Microbiology,* 84(22), pp. e01503-18.

Cheung, J., Murphy, Michael E. P. and Heinrichs, David E. (2012) 'Discovery of an Iron-Regulated Citrate Synthase in Staphylococcus aureus', *Chemistry & Biology,* 19(12), pp. 1568-1578.

Chudzik, A., Jalkanen, K., Täubel, M., Szponar, B. and Paściak, M. (2024) 'Identification of environmental Actinobacteria in buildings by means of chemotaxonomy, 16S rRNA sequencing, and MALDI-TOF MS', *Microbiology Spectrum,* 12(3), pp. e03596-23.

Cox-Georgian, D., Ramadoss, N., Dona, C. and Basu, C. (2019) 'Therapeutic and medicinal uses of terpenes', *Medicinal plants: from farm to pharmacy*, pp. 333-359.

Craney, A., Ozimok, C., Pimentel-Elardo, S. M., Capretta, A., & Nodwell, J. R. (2012) 'Chemical perturbation of secondary metabolism demonstrates important links to primary metabolism', *Chemistry & biology,* 19(8), pp. 1020-1027.

Curtiss III, R. (1969) 'Bacterial conjugation', *Annual review of microbiology,* 23(1), pp. 69-136.
Dang, T. and Süssmuth, R. D. (2017) 'Bioactive peptide natural products as lead structures for medicinal use', *Accounts of chemical research,* 50(7), pp. 1566-1576.

Dashti, Y., Grkovic, T., Abdelmohsen, U. R., Hentschel, U. and Quinn, R. J. (2014) 'Production of induced secondary metabolites by a co-culture of sponge-associated actinomycetes, Actinokineospora sp. EG49 and Nocardiopsis sp. RV163', *Marine drugs,* 12(5), pp. 3046-3059.

Dashti, Y., Grkovic, T., Abdelmohsen, U. R., Hentschel, U. and Quinn, R. J. (2017) 'Actinomycete Metabolome Induction/Suppression with N-Acetylglucosamine', *J Nat Prod,* 80(4), pp. 828-836.

Dashti, Y., Mohammadipanah, F., Zhang, Y., Cerqueira Diaz, P. M., Vocat, A., Zabala, D., Fage, C. D., Romero-Canelon, I., Bunk, B. and Spröer, C. (2024) 'Discovery and Biosynthesis of Persiathiacins: Unusual Polyglycosylated Thiopeptides Active Against Multidrug Resistant Tuberculosis', *ACS infectious diseases,* 10(9), pp. 3378-3391.

Dashti, Y., Tajabadi, F. M., Wu, L. J., Sumang, F. A., Escasinas, A., Ellis Allenby, N. E. and Errington, J. (2022) 'Discovery of demurilactone a: A specific growth inhibitor of L-form Bacillus subtilis', *ACS Infectious Diseases,* 8(11), pp. 2253-2258.

Dayan, F. E., Cantrell, C. L. and Duke, S. O. (2009) 'Natural products in crop protection', *Bioorganic & medicinal chemistry,* 17(12), pp. 4022-4034.

De Simeis, D. and Serra, S. (2021) 'Actinomycetes: A never-ending source of bioactive compounds—An overview on antibiotics production', *Antibiotics,* 10(5), pp. 483.

Deininger, P. L. (1983) 'Random subcloning of sonicated DNA: application to shotgun DNA sequence analysis', *Analytical biochemistry,* 129(1), pp. 216-223.

Demain, A. L. (2020) 'Carbon source regulation of idiolite biosynthesis in actinomycetes', *Regulation of secondary metabolism in Actinomycetes*: CRC Press, pp. 127-134.

Denis, F. and Brzezinski, R. (1992) 'A versatile shuttle cosmid vector for use in Escherichia coli and actinomycetes', *Gene,* 111(1), pp. 115-118.

Dos Santos, J. D. N., João, S. A., Martín, J., Vicente, F., Reyes, F. and Lage, O. M. (2022) 'iChip-inspired isolation, bioactivities and dereplication of actinomycetota from portuguese beach sediments', *Microorganisms,* 10(7), pp. 1471.

Doull, J. L., Singh, A. K., Hoare, M., & Ayer, S. W (1994) 'Conditions for the production of jadomycin B by Streptomyces venezuelae ISP5230: effects of heat shock, ethanol treatment and phage infection', *Journal of Industrial Microbiology and Biotechnology,* 13, pp. 120-125.

Du, D., Wang, L., Tian, Y., Liu, H., Tan, H. and Niu, G. (2015) 'Genome engineering and direct cloning of antibiotic gene clusters via phage ϕBT1 integrase-mediated site-specific recombination in Streptomyces', *Scientific reports,* 5(1), pp. 8740.

Duangmal, K., Ward, A. C. and Goodfellow, M. (2005) 'Selective isolation of members of the Streptomyces violaceoruber clade from soil', *FEMS microbiology letters,* 245(2), pp. 321-327.
Duggar, B. M. (1948) 'Aureomycin-a New Antibiotic', pp. 177-342.

Duke, R. C., Chervenak, R. and Cohen, J. J. (1983) 'Endogenous endonuclease-induced DNA fragmentation: an early event in cell-mediated cytolysis', *Proceedings of the National Academy of Sciences,* 80(20), pp. 6361-6365.

El-Hawary, S. S., Sayed, A. M., Mohammed, R., Khanfar, M. A., Rateb, M. E., Mohammed, T. A., Hajjar, D., Hassan, H. M., Gulder, T. A. and Abdelmohsen, U. R. (2018) 'New Pim-1 kinase inhibitor from the co-culture of two sponge-associated actinomycetes', *Frontiers in Chemistry,* 6, pp. 538.

El-Nakeeb, M. A. and Lechevalier, H. A. (1963) 'Selective isolation of aerobic actinomycetes', *Applied microbiology,* 11(2), pp. 75-77.

Elsayed, E. A., Farid, M. A. and El-Enshasy, H. A. (2019) 'Enhanced Natamycin production by Streptomyces natalensis in shake-flasks and stirred tank bioreactor under batch and fed-batch conditions', *BMC biotechnology,* 19, pp. 1-13.

Enghiad, B., Huang, C., Guo, F., Jiang, G., Wang, B., Tabatabaei, S. K., Martin, T. A. and Zhao, H. (2021) 'Cas12a-assisted precise targeted cloning using in vivo Cre-lox recombination', *Nature communications,* 12(1), pp. 1171.

Errington, J., Mickiewicz, K., Kawai, Y. and Wu, L. J. (2016) 'L-form bacteria, chronic diseases and the origins of life', *Philosophical Transactions of the Royal Society B: Biological Sciences,* 371(1707), pp. 20150494.

Eustáquio, A. S., Gust, B., Galm, U., Li, S.-M., Chater, K. F. and Heide, L. (2005) 'Heterologous expression of novobiocin and clorobiocin biosynthetic gene clusters', *Applied and Environmental Microbiology,* 71(5), pp. 2452-2459.

Farzam K, N. T., Quick J. (2023) 'Erythromycin', *In: StatPearls [Internet]. Treasure Island (FL)*.

Felnagle, E. A., Rondon, M. R., Berti, A. D., Crosby, H. A. and Thomas, M. G. (2007) 'Identification of the biosynthetic gene cluster and an additional gene for resistance to the antituberculosis drug capreomycin', *Applied and environmental microbiology,* 73(13), pp. 4162-4170.

Feng, Z., Kim, J. H. and Brady, S. F. (2010) 'Fluostatins produced by the heterologous expression of a TAR reassembled environmental DNA derived type II PKS gene cluster', *Journal of the American Chemical Society,* 132(34), pp. 11902-11903.

Feng, Z., Wang, L., Rajski, S. R., Xu, Z., Coeffet-LeGal, M. F. and Shen, B. (2009) 'Engineered production of iso-migrastatin in heterologous Streptomyces hosts', *Bioorganic & medicinal chemistry,* 17(6), pp. 2147-2153.

Fisch, K. M. (2013) 'Biosynthesis of natural products by microbial iterative hybrid PKS–NRPS', *RSC advances,* 3(40), pp. 18228-18247.

Fong, P., Francis, M. J., Hamblin, J. F., Korman, T. M. and Graham, M. (2018) 'Identification and diversity of Actinomyces species in a clinical microbiology laboratory in the MALDI-TOF MS era', *Anaerobe,* 54, pp. 151-158.

Franche, C., Lindström, K. and Elmerich, C. 2009. Nitrogen-fixing bacteria associated with leguminous and non-leguminous plants. Springer.

Fu, J., Bian, X., Hu, S., Wang, H., Huang, F., Seibert, P. M., Plaza, A., Xia, L., Müller, R. and Stewart, A. F. (2012) 'Full-length RecE enhances linear-linear homologous recombination and facilitates direct cloning for bioprospecting', *Nature biotechnology,* 30(5), pp. 440-446.

Gerber, N. and Lechevalier, H. (1965) 'Geosmin, an earthy-smelling substance isolated from actinomycetes', *Applied microbiology,* 13(6), pp. 935-938.

Godiska, R., Patterson, M., Schoenfeld, T. and Mead, D. A. 2005. Mini Review Beyond pUC: Vectors for Cloning Unstable DNA elucidations.

Goers, L., Freemont, P. and Polizzi, K. M. (2014) 'Co-culture systems and technologies: taking synthetic biology to the next level', *Journal of The Royal Society Interface,* 11(96), pp. 20140065.

Gomez-Escribano, J. P. and Bibb, M. J. (2012) 'Streptomyces coelicolor as an expression host for heterologous gene clusters', *Methods in enzymology*: Elsevier, pp. 279-300.

Gomez-Escribano, J. P. and Bibb, M. J. (2011) 'Engineering Streptomyces coelicolor for heterologous expression of secondary metabolite gene clusters', *Microbial biotechnology,* 4(2), pp. 207-215.

González-Cerón, G., Miranda-Olivares, O. J. and Servín-González, L. (2009) 'Characterization of the methyl-specific restriction system of Streptomyces coelicolor A3 (2) and of the role played by laterally acquired nucleases', *FEMS microbiology letters,* 301(1), pp. 35-43.

Goodfellow, M. (1989) 'Supregeneric classification of actinomycets', *Bergey's manual of systematic bacteriology,* 4, pp. 2333-2339.

Goodfellow, M. and Williams, S. (1983) 'Ecology of actinomycetes'.

Goris, J., Konstantinidis, K. T., Klappenbach, J. A., Coenye, T., Vandamme, P. and Tiedje, J. M. (2007) 'DNA–DNA hybridization values and their relationship to whole-genome sequence similarities', *International journal of systematic and evolutionary microbiology,* 57(1), pp. 81-91.

Grant, S. G., Jessee, J., Bloom, F. R. and Hanahan, D. (1990) 'Differential plasmid rescue from transgenic mouse DNAs into Escherichia coli methylation-restriction mutants', *Proceedings of the National Academy of Sciences,* 87(12), pp. 4645-4649.

Greunke, C., Duell, E. R., D'Agostino, P. M., Glöckle, A., Lamm, K. and Gulder, T. A. M. (2018) 'Direct pathway cloning (DiPaC) to unlock natural product biosynthetic potential', *Metabolic Engineering,* 47, pp. 334-345.

Grohmann, E., Muth, G. n. and Espinosa, M. (2003) 'Conjugative plasmid transfer in gram-positive bacteria', *Microbiology and molecular biology reviews,* 67(2), pp. 277-301.

Gullón, S., Olano, C., Abdelfattah, M. S., Braña, A. F., Rohr, J., Méndez, C. and Salas, J. A. (2006) 'Isolation, characterization, and heterologous expression of the biosynthesis gene cluster for the antitumor anthracycline steffimycin', *Applied and environmental microbiology,* 72(6), pp. 4172-4183.

Guo, J., Zhao, J., Li, L., Chen, Z., Wen, Y. and Li, J. (2010) 'The pathway-specific regulator AveR from Streptomyces avermitilis positively regulates avermectin production while it negatively affects oligomycin biosynthesis', *Molecular Genetics and Genomics,* 283, pp. 123-133.

Gust, B., Challis, G. L., Fowler, K., Kieser, T. and Chater, K. F. (2003) 'PCR-targeted Streptomyces gene replacement identifies a protein domain needed for biosynthesis of the sesquiterpene soil odor geosmin', *Proceedings of the National Academy of Sciences,* 100(4), pp. 1541-1546.

Haight, T. H., & Finland, M. (1952) 'Laboratory and clinical studies on erythromycin', *New England Journal of Medicine,* 247(7), pp. 227-232.

Harada, K.-i., Tomita, K., Fujii, K., Masuda, K., Mikami, Y., Yazawa, K. and Komaki, H. (2004) 'Isolation and structural characterization of siderophores, madurastatins, produced by a pathogenic Actinomadura madurae', *The Journal of antibiotics,* 57(2), pp. 125-135.

Harms, J. M., Wilson, D. N., Schluenzen, F., Connell, S. R., Stachelhaus, T., Zaborowska, Z., Spahn, C. M. and Fucini, P. (2008) 'Translational regulation via L11: molecular switches on the ribosome turned on and off by thiostrepton and micrococcin', *Molecular cell,* 30(1), pp. 26-38.

Hasebe, F., Matsuda, K., Shiraishi, T., Futamura, Y., Nakano, T., Tomita, T., Ishigami, K., Taka, H., Mineki, R. and Fujimura, T. (2016) 'Amino-group carrier-protein-mediated secondary metabolite biosynthesis in Streptomyces', *Nature Chemical Biology,* 12(11), pp. 967-972.

Hatano, K., Tamura, T. and Nishii, T. (1994) 'Taxonomic status of Streptomyces coelicolor A3 (2) and Streptomyces lividans 66', *Actinomycetologica,* 8(2), pp. 47-50.

Hayakawa, M. and Nonomura, H. (1989) 'A new method for the intensive isolation of actinomycetes from soil', *Actinomycetologica,* 3(2), pp. 95-104.

Hayakawa, M., Otoguro, M., Takeuchi, T., Yamazaki, T. and Iimura, Y. (2000) 'Application of a method incorporating differential centrifugation for selective isolation of motile actinomycetes in soil and plant litter', *Antonie van Leeuwenhoek,* 78, pp. 171-185.

Hayakawa, M., Sadakata, T., Kajiura, T. and Nonomura, H. (1991) 'New methods for the highly selective isolation of Micromonospora and Microbispora from soil', *Journal of fermentation and bioengineering,* 72(5), pp. 320-326.

Hirsch, C. and Christensen, D. (1983) 'Novel method for selective isolation of actinomycetes', *Applied and environmental microbiology,* 46(4), pp. 925-929.

Hollands, S., Tasch, J., Simon, D. J., Wassouf, D., Barber, I., Gessner, A., Bechthold, A. and Zechel, D. L. (2024) 'Analysis of the cryptic biosynthetic gene cluster encoding the RiPP curacozole reveals a phenylalanine-specific peptide hydroxylase', *Chemical Science,* 15(47), pp. 19858-19869.

Hopwood, D. A. (1967) 'Genetic analysis and genome structure in Streptomyces coelicolor', *Bacteriological reviews,* 31(4), pp. 373-403.

Hopwood, D. A. (1988) 'The Leeuwenhoek lecture, 1987-Towards an understanding of gene switching in Streptomyces, the basis of sporulation and antibiotic production', *Proceedings of the Royal society of London. Series B. Biological sciences,* 235(1279), pp. 121-138.

Hosaka, T., Ohnishi-Kameyama, M., Muramatsu, H., Murakami, K., Tsurumi, Y., Kodani, S., Yoshida, M., Fujie, A. and Ochi, K. (2009) 'Antibacterial discovery in actinomycetes strains with mutations in RNA polymerase or ribosomal protein S12', *Nature biotechnology,* 27(5), pp. 462-464.

Huang, B., Shi, Y., Qi, H., Wang, J., Zhang, Y., Bechthold, A., Yu, X. and Ma, Z. (2025) 'Enhancement or Activation of Agricultural Antibiotic Production in Streptomyces by an Identified Strong Promoter P30S', *Journal of Agricultural and Food Chemistry*.

Huang, S., Him Tong, M., Qin, Z., Deng, Z., Deng, H. and Yu, Y. (2015) 'Identification and characterization of the biosynthetic gene cluster of thiolutin, a tumor angiogenesis inhibitor, in Saccharothrix algeriensis NRRL B-24137', *Anti-Cancer Agents in Medicinal Chemistry-Anti-Cancer Agents),* 15(3), pp. 277-284.

Hung, M.-C. and Wensink, P. C. (1984) 'Different restriction enzyme-generated sticky DNA ends can be joined in vitro', *Nucleic acids research,* 12(4), pp. 1863-1874.

Hutchings, M. I., Truman, A. W. and Wilkinson, B. (2019) 'Antibiotics: past, present and future', *Current opinion in microbiology,* 51, pp. 72-80.

Igarashi, Y., Ogura, H., Furihata, K., Oku, N., Indananda, C. and Thamchaipenet, A. (2011) 'Maklamicin, an antibacterial polyketide from an endophytic Micromonospora sp', *Journal of natural products,* 74(4), pp. 670-674.

Isono, K. (1988) 'Nucleoside antibiotics: structure, biological activity, and biosynthesis', *The Journal of antibiotics,* 41(12), pp. 1711-1739.

Jacoby, R., Peukert, M., Succurro, A., Koprivova, A. and Kopriva, S. (2017) 'The role of soil microorganisms in plant mineral nutrition—current knowledge and future directions', *Frontiers in plant science,* 8, pp. 1617.

Jama-Kmiecik, A., Mączyńska, B., Frej-Mądrzak, M., Choroszy-Król, I., Dudek-Wicher, R., Piątek, D., ... & Sarowska, J (2025) 'The Changes in the Antibiotic Resistance of Staphylococcus aureus, Streptococcus pneumoniae, Enterococcus faecalis and Enterococcus faecium in the Clinical Isolates of a Multiprofile Hospital over 6 Years (2017–2022)', *Journal of Clinical Medicine,* 14(2), pp. 332.

Jessup, C. M., Kassen, R., Forde, S. E., Kerr, B., Buckling, A., Rainey, P. B. and Bohannan, B. J. (2004) 'Big questions, small worlds: microbial model systems in ecology', *Trends in ecology & evolution,* 19(4), pp. 189-197.

Jiang, W., Zhao, X., Gabrieli, T., Lou, C., Ebenstein, Y. and Zhu, T. F. (2015) 'Cas9-Assisted Targeting of CHromosome segments CATCH enables one-step targeted cloning of large gene clusters', *Nature communications,* 6(1), pp. 8101.

Jiao, H., Xu, W., Hu, Y., Tian, R. and Wang, Z. (2022) 'Citric acid in rice root exudates enhanced the colonization and plant growth-promoting ability of Bacillus altitudinis LZP02', *Microbiology Spectrum,* 10(6), pp. e01002-22.

Jung, W. S., Lee, S. K., Hong, J. S. J., Park, S. R., Jeong, S. J., Han, A. R., Sohng, J. K., Kim, B. G., Choi, C. Y. and Sherman, D. H. (2006) 'Heterologous expression of tylosin polyketide synthase and production of a hybrid bioactive macrolide in Streptomyces venezuelae', *Applied microbiology and biotechnology,* 72(4), pp. 763-769.

Just-Baringo, X., Albericio, F. and Álvarez, M. (2014) 'Thiopeptide antibiotics: retrospective and recent advances', *Marine drugs,* 12(1), pp. 317-351.

Kang, H.-S. and Kim, E.-S. (2021) 'Recent advances in heterologous expression of natural product biosynthetic gene clusters in Streptomyces hosts', *Current Opinion in Biotechnology,* 69, pp. 118-127.

Kawai, K., Wang, G., Okamoto, S. and Ochi, K. (2007) 'The rare earth, scandium, causes antibiotic overproduction in Streptomyces spp', *FEMS microbiology letters,* 274(2), pp. 311-315.

Khokhlov, A. S., Anisova, L. N., Tovarova, I. I., Kleiner, E. M., Kovalenko, I. V., Krasilnikova, O. I., ... & Pliner, S. A (1973) 'Effect of A-factor on the growth of asporogenous mutants of Streptomyces griseus, not producing this factor', *Zeitschrift für allgemeine Mikrobiologie,* 13(8), pp. 647-655.

Kieser, T., Bibb, M., Buttner, M., Chater, K. and Hopwood, D. (2000) 'Practical Streptomyces Genetics. John Innes Foundation; Norwich, England: 2000a', *Growth and preservation of Streptomyces*, pp. 43-62.

Kieser, T., Hopwood, D. A., Wright, H. M. and Thompson, C. J. (1982) 'pIJ101, a multi-copy broad host-range Streptomyces plasmid: functional analysis and development of DNA cloning vectors', *Molecular and General Genetics MGG,* 185, pp. 223-238.

Kim, U.-J., Shizuya, H., de Jong, P. J., Birren, B. and Simon, M. I. (1992) 'Stable propagation of cosmid sized human DNA inserts in an F factor based vector', *Nucleic acids research,* 20(5), pp. 1083-1085.

Klieneberger-Nobel, E. (1947) 'The life cycle of sporing Actinomyces as revealed by a study of their structure and septation', *Microbiology,* 1(1), pp. 22-32.

Klieneberger, E. (1935) 'The Natural Occurrence of Pleuro-Pneumonia-Like Organisms in Apparent Symbiosis with Streptobacillus moniliformis and Other Bacteria'.

Komaki, H. (2023) 'Recent progress of reclassification of the genus Streptomyces', *Microorganisms,* 11(4), pp. 831.

Komatsu, M., Komatsu, K., Koiwai, H., Yamada, Y., Kozone, I., Izumikawa, M., Hashimoto, J., Takagi, M., Omura, S. and Shin-ya, K. (2013) 'Engineered Streptomyces avermitilis host for heterologous expression of biosynthetic gene cluster for secondary metabolites', *ACS synthetic biology,* 2(7), pp. 384-396.

Küberl, A., Mengus-Kaya, A., Polen, T. and Bott, M. (2020) 'The iron deficiency response of Corynebacterium glutamicum and a link to thiamine biosynthesis', *Applied and environmental microbiology,* 86(10), pp. e00065-20.

Kuhstoss, S. and Rao, R. N. (1991) 'Analysis of the integration function of the streptomycete bacteriophage φC31', *Journal of molecular biology,* 222(4), pp. 897-908.

Labes, G., Bibb, M. and Wohlleben, W. (1997) 'Isolation and characterization of a strong promoter element from the Streptomyces ghanaensis phage I19 using the gentamicin resistance gene (aacC1) of Tn 1696 as reporter', *Microbiology,* 143(5), pp. 1503-1512.

Laureti, L., Song, L., Huang, S., Corre, C., Leblond, P., Challis, G. L. and Aigle, B. (2011) 'Identification of a bioactive 51-membered macrolide complex by activation of a silent polyketide synthase in Streptomyces ambofaciens', *Proceedings of the National Academy of Sciences,* 108(15), pp. 6258-6263.

Lechevalier, M. P. and Lechevalier, H. 1970. Chemical composition as a criterion in the classification of aerobic actinomycetes. Microbiology Society.

Lewis, K., Epstein, S., D'onofrio, A. and Ling, L. L. (2010) 'Uncultured microorganisms as a source of secondary metabolites', *The Journal of antibiotics,* 63(8), pp. 468-476.

Li, B., Wever, W. J., Walsh, C. T. and Bowers, A. A. (2014) 'Dithiolopyrrolones: biosynthesis, synthesis, and activity of a unique class of disulfide-containing antibiotics', *Natural product reports,* 31(7), pp. 905-923.

Li, L., Wei, K., Liu, X., Wu, Y., Zheng, G., Chen, S., Jiang, W. and Lu, Y. (2019a) 'aMSGE: advanced multiplex site-specific genome engineering with orthogonal modular recombinases in actinomycetes', *Metabolic engineering,* 52, pp. 153-167.

Li, T., Du, Y., Cui, Q., Zhang, J., Zhu, W., Hong, K. and Li, W. (2013) 'Cloning, characterization and heterologous expression of the indolocarbazole biosynthetic gene cluster from marine-derived Streptomyces sanyensis FMA', *Marine drugs,* 11(2), pp. 466-488.

Li, X., Xu, H., Li, Y., Liao, S. and Liu, Y. (2023) 'Exploring diverse bioactive secondary metabolites from marine microorganisms using co-culture strategy', *Molecules,* 28(17), pp. 6371.

Li, Z.-y., Bu, Q.-t., Wang, J., Liu, Y., Chen, X.-a., Mao, X.-m. and Li, Y.-Q. (2019b) 'Activation of anthrachamycin biosynthesis in Streptomyces chattanoogensis L10 by site-directed mutagenesis of rpoB', *Journal of Zhejiang University. Science. B,* 20(12), pp. 983.

Liang, L., Sproule, A., Haltli, B., Marchbank, D. H., Berrué, F., Overy, D. P., McQuillan, K., Lanteigne, M., Duncan, N. and Correa, H. (2019) 'Discovery of a new natural product and a deactivation of a quorum sensing system by culturing a “producer” bacterium with a heat-killed “inducer” culture', *Frontiers in Microbiology,* 9, pp. 3351.

Liang, M., Liu, L., Xu, F., Zeng, X., Wang, R., Yang, J., Wang, W., Karthik, L., Liu, J. and Yang, Z. (2022) 'Activating cryptic biosynthetic gene cluster through a CRISPR–Cas12a-mediated direct cloning approach', *Nucleic Acids Research,* 50(6), pp. 3581-3592.

Lin, J., Nishino, K., Roberts, M. C., Tolmasky, M., Aminov, R. I. and Zhang, L. (2015) 'Mechanisms of antibiotic resistance', *Frontiers in microbiology,* 6, pp. 34.

Lin, Z., Falkinham III, J. O., Tawfik, K. A., Jeffs, P., Bray, B., Dubay, G., Cox, J. E. and Schmidt, E. W. (2012) 'Burkholdines from Burkholderia ambifaria: antifungal agents and possible virulence factors', *Journal of natural products,* 75(9), pp. 1518-1523.

Liu, H., Jiang, H., Haltli, B., Kulowski, K., Muszynska, E., Feng, X., Summers, M., Young, M., Graziani, E. and Koehn, F. (2009) 'Rapid cloning and heterologous expression of the meridamycin biosynthetic gene cluster using a versatile Escherichia coli− Streptomyces artificial chromosome vector, pSBAC', *Journal of natural products,* 72(3), pp. 389-395.

Liu, X., Zhao, F.-P., Tian, T., Wang, W.-C., Liu, Z., Zhou, Q., Hou, X.-F., Wang, J., Guo, W. and Lin, S. (2024) 'Rational Engineering of Secondary Metabolic Pathways in A Heterologous Host to Enable The Biosynthesis of Hibarimicin Derivatives With Enhanced Anti-Melanomic Activity', *Engineering,* 38, pp. 113-123.

MacNeil, D. J. and Klapko, L. M. (1987) 'Transformation of Streptomyces avermitilis by plasmid DNA', *Journal of industrial microbiology and biotechnology,* 2(4), pp. 209-218.
Malik, V. (1980) 'Microbial secondary metabolism', *Trends in Biochemical Sciences,* 5(3), pp. 68-72.

Marahiel, M. A. (2016) 'A structural model for multimodular NRPS assembly lines', *Natural Product Reports,* 33(2), pp. 136-140.

Martín, J.-F. and Liras, P. (2010) 'Engineering of regulatory cascades and networks controlling antibiotic biosynthesis in Streptomyces', *Current opinion in microbiology,* 13(3), pp. 263-273.
Martín, J. F. (2004) 'Phosphate control of the biosynthesis of antibiotics and other secondary metabolites is mediated by the PhoR-PhoP system: an unfinished story', *Journal of bacteriology,* 186(16), pp. 5197-5201.

Martin, J. F. and Demain, A. L. (1980) 'Control of antibiotic biosynthesis', *Microbiological reviews,* 44(2), pp. 230-251.

Martinet, L., Naômé, A., Deflandre, B., Maciejewska, M., Tellatin, D., Tenconi, E., Smargiasso, N., De Pauw, E., van Wezel, G. P. and Rigali, S. (2019) 'A single biosynthetic gene cluster is responsible for the production of bagremycin antibiotics and ferroverdin iron chelators', *MBio,* 10(4), pp. 10.1128/mbio. 01230-19.

Martínez-Burgo, Y., Álvarez-Álvarez, R., Pérez-Redondo, R. and Liras, P. (2014) 'Heterologous expression of Streptomyces clavuligerus ATCC 27064 cephamycin C gene cluster', *Journal of Biotechnology,* 186, pp. 21-29.

Martinez, A., Kolvek, S. J., Yip, C. L. T., Hopke, J., Brown, K. A., MacNeil, I. A. and Osburne, M. S. (2004) 'Genetically modified bacterial strains and novel bacterial artificial chromosome shuttle vectors for constructing environmental libraries and detecting heterologous natural products in multiple expression hosts', *Applied and environmental microbiology,* 70(4), pp. 2452-2463.

Mazodier, P., Petter, R. and Thompson, C. (1989) 'Intergeneric conjugation between Escherichia coli and Streptomyces species', *Journal of Bacteriology,* 171(6), pp. 3583-3585.
Mazy-Servais, C., Baczkowski, D. and Dusart, J. (1997) 'Electroporation of intact cells of Streptomyces parvulus and Streptomyces vinaceus', *FEMS microbiology letters,* 151(2), pp. 135-138.

McCarthy, A. (1987) 'Lignocellulose-degrading actinomycetes', *FEMS Microbiology Reviews,* 3(2), pp. 145-163.

McInerney, B. V., Gregson, R. P., Lacey, M. J., Akhurst, R. J., Lyons, G. R., Rhodes, S. H., Smith, D. R., Engelhardt, L. M. and White, A. H. (1991) 'Biologically active metabolites from Xenorhabdus spp., Part 1. Dithiolopyrrolone derivatives with antibiotic activity', *Journal of Natural Products,* 54(3), pp. 774-784.

Meng, J., Feng, R., Zheng, G., Ge, M., Mast, Y., Wohlleben, W., Gao, J., Jiang, W. and Lu, Y. (2017) 'Improvement of pristinamycin I (PI) production in Streptomyces pristinaespiralis by metabolic engineering approaches', *Synthetic and Systems Biotechnology,* 2(2), pp. 130-136.

Merrouche, R., Yekkour, A., Coppel, Y., Bouras, N., Zitouni, A., Mathieu, F. and Sabaou, N. (2020) 'Saccharothrix algeriensis NRRL B-24137, the first non-Streptomyces actinobacterium, produces holomycin after cystine feeding', *Archives of Microbiology,* 202(9), pp. 2509-2516.

Miao, V., Coeffet-LeGal, M.-F., Brian, P., Brost, R., Penn, J., Whiting, A., Martin, S., Ford, R., Parr, I. and Bouchard, M. (2005) 'Daptomycin biosynthesis in Streptomyces roseosporus:

cloning and analysis of the gene cluster and revision of peptide stereochemistry', *Microbiology,* 151(5), pp. 1507-1523.

Moody, S. C. 2014. Microbial co-culture: harnessing intermicrobial signaling for the production of novel antimicrobials. Taylor & Francis.

Mordarska, H., Mordarski, M. and Goodfellow, M. (1972) 'Chemotaxonomic characters and classification of some nocardioform bacteria', *Microbiology,* 71(1), pp. 77-86.

Müller, M. M. (2018) 'Post-translational modifications of protein backbones: unique functions, mechanisms, and challenges', *Biochemistry,* 57(2), pp. 177-185.

Myronovskyi, M. and Luzhetskyy, A. (2019) 'Heterologous production of small molecules in the optimized Streptomyces hosts', *Natural product reports,* 36(9), pp. 1281-1294.

Myronovskyi, M., Rosenkränzer, B., Nadmid, S., Pujic, P., Normand, P. and Luzhetskyy, A. (2018) 'Generation of a cluster-free Streptomyces albus chassis strains for improved heterologous expression of secondary metabolite clusters', *Metabolic engineering,* 49, pp. 316-324.

Nah, H.-J., Pyeon, H.-R., Kang, S.-H., Choi, S.-S. and Kim, E.-S. (2017) 'Cloning and heterologous expression of a large-sized natural product biosynthetic gene cluster in Streptomyces species', *Frontiers in microbiology,* 8, pp. 394.

Nair, S. and Abraham, J. (2020) 'Natural products from actinobacteria for drug discovery', *Advances in Pharmaceutical Biotechnology: Recent Progress and Future Applications*, pp. 333-363.

Nett, M., Ikeda, H. and Moore, B. S. (2009) 'Genomic basis for natural product biosynthetic diversity in the actinomycetes', *Natural product reports,* 26(11), pp. 1362-1384.

Nguyen, L. T. T., Park, A. R., Van Le, V., Hwang, I. and Kim, J.-C. (2024) 'Exploration of a multifunctional biocontrol agent Streptomyces sp. JCK-8055 for the management of apple fire blight', *Applied Microbiology and Biotechnology,* 108(1), pp. 49.

Nichols, D., Cahoon, N., Trakhtenberg, E., Pham, L., Mehta, A., Belanger, A., Kanigan, T., Lewis, K. and Epstein, S. (2010) 'Use of ichip for high-throughput in situ cultivation of "uncultivable" microbial species', *Applied and environmental microbiology,* 76(8), pp. 2445-2450.

Nicolle, C., Gayrard, D., Noël, A., Hortala, M., Amiel, A., Grat, S., Le Ru, A., Marti, G., Pernodet, J.-L. and Lautru, S. (2024) 'Root-associated Streptomyces produce galbonolides to modulate plant immunity and promote rhizosphere colonization', *The ISME Journal,* 18(1), pp. wrae112.

Nierman, W. C. and Feldblyum, T. V. (2001) 'Genomic Library in Encyclopedia of Genetics', pp. Pages 865-872,.

Ochi, K. (2007) 'From microbial differentiation to ribosome engineering', *Bioscience, biotechnology, and biochemistry,* 71(6), pp. 1373-1386.

Ochi, K. and Hosaka, T. (2013) 'New strategies for drug discovery: activation of silent or weakly expressed microbial gene clusters', *Applied microbiology and biotechnology,* 97, pp. 87-98.

Oliva, B., O'Neill, A., Wilson, J. M., O'Hanlon, P. J. and Chopra, I. (2001) 'Antimicrobial properties and mode of action of the pyrrothine holomycin', *Antimicrobial agents and chemotherapy,* 45(2), pp. 532-539.

Onaka, H., Taniguchi, S.-i., Ikeda, H., Igarashi, Y. and Furumai, T. (2003) 'pTOYAMAcos, pTYM18, and pTYM19, actinomycete-Escherichia coli integrating vectors for heterologous gene expression', *The Journal of Antibiotics,* 56(11), pp. 950-956.

Oren, A. and Garrity, G. M. (2021) 'Valid publication of the names of forty-two phyla of prokaryotes', *International journal of systematic and evolutionary microbiology,* 71(10), pp. 005056.

Osoegawa, K., Woon, P. Y., Zhao, B., Frengen, E., Tateno, M., Catanese, J. J. and De Jong, P. J. (1998) 'An improved approach for construction of bacterial artificial chromosome libraries', *Genomics,* 52(1), pp. 1-8.

Otoguro, M., Hayakawa, M., Yamazaki, T. and Iimura, Y. (2001) 'An integrated method for the enrichment and selective isolation of Actinokineospora spp. in soil and plant litter', *Journal of applied microbiology,* 91(1), pp. 118-130.

Pansomsuay, R., Fukasem, P., Pittayakhajonwut, P., Intaraudom, C., Suriyachadkun, C., Yasawong, M., He, Y.-W., Tanasupawat, S., Qian, Y. and Thawai, C. (2025) 'Discovery of Streptomyces marinisediminis sp. nov., a new thiolutin producing actinomycete isolated from Thai marine sediment', *Scientific Reports,* 15(1), pp. 29301.

Park, H.-S., Park, J.-H., Kim, H.-J., Kang, S.-H., Choi, S.-S. and Kim, E.-S. (2022) 'BAC cloning and heterologous expression of a giant biosynthetic gene cluster encoding antifungal neotetrafibricin in streptomyces rubrisoli', *Frontiers in Bioengineering and Biotechnology,* 10, pp. 964765.

Passari, A. K., Chandra, P., Mishra, V. K., Leo, V. V., Gupta, V. K., Kumar, B. and Singh, B. P. (2016) 'Detection of biosynthetic gene and phytohormone production by endophytic actinobacteria associated with Solanum lycopersicum and their plant-growth-promoting effect', *Research in Microbiology,* 167(8), pp. 692-705.

Patil, H. J., Srivastava, A. K., Singh, D. P., Chaudhari, B. L. and Arora, D. K. (2011) 'Actinomycetes mediated biochemical responses in tomato (Solanum lycopersicum) enhances bioprotection against Rhizoctonia solani', *Crop protection,* 30(10), pp. 1269-1273.

Pham, J. V., Yilma, M. A., Feliz, A., Majid, M. T., Maffetone, N., Walker, J. R., Kim, E., Cho, H. J., Reynolds, J. M. and Song, M. C. (2019) 'A review of the microbial production of bioactive natural products and biologics', *Frontiers in microbiology,* 10, pp. 1404.

Pigac, J. and Schrempf, H. (1995) 'A simple and rapid method of transformation of Streptomyces rimosus R6 and other streptomycetes by electroporation', *Applied and Environmental Microbiology,* 61(1), pp. 352-356.

Pinu, F., Villas-Boas, S. and Aggio, R. 2017. Analysis of intracellular metabolites from microorganisms: Quenching and extraction protocols. Metabolites 2017; 7. DOI.

Prashar, P., Kapoor, N. and Sachdeva, S. (2014) 'Rhizosphere: its structure, bacterial diversity and significance', *Reviews in Environmental Science and Bio/Technology,* 13(1), pp. 63-77.
Preston, A. (2003) 'Choosing a cloning vector', *E. coli Plasmid Vectors: Methods and Applications*, pp. 19-26.

Price, N. P., Labeda, D. P., Naumann, T. A., Vermillion, K. E., Bowman, M. J., Berhow, M. A., Metcalf, W. W. and Bischoff, K. M. (2016) 'Quinovosamycins: new tunicamycin-type antibiotics in which the α, β-1 ″, 11′-linked N-acetylglucosamine residue is replaced by N-acetylquinovosamine', *The Journal of Antibiotics,* 69(8), pp. 637-646.

Qiu, C., Arora, P., Malik, I., Laperuta, A. J., Pavlovic, E. M., Ugochukwu, S., Naik, M. and Kaplan, C. D. (2024) 'Thiolutin has complex effects in vivo but is a direct inhibitor of RNA polymerase II in vitro', *Nucleic Acids Research,* 52(5), pp. 2546-2564.

Rebstock, M. C., Crooks, H. M., Controulis, J., & Bartz, Q. R. (1949) 'Chloramphenicol (chloromycetin). 1 IV. 1a chemical studies', *Journal of the American Chemical Society,* 71(7), pp. 2458-2462.

Ribeiro, M., Sousa, C. A. and Simões, M. (2022) 'Harnessing microbial iron chelators to develop innovative therapeutic agents', *Journal of Advanced Research,* 39, pp. 89-101.

Ritzau, M., Vettermann, R., Fleck, W. F., Gutsche, W., Dornberger, K. and Grafe, U. (1997) 'Benaphthamycin, a new dihydrobenzo [a] naphthacenequinone antibiotic from Streptomyces sp. HKI-0057', *The Journal of Antibiotics,* 50(9), pp. 791-793.

Rodríguez Estévez, M., Myronovskyi, M., Gummerlich, N., Nadmid, S. and Luzhetskyy, A. (2018) 'Heterologous expression of the nybomycin gene cluster from the marine strain Streptomyces albus subsp. chlorinus NRRL B-24108', *Marine Drugs,* 16(11), pp. 435.

Rosselló-Móra, R., Urdiain, M. and López-López, A. (2011) 'DNA–DNA Hybridization', *Methods in microbiology*: Elsevier, pp. 325-347.

Rubin, G. M. and Ding, Y. (2020) 'Recent advances in the biosynthesis of RiPPs from multicore-containing precursor peptides', *Journal of Industrial Microbiology & Biotechnology: Official Journal of the Society for Industrial Microbiology and Biotechnology,* 47(9-10), pp. 659-674.

Rutledge, P. J. and Challis, G. L. (2015) 'Discovery of microbial natural products by activation of silent biosynthetic gene clusters', *Nature Reviews Microbiology,* 13(8), pp. 509-523.

Santamarta, I., Rodríguez-García, A., Pérez-Redondo, R., Martín, J. F. and Liras, P. (2002) 'CcaR is an autoregulatory protein that binds to the ccaR and cefD-cmcI promoters of the cephamycin C-clavulanic acid cluster in Streptomyces clavuligerus', *Journal of bacteriology,* 184(11), pp. 3106-3113.

Saraswathy, N. and Ramalingam, P. (2011) 'High capacity vectors', *Concepts Tech. Genom. Proteom*, pp. 49-56.

Sasse, J., Martinoia, E. and Northen, T. (2018) 'Feed your friends: do plant exudates shape the root microbiome?', *Trends in plant science,* 23(1), pp. 25-41.

Schatz, A., Bugle, E. and Waksman, S. A. (1944) 'Streptomycin, a substance exhibiting antibiotic activity against gram-positive and gram-negative bacteria.∗', *Proceedings of the Society for Experimental Biology and Medicine,* 55(1), pp. 66-69.

Schwartz, D. C. and Cantor, C. R. (1984) 'Separation of yeast chromosome-sized DNAs by pulsed field gradient gel electrophoresis', *cell,* 37(1), pp. 67-75.

Selegato, D. and Castro-Gamboa, I. 2023. Enhancing chemical and biological diversity by co-cultivation. Front Microbiol.

Seng, P., Rolain, J.-M., Fournier, P. E., La Scola, B., Drancourt, M. and Raoult, D. (2010) 'MALDI-TOF-mass spectrometry applications in clinical microbiology', *Future microbiology,* 5(11), pp. 1733-1754.

Shapiro, S. (2020) 'Nitrogen assimilation in actinomycetes and the influence of nitrogen nutrition on actinomycete secondary metabolism', *Regulation of secondary metabolism in actinomycetes*: CRC press, pp. 135-211.

Sharma, M., Dangi, P. and Choudhary, M. (2014) 'Actinomycetes: source, identification, and their applications', *International Journal of Current Microbiology and Applied Sciences,* 3(2), pp. 801-832.

Shen, B. (2003) 'Polyketide biosynthesis beyond the type I, II and III polyketide synthase paradigms', *Current opinion in chemical biology,* 7(2), pp. 285-295.

Shilling, P. J., Mirzadeh, K., Cumming, A. J., Widesheim, M., Köck, Z. and Daley, D. O. (2020) 'Improved designs for pET expression plasmids increase protein production yield in Escherichia coli', *Communications biology,* 3(1), pp. 214.

Shin, Y.-H., Ban, Y. H., Kim, T. H., Bae, E. S., Shin, J., Lee, S. K., Jang, J., Yoon, Y. J. and Oh, D.-C. (2021) 'Structures and biosynthetic pathway of coprisamides C and D, 2-alkenylcinnamic acid-containing peptides from the gut bacterium of the carrion beetle Silpha perforata', *Journal of Natural Products,* 84(2), pp. 239-246.

Shiozawa, H., Kagasaki, T., Kinoshita, T., Haruyama, H., Domon, H., Utsui, Y., Kodama, K. and Takahashi, S. (1993) 'Thiomarinol, a new hybrid antimicrobial antibiotic produced by a marine bacterium fermentation, isolation, structure, and antimicrobial activity', *The Journal of antibiotics,* 46(12), pp. 1834-1842.

Shizuya, H., Birren, B., Kim, U.-J., Mancino, V., Slepak, T., Tachiiri, Y. and Simon, M. (1992) 'Cloning and stable maintenance of 300-kilobase-pair fragments of human DNA in Escherichia coli using an F-factor-based vector', *Proceedings of the National Academy of Sciences,* 89(18), pp. 8794-8797.

Silvestre, A. J. and Gandini, A. (2008) 'Terpenes: major sources, properties and applications', *Monomers, polymers and composites from renewable resources*: Elsevier, pp. 17-38.
Sime, F., Tovmassian, D., & Falk, G. L. (2025) 'Positive effect of erythromycin on ineffective oesophageal motility in laryngopharyngeal reflux patients: Room for a novel treatment?', *Clinical Physiology and Functional Imaging,* 45(1).

Simon, R., Priefer, U. and Pühler, A. (1983) 'A broad host range mobilization system for in vivo genetic engineering: transposon mutagenesis in gram negative bacteria', *Bio/technology,* 1(9), pp. 784-791.

Singh, P. K., Singh, P., Singh, R. P. and Singh, R. L. (2021) 'From gene to genomics: tools for improvement of animals', *Advances in Animal Genomics*: Elsevier, pp. 13-32.

Smanski, M. J., Casper, J., Peterson, R. M., Yu, Z., Rajski, S. R. and Shen, B. (2012) 'Expression of the platencin biosynthetic gene cluster in heterologous hosts yielding new platencin congeners', *Journal of Natural Products,* 75(12), pp. 2158-2167.

Snyder, L., Champness, W. and Champness, W. (2007) *Molecular genetics of bacteria.* ASM press Washington, DC.

Sosio, M., Bossi, E. and Donadio, S. (2001) 'Assembly of large genomic segments in artificial chromosomes by homologous recombination in Escherichia coli', *Nucleic acids research,* 29(7), pp. e37-e37.

Staunton, J. and Weissman, K. J. (2001) 'Polyketide biosynthesis: a millennium review', *Natural product reports,* 18(4), pp. 380-416.

Stringlis, I. A., Zhang, H., Pieterse, C. M., Bolton, M. D. and de Jonge, R. (2018) 'Microbial small molecules–weapons of plant subversion', *Natural Product Reports,* 35(5), pp. 410-433.

Strzelczyk, E. and Pokojska-Burdziej, A. (1984) 'Production of auxins and gibberellin-like substances by mycorrhizal fungi, bacteria and actinomycetes isolated from soil and the mycorrhizosphere of pine (Pinus silvestris L.)', *Plant and Soil*, pp. 185-194.

Sumang, F. A., Errington, J. and Dashti, Y. (2025) 'Biosynthesis of the quinovosamycin nucleoside antibiotics diverge from tunicamycins by additional sugar processing genes', *Bioorganic Chemistry*, pp. 108431.

Sumang, F. A., Ward, A., Errington, J. and Dashti, Y. (2024) 'Hibiscus acid and hydroxycitric acid dimethyl esters from Hibiscus flowers induce production of dithiolopyrrolone antibiotics by Streptomyces Strain MBN2-2', *Natural Products and Bioprospecting,* 14(1), pp. 40.

Takano, E., Kinoshita, H., Mersinias, V., Bucca, G., Hotchkiss, G., Nihira, T., Smith, C. P., Bibb, M., Wohlleben, W. and Chater, K. (2005) 'A bacterial hormone (the SCB1) directly controls the expression of a pathway-specific regulatory gene in the cryptic type I polyketide biosynthetic gene cluster of Streptomyces coelicolor', *Molecular microbiology,* 56(2), pp. 465-479.

Takano, E., White, J., Thompson, C. J. and Bibb, M. J. (1995) 'Construction of thiostrepton-inducible, high-copy-number expression vectors for use in Streptomyces spp', *Gene,* 166(1), pp. 133-137.

Takeuchi, T., Sawada, H., Tanaka, F. and Matsuda, I. (1996) 'Phylogenetic analysis of Streptomyces spp. causing potato scab based on 16S rRNA sequences', *International Journal of Systematic and Evolutionary Microbiology,* 46(2), pp. 476-479.

Tamura, T., Hayakawa, M. and Hatano, K. (1997) 'A New Genus of the Order Actinomycetales, Spirilliplanes gen. nov., with Description of Spirilliplanes yamanashiensis sp. nov', *International journal of systematic bacteriology,* 47(1), pp. 97-102.

Tan, G.-Y., Deng, K., Liu, X., Tao, H., Chang, Y., Chen, J., Chen, K., Sheng, Z., Deng, Z. and Liu, T. (2017) 'Heterologous biosynthesis of spinosad: an omics-guided large polyketide synthase gene cluster reconstitution in Streptomyces', *ACS synthetic biology,* 6(6), pp. 995-1005.

Tanaka, Y., Hosaka, T. and Ochi, K. (2010) 'Rare earth elements activate the secondary metabolite–biosynthetic gene clusters in Streptomyces coelicolor A3 (2)', *The Journal of antibiotics,* 63(8), pp. 477-481.

Tang, X., Li, J., Millán-Aguiñaga, N., Zhang, J. J., O'Neill, E. C., Ugalde, J. A., Jensen, P. R., Mantovani, S. M. and Moore, B. S. (2015) 'Identification of thiotetronic acid antibiotic biosynthetic pathways by target-directed genome mining', *ACS Chemical Biology,* 10(12), pp. 2841-2849.

Tao, W., Chen, L., Zhao, C., Wu, J., Yan, D., Deng, Z. and Sun, Y. (2019) 'In vitro packaging mediated one-step targeted cloning of natural product pathway', *ACS Synthetic Biology,* 8(9), pp. 1991-1997.

Tarasova, E. V., Luchnikova, N. A., Grishko, V. V. and Ivshina, I. B. (2023) 'Actinomycetes as producers of biologically active terpenoids: Current trends and patents', *Pharmaceuticals,* 16(6), pp. 872.

Thaker, M. N., Waglechner, N. and Wright, G. D. (2014) 'Antibiotic resistance–mediated isolation of scaffold-specific natural product producers', *nature protocols,* 9(6), pp. 1469-1479.
Thompson, C., Ward, J. and Hopwood, D. (1982) 'Cloning of antibiotic resistance and nutritional genes in streptomycetes', *Journal of Bacteriology,* 151(2), pp. 668-677.

Thorpe, H. M., Wilson, S. E. and Smith, M. C. (2000) 'Control of directionality in the site-specific recombination system of the Streptomyces phage φC31', *Molecular microbiology,* 38(2), pp. 232-241.

Traxler, M. F., Watrous, J. D., Alexandrov, T., Dorrestein, P. C. and Kolter, R. (2013) 'Interspecies interactions stimulate diversification of the Streptomyces coelicolor secreted metabolome', *MBio,* 4(4), pp. 10.1128/mbio. 00459-13.

Umezawa, H., Ueda, M., Maeda, K., Yagishita, K., Kondō, S., Okami, Y., ... & Takeuchi, T. (1957) 'Production and isolation of a new antibiotic, kanamycin', *The Journal of Antibiotics, Series A,,* 10(5), pp. 181-188.

Undabarrena, A., Pereira, C. F., Kruasuwan, W., Parra, J., Sélem-Mojica, N., Vind, K. and Schniete, J. K. (2021) 'Integrating perspectives in Actinomycete research: an ActinoBase review of 2020–21', *Microbiology,* 167(9), pp. 001084.

Van Der Heijden, M. G., Bardgett, R. D. and Van Straalen, N. M. (2008) 'The unseen majority: soil microbes as drivers of plant diversity and productivity in terrestrial ecosystems', *Ecology letters,* 11(3), pp. 296-310.

Van der Meij, A., Worsley, S. F., Hutchings, M. I. and van Wezel, G. P. (2017) 'Chemical ecology of antibiotic production by actinomycetes', *FEMS microbiology reviews,* 41(3), pp. 392-416.

Van Middlesworth, F. and Cannell, R. J. (1998) 'Dereplication and partial identification of natural products', *Natural products isolation*, pp. 279-327.

Viaene, T., Langendries, S., Beirinckx, S., Maes, M. and Goormachtig, S. (2016) 'Streptomyces as a plant's best friend?', *FEMS microbiology ecology,* 92(8), pp. fiw119.

Vinogradov, A. A. and Suga, H. (2020) 'Introduction to thiopeptides: biological activity, biosynthesis, and strategies for functional reprogramming', *Cell Chemical Biology,* 27(8), pp. 1032-1051.

Vior, N. M., Olano, C., García, I., Mendez, C. and Salas, J. A. (2014a) 'Collismycin A biosynthesis in Streptomyces sp. CS40 is regulated by iron levels through two pathway-specific regulators', *Microbiology,* 160(3), pp. 467-478.

Vior, N. M., Olano, C., García, I., Méndez, C. and Salas, J. A. (2014b) 'Collismycin A biosynthesis in Streptomyces sp. CS40 is regulated by iron levels through two pathway-specific regulators', *Microbiology (Reading),* 160(Pt 3), pp. 467-478.

Vurukonda, S. S. K. P., Giovanardi, D. and Stefani, E. (2018) 'Plant Growth Promoting and Biocontrol Activity of Streptomyces spp. as Endophytes', *International Journal of Molecular Sciences,* 19(4), pp. 952.

Waksman, S. A. and Henrici, A. T. (1943) 'The nomenclature and classification of the actinomycetes', *Journal of bacteriology,* 46(4), pp. 337-341.

Wan, J., Ma, N. and Yuan, H. (2023) 'Recent advances in the direct cloning of large natural product biosynthetic gene clusters', *Engineering Microbiology,* 3(3), pp. 100085.

Wang, W., Li, X., Wang, J., Xiang, S., Feng, X. and Yang, K. (2013) 'An engineered strong promoter for streptomycetes', *Applied and environmental microbiology,* 79(14), pp. 4484-4492.
Wellington, E. and Toth, I. (1994) 'Actinomycetes', *Methods of Soil Analysis: Part 2 Microbiological and Biochemical Properties,* 5, pp. 269-290.

Wild, J., Hradecna, Z. and Szybalski, W. (2002) 'Conditionally amplifiable BACs: switching from single-copy to high-copy vectors and genomic clones', *Genome research,* 12(9), pp. 1434-1444.

Wilkinson, C. J., Hughes-Thomas, Z. A., Martin, C. J., Bohm, I., Mironenko, T., Deacon, M., Wheatcroft, M., Wirtz, G., Staunton, J. and Leadlay, P. F. (2002) 'Increasing the efficiency of heterologous promoters in actinomycetes', *Journal of molecular microbiology and biotechnology,* 4(4), pp. 417-426.

Williams, S. and Wellington, E. (1982) 'Actinomycetes', *Methods of Soil Analysis: Part 2 Chemical and Microbiological Properties,* 9, pp. 969-987.

Willson, T. A. and Gough, N. M. (1988) 'High voltage E. coli electro-transformation with DNA following ligation', *Nucleic acids research,* 16(24), pp. 11820.

Wimberly, B. T., Guymon, R., McCutcheon, J. P., White, S. W. and Ramakrishnan, V. (1999) 'A detailed view of a ribosomal active site: the structure of the L11–RNA complex', *Cell,* 97(4), pp. 491-502.

Winn, M., Fyans, J., Zhuo, Y. and Micklefield, J. (2016) 'Recent advances in engineering nonribosomal peptide assembly lines', *Natural product reports,* 33(2), pp. 317-347.
Woese, C. R., Fox, G. E., Zablen, L., Uchida, T., Bonen, L., Pechman, K., Lewis, B. J. and Stahl, D. (1975) 'Conservation of primary structure in 16S ribosomal RNA', *Nature,* 254(5495), pp. 83-86.

Woo, M.-W., Nah, H.-J., Choi, S.-S. and Kim, E.-S. (2014) 'Pikromycin production stimulation through antibiotic down-regulatory gene disruption in Streptomyces venezuelae', *Biotechnology and Bioprocess Engineering,* 19, pp. 973-977.

Woo, S.-S., Jiang, J., Gill, B. S., Paterson, A. H. and Wing, R. A. (1994) 'Construction and characterization of bacterial artificial chromosome library of Sorghum bicolor', *Nucleic acids research,* 22(23), pp. 4922-4931.

Woodgate, J., Sumang, F. A., Salliss, M. E., Belousoff, M., Ward, A. C., Challis, G. L., Zenkin, N., Errington, J. and Dashti, Y. (2024) 'Mode of Action and Mechanisms of Resistance to the Unusual Polyglycosylated Thiopeptide Antibiotic Persiathiacin A', *ACS Infectious Diseases,* 11(1), pp. 155-163.

Wu, C., Zacchetti, B., Ram, A. F., Van Wezel, G. P., Claessen, D. and Hae Choi, Y. (2015) 'Expanding the chemical space for natural products by Aspergillus-Streptomyces co-cultivation and biotransformation', *Scientific Reports,* 5(1), pp. 10868.

Xia, H., Li, X., Li, Z., Zhan, X., Mao, X. and Li, Y. 2020. The application of regulatory cascades in Streptomyces: yield enhancement and metabolite mining. Front Microbiol 11: 406.

Xie, F., Zhao, H., Liu, J., Yang, X., Neuber, M., Agrawal, A. A., Kaur, A., Herrmann, J., Kalinina, O. V. and Wei, X. (2024) 'Autologous DNA mobilization and multiplication expedite natural products discovery from bacteria', *Science,* 386(6727), pp. eabq7333.

Xu, M., Wang, Y., Zhao, Z., Gao, G., Huang, S.-X., Kang, Q., He, X., Lin, S., Pang, X. and Deng, Z. (2016) 'Functional genome mining for metabolites encoded by large gene clusters through heterologous expression of a whole-genome bacterial artificial chromosome library in Streptomyces spp', *Applied and Environmental Microbiology,* 82(19), pp. 5795-5805.

Xu, M. and Wright, G. D. (2019) 'Heterologous expression-facilitated natural products' discovery in actinomycetes', *Journal of Industrial Microbiology and Biotechnology,* 46(3-4), pp. 415-431.

Yamada, Y., Sugamura, K., Kondo, K., Yanagimoto, M., & Okada, H (1987) 'The structure of inducing factors for virginiamycin production in Streptomyces virginias', *The Journal of antibiotics,* 40(4), pp. 496-504.

Yamamura, H., Hayakawa, M. and Iimura, Y. (2003) 'Application of sucrose-gradient centrifugation for selective isolation of Nocardia spp. from soil', *Journal of Applied Microbiology,* 95(4), pp. 677-685.

Yamanaka, K., Reynolds, K. A., Kersten, R. D., Ryan, K. S., Gonzalez, D. J., Nizet, V., Dorrestein, P. C. and Moore, B. S. (2014) 'Direct cloning and refactoring of a silent lipopeptide biosynthetic gene cluster yields the antibiotic taromycin A', *Proceedings of the National Academy of Sciences,* 111(5), pp. 1957-1962.

Yan, B., Liu, N., Liu, M., Du, X., Shang, F. and Huang, Y. (2021) 'Soil actinobacteria tend to have neutral interactions with other co-occurring microorganisms, especially under oligotrophic conditions', *Environmental Microbiology,* 23(8), pp. 4126-4140.

Yang, X. and Van Der Donk, W. A. (2013) 'Ribosomally synthesized and post-translationally modified peptide natural products: New insights into the role of leader and core peptides during biosynthesis', *Chemistry–A European Journal,* 19(24), pp. 7662-7677.

Yu, L., Hu, Z. and Ma, Z. (2015) 'Production of bioactive tryptamine derivatives by co-culture of marine Streptomyces with Bacillus mycoides', *Natural Product Research,* 29(22), pp. 2087-2091.

Yuan, H., Zheng, Y., Yan, X., Wang, H., Zhang, Y., Ma, J. and Fu, J. (2023) 'Direct cloning of a herpesvirus genome for rapid generation of infectious BAC clones', *Journal of Advanced Research,* 43, pp. 97-107.

Zabarovsky, E. R. and Allikmets, R. L. (1986) 'An improved technique for the efficient construction of gene libraries by partial filling-in of cohesive ends', *Gene,* 42(1), pp. 119-123.
Zein, N., Sinha, A. M., McGahren, W. J. and Ellestad, G. A. (1988) 'Calicheamicin γ1I: an antitumor antibiotic that cleaves double-stranded DNA site specifically', *Science,* 240(4856), pp. 1198-1201.

Zeph, L. R. and Casida Jr, L. (1986) 'Gram-negative versus gram-positive (actinomycete) nonobligate bacterial predators of bacteria in soil', *Applied and environmental microbiology,* 52(4), pp. 819-823.

Zhang, H., Shinkawa, H., Kinashi, H. and Hasegawa, T. (1999) 'Protoplasting, Regeneration and Transformation of Rare Actinomycetes', *Actinomycetologica,* 13(1), pp. 42-48.

Zhang, M., Zhang, Y., Scheuring, C. F., Wu, C.-C., Dong, J. J. and Zhang, H.-B. (2012) 'Preparation of megabase-sized DNA from a variety of organisms using the nuclei method for advanced genomics research', *nature protocols,* 7(3), pp. 467-478.

Zhou, S., Bhukya, H., Malet, N., Harrison, P. J., Rea, D., Belousoff, M. J., ... & Corre, C (2021) 'Molecular basis for control of antibiotic production by a bacterial hormone', *Nature,* 590(7846), pp. 463-467.

Ziermann, R. and Betlach, M. C. (1999) 'Recombinant polyketide synthesis in Streptomyces: engineering of improved host strains', *Biotechniques,* 26(1), pp. 106-110.